ADDIS ABABA INSTITUTE OF TECHNOLOGY

SCHOOL OF CIVIL AND ENVIRONMENTAL ENGINEERING

An Investigation into the Ground Motion Amplification Potential of Selected Sites of Addis Ababa City

By

Zetseat Gashaye

A thesis submitted to the School of Graduate Studies of Addis Ababa University in Partial fulfillment of the requirement for the Degree of Master of Science in Geotechnical Engineering.

Advisor

Dr.-Ing. Asrat Worku

Addis Ababa, Ethiopia

July 2018

DECLARATION

I hereby declare to the senate of Addis Ababa University that this thesis is entirely original work and all other materials are duly acknowledged. This work has not been submitted for academic degree award at any University.

_____

ACKNOWLEDGEMENT

This study would not have been possible without the guidance of my advisor Dr.-Ing. Asrat Worku, associate professor of the School of Civil and Environmental Engineering at Addis Ababa Institute of Technology. He steered me in the right direction whenever I run into a trouble spot or had a question about the work. He really has been a tremendous advisor for me.

I am extremely grateful to the experts of the Institute of Geophysics Space Science and Astronomy (IGSSA) at Addis Ababa University: Dr. Atalay Ayele, Dr. Getnet Mewa and Dr. Genet Tamiru, for their limitless contribution in conducting the seismic refraction survey. They sacrificed their knowledge, skill, effort and time to conduct the field survey. Nobody has been more important to me in acquiring the geophysical data.

I would like to express my deep and sincere gratitude to the following consulting companies who provided me with all necessary and relevant geotechnical data: ARCON Design Build PLC, BEST Consulting Engineers PLC, SABA Engineering PLC, ADDIS GEOSYSTEMS PLC, Ethiopian Construction Design and Supervision Works Corporation, Gia Engineering PLC, MH Engineering PLC, JDAW Consulting Architects and Engineers PLC, MGM Consults PLC and BEACON Consulting Engineers PLC. Thank you for your sincere cooperation.

I would also like to express my profound gratitude to my friends: Besrat Eshetu, Leamlak Minwuyelet and Tenaw Workie for their continuous encouragement and support through the process of the study. Besrat, I really thank you for your reviewing and valuable comments on my work.

Finally, I am extending my thanks to all the people and the institutions whose name I cannot mention but have supported me to complete the study directly or indirectly.

ABSTRACT

Located on the western margin of the Main Ethiopian Rift, Addis Ababa, the capital city of Ethiopia, has experienced a number of earthquakes since its establishment. Thick soil formations which are predicted to have an effect on ground motion parameters characterize portions of the city. This site effect is even more significant considering the fact that the city is located in a region characterized by moderate seismicity. A one-dimensional ground response analysis using equivalent linear method was conducted to investigate the influence of selected sites on input ground motions. Input soil data were acquired from geotechnical investigation reports and seismic refraction surveys to characterize the soil profile of the selected sites. By considering the geologic and tectonic conditions of the vicinity, input ground motions were selected from PEER ground motion database. Ground motions of unique parameters that are customarily used in engineering practices were also included. Ground response analyses were performed employing the input soil data to the DEEPSOIL program subjected to the selected input ground motions at the base of the soil profile. The outcomes of the analyses show that the selected sites have significant potential of amplifying the ground motions. This amplification effect is observed to be exceedingly higher than the up-to-date code-specified predictions. Therefore, the study suggests that it would be worth investigating further in order to come up with more comprehensive study.

TABLE OF CONTENTS

Chapter Five

Chapter Six

LIST OF TABLES

LIST OF FIGURES

CHAPTER ONE

INTRODUCTION

1.1 Background

In recent times, the effect of thick soft soil deposits on strong ground motion characteristics has become a well-accepted fact. A number of recorded earthquake ground motions provided numerous evidences associated with the effect of soil deposits on ground motion characteristics (Kramer 1996; Villaverde 2009). Moreover, the effect is observed to be significant in moderately seismic areas like Addis Ababa city (Worku 2014).

Ground response analysis with different techniques of computation has become popular in quantifying site effects following the development of computer programs. "SHAKE" is the pioneering program to be used in site response analysis (Schnabel et al. 1972). Since then, a number of programs were developed to perform ground response analysis in order to assess the effect of soft soil deposits critically. Among the latest programs, DEEPSOIL developed at the University of Illinois at Urbana-Champaign, is one used to perform analysis both in frequency domain and time domain procedures.

Addis Ababa, the capital city of Ethiopia, is situated on the margins of the Ethiopian Rift System having moderate seismicity in the region. It has felt a number of earthquakes of magnitude up to M_s 6.8 in the near past. According to studies, an earthquake of nearly same magnitude (M_s of 6.8) is anticipated in the near future at about 27 km away from the city (Kinde 2002; Mammo 2005). The city is characterized by varied ground formations and is dominated by soft soil deposits in the south and south-eastern parts. Geotechnical reports from different locations and studies on engineering geology of the area provide a brief description of general characteristics of soil conditions in the city (Tsehayu and H.Mariam 1990). These thick soft soil formations presumably have the potential to alter the characteristics of ground motions emerged from stiff materials below these soil deposits.

Extensive infrastructures and high-rise buildings are being built in the rapidly growing city of Addis Ababa. The population of the city is progressively increasing day by day as well. The combined effect of such growths with the moderate seismicity of the area and

local soil conditions exacerbate susceptibility of the city to damages from earthquake hazards. This calls for detailed studies of local site effects and incorporating the results to local seismic design provisions in order to have earthquake resistant structures in the city.

1.2 Objectives

The main objective of this study is to undertake one-dimensional ground response analysis at selected sites in Addis Ababa city. In the meantime, the study comprises the following specific objectives, as well.

- investigating how ground motion parameters at the ground surface are affected as the input motions pass through the soil profile of the selected sites;
- investigating the potential of the selected sites to amplify/deamplify the input earthquake ground motions;
- examining how peak ground acceleration (PGA) varies through a soil profile as the input motions propagate from proposed bedrock (seismic base layer) to the ground surface;
- comparing the mean response spectrum obtained from the analysis with spectra of current local and applicable code provisions so as to check out the adequacy of the spectra provided in the codes.

1.3 Methodology

Ground response analysis is performed mainly to estimate the ground motion parameters as soil formations are subjected to the considered input earthquake motions. The analysis can be performed in one-, two- or three – dimensional techniques based on the spatiality of the problems. Having some simplifying assumptions, one-dimensional ground response analysis is carried out in linear, equivalent linear (EQL) or non-linear methods of analysis depending on the stress-strain behavior of soils under dynamic loading.

Equivalent linear method of analysis (in frequency domain) is an approximate method of simulating the non-linear behavior of soils. This method is popular in that it gives

reasonable analysis outputs for up to threshold strain level of soils (Udaka 1983, as cited by Haile 1996). The method is preferred in that it needs straightforward input soil parameters to perform the analysis. Several computer programs have been developed having the option to carry out EQL analyses of a soil profile. The DEEPSOIL program with EQL method has been opted to investigate the amplification potential of selected sites in Addis Ababa city.

The selected sites were characterized using soil data obtained from geotechnical investigation results of different projects. Seismic refraction survey was also conducted at four selected sites to collect geophysical data. The field test was repeated for a second time as the results from the first survey were not adequate. Soil parameters from these sources have been used to define soil models of the site profiles to perform the analysis.

The input ground motions have been obtained from PEER ground motion database based on geologic and tectonic conditions of the study area. In addition, commonly used historical earthquake ground motions have also been incorporated in order to have best representative design ground motions.

1.4 Scope of the Study

Complete and detailed ground amplification potential investigation of the entire area of the city requires cost-intensive and extended time frame. A number of field and laboratory tests need to be conducted in order to obtain soil parameters for characterizing sites using state of the art soil models in performing ground response analyses. This broad investigation, however, is beyond the scope of this study. As a more viable option, geotechnical investigation reports of different recent projects and seismic refraction survey have been conducted to obtain input soil data that characterize selected sites in the city. The method of analysis is also limited to equivalent linear method as dependable soil data were not available for the actual non-linear soil modeling.

1.5 Organization of the Study

This research is devised into seven chapters. Chapter Two reviews relevant literature about ground response analysis. Different techniques and methods of response analyses

will be discussed in this chapter. Chapter Three talks about geomorphology, geology, engineering geology and seismicity of the study area.

Input ground motions that will be used in the analysis are discussed in Chapter Four. In Chapter Five, the detail about input soil data from geotechnical reports and seismic refraction survey to characterize the selected sites is presented. The input ground motions obtained in Chapter Four and the soil models in Chapter Five will be employed for the analysis; and the results will be discussed in Chapter Six. Chapter Seven concludes the work along with recommendations.

CHAPTER TWO

LITERATURE REVIEW

2.1 Stress-Strain Behavior of Cyclically Loaded Soils

Most soils exhibit a nonlinear hysteretic behavior when loaded under symmetric cyclic loading. A typical stress-strain relationship (hysteretic loop) within a soil can be represented by the sketch in Figure 2.1. The hysteresis loop is described either by the actual path of the loop itself or by the parameters that describe its general shape (or both). Inclination and breadth are the two important parameters that describe the shape of the hysteresis loop (Kramer 1996).

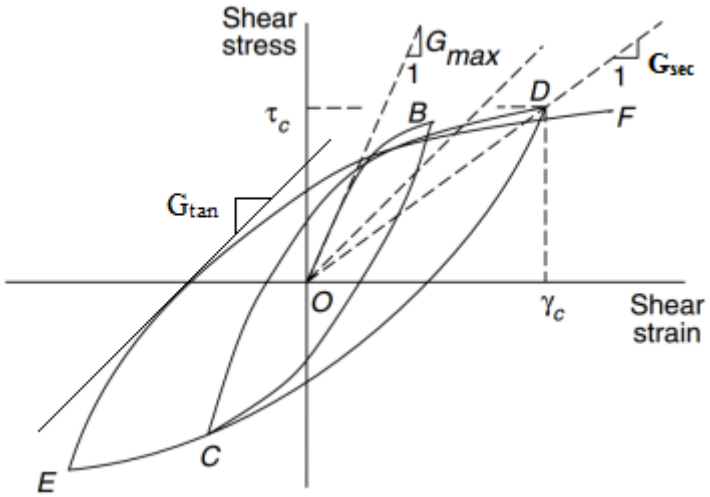

Figure 2.1 Typical stress–strain behavior of soils and variation of shear modulus with strain level (After Villaverde 2009)

The inclination, which represents the stiffness of the soil, is depicted by shear modulus of the soil. Shear modulus which is defined as ratio between incremental shear stress and shear strain can be measured in different ways. The low-strain amplitude shear modulus called maximum shear modulus, G_{max} is usually obtained from seismic geophysical tests (in situ low strain tests). In the absence of direct measurements, G_{max} can be estimated from empirical correlations. It is analytically related to basic soil properties using the following relation (Kramer 1996):

$$G_{\max} = \rho v_s^2 \tag{2.1}$$

Where, ρ is mass density and v_s shear wave velocity

Tangent shear modulus, G_{tan}, represents the gradient of the stress-strain curve at any specified strain or stress. Since stiffness of soil varies throughout a loading cycle, G_{tan} is approximated by the secant shear modulus. Secant shear modulus measures the average inclination of the loop.

$$G_{sec} = \frac{\tau_c}{\gamma_c} \tag{2.2}$$

Where, τ_c and γ_c are the shear stress and shear strain corresponding to the tip of the loop, respectively.

The secant shear modulus of soils varies with cyclic shear strain amplitude because of change in stiffness of the soil. Slippage between grains owing to increment in shear stress and shear strain causes a decrease in shear strength and stiffness of the soil. This condition results in rotation of the hysteresis loop towards horizontal axis; and this leads to the usual custom of characterizing the backbone curve (locus of points corresponding to tips of hysteresis loops of various cyclic strain amplitudes) in terms of modulus ratio, G_{sec}/G_{max}. Modulus reduction curve which presents the plot of variation of modulus ratio with shear strain is another way of describing the backbone curve (Figure 2.2).

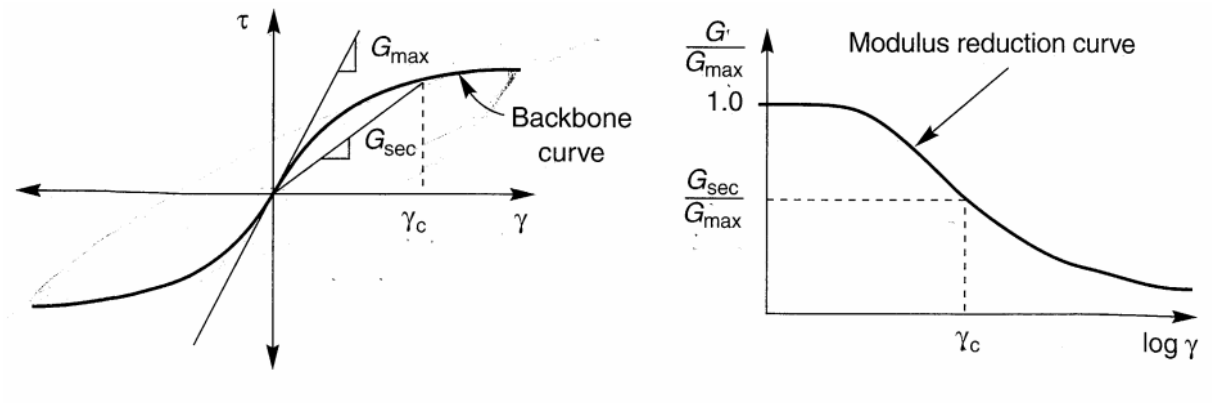

Figure 2.2 Backbone curve showing variation of G_{sec} with shear strain (after Kramer 1996)

The second important parameter related to area of the hysteresis loop is its breadth. It is the measure of energy dissipation by friction of soil particle movements. The input energy varies linearly with the displacement amplitude and the energy dissipated is proportional to the square of the displacement amplitude of motion (Chopra 2007). A

damping ratio ξ is frequently used as a measure of the energy dissipation (Kramer 1996).

$$\xi = \frac{W_D}{4\pi W_S} = \frac{1}{2\pi}\frac{A_{loop}}{G_{sex}\gamma_c^2} \tag{2.3}$$

Where: W_D is the dissipated energy, W_S is the maximum strain energy, i.e. the area of the triangle in Figure 2.3; and A_{loop} is the area of the hysteresis loop.

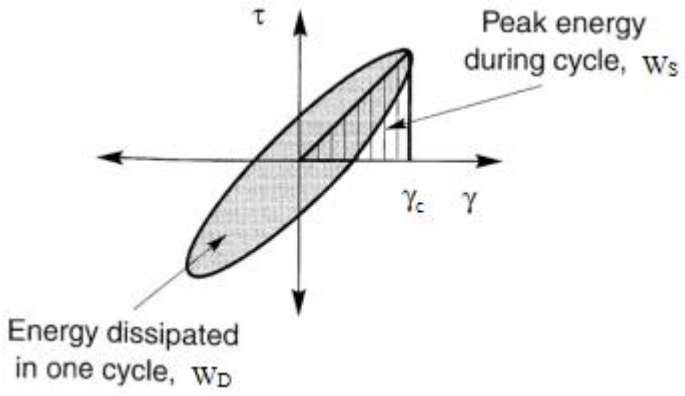

Figure 2.3 Relationship between hysteresis loop and damping ratio (After Kramer 1996)

The damping curve, which describes the manner in which the damping ratio varies with shear strain amplitude, increases with increasing strain level. In consequence, different soils exhibit different damping characteristics.

2.2 Material Curves: Modulus Reduction and Damping Curves

It should be noted that the aforementioned parameters of a soil and their variation with strain level depend on the type of soil. Besides this, investigations show that soil stiffness and damping properties are also influenced by mean confining pressure, plasticity index, over consolidation ratio, number of loading cycles and void ratio of the soil (Kramer 1996).

Modulus reduction and damping ratio curves can be measured on site-specific and material-specific basis using dynamic testing (e.g. cyclic simple shear, resonant column/torsional shear tests) or estimated using empirical correlations. When material-specific test results are unavailable, different sets of empirical correlations that consider the effect of different factors have been proposed for different soil types. A number of empirical correlations studied by different researchers are available in the

form of a set of curves. These generic curves include the pioneering works by Seed and Idriss (1970) (curves for clay and sand), Vucetic and Dobry (1991) (PI-dependent curves for clay), Ishibashi & Zhang (1993) and Darendeli (2001).

The influence of effective confining pressure on modulus reduction and damping behaviors is substantial for soils of low plasticity. Regarding the curves, the pioneering works of Seed and Idriss (1990) for sand soils after being re-analyzed and re-proposed by Seed et al. (1986) are shown in Figure 2.4.

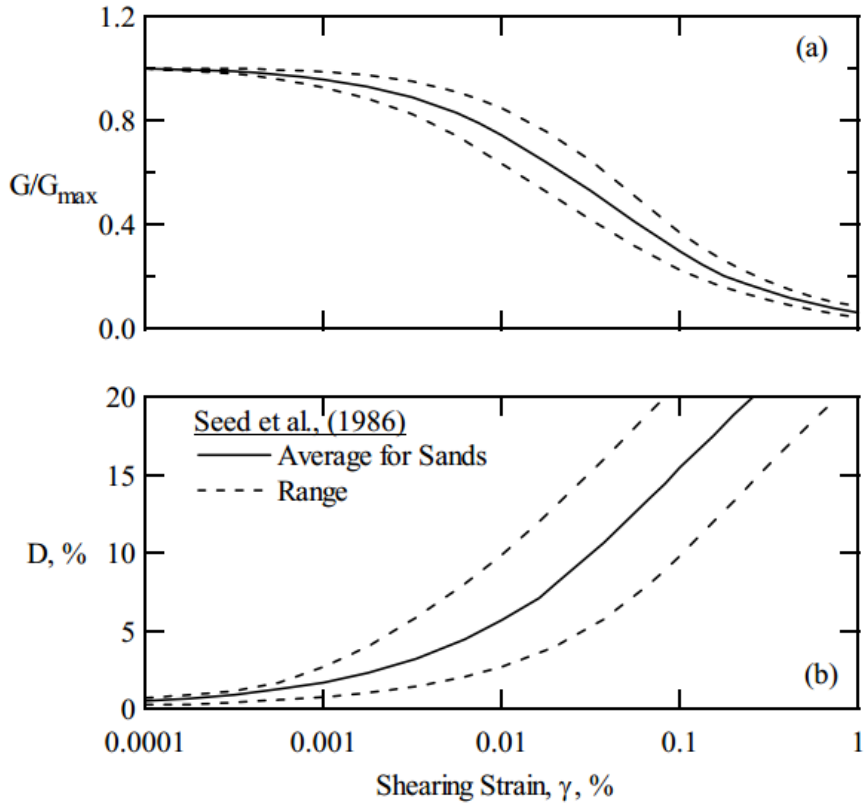

Figure 2.4 Empirical curves proposed by Seed et al. (1986): (a) normalized modulus reduction curve; (b) material damping curve (as replotted by Darendeli 2001)

In general, a modulus reduction curve increases with plasticity index and damping increases with decreasing plasticity index. The material curves generated in Figure 2.5 show the noteworthy works of Vucetic and Dobry (1991) keeping plasticity index as a controlling variable. Comparing the zero plasticity curves of Vucetic and Dobry (1991) with that of the average curves used for sands (Seed and Idriss 1970), one can conclude that the Vucetic-Dobry curves are applicable to both fine- and coarse-grained soils of low plasticity (Kramer 1996).

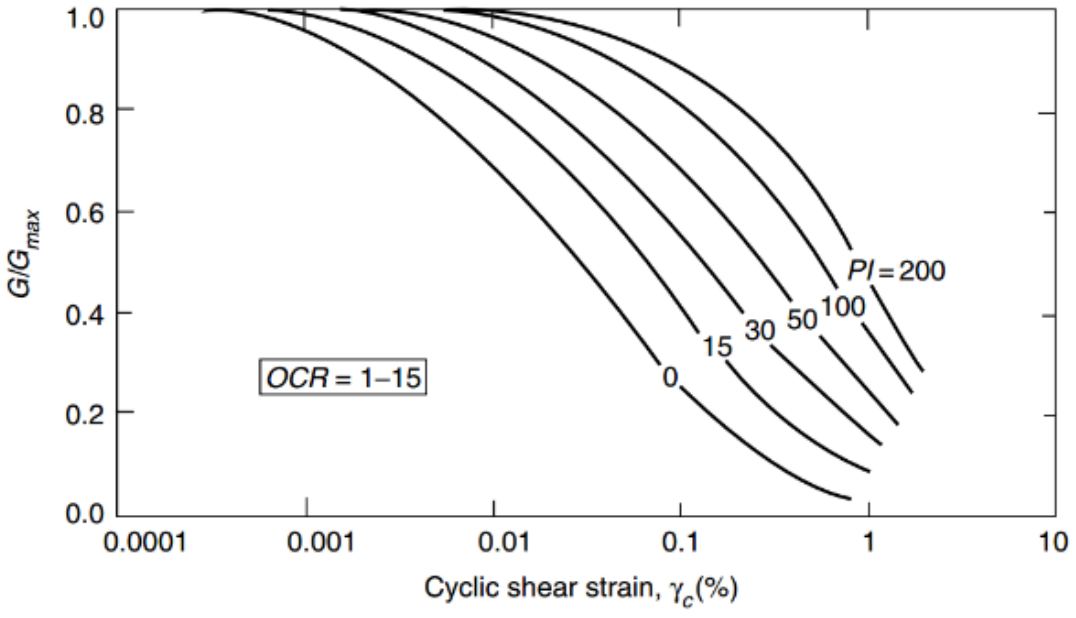

(a)

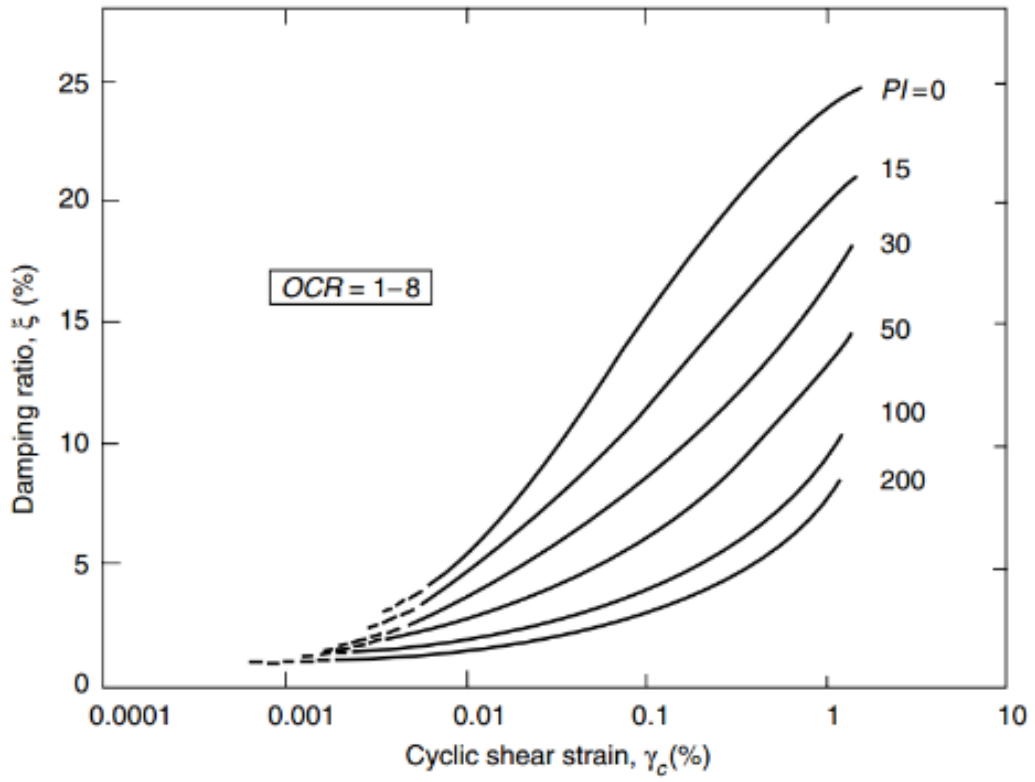

(b)

Figure 2.5 Variation of (a) normalized shear modulus and (b) damping ratio with shear strain and plasticity index (as reproduced by Villaverde 2009)

Ishibashi (1992) proposed curves characterizing the influence of effective confining pressure and plasticity index on modulus reduction behavior as drawn in Figure 2.6.

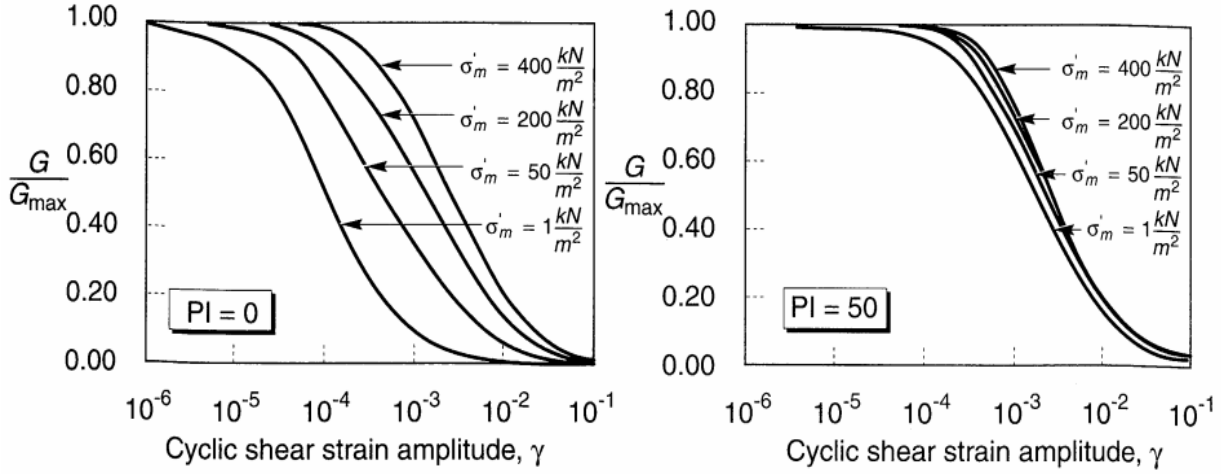

(a) (b)

Figure 2.6 influence of mean effective confining pressure on modulus reduction curves for (a) non-plastic (PI=0) soil, (b) plastic (PI=50) soil (After Ishibashi (1992) as referred by Kramer 1996)

Recent studies on material curves with the effects of plasticity index, mean effective confining pressure, over consolidation ratio and number of loading cycles were performed by Darendeli (2001). Comparing his works with those results from Seed et al (1986) and Vucetic and Dobry (1991), he observed some discrepancies. These discrepancies were attributed to the accuracy problems of old generation cyclic triaxial equipment in material damping measurements in the previous studies. The effect of confining pressure and soil plasticity on modulus reduction and damping curves as proposed by Darendeli (2001) are indicated in Figure 2.7.

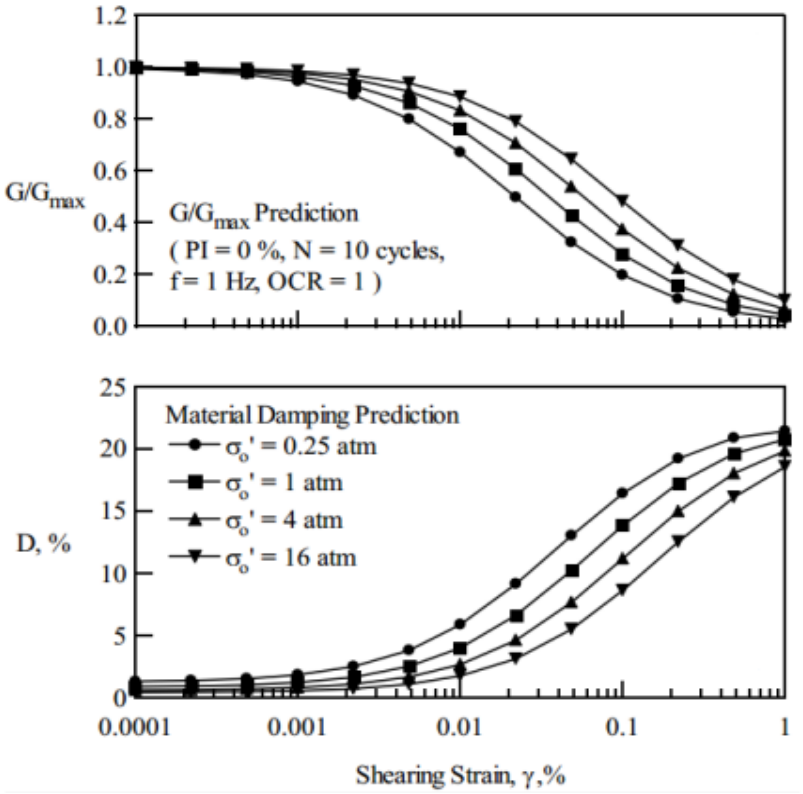

(a)

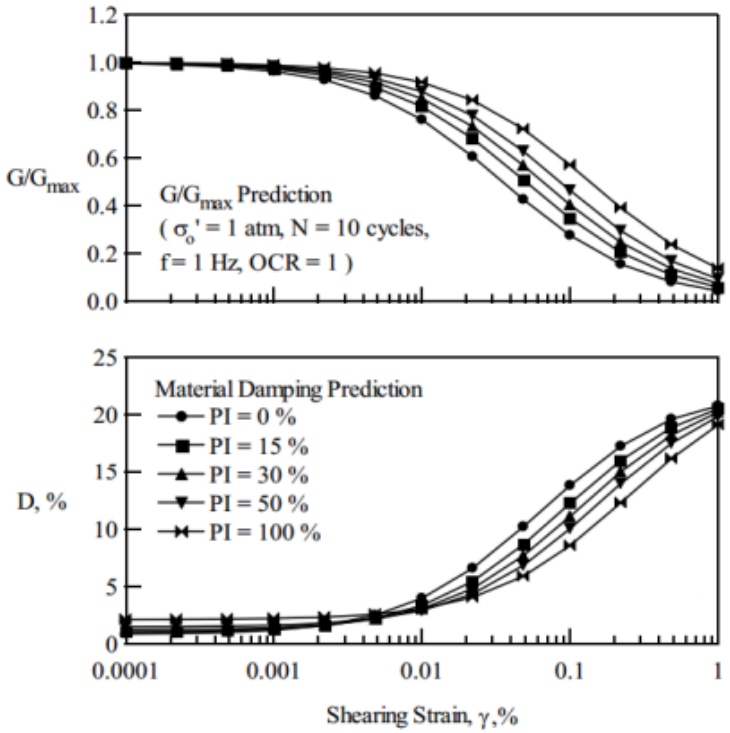

(b)

Figure 2.7 Effects on normalized modulus reduction and material damping curves (a) of confining pressure; (b) of soil plasticity

2.3 Local Site Effects

When a wave propagates through the path from a source to bedrock surface, it radiates in all directions. As the distance from the source increases and the wave radiates in all directions, the amplitude becomes smaller and a phenomenon known as attenuation of earthquake waves takes place. Because of successive refraction, the propagation of waves through soil deposits is nearly vertical along one direction. When waves propagate in one direction a phenomenon called amplification is likely to occur instead of attenuation (Yoshida 2015).

Early observations: MacMurdo (1824); Mallet (1857); Wood (1908) and Reid (1910); Gutenberg (1927) noted the effect of local site conditions on ground motions (as cited by Kramer (1996)). The existence and nature of local site effects is supported by considerable evidences. Actual amplification functions computed from instruments installed at surface and subsurface of the same location indicate the presence of local site effects. Measured ground surface motions from sites with different subsurface conditions have also corroborated modifications in ground surface motion characteristics. The 1985 Michoacan (Mexico) earthquake, the 1989 Loma Prieta (California) and the 2000 Tottoriken-seibu (Japan) earthquake are three of the most significant and well-documented earthquakes to show the significant relationship between local soil conditions and ground motions (Yoshida 2015; Kramer 1996).

Currently, the effect of local geology, topography and soil properties on ground shaking intensity has become well-accepted fact. Structures built on soft soils were generally observed to experience more damage than those situated on rock. Important characteristics (amplitude, frequency content and duration) of ground surface motions are significantly influenced by local soil conditions. The extent of influence of local soil conditions is contingent on characteristics of input motion, site topography, geometry and properties (stiffness density and damping) of the soil formation (Villaverde 2009; Kramer 1996).

Idriss (1990) related peak accelerations on soft soils to those on rock sites based on data from Mexico City and San Francisco Bay area. On the basis of this study, it was found that rock accelerations (less than about 0.4g) might be amplified several times at soft soil deposits (Figure 2.8). At higher rock acceleration levels, development of peak accelerations at the surface of soft soils is hindered by the low stiffness and non-linearity

of the soils (Figure 2.1). This implies that moderately seismic areas like Addis Ababa are severely exposed for such high amplifications effects (Worku 2014). Besides, deep and soft soil deposits have the tendency of amplifying low frequency input motions much more (Villaverde 2009).

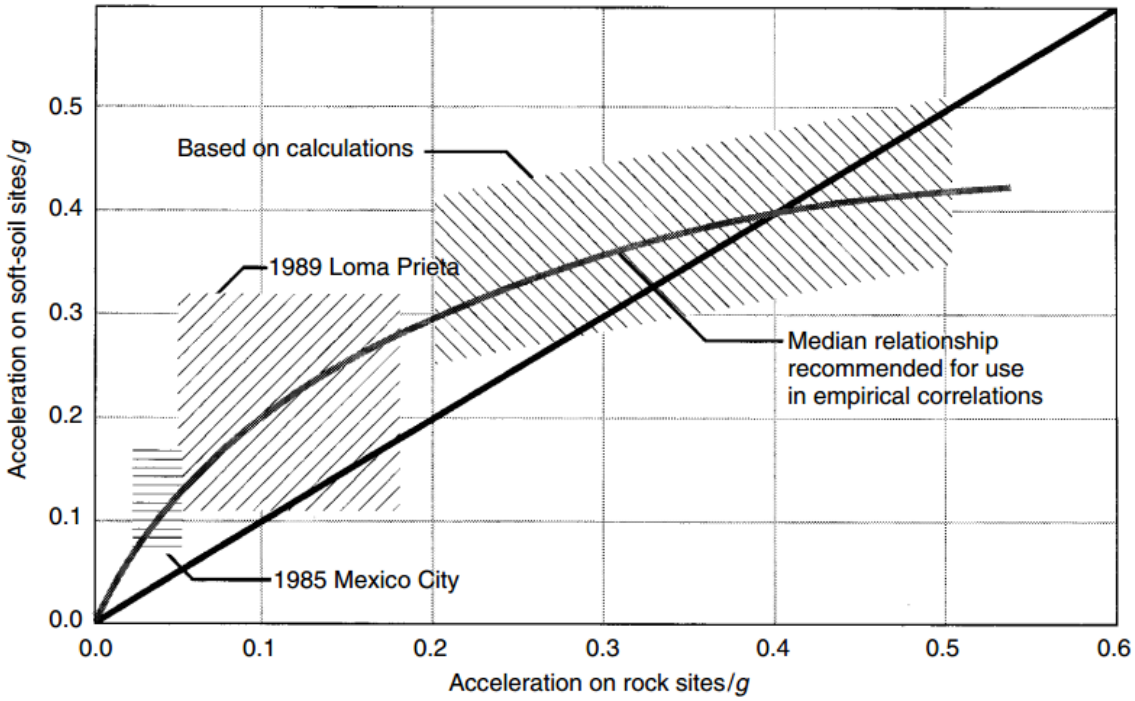

Figure 2.8 Empirical relationships between peak accelerations recorded on rock and soil sites (as reproduced by Villaverde 2009)

2.4 Ground Response Analysis

A complete characterization of earthquake ground motions for which structures should be designed constitutes ground response analysis. It encompasses the path from the earthquake source mechanism to the soil condition at the site of interest to study the influence on ground surface motion characteristics.

Seismic hazard analysis involves quantitative estimation of ground motion characteristics at a particular site by means of identifying and characterizing all potential sources of seismic activity that could produce significant ground motions at a site. Both deterministic and probabilistic seismic hazard analyses utilize predictive relationships to produce a set of ground motion parameters that may or may not correspond to the subsurface conditions at the site of interest. If the site of interest is located on a similar

profile, these parameters may be taken directly as the design ground motion parameters. If it is not, however, the parameters from the seismic hazard analysis must be modified to account for the effects of local site conditions.

As seismic waves from an earthquake propagate through overlying soil and reach the ground surface, ground motion parameters such as amplitude of motion, frequency content, and duration are affected. This physical process of filtering and modifying ground motion characteristics by local soils is termed as site effect. Site effects are quantified via ground response analysis, which involves the simulation of propagation of earthquake motions from the base rock through the overlying soil layers to the ground surface. The main objective of ground response analysis is, therefore, determining the response of soil deposit to the motion of bedrock immediately beneath it.

The development of a number of techniques for ground response analysis made the quantitative prediction of the influence of local soil conditions on strong ground motions possible. Depending on the spatiality of the problem to be addressed, ground response analysis techniques can be conducted in three ways: one, two or three-dimensional ground response analysis (Kramer 1996).

2.4.1 One-Dimensional Ground Response Analyses

Ground response analysis as a whole is considerably complex and hence it only simulates a portion of the physical properties controlling the site response. The important controlling features of local soil conditions and local geology include horizontal extent and depth of the soil deposits overlying bedrock, slopes of the bedding planes of the soils, horizontal variability of soils, topography of both bedrock and deposited soils, faults crossing soil deposits and basin effects.

One-dimensional (1D) ground response analysis (GRA) is recommended for level or gently sloping sites with the assumptions that: (1) ground surface and all material boundaries below the ground surface are horizontal and extend infinitely in all lateral directions; and (2) response of soil is predominantly caused by vertically propagating shear waves (SH-waves) from underlying bedrock (Kramer 1996).

Based on simplifying assumptions that are made in the representation of stress-strain relations of soils and in the methods used to integrate the equation of motion,

one-dimensional ground response analysis is grouped into three broad categories: linear analysis, equivalent-linear analysis and nonlinear analysis (Kramer 1996).

2.4.1.1 Linear Analysis

The method of linear analysis is based on the assumption that shear modulus and damping are strain independent and constant for each layer. Because of its simplicity, linear approach is extensively used. Closed form analytical solutions for idealized geometries and soil properties can be derived. In general, however, soil does not behave elastically and its material properties change in space. In such situations, no analytical solutions are possible and numerical techniques are required. For this reason, the approach is usually not convenient for ground response analyses of strong earthquake ground motions which induce strains in soils beyond the elastic range.

The key for linear approach is the evaluation of transfer functions of the soil deposit under investigation. Transfer functions are used to relate the various response parameters (such as displacement, velocity, acceleration, shear stress and shear strain) at the surface or at any point within the soil to an input bedrock motion. These functions are influenced by thickness, stiffness and damping characteristics of the soil. The general procedure can be summarized as follows (R. Villaverde 2009).

1. The bedrock motion is first represented in the frequency domain in the form of Fourier series (as the sum of a series of sine waves of different amplitudes, frequencies, and phase angles) through the use of Fast Fourier Transform (FFT).
2. Each term in the Fourier series is multiplied by the transfer function of the soil to obtain the Fourier series of the motion at the ground surface.
3. The Fourier series of the output (ground surface) motion is computed as the product of the Fourier series of the input (bedrock) motion and the transfer function.
4. The ground surface motion is expressed in the time domain by means of the inverse fast Fourier transform.

2.4.1.2 Equivalent Linear Analysis (EQL): Frequency Domain

This frequency domain method of analysis was developed to analyze the nonlinear response of soil using linear transfer functions. The model approximates the actual

nonlinear behavior of cyclically loaded soils by equivalent linear properties for a range of strain values. These equivalent-linear properties correspond to the effective shear strain obtained using an iterative procedure. The target of the iterative procedures is to determine shear modulus, G and damping, ξ values that are consistent with the amount of strain developed in each layer during the modeling process.

The strain level of transient (earthquake) record is characterized in terms of effective shear strain to account for the severe loading condition of the harmonic record. Generally, the effective shear strain is considered to be 65% (a factor determined from statistical analyses of many shear stress time histories) of the maximum shear strain developed in the layer.

The following iterative procedure is used to ensure that the equivalent linear properties used in the analysis are compatible with the computed strain levels in all layers (Kramer 1996).

1. Initial estimation of low-strain (same strain level) G and ξ values are made for each layer.
2. Ground response is performed using the estimated G and ξ values and shear strain time histories are obtained for each layer.
3. The effective shear strain in each layer is determined from the maximum shear strain in the computed shear strain time history.
4. Using this effective shear strain, new equivalent linear G and ξ values are chosen for the next iteration. This process is repeated until the differences between the assumed and realized values fall below a predetermined value in all layers. The shear modulus and damping used in each iteration remains constant for the whole time-history.

The general procedure of the analysis is similar to that of linear approach and can be summarized by the following flow chart.

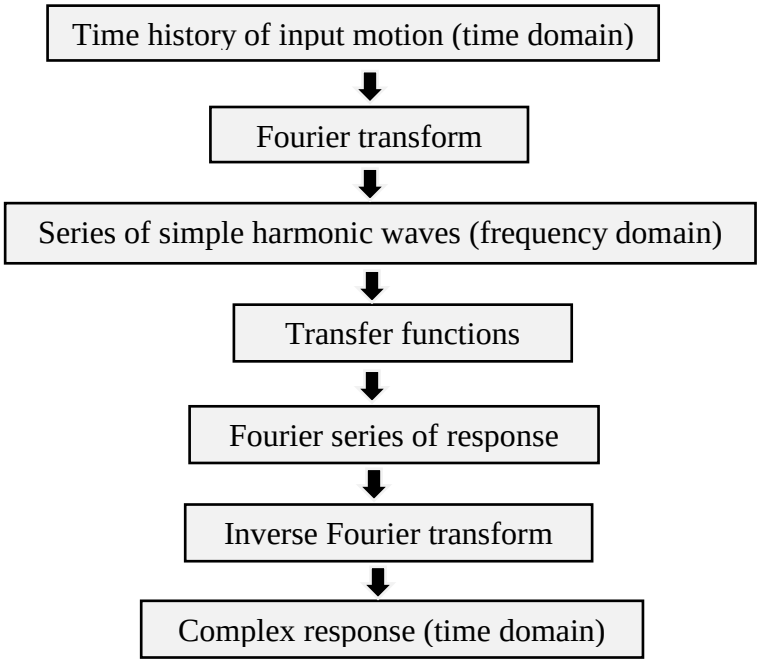

Figure 2.9 Flow chart showing the general procedure of EQL analysis method

According to Udaka (1983), equivalent-linear method of ground response analysis gives satisfactory results for strain level of about 0.5% (as cited by Haile 1996). This method is computationally efficient with the availability of several codes and provides reasonable results. In spite of this advantage, the method is incapable of representing the change in soil stiffness that actually occurs during large earthquakes (Kramer, 1996). It also gives unreliable results for problems involving permanent shear deformation as the model does not follow the actual hysteresis loop.

2.4.1.3 Non-Linear Analysis (NL): Time Domain

Equivalent linear analysis has limitations in the representations of actual strain dependent modulus degradation and damping curves under cyclic loading. The analysis does not consider the generation of excess pore water pressure. It is also limited to low to moderate strain levels (not appropriate for large strain levels). These problems can be addressed by characterizing the realistic stress-strain soil behavior and adopting nonlinear ground response analysis.

In nonlinear method of analysis realistic stress-strain behavior of soil is modeled for accurate measurement of soil behavior. Several nonlinear inelastic stress-strain models or advanced constitutive models are available. The nonlinear analysis can be done with or

without pore water pressure generation using appropriate soil models. Equations of motions are solved in time domain using step by step numerical integration.

For problems with low strain levels, both equivalent linear and nonlinear analyses give close results of ground response analysis. The main difference between the two analyses is the degree of non-linearity in the actual soil response. Still, nonlinear analysis has the following advantages over the equivalent linear one (Kramer 1996).

- stress-strain behavior is more realistically modeled;
- it provides reasonable results for problems involving high strain levels (as shear stress approaches shear strength of the soil); and
- it can be formulated in terms of effective stresses to allow generation, redistribution and eventual dissipation of excess pore water pressure during and after earthquake shaking.

Though the nonlinear method has a number of advantages over the equivalent linear, the parameters used to describe soil models are not well established as those of equivalent linear model. The evaluation of nonlinear model parameters demands advanced field and laboratory testing. These conditions give limitations on the implementation of nonlinear ground response analysis in some problems.

2.4.2 Two-Dimensional and Three-Dimensional Ground Response Analyses

Some controlling features of sites make one-dimensional ground response analysis impractical. The presence of surface irregularities such as ridges and valleys, subsurface topography, heavy structures, embedded structures and tunnels calls for the use of two-dimensional or possibly even three-dimensional analysis.

The substantial effect of alluvial basin geometry on ground surface motions was observed from a number of recordings. From measured ground motions along transverse and longitudinal profiles across Chusal Valley (Afghanistan), King and Tucker (1984) suggested that one-dimensional ground response analysis is not feasible to measure amplification functions particularly near the edge of the valley. By comparing computed amplification functions for two-dimensional case, Bard and Gabriel (1986) showed analytically that amplification functions closer to the edge of a valley were considerably different (as cited by Kramer 1996). This impracticality of 1D ground response analysis

is mainly caused for the reason that multiple wave reflections and surface wave generation take place at basin edges.

Numerous studies also showed that the unusually high peak ground motion parameters recorded on ridges are attributed to a topographic effect. Peak ground accelerations recorded from an accelerograph located at the crest of narrow, rocky ridge (on the abutment of Pacoima Dam in southern California) were substantially larger. This effect was corroborated by similar patterns of amplifications on ridges from five earthquakes in Matuazaki, Japan, (Jibson 1987) and from earthquakes in Italy and Chile (Finn 1991) (as cited by Kramer 1996). For these types of problems, 1D analysis may not be able to describe the complex wave patterns produced by topographic irregularities.

Similarly, these effects have been observed in the city of Addis Ababa following the 1979 earthquake of local magnitude 4.1. The intensity map prepared at the time showed significantly higher intensities at some locations because of topographic and the Filwoha fault effects (Figure 3.3).

Two-dimensional and three-dimensional dynamic response analyses solve problems in much the same way both in time domain and frequency domain. They are usually performed using dynamic finite element analyses in equivalent linear and nonlinear methods which are analogous to their one-dimensional counterparts. 2D simulation yields satisfying results for site conditions which show significant variation in two directions and are uniform in the other one direction. But some problems involving conditions such as three-dimensional variation of soil conditions and boundary problems and three-dimensional response of structures, necessitate the use of 3D ground response analysis. Be that as it may, these analyses are complicated and time consuming and demand more detailed site characterizations (Kramer 1996).

CHAPTER THREE

GEOLOGY AND SEISMICITY OF THE STUDY AREA

3.1 Location and Geomorphology

Addis Ababa, located between 8º 49’ 55.929’’ and 9º 5’ 53.853’’ North latitude and 38º 38’ 16.555’’ and 38º 54' 19.547" East longitude is not only the capital city of Ethiopia but also the political and social center of Africa and the seat for regional and international organizations. It is speedily expanding and is represented by the large population with rapid growth rate.

The city, sited in the central high plateau of the country, has an altitude ranging from 3100 m (at Mt. Entoto) to 2050 m (at Akaki plains) above sea level. The rugged topography of the city is characterized by well-drained plateau surrounded by trachyte and rhyolite hills. While the central part of the city has gentle and rolling topography with scattered plots of hills, the southern and south-eastern part is predominantly flat. The area of Addis Ababa is generally characterized by the following noticeable landforms (Tsehayu and H.Mariam 1990).

Entoto Ridges: The south and south-west acidic flow of rhyolite and trachyte from the east-west trending fault during the lower Miocene process formed ridges along the fault line as a result of the high viscosity of the lava. This created the highest ridge of 3100 m above sea level and gave topography that lowers the flow direction.

Flat and Undulating Topography: The eruption of low-viscosity (high mobility) Addis Ababa basalt during the lower Pliocene (after a long period of erosion of Entoto silicic) formed flatter topography. This activity resulted in the relatively flat and undulating topography of the central part of the city with a gradual decrease in topography to the south-east.

Young Volcanic Hills: During the upper Pliocene, young volcanic mountains such as Wachecha (3350 meters), Furi (2850 meters) and Yerer (3099 meters) were formed.

Kebena and Akaki rivers: Draining towards south to join Awash River, these are the main rivers crossing the city. They form terraces and alluvium deposits in west, south-west and central part of the city.

3.2 Local Geology

Addis Ababa is located on the western margin of the main Ethiopian rift system, which was formed as a result of fracturing of the earth's crust by tension forces. As a consequence, the city comprises volcanic rocks that range from basic to acidic composition. These rocks age from quaternary to tertiary. Recent quaternary superficial deposits predominate the area (Mammo 2005; Tsehayu and H.Mariam 1990). Figure 3.1 shows the distribution of different rocks constituting the city's region.

Following the major uplift that occurred in the horn of Africa, an early volcanic event gave Ashangi basalts and initiated opening of the southern red sea from east-west trending extensional fractures. Aiba basalts resulted from the second cycle of the uplift followed by a third volcanic activity which contributed the Oligocene Alaji basalts.

Ashangi basalts, Aiba basalts and Miocene basaltic shield volcanoes (Termaber basalts) are dominant in the northern area of Addis Ababa city. Rhyolites and trachytes (Entoto silicic) and Alaji rhyolites of Miocene origin (pyroclastics) predominate the immediate north and the Entoto hill chains. Outcropping basalts on top of Entoto silicic are the product of the Termaber basalt.

Addis Ababa basalts (Pliocene in age) and Younger Volcanics (Pliocene-Pleistocene) are widespread within the city. The Addis Ababa basalts comprise olivine basalts, feldspar basalts, and aphanitic basalts. The youngest porphyritic olivine basalts cover a large area from Legehar to the foot of Entoto hills. The area from the central part to the westernmost limit of the city (Burayo) is occupied by intermediate age porphyritic feldspar basalts whereas the oldest aphanitic basalts extend from east to west (Yeka to Gulele) and are exposed at the southern parts of the city along the Bole International airport and following the rivers of Akaki and Kebena.

Younger Volcanics cover the entire area south, east and west of the city. These rocks include the Balchi rhyolites and the Bishoftu basalts. The Balchi rhyolites, which include tuffs, ignimbrites, rhyolites, and trachytes, are exposed in the southern and eastern part of the city and beyond. The Bishoftu basalts, on the other hand, are exposed in the southeast direction from the city towards Akaki and Debrezeit (Bishoftu) town.

Ignimbrites, tuffs, and trachybasalts of Addis Ababa volcanic hills are also results of volcanism in the Ethiopian Rift. The hills are mainly trachyte in composition. These

trachytic hills include Wachecha in the south-west, Furi in the southern part and Yerer in the southeastern part of Addis Ababa.

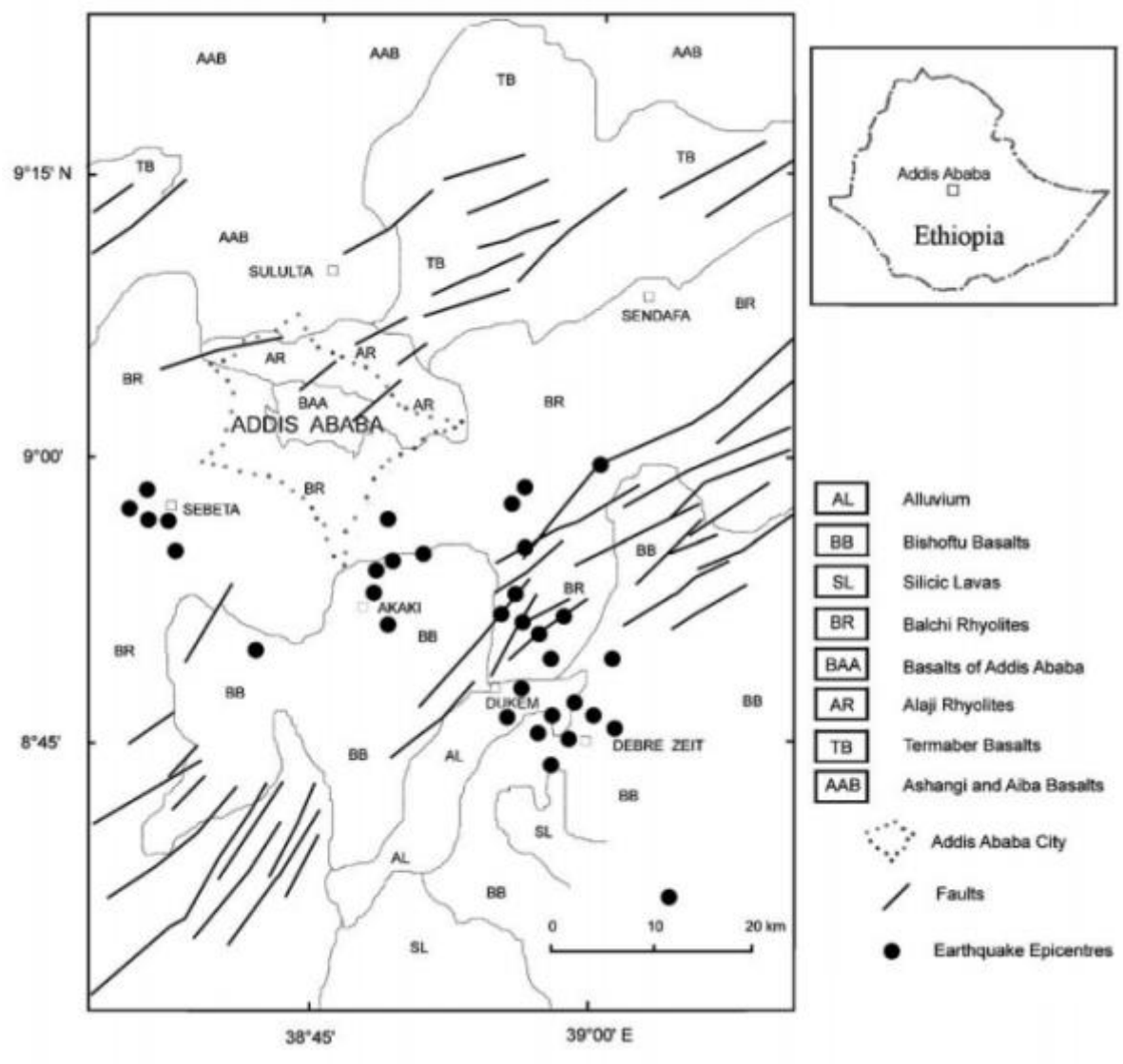

Figure 3.1 The geology, tectonic structures, and seismicity of Addis Ababa area (After Mammo 2005)

3.3 Engineering Geology

3.3.1 Soils

The climatic condition and topography of the city favor development of thick soil profile by decomposition of rocks on which it lies. Engineering geological soils in Addis Ababa are genetically (originally) grouped into alluvial, alluvial fan, residual, colluvial and lacustrine soil units (Tsehayu and H.Mariam 1990).

Alluvial Soils: These are layered deposits transported by streams from higher to lower ground. Places along the Akaki River in the west and south-west of the city and along Kebena river north-west of Bole area are occupied by alluvial deposits.

Alluvial fan deposit: They are sediment deposits along a river having decreasing gradient from a hill or mountain to a plain. These deposits, currently dissected by a deep gully, are mainly found in the Entoto region.

Residual Soils: Residual soils of intermediate to high plasticity developed from the decomposition of rocks are mainly found in central part, Gulele and Kolfe regions of the city.

Lacustrine Soils: These are black cotton soils formed as a result of deposition of initially water covered places by river sediments. Flat and relatively low altitude regions of the city such as Bole, Lideta, and Mekanisa are occupied by soils of lacustrine origin.

Colluvial soils: They are deposits such as talus and debris formed because of downward movement of soils and disintegrated bedrock. Soils at the foot slope of northeastern part of Entoto silicic and other few places are colluvial.

3.3.2 Rocks

Furthermore, the Geological Survey classifies rocks of the region into engineering geological rock units based on rock mass strength evaluated from field observation, field tests and laboratory tests (Tsehayu and H.Mariam 1990).

Rocks with very high mass strength: Includes basalts situated mainly in the central part and outcrops (porphyritic olivine, porphyritic feldspar and aphanitic) in the south-eastern part of the city.

Rocks with high mass strength: This unit consists of trachybasalt, trachyte, rhyolite and more jointed basalts. Young trachyte in south-west and southern part and rhyolite and trachyte of Entoto silicic outcropping in the northeast of the city are rocks with high mass strength.

Rocks with medium mass strength: Includes the widely spread ignimbrite throughout the city (outcropping mainly in southern and eastern part) and some narrowly spaced jointed rocks of rhyolite and trachyte.

Rocks with low mass strength: Tuff and agglomerate and tuff which are available in the north-west, north-east and south-eastern part and all highly weathered jointed rocks have low mass strength. They are highly weathered and changed into soils in places they outcrop.

3.4 Seismicity

3.4.1 Seismicity of the Region

The East African Rift System (EARS) is the main cause of significant seismic hazard in the horn of Africa. The tectonic features of Ethiopia are mainly controlled and influenced by the well-known geological structure called the Main Ethiopian Rift (MER) as part of the EARS. This geological structure divides the country into two along the NE-SW direction (Somalian Plate and Nubian Plate). The capital city of Ethiopia, Addis Ababa, is situated on the margin of the MER system. Hence the geology and structural features within and around the city are also influenced by all processes related to the formation and subsequent growth of this rift system.

Three main seismic source zones with specific tectonic, geologic and seismic characteristics are known to exist in the horn of Africa as shown in Figure 3.2 (Mammo 2005). Most of the earthquakes felt at Addis Ababa originated from the escarpment and the Ethiopian Rift System seismic source zones.

The Afar Depression: This zone represents the area of a triple joint junction where the three rift structures (the Red Sea, Gulf of Aden and the Main Ethiopian Rift System) meet. The depression is recognized by complicated fault systems including extended faults of the Main Ethiopian Rift System. Small to intermediate size earthquakes are expected in this seismic zone. The 1969 Serdo earthquake (magnitude 6.1) which completely destroyed the nearby town Serdo and the 1989 Dobi earthquake (magnitude 6.3) are the two most notable destructive earthquakes occurred in this zone.

The Escarpment: This seismic zone, dominated by almost N-S running faults, is one of the most seismically active zones in the region. The 1961 Kara Kore earthquake and intermediate size earthquakes in 1971 (magnitude of 5.3 and 5.1) originated from this region.

The Main Ethiopian Rift System: This zone is characterized by the NE-SW trending fault system (mainly the rift margins) and Wonji Fault Belt (WFB) which is oblique to the rift margins. Small to intermediate earthquakes generated from this seismic source zone. Prominent earthquakes in 1906, in 1960 (M_s =6.3) and in 1987 (M_s = 6.2) originated from this seismic zone.

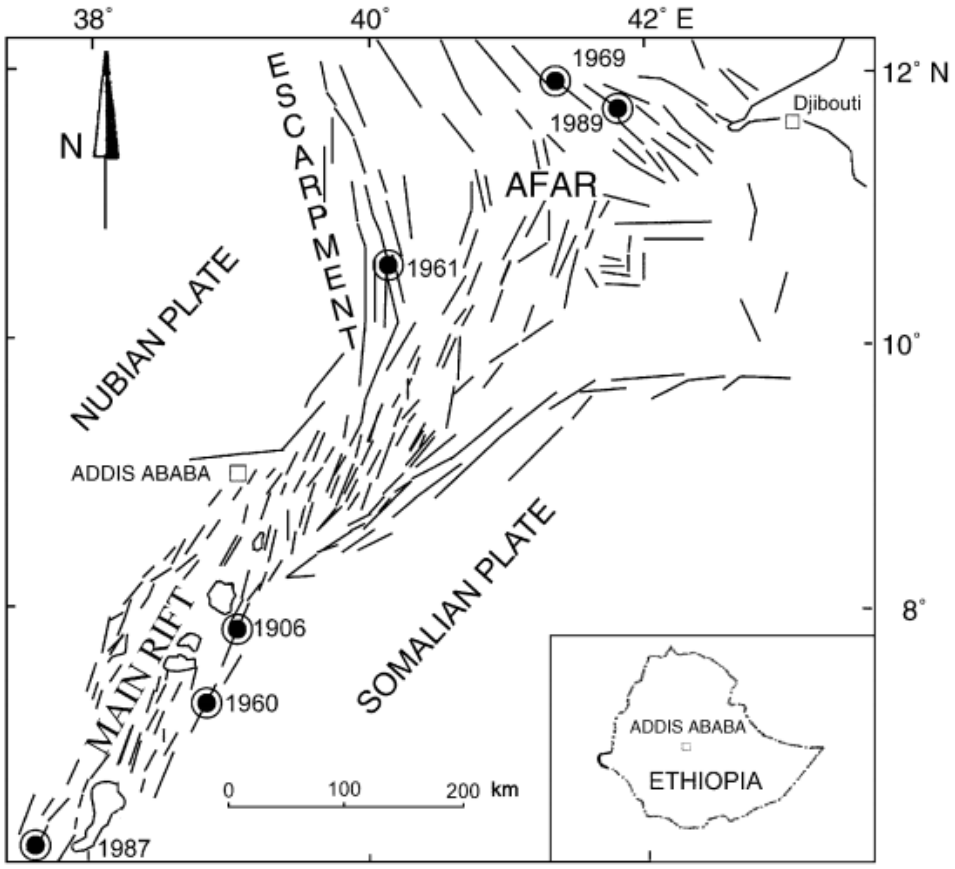

Figure 3.2 Structural pattern of the East African region and epicenters of major earthquakes of magnitude above 6.0. (After Mammo 2005)

3.4.2 Seismicity of the Study Area

Since its establishment, Addis Ababa has experienced a number of earthquakes from adjacent seismic source zones. The 1906 earthquake near Langano (M_s = 6.8) and the 1961 earthquake (M_s = 6.7) near Kara Kore town were with highest intensities to cause widespread panic and damages in the city. The 1906 earthquake at an estimated epicentral distance of 100 km south of Addis Ababa occurred during the infancy stage of the city (low populations, few buildings, and almost no infrastructure). For this reason, no significant damages were registered. However, the 1961 earthquake at about 200 km away from the city resulted in relatively bigger damages such as cracking of masonry

structures and dislocation of partition walls. The intensity was observed to be significant along the Filowoha fault zone of the city (Mammo 2005; Kinde 2002; Kebede and van Eck 1997).

The intensity map (Figure 3.3) prepared following the 1979 earthquake of local magnitude 4.1 (about 22 km south west of the city) also shows that maximum intensities in the city were observed due to topographic and the Filwoha fault effects (Mammo 2005).

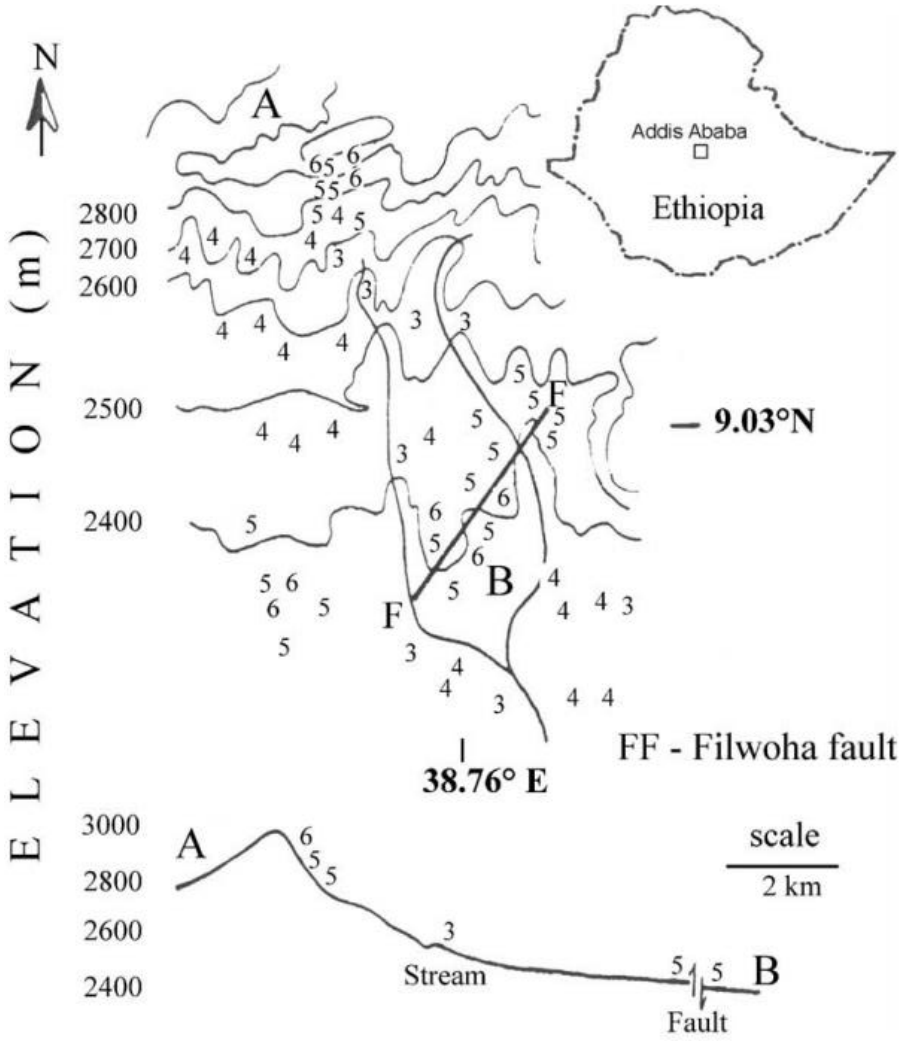

Figure 3.3 Intensities in Modified Mercalli Scale reported in Addis Ababa following the July 1979 earthquake (after Asfaw 1990 as referred by Mammo 2005)

RADIUS (Risk Assessment Tools for Diagnosis of Urban areas against Seismic disasters) project of Addis Ababa was initiated under the demonstration project of International Decade for Natural Disasters Reduction, IDNDR (1900-2000), of United Nations for the mitigation of the effects of major earthquakes in urban areas. According to the report from this project, an earthquake of magnitude 6.5 is anticipated at about 27 km away from the city. A collapse of 15% of buildings, 4000-5000 deaths, 8000-10,000 injuries and displacement of as many as 500,000 people with total damage in property of more than 12 Billion Birr has been estimated related to this earthquake (Kinde 2002).

Mammo (2005) confirms this conclusion by looking into the generic relationship between faults and epicenters of earthquakes from geology, tectonics, and seismicity of the neighborhood of the region (Mammo 2005). Using an empirical relationship between known fault rupture length from the region and an earthquake magnitude, he estimates a maximum possible earthquake of magnitude 6.8.

3.4.3 Seismic Hazard of Addis Ababa City

The design level of ground shaking for which structures and facilities are expected to perform satisfactorily is described in terms of ground motion parameters. Since inertial forces in structural response are directly related to ground accelerations, peak ground acceleration (PGA) is the parameter that is commonly used to characterize ground motion intensity and severity. Most building codes utilize PGA value to describe the ground motion intensity expected at given seismic region. This ground motion parameter is ordinarily expressed using seismic hazard of a region defined as the probability that a certain level of this parameter will be exceeded at a given place and within a given time period.

Reference peak ground acceleration at rock level is an essential parameter to develop input ground motions for the purpose of ground response analyses. Consequently, a number of sources have been consulted so as to extract this single parameter (PGA) that best describes the seismic hazard of the study area.

3.4.3.1 Ethiopian Building Code Standard, EBCS 8, 1995

This earlier version of the country's code was drafted based on the Universal Building Code (UBC). The seismic hazard map in the EBCS 8, 1995 of Ethiopia was developed

for a 100-year return period. According to this map, seismic prone areas of the country are divided into four distinct zones depending on bedrock acceleration ratio (α_o) (Table 3.1; Figure 3.4). Zone 0 represents seismic free areas. Addis Ababa located at 09º 02' N latitude and 38º 43' E longitude goes to zone 2 with peak ground acceleration of 0.05g.

Table 3.1 Bedrock Acceleration Ratio, α_o (EBCS 1995)

Zone	4	3	2	1
α_o	0.10	0.07	0.05	0.03

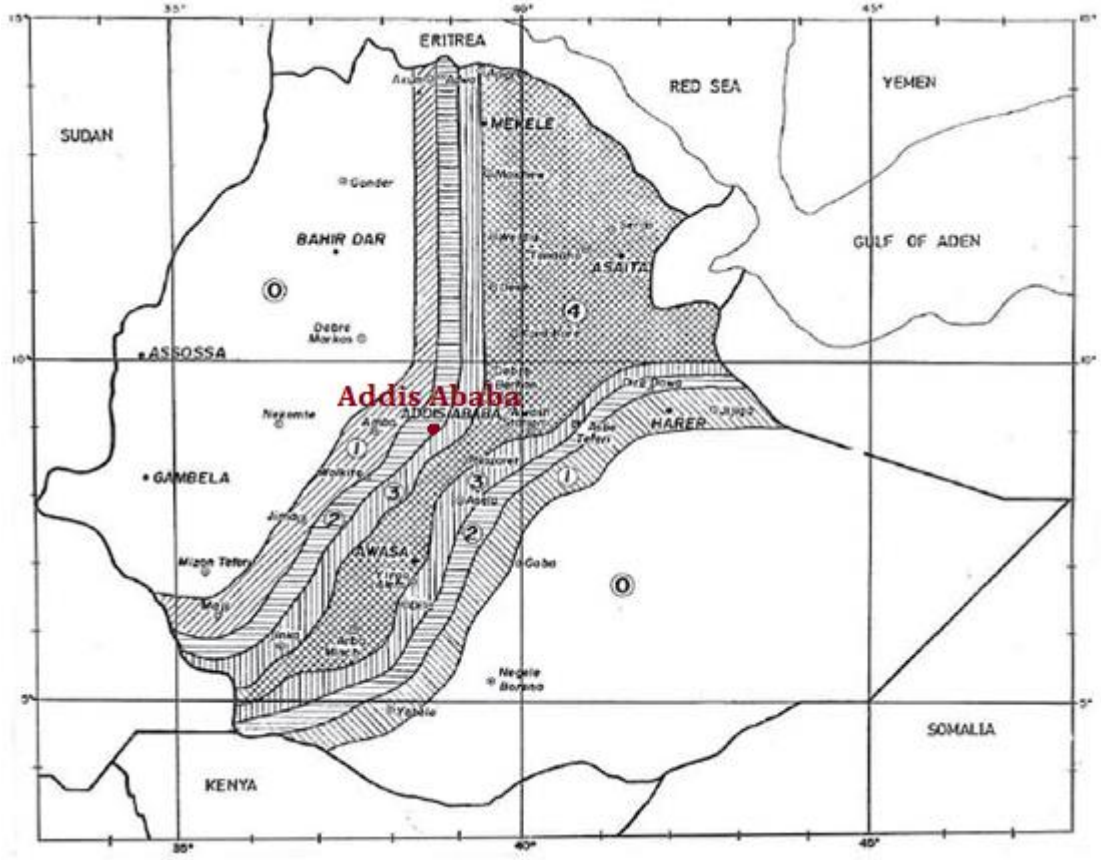

Figure 3.4 Seismic Hazard Map of Ethiopia for 100-year return period as per EBCS 8: 1995 (MWUD 1995)

Other seismic prone African countries have often been referring to this code for their seismic design provisions. In fact, it has been pointed out that the seismic code significantly underestimates seismic designs. This pitfall was mainly attributed to insufficient consideration of site effects and to the irrational acceptance of the 100-year return period. This return period is not the case in almost all seismic codes outside of Ethiopia (Worku 2011, Worku 2014). The code is now obsolete and may not be applicable any further due to the recent issuance of an updated version. This implies that

old structures designed according to this code could be at significant risk and may require reinforcement to prevent serious damage or collapse from future strong ground motions.

3.4.3.2 Ethiopian Building Code Standard, ES EN 1998:2015

This new seismic code was drafted in 2015 based on Euro norms. The code has brought advancement in terms of site effect consideration and in the use of a 475-year return period (exceedance rate of 10% within 50 years). As usual, the seismic hazard of areas is characterized in terms of the ratio of peak ground acceleration at rock level to gravitational acceleration, g (bedrock acceleration ratio). The seismic hazard maps developed are shown in Figure 3.5.

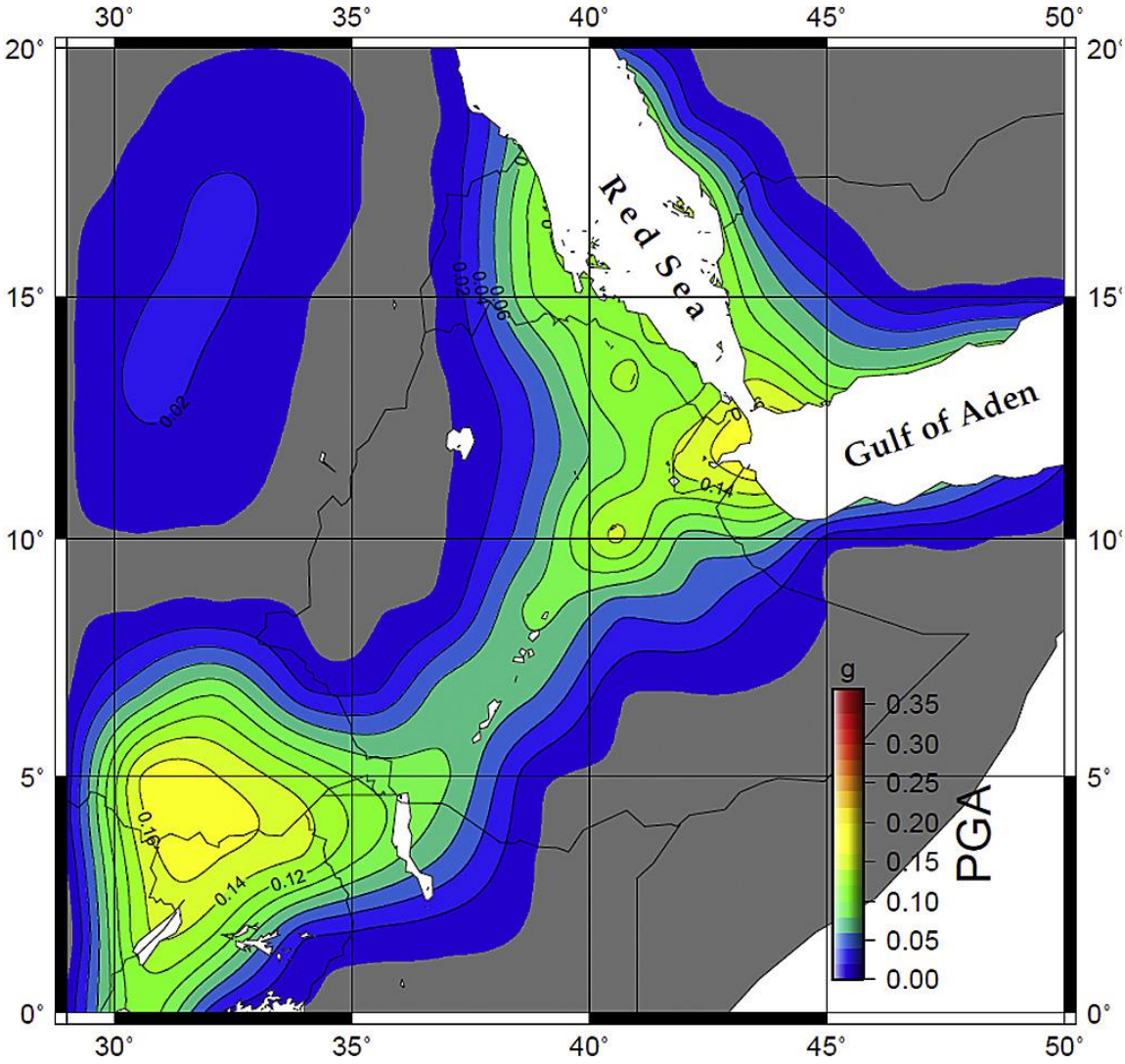

(a)

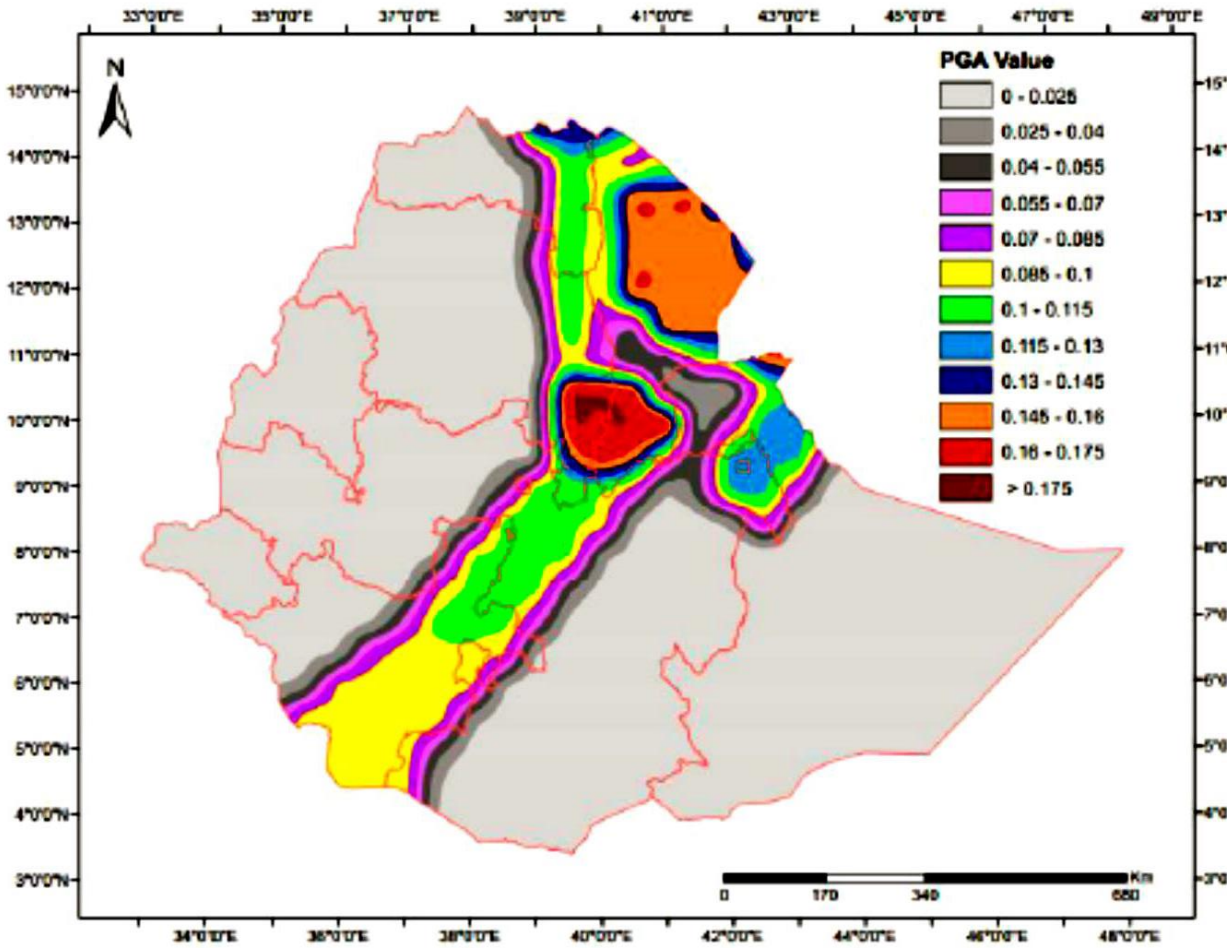

(b)

Figure 3.5 Seismic hazard map: (a) along the Horn of Africa, and (b) of Ethiopia, in terms of PGA (ES EN 1998:2015)

The code groups the country into six distinct seismic zones based on bedrock acceleration ratios as shown in Table 3.2.

Table 3.2: Bedrock Acceleration Ratio α_o (ES EN 1998:2015)

Zone	5	4	3	2	1	0
$a_o = a_g/g$	0.20	0.15	0.10	0.07	0.04	0.00

Tabular listing of seismic hazard zonation for selected towns is also included in the provision. Addis Ababa with an approximate location of latitude 8.9757^o N and longitude 38.7645^o E is assigned in zone 3, PGA of 0.1g. This entails that the seismic hazard of the city has been improved by two-fold from the value provided in the old code provision. In spite of this improvement, there is a significant discrepancy in the values of

PGA obtained from the hazard maps and from the tabular listing of seismic zones. The PGA for Addis Ababa obtained from the map (seismic hazard map along the Horn of Africa) is approximated to 0.08g (closer value from the second map, as well) which is lesser than the value found earlier. This discrepancy is a case not only for Addis Ababa but also for many cities in the listing. Table 3.3 shows dramatic discrepancies in PGA values for selected cities obtained from the tabular listing and the two seismic hazard maps.

Table 3.3 PGA values of selected cities in Ethiopia (ES EN 1998:2015)

City	Longitude	Latitude	PGA Value		
			Tabular Listing	Map (Fig. 3.5a)	Map (Fig. 3.5b)
Adama	39.2682	8.5386	0.15	0.08	0.1-0.115
Hawassa	38.4741	7.0080	0.15	0.08	0.1-0.115
Mekelle	39.5515	13.4056	0.15	0.10	0.1-0.115
Semera	41.1321	11.7297	0.20	0.12	0.145-0.16
Shashemene	38.5881	7.2003	0.10	0.08	0.1-0.115

3.4.3.3 Hazard Estimates from Other Notable Studies

i. Lubkowski et al. (2014)

This study, presented as part of proceedings for the second European Conference on Earthquake Engineering and seismology organized by the Turkish Earthquake Foundation-Earthquake Engineering Committee, investigated the suitability and appropriateness of local codes for countries in the East African region. The study paid special emphasis on the seismic hazard of principal cities in the region. It developed a new attenuation relationship model to estimate the seismic hazard of the region. Revised hazard values were derived by making use of the latest earthquake data and ground motion predictive equations. The methodology used for ground motion prediction equation has also been validated using the Pacific Earthquake Engineering Research Center tests (Lubkowski et al. 2014).

The major output of the probabilistic seismic hazard assessment (PSHA) for different principal cities has been expressed in terms of 5% damped uniform hazard response spectra (UHRS) for a fixed annual probability of exceedance (return period). From this result, the peak ground acceleration (PGA) of Addis Ababa at a rock level was computed to be 0.13g for a return period of 475 years as depicted in Figure 3.6. Examining the seismic hazard and reviewing the local codes, the study concludes that the existing local seismic codes significantly underestimate the seismic hazard of the area, including Addis Ababa.

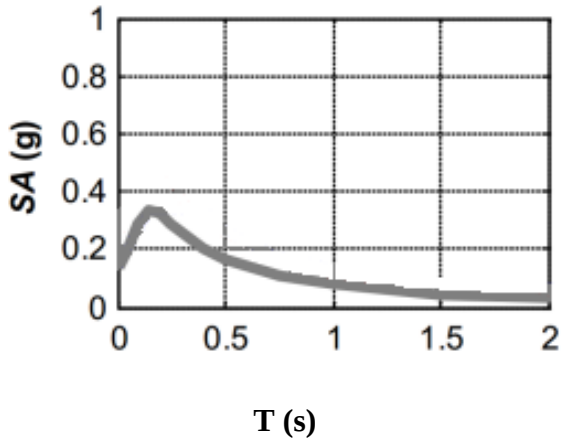

Figure 3.6 Uniform hazard spectra at Addis Ababa city for a return period of 475 years (After Lubkowski et al. 2014)

ii. Poggi et al. (2017)

Poggi et al. (2017) conducted a seismic hazard assessment for the East African Rift System (EARS) by making use of new data and Global Earthquake Model (GEM) computational tools. Most recent information available from scientific literature, global bulletins, and regional earthquake catalogues (including those from African Array projects) have been used to formulate the hazard model of the study.

Based on the distribution of seismicity sources new probabilistic seismic hazard assessment models were developed for regions surrounding the EARS. The seismicity sources were characterized by up to date data such as local earthquake catalogues, faults, and focal mechanisms. Regional strain-rate model developed for the area has also been considered in this study.

The major output of the attenuation relationship is provided in terms of hazard curves, hazard maps and uniform hazard spectra as a ground motion intensity measure. Hazard

curves for a range of spectral periods (including PGA curve) for a probability of exceedance in 50 years were prepared for four selected African capitals: Addis Ababa, Kampala, Nairobi, and Bujumbura. Peak ground acceleration (PGA) for 10% probability of exceedance in 50 years (475 years return period) from the proposed hazard curve is read as 0.11g for Addis Ababa (Figure 3.7).

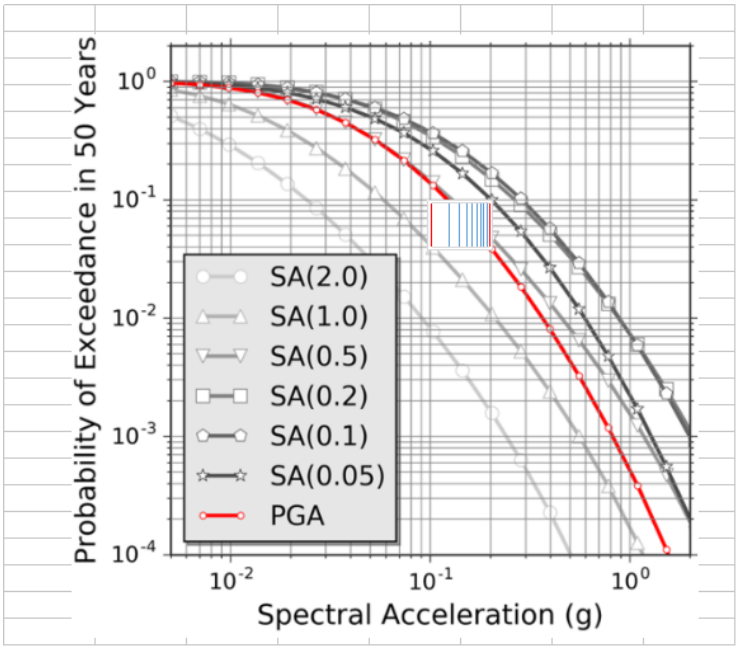

Figure 3.7 Mean hazard curves computed for a range of spectral periods, including PGA (in red) for Addis Ababa (After Poggi et al. 2017)

3.4.3.4 Global Seismic Hazard Assessment Program (GSHAP)

The United Nations designated the period from 1990-2000 as International Decade for Natural Disaster Reduction (UN/IDNDR) to increase worldwide awareness, foster the prevention and reduce the risks of natural disasters through the widespread application of modern science and technology. As part of UN/IDNDR, global seismic hazard assessment program (GSHAP) was established as a decade demonstration project by the International Lithosphere Program (ILP) with the support of the International Council of Scientific Unions (ICSU).

GSHAP worked in coordination with International Union of Geophysics and Geodesy (IUGG), International Union of Geological Sciences (IUGS), international hazards projects of various regions, and national seismological agencies and institutes. The link with geological and geophysical fields ensures suited integration of seismology for a better assessment of seismic hazards. It was endorsed by the International Association of

Seismology and Physics of the Earth's Interior (IASPEI) as one of the main contributions of the seismological-geological community to the decade (Giardini and Basham 1993).

The GSHAP promoted regionally coordinated, homogeneous approach to seismic hazard evaluation in order to mitigate the risk associated with the recurrence of an earthquake. It made its principal target on developing countries located in active earthquake belts allied with the existing hazard projects with similar purposes and methodologies. Seismic hazard assessment has been computed in a regionally coordinated fashion and with the most advanced methods of the time. Nine regional centers were established for the implementation of the seismic hazard assessment. The assessment for the African Rift area was performed under the group so-called "Eastern and Southern Africa Regional Seismological Working Group". Seismic hazard map, including site-specific hazard estimates for the capital cities along the rift, was made available. RADIUS project of Addis Ababa was part of this program (Mammo 2005).

This world-wide accepted program furnished a global seismic hazard map in terms of PGA values for 10% probability of exceedance in 50 years (return period of 475 years) as a major output. The data are available freely on the GSHAP homepage. Hence, using appropriate data, a user can easily extract hazard map of a desired region. The seismic hazard map extracted from this source for the region containing Ethiopia is depicted in Figure 3.8. Addis Ababa is characterized by a PGA of 0.11g.

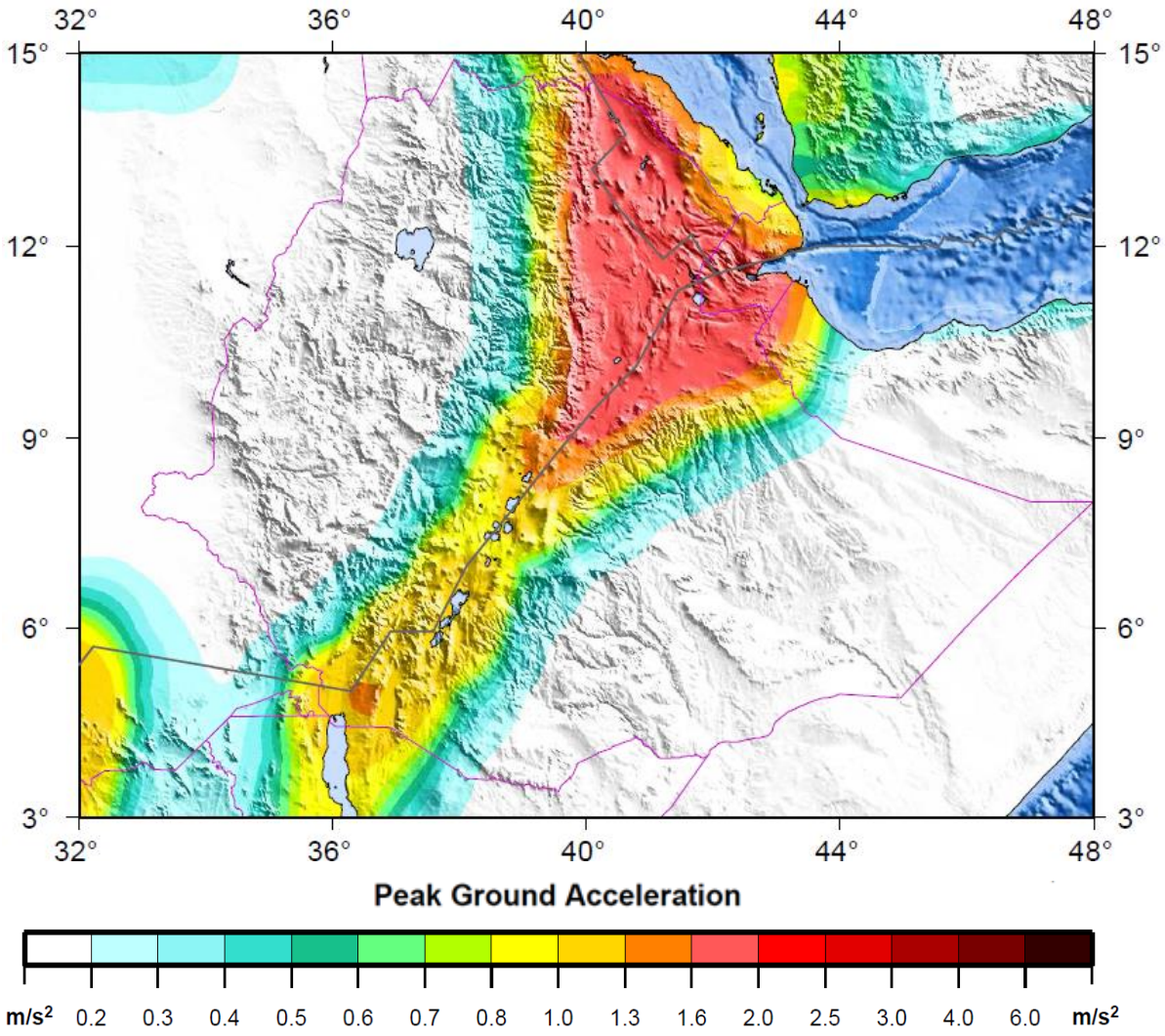

Figure 3.8 Seismic hazard map of Ethiopia based on the GSHAP data for a return period of 475 years

In conclusion, excepting the obsolete EBCS 8, 1995 code provision, PGA values for Addis Ababa city from different sources mentioned above are summarized in Table 3.4. In addition to the irrational discrepancy of PGA values for a specific site, the new code provision appears to underestimate the seismic hazard of Addis Ababa city and the whole country in general. Accordingly, PGA value from the widely accepted seismic hazard assessment program, GSHAP, has been adopted for the purpose of this study.

Table 3.4 PGA value of Addis Ababa obtained from different sources

Source	ES EN 1998:215		GSHAP	Lubkowski et al. (2014)	Poggi et al. (2017)
	Table	Map			
PGA (g)	0.10	0.08	0.11	0.13	0.11

CHAPTER FOUR

INPUT GROUND MOTIONS

4.1 Introduction

Ground response analyses involve the specification of acceleration time-histories as an input. This necessitates that the analyst identifies suites of ground motions that match the desired ground motion parameters at the site of interest. An increased ground motion instrumentation and the natural occurrence of earthquakes over time provide the access to thousands of recorded earthquake ground motions that have occurred around the world. These records include a wide range of earthquake magnitudes, source-to-site distances, types of faulting, and site conditions. While locations such as California and Japan are known for their numerous recorded ground motions, many regions of the world have scarce records.

In the absence of representative ground motions, however, studies encourage the use of motions recorded at other sites under similar conditions as that of the site of interest (Kramer 1996). The similarity of the site of interest and those sites where actual strong ground motions have previously been recorded is principally described by the local and regional geologic and tectonic conditions. Factors such as the magnitude of an earthquake, the distance of the site from the causative fault, fault mechanism, geology of the travel path of seismic waves from the source to the site and the local soil conditions at the site are among the parameters that should be considered in the process of selecting a suite of motions (Stewart et al. 2014; Kramer 1996).

The East African Rift is one of the well-known seismic regions in the world that is hampered by insufficient records of strong ground motions. Because of this, there are no attenuation relationships proposed for the region directly based on strong motion data recorded in the region. In his study of probabilistic seismic hazard analysis for Ethiopia and the neighboring region, Atalay (2017) mentions that attenuation models can be extended and adopted as they suit the region of interest. He used ground motion prediction equations from the Next Generation Attenuation (NGA) for the hazard assessment study in Ethiopia based on the argument that Western United States and the East African Rift System are characterized by shallow crustal earthquakes.

Kebede and van Eck (1997) have also adopted strong ground motion attenuation relation of the Western USA in their study of seismic hazard assessment for the Horn of Africa indicating the following points:

1. both California and the Horn of Africa have substantial parts of their surface areas as plate boundaries running all along their lengths; and
2. the hypo-central depths of earthquakes are in both regions constrained to the crust.

As a result of the aforementioned points, this study was drawn to take input ground motions recorded elsewhere from available ground motion database. The Pacific Earthquake Engineering Research (PEER) database is well-developed ground motion database in existence which has collected, processed and archived ground motion data for more than 20 years to date (Kramer et al. 2012). This well-designed and implemented online utility is freely available to the users. For the purpose of this study, a number of suited ground motions on the basis of filtering conditions were picked out. Additional historical earthquake ground motions which are largely used in the engineering practice were also acquired. Details of acquisition process of these input motions are discussed in the subsequent sections.

4.2 Input Motions from PEER Ground Motion Database

The PEER ground motion database contains most motions from shallow crustal earthquakes in active tectonic regimes to the contrary of subduction zone earthquakes which emanate from greater depths with a considerably greater magnitude and longer duration (Kramer et al. 2012). This makes the motions selected from this database more befitting for the study area because of the fact that the East African Rift System regime is dominated by shallow crustal earthquakes.

The database is an interactive web-based application that allows the user to select sets of strong ground motion time series that are representative of design ground motions. The user is expected to specify the ground motions in terms of a target response spectrum and desired characteristics of the motions such as earthquake magnitude, source to site distance and other general characteristics. The database tool then selects motions that satisfy the user-specified selecting criteria. The following filtering parameters were applied to select appropriate records from the database.

4.2.1 User Defined Target Response Spectrum

Target spectrum for the study site condition is among the critical issues associated with the selection of input motion time series for use in ground response analysis (GRA). Target spectrum represents the response spectrum of ground shaking for the reference site condition. The term "reference site condition" here describes the site condition below the geotechnical layers being considered in GRA (Stewart et al. 2014).

The ES EN 1998:2015 provides two different types of response spectra. Type 2 response spectra are used when the earthquakes that contribute most to the probabilistic seismic hazard assessment for the site have surface wave magnitude, M_s, not greater than 5.5. In spite of the provision of two different response spectra, the Main Ethiopian Rift System is generally characterized by intermediate size (5.5 to 6.5, surface magnitude) earthquakes (Kebede and van Eck 1997; Kebede and Asfaw 1996). Accordingly, Type 1 response spectrum was applied as worthy of the ground motion selection process for the purpose of this study.

Peak ground acceleration of 0.11g for a return period of 475 years which is obtained under section 3.4.3 is used to develop the user-defined response spectrum. Presuming that the reference site condition matches with the site condition described by ground Type A of ES EN 1998:2015, the target spectrum was developed for ground Type A (rock material).

In accordance with the ES EN 1998:2015, the elastic response spectrum S_e (T) (5% damping) for the horizontal components of the seismic action is defined by the following expressions:

$$0 \le T \le T_B : S_e(T) = a_g.S.\left[1 + \frac{T}{T_B}.(\eta.2.5 - 1)\right]$$

$$T_B \le T \le T_C : S_e(T) = a_g.S.\eta.2.5 \quad (4.1)$$

$$T_C \le T \le T_D : S_e(T) = a_g.S.\eta.2.5\left[\frac{T_C}{T}\right]$$

$$T_D \le T \le 4s : S_e(T) = a_g.S.\eta.\left[\frac{T_C T_D}{T^2}\right]$$

Where:

$S_e(T)$ is the elastic response spectrum;

T is the vibration period of a linear single-degree-of-freedom system;

a_g is the design ground acceleration on type A ground;

T_B is the lower limit of the period of the constant spectral acceleration branch;

T_C is the upper limit of the period of the constant spectral acceleration branch;

T_D is the value defining the beginning of the constant displacement response range of the spectrum;

S is the soil factor and

η is the damping correction factor with a reference value of $\eta = 1$ for 5% viscous damping

Parameters used to describe the response spectrum are shown in Table 4.1 and the response spectrum is depicted in Figure 4.1.

Table 4.1 Values of the parameters describing the recommended Type 1 elastic response spectrum (ES EN998:2015)

Type 1 elastic response spectrum	Ground Type	S	T_B	T_C	T_D
	A	1	0.15	0.4	2

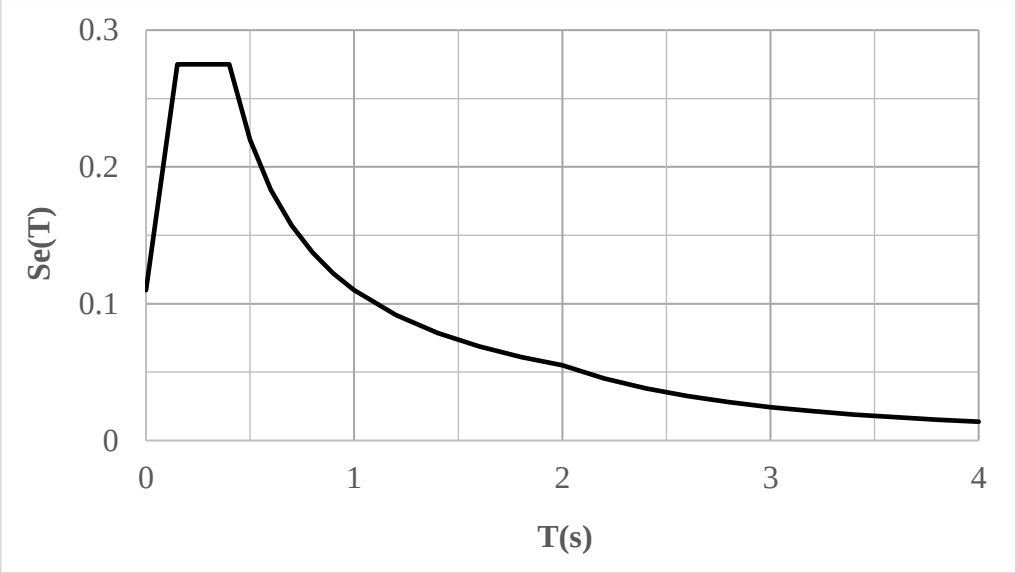

Figure 4.1 Recommended Type 1 elastic response spectrum for ground type A (ES EN 1998:2015)

4.2.2 Range of Moment Magnitude

Magnitude range is another important consideration when selecting input ground motions for GRA. Kebede and van Eck (1997) made a brief review of several seismicity studies for the Horn of Africa. These different studies suggest that eight seismic source zones were distinguished as main contributors of damaging earthquakes in the region. Among these source zones, zone 2 makes up the southernmost rifts of Ethiopia and the main Ethiopian Rift (MER) system. Addis Ababa is bounded in the MER system which comprises the Wonji Fault Belt. According to this study, the seismic source zone is characterized by lower bound magnitude M_o of 4.0 and upper bound magnitude M_{max} of 7.0. This magnitude range has been directly applied as ground motion filtering criteria from PEER database system.

4.2.3 Source to Site Distances

Rupture distance, $R_{rup,}$ being defined as the closest distance from a site to the rupture plane and Joyner-Boore distance, $R_{JB,}$ determined as the closest distance from a site to the vertical projection of a fault plane on the Earth's surface (Figure 4.2), are among the required input parameters in the filtering process. Despite the presence of different ways of interpreting the distance between the site of interest and the source of an earthquake (fault rupture), PEER ground motion database needs the definition of these two distance measures.

Significant earthquakes felt at Addis Ababa during the last century which are listed in Table 4.2 as compiled by Mammo (2005), have been used to define a reasonably rough source to site distances. This list of earthquakes is indeed without the description of the depth of the source from the surface. Furthermore, there is no clearly articulated information regarding the type of fault and fault geometry. However, shallow crustal earthquakes in the Ethiopian Rift System can be characterized by a conservative average depth of 10 km (Atalay 2017). From computed distances summarized in Table 4.2, the closest distance to the rupture plane is found to vary from 18.6 km to 266 km and that of Joyner-Boore distance from 15.7 km to 265.8 km.

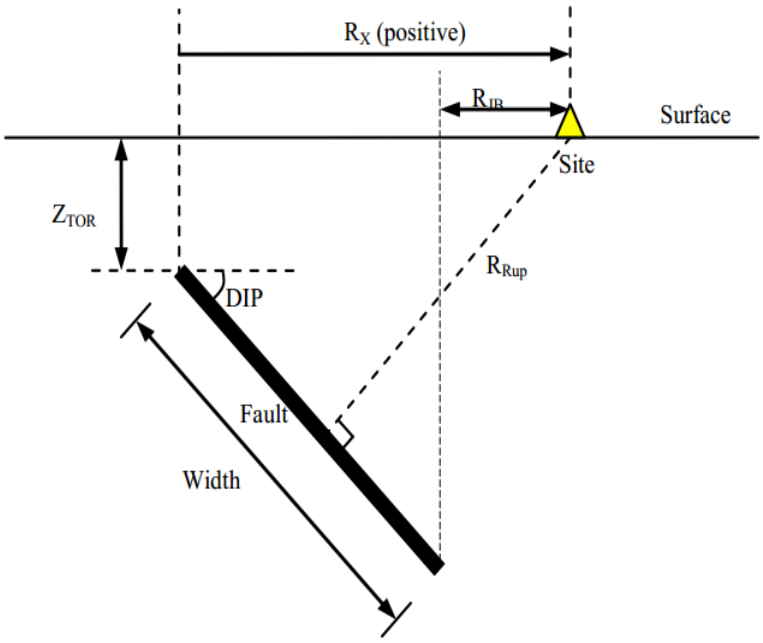

(a)

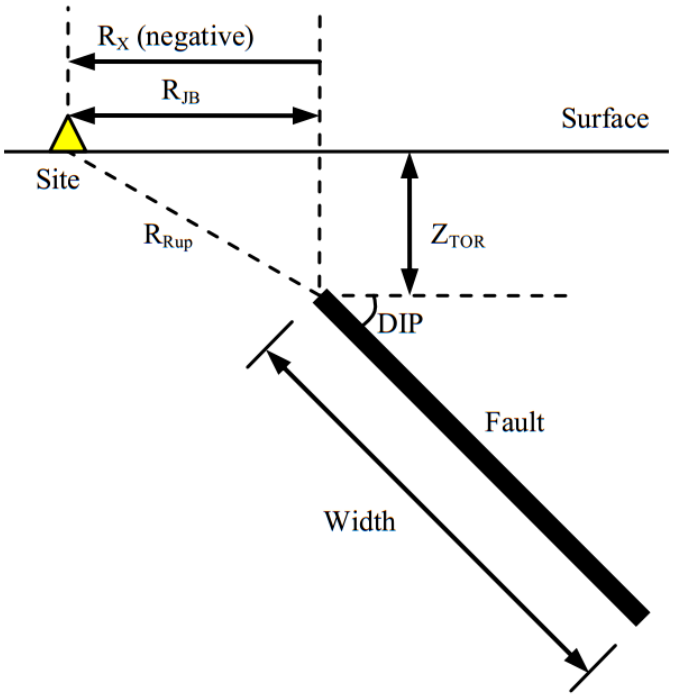

* Z_{TOR} is depth to top of rupture plane

(b)

Figure 4.2 Definition of Fault Geometry and Distance Measures (PEER database): (a) Reverse and normal faulting, hanging-wall site; (b) Reverse and normal faulting, foot-wall site

Table 4.2 Earthquakes felt at Addis Ababa during the last century (Mammo 2005)

Year	Month	Day	Time	Latitude (ºN)	Longitude (ºE)	Magnitude	Intensity (M.M*)	R_{JB} (km)	R_{rup} (km)
1906	08	25	11:55	7.70	38.80	6.6	7	141.7	142.0
1906	08	25	13:47	7.70	38.80	6.8	8	141.7	142.0
1961	06	01	23:29:18	10.54	39.89	6.7	7	213.9	214.1
1961	08	25	21:43:49	10.65	40.10	4.5	4	237.7	237.9
1968	01	23	19:18:13	8.71	37.66	5.1	4	126.1	126.5
1973	03	08	AM	9.00	39.00	4.1	4	26.3	28.1
1974	02	25	16:05:40	9.90	39.70	4.5	3	146.0	146.3
1977	07	08	06:23:02	10.94	39.63	5.0	5	238.3	238.5
1979	07	28	19:22:16	8.85	38.70	4.1	6	15.7	18.6
1984	04	10	08:17:26	11.37	38.71	5.2	4	265.8	266.0
1985	10	28	12:08:45	9.47	39.61	4.8	5	108.7	109.2
1993	02	13	02:25:50	8.33	39.31	5.0	---	93.8	94.4

*M.M = Modified Mercalli Scale; AM=morning

4.2.4 Duration of Ground Motion

Duration of strong earthquake ground motion significantly affects the damage to be incurred by structures in comparison to other ground motion parameters. Long duration motions (even if they are low amplitude motions) produce enough load reversals to cause damage and conversely, short duration motions (even if they are high amplitude motions) may not produce enough load reversals to damage a structure (Villaverde 2009). Hence, specification of duration of strong ground motion is a crucial measure step in order to select suited motions.

The entire time interval of ground motions recorded by accelerographs is not of interest for engineering purposes. Different definitions have been proposed regarding the portion of strong motion interval during which substantial response of structures develops. These definitions are generally grouped into three generic categories: bracketed, uniform, and significant (Boomer et al. 2009). For engineering purposes, bracketed duration based on relative acceleration levels is most commonly used (Kramer 1996).

Significant duration, demanded by PEER ground motion database, is defined by Trifunac and Brady (Villaverde 2009) as the time interval between the points at which the integral of the acceleration square is equal to 5 to 95% of the total value. Bommer et al. (2009) made a brief review of previous works and have developed a new empirical predictive equation for the significant duration (Figure 4.3) using records of NGA database. This equation is used to estimate the duration of shallow crustal earthquakes of magnitude between M_w 4.8 and 7.9 at distances up to 100 km from the source. Using maximum magnitude M_w 7.0 of a shallow crustal earthquake from the seismic region under consideration, the significant duration can be approximated to 20 seconds.

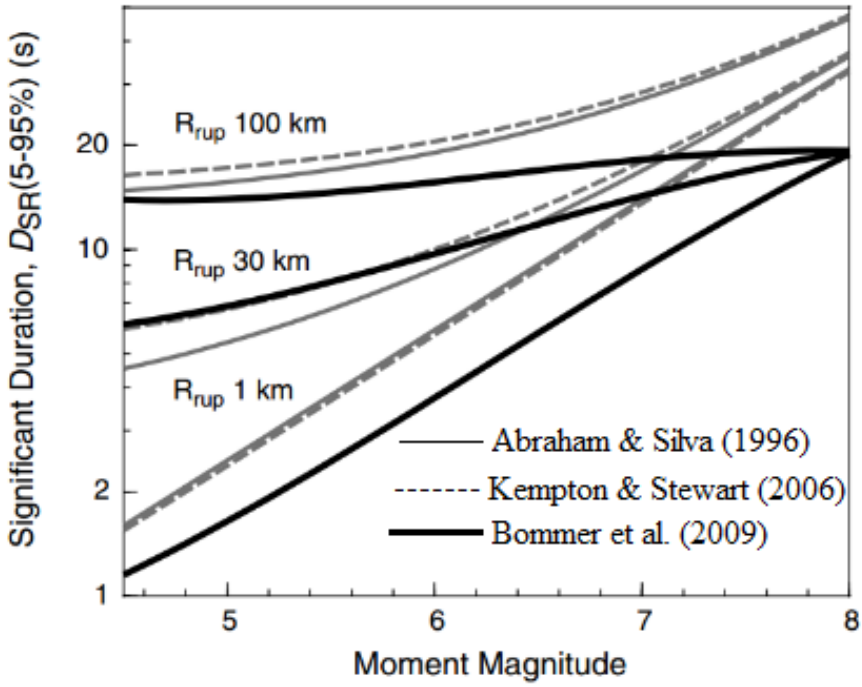

Figure 4.3 Comparison of empirical predictive models for significant duration (Bommer et al. 2009)

4.2.5 Style of Faulting

The fault type characterizing the region of interest is another input parameter in the filtering process. According to Kebede and van Eck (1997), surface geology studies indicate that the Main Ethiopian Rift is dominated by normal faulting. Most of the faults in Addis Ababa region are mainly located in the SE part of the city and have a structure trending in NE-SE directions. These faults are also principally normal faults (Getahun 2007).

4.2.6 Average shear wave velocity of top 30 meters of the site

The average shear wave velocity of top 30 meters of the site of interest (which is expected to have coincident velocity with the site on which recordings of earthquake ground motions took place) is again another crucial filtering criterion. This shear wave velocity should be the velocity corresponding to the reference site condition which is the site condition below the site profiles being analyzed in GRA. The reference site condition is the site class that has been used to develop the user-defined target response spectrum. Therefore, shear wave velocity range of a rock or other rock-like geological formation (ground type A of ES EN 1998:2015) was applied for filtering process. In

doing so, the site effects on ground motions are presumed to be removed since the ground motions to be selected are those recorded on rock sites (Finn et al. 1995).

4.2.7 Ground Motion Time Series Scaling

The characteristics of actual recorded ground motions are required to match with the target ground motion parameters. Then the concept of scaling comes with an objective of coinciding the records with target spectrum in terms of amplitude and frequency content. This is accomplished without changing the shape of the response spectrum.

For this purpose, recommended scaling factor (defined as the ratio of target amplitude to the amplitude of the record to be scaled) is applied to strong ground motions in selecting process. Scaling factor is commonly limited from 0.25 to 4.0 and should be kept as close to 1 as possible (Kramer 1996). This range is also recommended during motion selection for ground response analysis (Stewart et al. 2014). Hence, a sensible scale factor range 0.5-2.0 has been applied to this process of motion selection.

The scale factors are selected to achieve best agreement between the average square root of the square of sums (SRSS) spectrum and the target spectrum over a period range. Two options are provided for scaling the records to match the target response spectrum (Figure 4.4).

i. Scaling the record to match the target spectrum over a period range

Ground motions are selected and scaled in such way that the record is scaled by a factor that minimizes the mean squared error between the spectrum of the scaled record and the target spectrum over a defined period range. This approach provides a more formal match of the recording suite to the target spectrum.

ii. Scaling the records to match the target spectrum to a single period

In this approach, the records are scaled to match the target spectrum at a specific spectral period, T but do not enforce matching elsewhere.

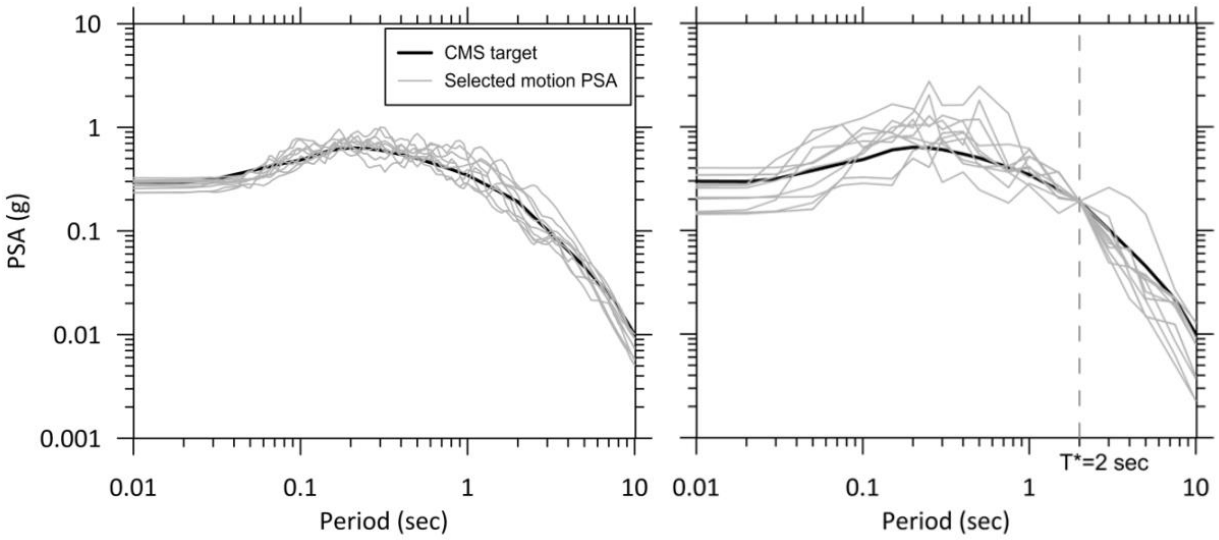

(a) (b)

Figure 4.4 Conditional Mean Spectrum (CMS)-based target spectrum and PSA for 11 selected and scaled motions: (a) Approach 1, using a range of periods (0.01-10 sec); (b) Approach 2, using a single matching period at 2.0 sec (After Stewart et al. 2014)

Strict procedures and requirements regarding the period over which scaled motions must approximately match the target spectrum are followed if the motions are to be used for direct performance evaluation of structures (Haselton et al. 2014). For the application of ground response analysis, however, it is different in that the input motions are being used to estimate ground surface motions. On this account, it is not strictly necessary for input motions to match the target spectrum. But it allows some desirable variability in the input ground motions (Stewart et al. 2014).

For ground response applications, a period range based on the period of the structural system is generally recommended. For instance, in building codes, the period range is taken from 0.2T-2.0T, where T is the elastic first mode period of a structure (Stewart et al. 2014).

In accordance with ES EN 1998:2015, the fundamental periods of vibration T_1 of buildings whose response is not significantly affected by higher modes of vibration is given by the following expression.

$$T_1 \leq \begin{cases} 4.T_c \\ 2.0s \end{cases} \quad (4.2)$$

Where; T_c is the upper limit of the period of the constant spectral acceleration branch (equals 0.4 seconds for Type 1 response spectrum of ground type A).

From this, the fundamental period for Type 1 response spectrum can be estimated to be 1.6 s. Accordingly, a period range of 0.32 - 3.2 is obtained and the range is directly used to filter recorded ground motions. Finally, a weighting function that allows the matching algorithm to consider matching at some periods to be more important than others has also been assigned.

Applying these filtering criteria all the way to the end, ground motions were downloaded from PEER ground motion database. The database gives unscaled, processed and as-recorded (unrotated) displacement, velocity and acceleration time history files as an output. But only one horizontal component of acceleration time history was selected based on recommendations. It is also urged to limit the number of motions from a single event to three or four (Stewart et al. 2014). As per this recommendation, only one ground motion was taken from the five suited motions obtained from Loma Prieta event in order to avoid the undue influence from a single event. The earthquakes of San Fernando, Loma Prieta and Northridge are important recorded strong ground shaking events in California (Chopra 2007).

Finally, the four out of eight ground motions selected from the database are listed in Table 4.3. These motions scaled to Addis Ababa's PGA of 0.11g are depicted in Figure 4.5.

Table 4.3 Ground motions selected from PEER ground motion database

SN	D5-95 (s)	Event	Year	Station	Magnitude	R_{JB} (km)	R_{rup} (km)	V_{S30} (m/s)
80	14.1	San Fernando	1971	Pasadena-Old Seismo Lab	6.61	21.5	21.5	969.07
804	12.1	Loma Prieta	1989	So. San Francisco, Sierra Pt.	6.93	63.03	63.15	1020.62
1091	8.3	Northridge-01	1994	Vasquez Rocks Park	6.69	23.1	23.64	996.43
8167	16.9	San Simeon, CA	2003	Diablo Canyon Power Plant	6.52	37.92	37.97	1100

* RSN is Record Sequence Number

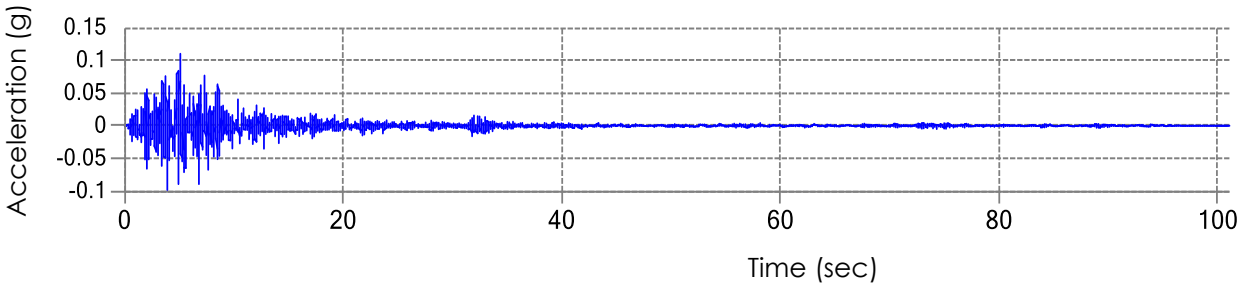

(a)

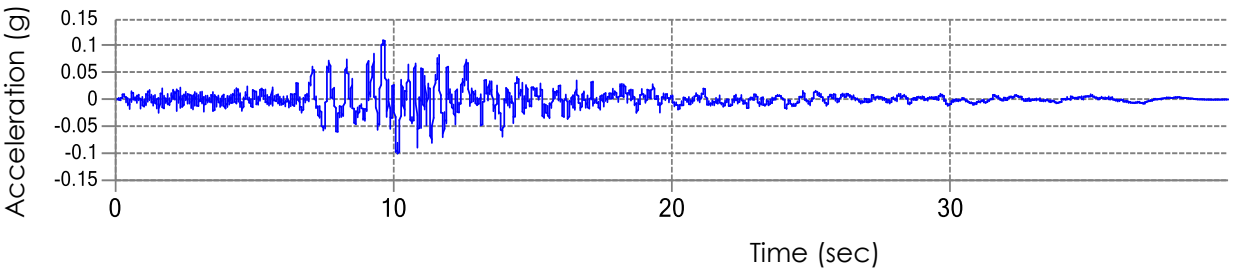

(b)

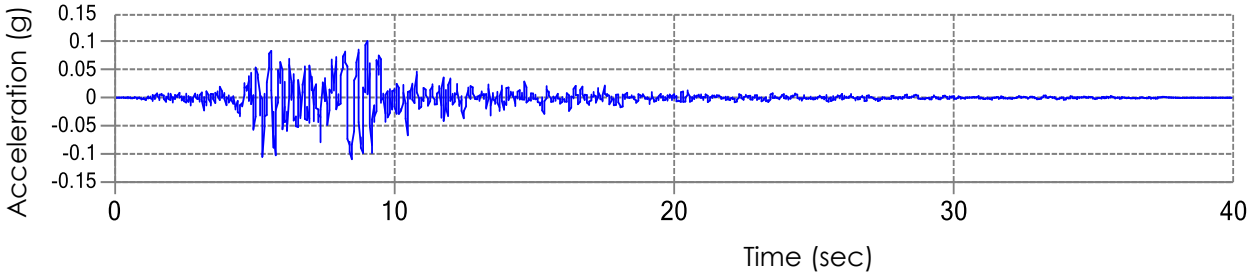

(c)

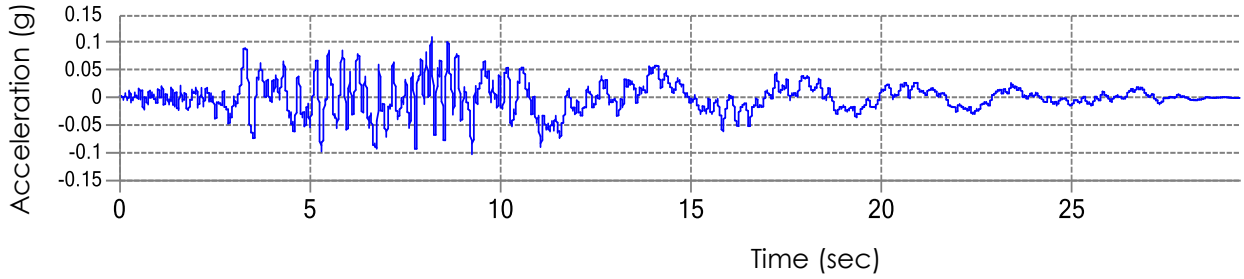

(d)

Figure 4.5 Ground motions selected from PEER database and scaled to 0.11g: (a) the 1971 San Fernando earthquake; (b) the 1989 Loma Prieta earthquake; (c) the 1994 Northridge-01 earthquake; (d) the 2003 San Simeon, CA earthquake

4.3 Historical Earthquake Motions

In addition to the selected motions from PEER ground motion database by means of the aforesaid selecting criteria, historical earthquake motions that have been frequently used in earthquake resistant design in the world were also employed for this study. The reason why these motions are commonly used in practice is that they are representatives of large earthquake records with unique characteristics concerning strong ground motion parameters; amplitude, frequency content and duration (Yoshida 2015).

The ground motions observed at recording sites are usually deconvolved back by using the soil profile through which they passed, to determine the time histories of bedrock motions so that they can be used as input motions at other sites of interest. This usage is based on the assumption that the incident waves are unique regardless of the subsurface conditions (site effects). The deconvolved horizontal ground acceleration time histories of four representative ground motions used for this study are depicted in Figures 4.6 through 4.9. Wider variability of characteristics is observed in these input motions (Haile 1996; Yoshida 2015).

- El Centro record during the 1940 Imperial Valley earthquake of magnitude M=6.7 (7.1, according to Yoshida 2015) and significant duration 24.4 s with a maximum acceleration more than 3 m/s^2. Different versions of this record exist because of differences in the method of digitization of the original analogue trace acceleration and the procedure chosen to introduce the missing baseline in the record (Chopra 2007; Yoshida 2015).

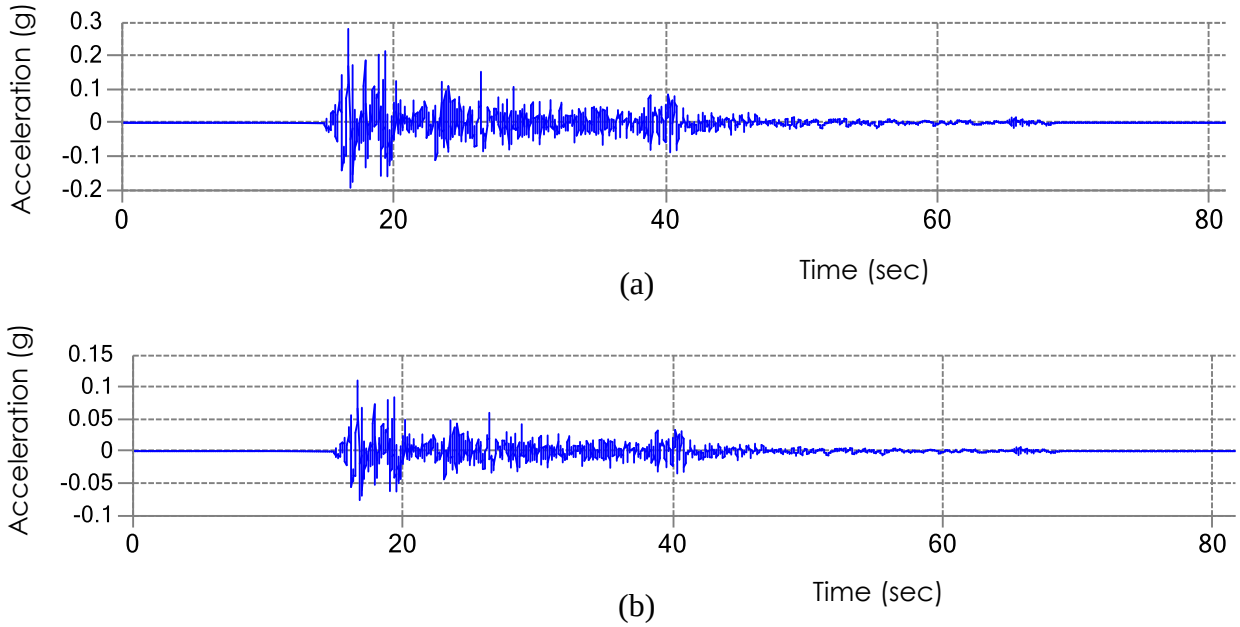

Figure 4.6 Imperial Valley earthquake, 1940 El Centro record: (a) Deconvolved (Haile 1996); (b) Scaled to PGA of 0.11g

- Taft record during the 1952 Kern County earthquake of magnitude 7.7 and significant duration 28.7 s.

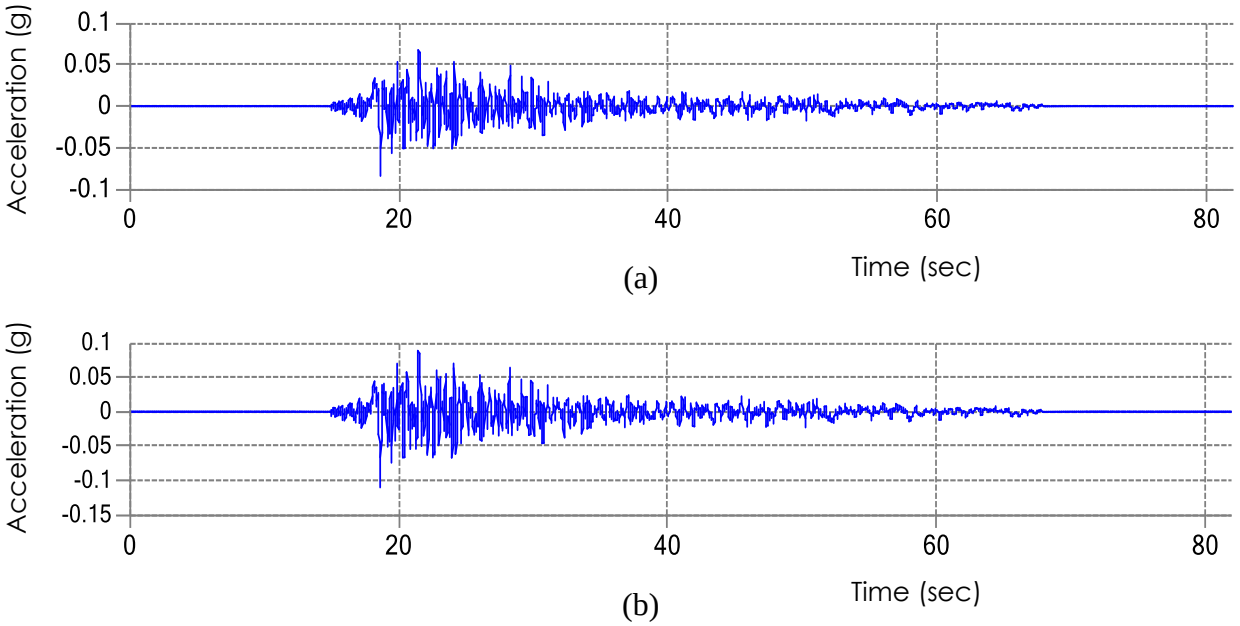

Figure 4.7 Kern County earthquake, 1952 Taft record: (a) Deconvolved (Haile 1996); (b) Scaled to PGA of 0.11g

- Hachinohe record during the 1968 Tokachi-Oki earthquake of magnitude M = 7.9 and significant duration 23.9 s. This record contains long period component significantly, which is the reason why it is commonly used in practical designs (Yoshida 2015).

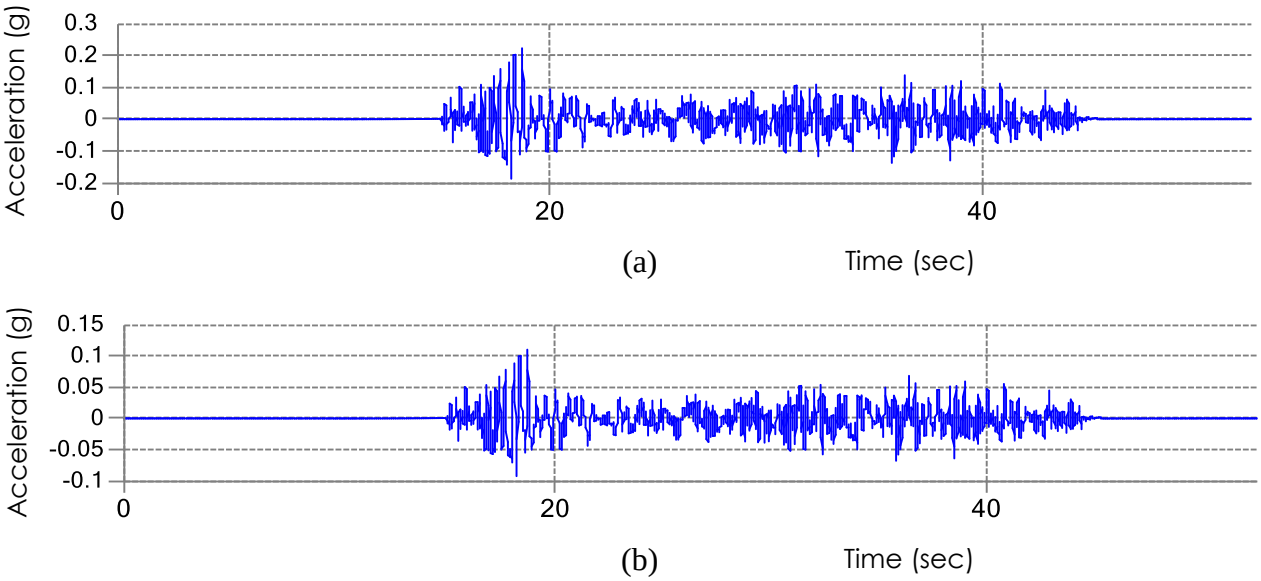

Figure 4.8 Tokachi-Oki earthquake, 1968 Hachinohe record: (a) Deconvolved (Haile 1996); (b) Scaled to PGA of 0.11g

- Kobe record during the 1995 Hyogoken-Nambu earthquake of magnitude M =7.2 and significant duration 8.9 s.

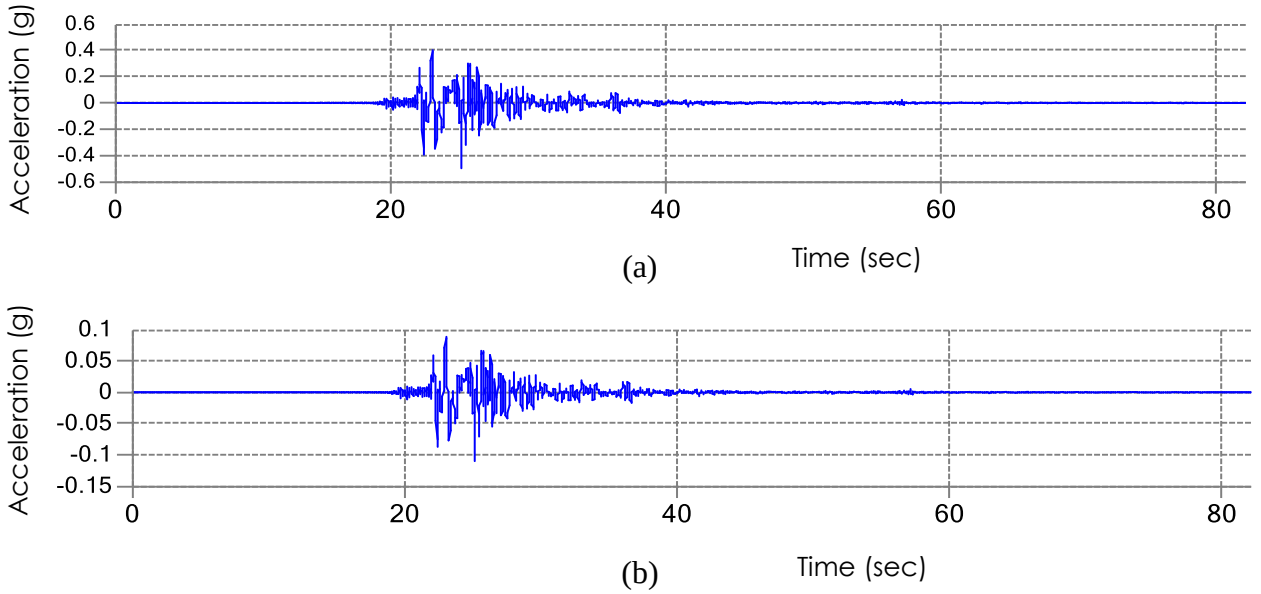

Figure 4.9 Hyogoken-Nambu earthquake, 1995 Kobe record: (a) Deconvolved (Haile 1996); (b) Scaled to PGA of 0.11g

The smoothed Fourier Amplitude spectra (quantitative representation of amplitude distribution among different frequencies) of the total eight input motions selected for the response analyses of this study are presented in Figure 4.10.

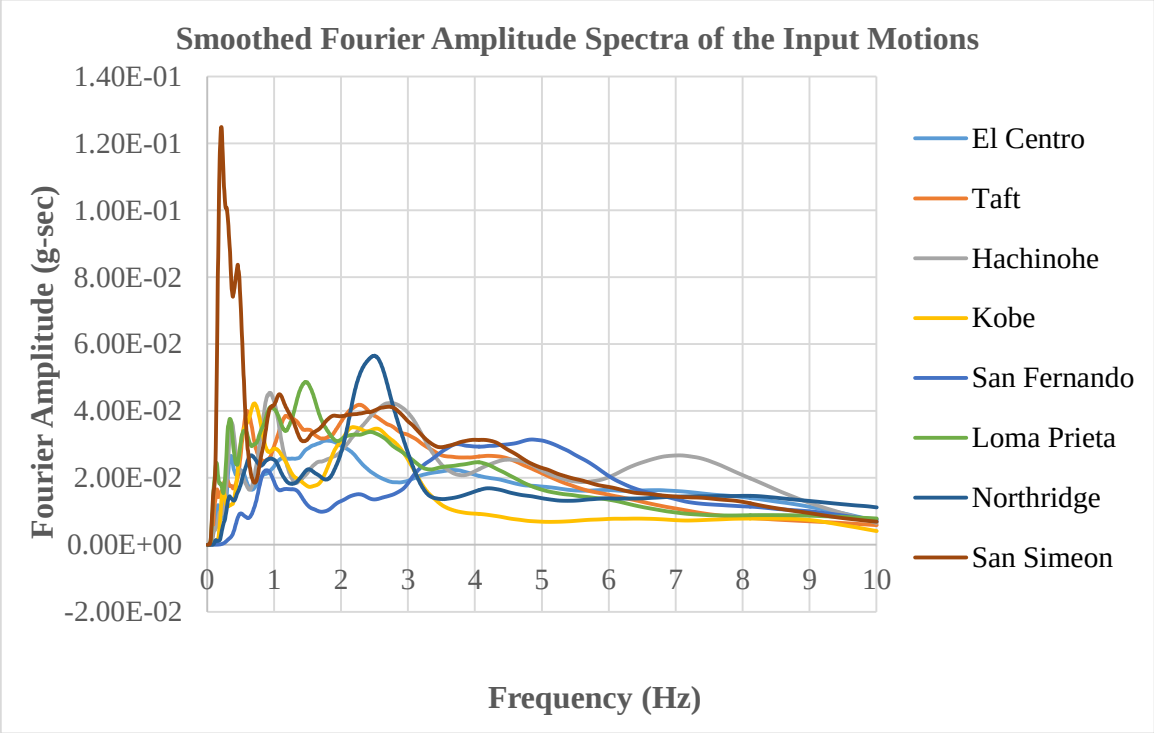

Figure 4.10 smoothed Fourier Amplitude of the selected input motions

CHAPTER FIVE

SITE CHARACTERIZATION/INPUT SOIL DATA

5.1 Introduction

Dynamic mechanical properties of a soil such as stiffness and damping are important input parameters to perform ground response analysis. Stiffness and damping are the most crucial properties that influence wave propagation through soils. Other properties like plasticity index (PI) and over-consolidation ratio (OCR) also have an effect in defining stiffness and damping curves.

As noted in section 2.1, shear wave velocity (V_S) is a valuable indicator of the dynamic properties of a soil due to its inherent relationship with low strain-level stiffness of the soil (G_{max}). It is an integral component in characterization of the stress-strain behavior of soils in ground response analysis. Several laboratory and field tests are available for its measurement. In the absence of direct measurements, however, estimations based on correlations with in situ penetration tests can be used, having in mind the uncertainties introduced by such methods (Wair et al., 2012).

For this indicative study, two different methods were used in determining the shear wave velocity profiles of selected sites: (1) seismic refraction survey and (2) correlations with in situ standard penetration tests (geotechnical investigation). These methods will be discussed in detail in the following sub-sections of this chapter.

5.2 Considerations to Site Selection

In section 3.3 it was mentioned that the study of Tsehayu and H.Mariam (1990) indicates that the south-west (along Akaki River), Bole area and central parts of the city are constituted of alluvial, residual and lacustrine deposits. These are comparatively the most constructed areas of the city (and probably increasingly in the future). On the other hand the less built areas in the north, west and south-west of the city are dominated by ridges and

valleys. For the sake of site selection, more focus was given to majorly constructed sites (condominium houses, real estates and high-rise buildings).

Furthermore, the controlling features noted under section 2.4.2 that make 1D ground response analysis ineffective for some problems of interest were also considered. In order to obtain befitting selected sites in a study area, one has to take into account these controlling factors. The presence of slopping or irregular ground surfaces and sub-surfaces (topographic effects) and basin effects are the main factors that are likely to control the degree of accuracy of 1D response analysis of sites in the study area.

Results of studies suggest that 1D ground response analysis is better to measure ground response analyses at the center of a valley than near the edge. Haile (1996) also made a comparison between 1D and 2D analyses to determine the limiting geometric conditions at which geometric effects become insignificant. He observed that for width to depth ratios of greater than 4, the 2D geometric effect is insignificant and 1D analysis can be used as a good approximation for 2D valleys. The presence of irregular surface topography is also another factor that constricts the applicability of 1D analysis.

Therefore, assessing the appropriateness of the sites to perform 1D analysis is indispensable and the first step to go ahead with the analysis. Borehole profiles and cross sections through different boreholes of sites were integrated in order to achieve the requirements.

5.3 Input Soil Data from Geotechnical Investigation

Data from geotechnical investigation results conducted for different projects were collected at different locations. These project sites encompass parts of the city where major construction (such as high-rising buildings and condominium houses) is taking place. These sites are also from areas of the city which have flat topography with gentle slopes. As mere flatness of the general area of a site does not secure the suitability of 1D analysis, surface and subsurface topography of the local area represented by the site profiles were also evaluated from geotechnical investigation reports.

Most geotechnical reports comprise borehole logs and laboratory test results. They provide data such as thickness of soil stratification, standard penetration test (SPT) values with

varying depth, the over-consolidation ratio (OCR) and index properties. In addition to the suitability of sites for 1D analysis, depth of investigation and completeness of relevant data have also been regarded as additional filtering criteria applied in the collection of geotechnical reports. All available geotechnical reports collected are summarized and presented in Table 5.1.

Table 5.1 Summary of collected geotechnical reports of different projects sites

Firms (Consulting Companies)	**Number of Project Sites Obtained**
ADDIS GEOSYSTEMS PLC	4
ARCON Design Build PLC	12
BEACON Consulting Engineers PLC	1
BEST Consulting Engineers PLC	3
Ethiopian Construction Design and Supervision Works Corporation (Previously Construction Design Share Company)	11
Gia Engineering PLC	3
JDAW Consulting Architects and Engineers PLC	2
MGM Consults PLC	1
MH Engineering PLC/ ETG Designers and Consultants PLC	1
SABA Engineering PLC	2
TOTAL	**40**

All these reports do not extend their investigation to the required depth. In addition, these project sites are cumbersome to come up with all necessary outputs of ground response analysis within the scope of this study. Therefore, looking into the depth of investigations and availability of relevant parameters that are used to define soil models in the analysis, the sites were further filtered to a manageable size of seven representative sites. A brief description of these finally selected representative sites is shown in compact form in Table 5.2. Their locations are also depicted in Figure 5.1 on Google map.

Table 5.2 Summary of selected borehole profiles for response analysis

No.	Site Code	Project Name/ Client/Description	Consulting Firm	Depth of Investigation	Location
1	Ayat	Ethio-American Doctors Group/Medical Center	SABA Engineering PLC (Nov-2016)	30 m	Ayat Area
2	CMC	Addis-Africa International Convention and Exhibition Center/Share Company	BEST Consulting Engineers PLC (Dec-2015)	33 m	CMC
3	Bole Site 1	Bole International Terminal Expansion	BEST Consulting Engineers PLC (Dec-2013)	30 m	Bole Airport
4	Bole Site 2	SOLTA Hotel and Apartment Business PLC- B+G+9 Building	ARCON Design Build PLC (July 2015)	25 m	Millennium hall area
5	Mexico Site 1	Bank of Abyssinia- 3B+G+20 Branch Building	ARCON Design Build PLC (Dec-2017)	31.6 m	Around Mexico Square
6	Mexico Site 2	Organization for Rehabilitation and Development in Amhara, ORDA	Ethiopian Construction Design and Supervision Works Corporation, (Dec-2013)	30 m	Legehar
7	Jemmo	Tracon Trading PLC- 3B+G+20 Apartment Building	ARCON Design Build PLC (Jan-2016)	40 m	Jemmo

Figure 5.1 location of selected sites using geotechnical data

A number of geotechnical data from around the Airport area verify the existence of a hard stratum (Ignimbrite) at about 20 m depth overlain by soft soil formation. Two typical sites have been selected from this area: Bole site 1 and Bole site 2. The only and satisfactory geotechnical data obtained from Jemmo area is the project site for Tracon Trading PLC. The report shows two highly varying profiles 150 m far apart. One profile consists of clay and silt soils of about 19 m thickness underlain by slightly-to-moderately weathered ignimbrite, whereas the other profile is composed of soft soil formation extending to 40 m depth. Three available boreholes (to each profile) have been used to characterize and analyze these profiles independently.

The averaged stratification of the seven site profiles found from borehole logs and laboratory reports is summarized in Tables 5.3 and 5.4. Typical and pertinent data about each site as obtained from consulting firms are presented in the appendix A.

Table 5.3 Average stratification of selected site profiles

Site	Depth (m)	Field Description of Soil/Rock
Ayat	0-9.4	Silty Clay
	9.4-17	Sandy Silt with some gravel (Residual soil of weathered Rhyolite)
	17-20.1	Moderately weathered and fractured Rhyolite
	20.1-22.3	Sandy Silt
	22.3-25.4	Moderately weathered and fractured Rhyolite
	25.4-30	Sandy Silt
CMC	0-6.3	medium stiff, dark gray to light brown, highly plastic Clay
	6.3-8.8	slightly to moderately weathered Ignimbrite
	8.8-25	Clayey Silt/Silty Clay
	25-30	slightly to moderately weathered Basalt
	30-33	Clayey Silt/Silty Clay
Bole Site 1	0-0.7	Fill material
	0.7-3	Sandy Silt
	3-19.0	Clayey Silt
	19-21.0	Clayey Silt (Decomposed Basalt)
	21-30.0	Slightly to moderately weathered Vesicular Basalt
Bole Site 2	0-7	Silty Clay
	7-19.0	Silty/Clayey Sand
	19-25	Silty Gravel (Weathering product of Basalt)

Table 5.4 Average stratification of selected site profiles

Site	Depth (m)	Field Description of Soil/Rock
Mexico Site 1	0-2.2	Silty Clay
	2.2-4	Decomposed Ignimbrite
	4-9.5	Clayey Silt with trace sand soil layer
	9.5-21.5	Sandy silt with trace clay
	21.5-27	Slightly to highly weathered Vesicular Basalt
	27-31.6	Silty Gravel/Sand
Mexico Site 2	0-2.5	soft expansive silty clay with some gravel
	2.5-9	clayey silt with some sand
	9-19.0	Gravelly silty sand (Derived from highly to completely weathered Basalt)
	19-23.6	Gravelly silty sand (Derived from highly to completely weathered Basalt)
	23.6-30	clayey silt with some sand
Jemmo Profile 1	0-2.0	Silty Clay
	2.0-20	Clayey Silt
	20-40	Sandy Silt
Jemmo Profile 2	0-6	Silty Clay
	6-18.8	Clayey Silt
	18.8-30	Slightly to Moderately weathered Ignimbrite

5.4 SPT-N and Shear wave Velocity (V_s) Correlation

As discussed in the previous subsections, the shear wave velocity used in characterizing the stress-strain behavior of soils for the purpose of ground response analysis can be estimated from in situ penetration tests. The standard penetration test is one of the most widely used in situ geotechnical test throughout the world. Since the 1960s, researchers have studied the relationship between Vs and SPT-N values (Wair et al. 2012). These relationships are available in many publications.

Pacific Earthquake Engineering Center (PEER) has made a study and prepared a well-documented guideline for estimation of shear wave velocity profiles from penetration test results (Wair et al. 2012). In this study brief review of previous works

has been presented: Kanai (1966); Shibata (1970); Ohba & Toriuma (1970); Ohsaki & Iwasaki (1973); Ohta & Goto (1978); Imai & Tonouchi (1982); Seed, Idriss & Arango (1983); Sykora & Stokoe (1983); Lin et al. (184); Jinan (1987); Yoshida et al. (1988); Lee (1992); Andrus (1994); Dickenson (1994); Lum & Yan (1994); Sisman (1995); Iyisan (1995); Jafari et al. (1997); Rollins et al. (1998); Pitilaki et al. (1999); Kiku et al. (2001); Jafari et al. (2002); Hasancebi & Ulusay (2007) and Piratheepan 92002).

From these studies, correlation equations for clays and silts, sands, and gravels were developed based on regression analysis of available datasets. SPT values were converted to uniform reference energy ratio of 60% in order to minimize variability due to differences in equipment efficiency. Other corrections are also applied to field SPT values to account for variations from standard practice. It was observed that Vs-N_{60} equations that took into account the effect of overburden Stress (or depth) provided better correlations (from comparison of coefficients of determination). In general, the equations took the form:

$$V_S = a.N^b\sigma_v^{'c} \tag{5.1}$$

Where; a, b and c are regression coefficients, N_{60} is corrected SPT value and $\sigma_v^{'}$ is effective overburden stress.

Having examined these studies, Wair et al. (2012) recommended correlation equations for different categories of soils: all soils, clays and silts, sands, and gravels (Table 5.5). This study describes the need for correction of field SPT values while using these recommended equations. The equations were proposed for Quaternary soils (Holocene and Pleistocene soils). Applying age scaling factors (Table 5.5) for soils of known age improves the accuracy of the correlation equations.

Table 5.5 Recommended SPT–stress–V_S correlation equations (after Wair et al. 2012)

Soil Type	Shear Wave Velocity (m/s)	Age Scaling Factors	
		Holocene	Pleistocene
All soils	$30N_{60}^{0.215}\sigma'^{0.275}_{v}$	0.87	1.13
Clays and Silts	$26N_{60}^{0.17}\sigma'^{0.32}_{v}$	0.88	1.12
Sands	$30N_{60}^{0.23}\sigma'^{0.23}_{v}$	0.90	1.17
Gravels-Holocene	$53N_{60}^{0.19}\sigma'^{0.18}_{v}$	----	----
Gravels-Pleistocene	$115N_{60}^{0.17}\sigma'^{0.12}_{v}$	----	----

σ'_v Measured in kPa

Concerned bodies and organizations (Geological survey of Ethiopia; Department of Geology, AAU; and experts) were consulted on issues related to the ages of soils around Addis Ababa. As no dependable data were found, the correlation equations have been applied without modifying them by age scaling factors. Even if the equations were used without age scaling factors, trial ground response analyses outputs found by considering and neglecting these factors were smoothly agreeable.

As mentioned previously, the recommended equations are suited for corrected and normalized (to reference energy ratio of 60%) field SPT values. The need for corrections is to account for variations due to differences in equipment and procedures of the test (i.e., hammer energy, borehole diameter, and rod length). These corrections to SPT field values were applied as per the recommendations of ES EN 1997: 2015 provision. The correction factor for borehole diameter is unity since all borehole logs have diameters between 60 mm and 115 mm. Therefore, corrections only for equipment type and rod length were applied.

For the purpose of estimation of V_S from penetration tests, normalizing the SPT values to reference effective overburden stress (correction for overburden pressure) has been found to be inappropriate. Wair et al. (2012) describes that several studies concluded that using stress normalized SPT values in V_S estimations proved to be considerably less accurate than relations based on non-normalized values.

In general, corrections for equipment (Hammer energy) and rod length were employed for this study and corrected SPT values were computed using the expression:

$$N_{60} = \frac{ER_r}{60} * \lambda * N \qquad (5.2)$$

Where;

ER_r is the energy ratio of the equipment used at field

λ is correction for rod length

N is measured field SPT value

All the procedures of corrections and correlations were thoroughly applied to those SPT values of the selected sites in section 5.3 to estimate the shear wave velocities. Computed shear wave velocity profiles for these sites are summarized in Tables 5.6 and 5.7.

Consideration of Rocks

At some of the selected sites, slightly-to-moderately weathered rhyolite, ignimbrite and basalt rocks were encountered at varying depths. As identified in geological aspect of the study area under section 3.2, basalt and weathered products of basalt were found at Mexico, Bole and CMC sites. Ignimbrites and rhyolites (younger volcanic rocks) were also observed at eastern and southern sites: ignimbrites at CMC and Jemmo sites and ryolites at Ayat site.

Euro-code describes six grades of simplified weathering classification of rocks. According to this classification, grade I represents fresh rocks which show no visible sign of rock material weathering. If discoloration that indicates weathering of rock material and discontinuity surfaces is observed, then, the rocks are grouped into grade II (slightly weathered rock). Grade III contains moderately weathered rocks wherein less than half of the rock material is decomposed or disintegrated to a soil whereas grade IV (highly weathered rock) is assigned to rocks whose more than half part is decomposed/disintegrated to a soil. Grades V and VI are attributed to completely weathered rocks and residual soils, respectively.

The study of Tsehayu and H.Mariam (1990) and field description of rocks provide nearly identical rock mass strengths. Accordingly, closely to very closely jointed basalts, rhyolites and all the ignimbrites in the city have medium rock mass strength. For these

slightly to moderately weathered rocks having a medium rock mass strength, the lower limit shear wave velocity of NEHRP provision (760 m/s) has been used. Using greater shear wave velocity values than 760 m/s induces very slight changes in the analysis output.

Table 5.6 Shear wave velocity of profiles for selected sites

Ayat Site		**CMC Site**		**Bole Site 1**		**Bole Site 2**	
Depth (m)	Vs (m/s)	Depth (m)	Vs (m/s)	Depth (m)	Vs (m/s)	Depth (m)	Vs (m/s)
0-3	107	0-2.28	114	0-2.25	104	0-3	106
3-5.0	148	2.28-3.78	139	2.25-3.75	139	3-5.0	152
5-7.0	168	3.78-6.3	158	3.75-5.25	151	5-7.0	189
7-9.0	191	6.3-8.8	760	5.25-6.75	165	7-9.0	215
9-11.0	240	8.8-10.28	185	6.75-8.25	199	9-11.0	231
11-13.0	272	10.28-12	205	8.25-9.75	211	11-13.0	240
13-15.0	294	12-14.0	247	9.75-11.25	217	13-15.0	241
15-17.0	311	14-16.0	261	11.25-13	229	15-17.0	248
17-20.1	760	16-17.78	271	13-15	243	17-19.0	261
20.1-22.3	322	17.78-19.28	302	15-17	254	19-25	389
22.3-25.4	760	19.28-21	308	17-19	289	25-30	760
25.4-30	355	21-22.75	319	19-21	369		
		22.75-25	342	21-30	760		
		25-30	760				
		30-33	366				

Table 5.7 Shear wave velocity of profiles for selected sites

Mexico Site 1		**Mexico Site 2**		**Profile 1**		**Profile 2**	
Depth (m)	**Vs (m/s)**	**Depth (m)**	**Vs (m/s)**	**Depth (m)**	**Vs (m/s)**	**Depth (m)**	**Vs (m/s)**
0-2.25	124	0-4	145	0-3	120	0-3	107
2.25-3.75	149	4-6.0	199	3-5.0	151	3-5.0	142
3.75-5.25	187	6-8.0	236	5-7.0	180	5-7.0	173
5.25-6.75	191	8-10.0	231	7-9.0	204	7-9.0	204
6.75-8.25	197	10-12.0	196	9-11.0	223	9-11.0	225
8.25-9.75	209	12-14.0	196	11-13.0	254	11-13.0	267
9.75-11.25	231	14-16.0	203	13-15.0	265	13-15.0	250
11.25-12.75	251	16-18.0	223	15-17.0	273	15-18.8	263
12.75-14.75	261	8-120.0	244	17-19.0	283	18.8-30	760
14.75-16	284	20-22.0	234	19-21.0	279		
16-18	311	22-24.0	248	21-23.0	294		
18-21.5	302	24-26.0	298	23-25.0	311		
21.5-27	760	26-28.0	300	25-27.0	322		
27-31.6	419	28-30.0	284	27-29.0	314		
				29-31.0	320		
				31-33.0	326		
				33-35.0	346		
				35-37.0	320		
				37-40.0	322		

5.5 Input Soil Data from Seismic Refraction Survey

5.5.1 Theoretical Background

Seismic refraction test, which makes use of longitudinal wave propagation, is used to determine stratigraphy of soil layers, wave propagation characteristics of layers and depth to bedrock. Longitudinal waves are chosen since they travel faster through the ground and arrive first at distant points. Their arrival and the time they arrive can easily be detected using receivers. The test involves measurement of the travel time of longitudinal wave propagation from an impulse source to a receiver (geophone) on the ground surface. Geophones, tightly pressed against the ground, are commonly located in a linear arrangement along the ground surface at different distances from the source as depicted in Figure 5.2.

When a wave approaches a boundary of two layers (incident wave), part of it may return back to the surface (reflected wave) and part of it may pass through to the next layer (refracted wave). When longitudinal waves from a source at the surface travel to the interface of two materials of different wave propagation velocities, refraction of waves take place according to Snell's law. Snell's law for wave propagation at the interface states that the ratio of the angle between a ray and the normal to the interface to the velocity of the wave remains constant (no change in wave frequency as the wave enters the next layer).

$$\frac{\sin \alpha_1}{v_1} = \frac{\sin \alpha_2}{v_2} \tag{5.3}$$

Where; v_1 and v_2 are wave velocities in the upper layer and lower layer and α_1 and α_2 are angle of incidence and angle of refraction respectively.

When v_2 is larger than v_1 (lower layer being stiffer than the upper one), there is an angle of incidence called critical angle beyond which only reflection (no refraction) takes place. Waves that refract at a critical angle (critically refracted waves) travel parallel to the boundary. These critically refracted waves that travel along the interface of the two layers (also referred to as a refractor) refract back into the upper layer and strike geophones on the ground surface (Figure 5.2).

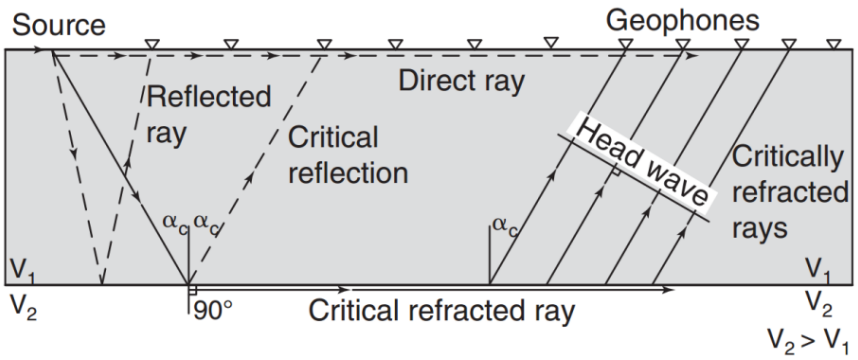

Figure 5.2 Seismic refraction test. (After Bechtel as referred by Briaud 2013)

At the commencement of recording, waves traveling directly in the upper layer arrive first at a given geophone. Later on, because of the higher stiffness of the lower layer, refracted waves arrive at a geophone before the direct or reflected waves. Crossover time, t_c represents the time gap at which this change occurs. The corresponding distance to this time interval is termed as crossover distance, X_c. Both velocity of wave propagation and depth to the interface of the two layers can be obtained using plots of arrival times of longitudinal waves at geophones of different distances on the ground surface (Figure5.3). Manipulation of measured parameters gives thickness of the upper layer (depth to refractor) to be computed as (Briaud 2013):

$$Z = \frac{X_c}{2}\frac{\sqrt{v_2 - v_1}}{\sqrt{v_2 + v_1}} \tag{5.4}$$

Where crossover distance, X_c is $t_c v_1$.

For the case of multiple layers, time arrival-distance plots have more than one break in slope. The slopes of plots along with the slope breaks are used to determine thicknesses of the deeper layers by extending the derivation used for a single layer. The longitudinal wave velocities of layers can also be extracted with the help of a computer program and an interpreter.

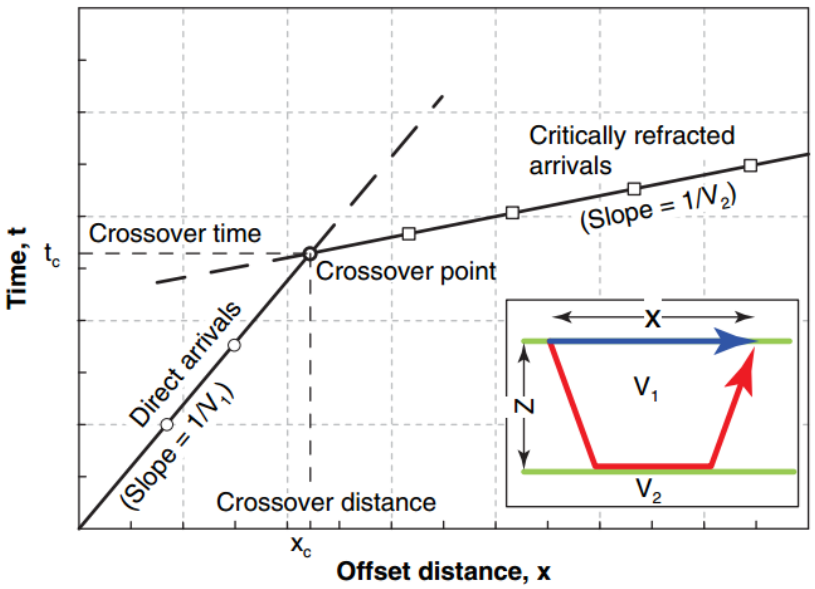

Figure 5.3 Interpreted signal from seismic refraction (After Briaud 2013)

The above derivations of thicknesses of different layers are based on the following assumptions (ASTM D 5777).

i. The boundaries between layers are planar (either horizontal or dipping at a constant angle).

ii. There are no ground surface undulations.

iii. Each layer is assumed to be homogeneous and isotropic.

iv. The wave velocity increases with depth (weak layer underlain by a strong layer).

v. Intermediate layers must have sufficient velocity contrast, thickness and the lateral extent to be detected.

5.5.2 Site Selection to Field Survey

Characteristics of sites upon which it is intended to conduct seismic refraction survey should be carefully considered at the very beginning of the survey. Looking into conditions of the site such as access to the site, absence of noise generating activities and topography and geology of the site must be done prior to the field work. Moreover, subsurface conditions of the sites can also be inferred from closer boreholes and geologic logs so that the feasibility is supported before the commencement.

The city of Addis Ababa has varied ground formations ranging from rocks to soft soil deposits. It is also represented by undulating ground surfaces (rugged topography).

Borehole logs from geotechnical investigations show that subsurface conditions are heavily erratic as well. The geotechnical profiles amassed from different sites testify this variability. Accordingly, subdividing the city into a number of sub-regions of nearly similar subsurface conditions and selecting representative sites for field tests has been found difficult.

The city is crowded with a lot of construction activities, vehicular traffic flow and busy day to day human activities. The equipment of seismic refraction test requires enough open space to spread its components and conduct the test. The space required mainly depends on the number of geophones to be used and the spacing between them. Therefore, the sites must be selected by searching all available open and feasible spaces and by making an effort to minimize the factors that limit the quality of the investigation result. Having the above conditions in mind, the following important considerations were used to pick out feasible sites for conducting the seismic refraction survey.

Proximity to Geotechnical Data: Seismic refraction survey alone is not a complete assessment of subsurface conditions of a site. It needs proper integration with other geological or geotechnical information. Spatial proximity of data from the two methods (geotechnical and geophysical) will be beneficial not only to supplement missing data but also to compare results from the two methods. Thus, sites selected for the seismic refraction test were made as much closer to sites with geotechnical data as possible.

Interference: Seismic refraction test is sensitive to ground vibrations from various sources. Sources of indirect noises such as wind, rainfall on geophones, movement of field crew, nearby vehicles, blasting, buried power-lines, and construction activity cause ground vibrations. Most vibrations from these sources produce compressional waves. Theses waves will easily overlap with the induced waves from triggering sources to give erroneous results. To find such completely free sites in the city is, however, hardly possible. An effort has been made in selecting sites to do away with noises from indirect sources.

Potential Amplification: Sites satisfying all the aforementioned criteria can be filtered in advance based on their potential susceptibility to amplification. This condition has already been considered during the geotechnical data filtering stage.

Scope: Most importantly, the seismic refraction survey has been conducted in cooperation with experts from IGSSA (Institute of Geophysics Space Science and

Astronomy) of Addis Ababa University. The crew contributed its unlimited knowledge, skill, effort and the seismic equipment gratefully to conduct the test for this study. Though the seismic refraction survey is comparatively simple as compared to most geophysical tests, it needs a time budget that takes a number of days. Accordingly, the scope of the field work and the number of field tests have to be limited to an extent that accommodates this constraint.

Following these considerations, the four sites shown in Figure 5.4 were selected to conduct the seismic refraction survey. The Ayat and the CMC project sites were feasible sites to conduct the field survey and thus the seismic refraction line was performed at the project sites closer to the drilling locations, while the Jemmo and Bole sites do not have practicable open spaces. Therefore, an open space adjacent to the project site has been preferred for the field work at Jemmo site. Whereas, for Bole sites closer working space to the selected geotechnical data is found near Bole Community School.

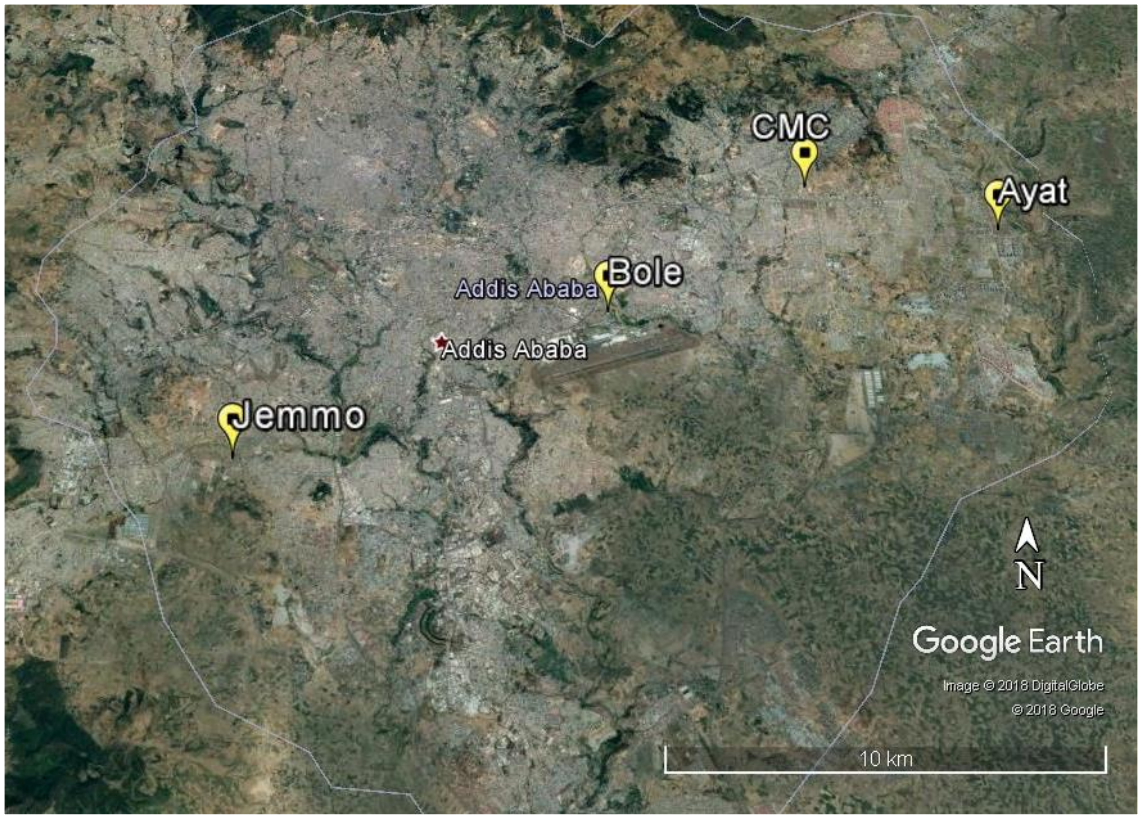

(a)

(b)

(c)

(d)

(e)

Figure 5.4 Location of selected sites for seismic refraction survey: on Google map (a); Ayat site (b); CMC site (c); Bole site (d) and Jemmo site (e)

5.5.3 Equipment and Field Procedure

A seismic refraction method of measuring subsurface conditions requires an energy source, trigger cable, geophones, geophone cable, and seismograph in order to meet the objectives of the survey.

Energy Source and Trigger Cable

Energy sources generate elastic waves that travel through the soil from the source. Among the waves generated, the longitudinal wave has the highest velocity and arrives first at each geophone. Different types of energy sources are commonly used in seismic refraction survey: sledgehammer, mechanical weigh-drop (or impact devices), projectile (gun)

sources and explosives. Selection of the energy source depends upon the required depth of investigation and geologic conditions. More energy is required for deeper investigations.

For the purpose of this investigation, sledgehammer energy source has been used. A metal plate (strike plate) on the ground is used to improve the coupling of energy from the hammer to the soil. An electrical timing device at the head of the hammer is used to generate the initial time impulse and is connected to the seismograph by a cable.

Figure 5.5 sledgehammer and metal plate used for seismic refraction survey

Geophones and Cabling

Geophones are commonly arranged in a linear array form of spreading. The length of geophone array is usually on the order of 4 to 5 times the depth of investigation. A 92 m length of linear array of geophones with 4 m spacing between successive geophones has been utilized for this seismic refraction survey. Though this arrangement entails that the investigation can extend to a depth of about 25 m, very large shock sources are required to detect to this depth.

After determining the direction along which a geophone cable is to be situated, a measuring tape was laid out along the survey axis and geophones were spread at the desired spacing. A typical geophone cable has electrical connection points (takeouts) at intervals along the cable. The geophone cable was then deployed with a takeout placed at each geophone location. Geophones were connected to the geophone cable at the takeout

points. They have spikes that are driven into the ground for effective coupling to detect the seismic signal.

Figure 5.6 Geophone and geophone cable

Seismographs

A wide variety of seismographs ranging from simple, single channel units (with single geophone) to very sophisticated multichannel units is available. They sample, record and display the seismic wave digitally. A multi-channel seismograph with 24 geophones was used for this survey. The survey was conducted by moving the hammer shot point to successive positions along the geophone array and repeatedly hammering the strike plate at those shot points.

Figure 5.7 Seismograph

5.5.4 Data Processing and Output

The seismic refraction test provides the velocity of compressional waves in subsurface materials. However, the contribution of the interpreter based on knowledge of local conditions and other data is significant. He must interpret the seismic refraction data and arrive at a sensible description of the site.

Geophones convert ground vibrations into electrical signals by transforming P-wave energy into electrical signal. This electrical signal is recorded and processed by seismographs. Travel time, which is the time it takes for the seismic P-wave to travel from the seismic energy source to the geophone, is determined. It is a function of the distance between geophones, depth to the refractor and the seismic velocities of materials through which the wave passes. Travel time plots are the basic format for presentation of first arrival data needed for refraction interpretation. The travel times are plotted against the distance between the source (shot points) and the geophone array to make travel-time curves.

The depth of refractors (interface between two layers) is described using the rigorous application of Snell's law to a subsurface model consisting of homogeneous layers and horizontal or dipping planar interfaces as discussed under section 5.5.1. Pickwin95 and Plotrefa packages of SeisImager were used to generate the interpretations. This process

resulted in an output of tomographic inversions showing the compressional wave (P-wave) velocity profiles. The tomographic inversion outputs of the survey for the selected sites are depicted in Figures 5.8 and 5.9.

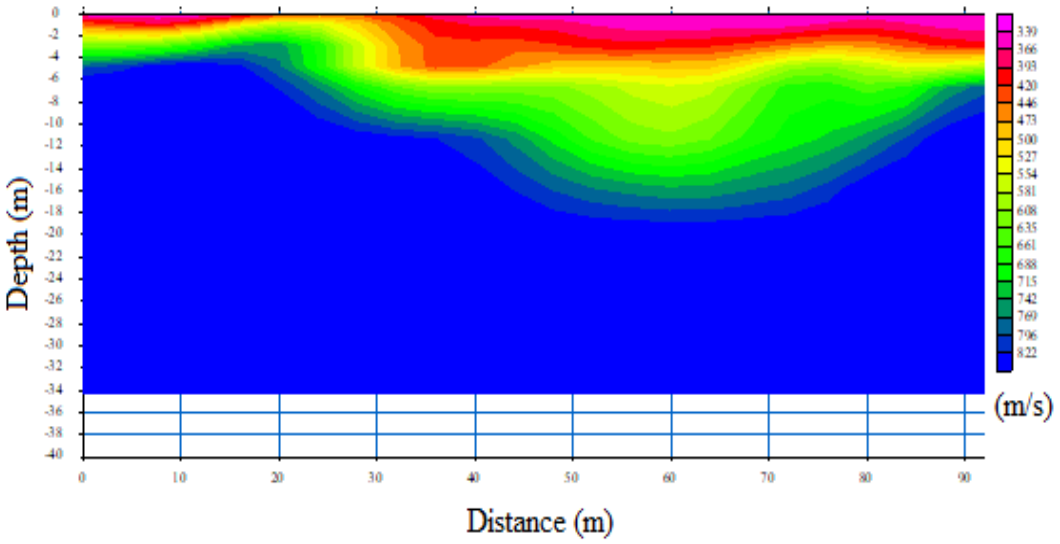

(a)

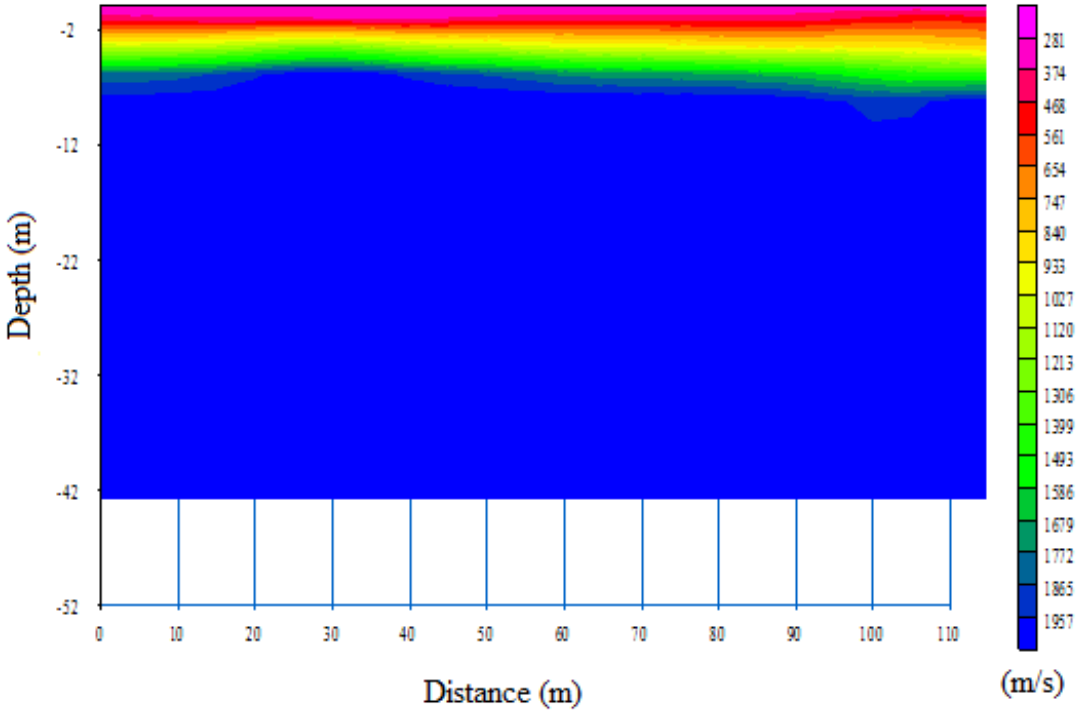

(b)

Figure 5.8 Tomographic inversions: (a) for Ayat site; (b) for CMC site

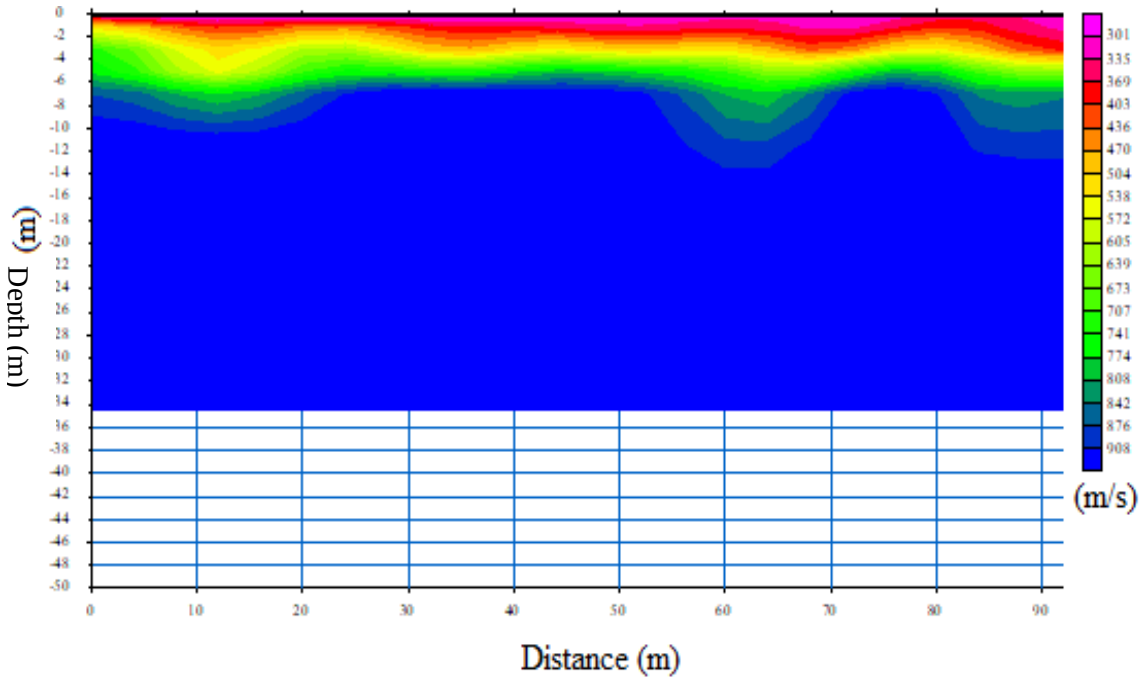

(a)

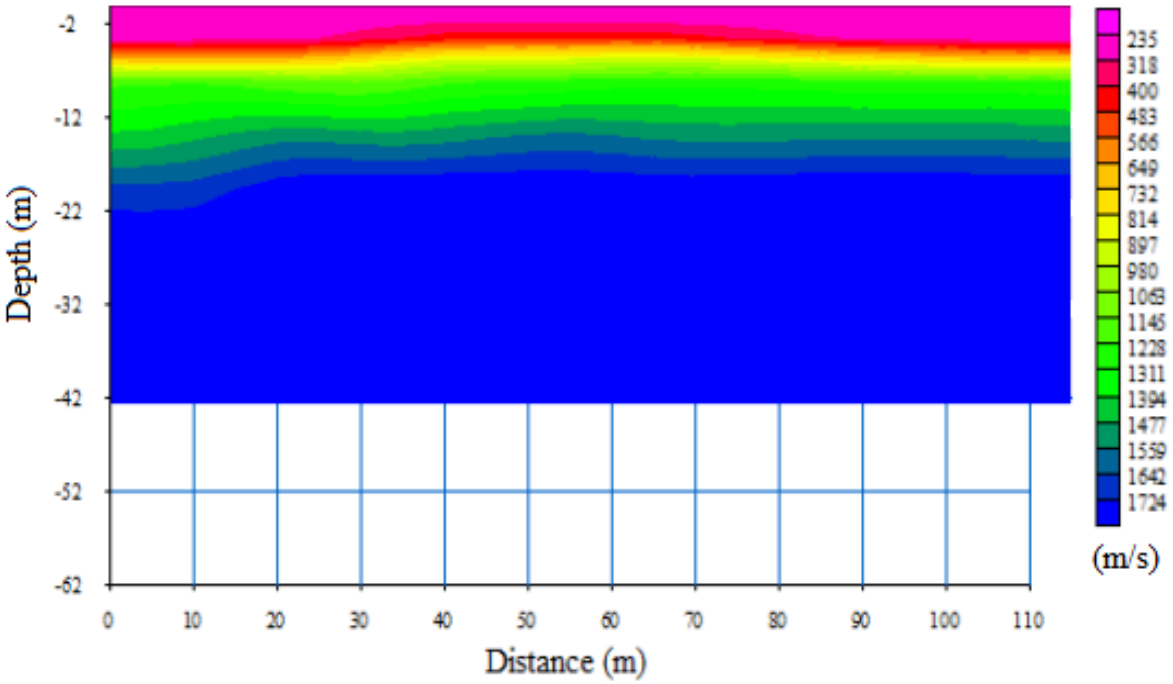

(b)

Figure 5.9 Tomographic inversions: (a) for Bole site; (b) for Jemmo site

5.5.5 Shear Wave Velocity Determination

Geophysical methods are generally limited as far as comprehensive data is concerned and hence are best complemented by geotechnical or by other geophysical investigations. In other words, seismic refraction survey cannot solely be relied upon to provide all set of data required for subsurface characterization. S-wave velocities of site profiles must be determined using the seismic refraction results in hand. Qualitative description of site profiles from borehole logs of the geotechnical investigations were examined for this instance.

Based on the geotechnical field description of soils closer to the seismic survey sites, a sensible Poisson's ratio of the materials has been estimated. The shear wave velocity is then related to longitudinal wave velocity using the property of the material (expressed through its Poisson's ratio, υ). The following expression derived from theory of elasticity is used to relate the P-wave and S-wave velocities of a homogeneous, isotropic and elastic soil (Kramer 1996). This expression was applied to this study with reasonable Poisson's ratio value of soils which was obtained based on qualitative description of borehole profiles and the laboratory results.

$$\frac{v_p}{v_s} = \sqrt{\frac{2-2\upsilon}{1-2\upsilon}} \tag{5.5}$$

Finally, the longitudinal wave velocities and the shear wave velocity profiles computed from the seismic refraction survey are summarized in Table 5.8.

Table 5.8 P-wave and correlated S-wave velocity profiles from seismic refraction survey

Depth (m)	**Ayat Site**		**CMC Site**		**Bole Site**		**Jemmo Site**	
	V_p (m/s)	V_s (m/s)	V_p (m/s)	V_s (m/s)	V_p (m/s)	V_s (m/s)	V_p (m/s)	V_s (m/s)
2	366	176	374	180	335	161	235	113
4	420	202	840	404	436	209	318	153
6	473	227	1120	538	605	291	566	272
8	527	253			707	340	814	391
10	581	279			808	388	1063	511
12	635	305			908	436	1228	590
14	688	331					1394	670
16	742	356						
18	796	382						
20	822	395						

5.5.6 Statistical Extrapolation of Shallow Velocity Profiles

The development of design response spectra is customarily performed considering the upper 30 m formation of the ground. Despite this necessity, the shear wave velocity profiles from an investigation may not extend to the required depth of 30 m. The field survey outputs of this study (Table 5.8), can be easily observed that their depth of investigation (and hence the velocity profiles) does not run to 30 m.

Boore (2004) made a regression analysis using 135 boreholes that extend to a depth of at least 30 m and suggested a method for extrapolating velocity profiles (Wair et al. 2012). The method involves a statistical correlation between V_{s30} and the time averaged velocity to the terminal depth of investigation (V_{sd}). Time averaged velocity (V_{sd}) to the terminal depth of investigation ($\sum_{i=1}^{n} d_i$) can be computed as (Boore 2004):

$$V_{sd} = \frac{\sum_{i=1}^{n} d_i}{\sum_{i=1}^{n} \frac{d_i}{V_{si}}} \tag{5.6}$$

Where; V_{si} is the velocity at a depth, d_i

After computing the time averaged velocity, V_{s30} of the top 30 m profile is obtained from the equation;

$$\log V_{s,30} = a + b * \log V_{sd} \tag{5.7}$$

Where; a and b are depth dependent Boore (2004) regression coefficients (presented in Appendix B).

Using these two equations (V_{s30} being constant throughout the computation), the shear wave velocity at the required depth beyond the depth of investigations is computed.

This method of extrapolation is found to be reliable for most sites with relatively uniform soil conditions (erroneous for sites with considerable velocity contrast). For this very reason, stiff and rock like materials that show high velocity contrast were excluded during the extrapolation process. Finally, the computed shear wave velocity profiles for the four sites are summarized in Table 5.9.

Table 5.9 Extrapolated shear wave velocities of geophysical profiles

Depth (m)	Ayat Site		CMC Site		Bole Site		Jemmo Site	
	V_p (m/s)	V_s (m/s)	V_p (m/s)	V_s (m/s)	V_p (m/s)	V_s (m/s)	V_p (m/s)	V_s (m/s)
2	366	176	374	180	335	161	235	113
4	420	202	840	404	436	209	318	153
6	473	227	1120	404	605	291	566	272
8	527	253	---	404	707	340	814	391
10	581	279	---	404	808	388	1063	391
12	635	305	---	401	908	436	1228	259
14	688	331	---	470	---	375	1394	294
16	742	356	---	457	---	364	---	285
18	796	382	---	488	---	384	---	296
20	822	354	---	504	---	400	---	312
22	---	370	---	532	---	419	---	324
24	---	387	---	540	---	434	---	342
26	---	403	---	564	---	453	---	357
28	---	418	---	594	---	472	---	367

5.6 Soil Model

Major elements that influence the ground response analysis include characteristics of input ground motion, soil properties, soil model and the analytical method to be used. In short, the evaluation of site effects using analytical techniques is inconceivable without the knowledge of shear modulus and damping ratio of the different layers that compose a soil profile. Therefore, accurate evaluation of these parameters is an important step in ground response analysis.

Secant shear modulus, G_{sec} and damping ratio, ξ are often referred to as equivalent linear soil parameters. These are properties of different soils upon which most 1D ground response analyses are dependent. The parameters can be estimated from available empirical correlations that have been proposed based on previous studies or obtained from laboratory and field tests on the site of interest. Some noteworthy previous works related to these material curves has been introduced in the literature review section.

DEEPSOIL is a freely available software for research purposes to perform one-dimensional ground response analyses in linear, equivalent linear (EQL) and nonlinear (NL) methods. It performs linear and EQL analyses in the frequency domain; and linear and NL analyses in the time domain.

This study uses the equivalent linear method in the frequency domain to investigate the response of selected sites in Addis Ababa under earthquake loading. Determining material curves for these selected sites based on field or laboratory tests is beyond the scope of this study. Therefore, a set of strain-dependent modulus reduction and damping ratio curves inbuilt in DEEPSOIL were applied instead. The software also allows one to define his own material curves for different soil types using additional data in hand. Effective vertical stress for sand and clay and plasticity index for clay should be specified for defining these curves.

Accordingly, curves proposed by Vucetic and Dobry (1991) and Seed and Idriss (1991) were used to define the dynamic behavior of fine- and coarse-grained soils. They are being extensively used in several studies and are considered to be better alternatives (Hashash *et al*., 2016). Soil parameters such as over-consolidation ratio and plasticity index were obtained from amassed geotechnical reports for defining these curves.

CHAPTER SIX

ANALYSIS AND DISCUSSION

As discussed under section 2.4.1.2, EQL method of analysis is one of the most popular techniques in site response analysis because of relatively straightforward soil properties required and satisfactory outputs for recommended induced strain level. Different computer programs with similar computational approach are available to perform EQL site response analysis (e.g. SHAKE, STRATA, and DEEPSOIL). This method of analysis was originally implemented in SHAKE (Schnabel et al. 1972) in a frequency domain.

With an acquired official permission, DEEPSOIL, a program developed from the University of Illinois at Urbana-Champaign, is used to perform 1D ground response analysis of this study. The version considered in this study is v6.1 (Hashash et al. 2016).

6.1 Equivalent Linear Approach

One dimensional ground response analysis is associated with vertical propagation of shear waves through a linear viscoelastic system. The method of Equivalent linear approach treats soils as linear viscoelastic materials (soil behavior is approximated as Kelvin-Voigt solid). The shearing resistance to deformation of Kelvin-Voigt solids is the sum of an elastic part (linear elastic shear modulus) and a viscous part (viscous damping). The stress-strain relationship for a Kelvin-Voigt solid in shear is given as (Kramer 1996):

$$\tau = G\gamma + \eta\frac{\partial\gamma}{\partial t} \tag{6.1}$$

Where; τ is the shear stress, G is the shear modulus, $\gamma = \frac{\partial u}{\partial t}$ is the shear strain and η is the coefficient of viscous damping.

One dimensional equation of motion for vertically propagating shear (SH) waves can be written as:

$$\rho\frac{\partial^2 u}{\partial t^2} = \frac{\partial\tau}{\partial z} \tag{6.2}$$

Substituting Equation (6.1) into Equation (6.2) gives the basic wave equation for uniform damped soil expressed as follows.

$$\rho \frac{\partial^2 u}{\partial t^2} = G \frac{\partial^2 u}{\partial z^2} + \eta \frac{\partial^3 u}{\partial t^3} \tag{6.3}$$

Where; ρ is the mass density of the medium and u is the displacement of the medium along the lateral direction.

The solution to the above wave Equation (6.3) yields the one-dimensional ground response analysis and is of the form (Kramer 1996):

$$u(z,t) = Ae^{i(\omega t + k^* z)} + Be^{i(\omega t - k^* z)} \tag{6.4}$$

Where; u(z, t) is horizontal displacement at a depth z below the ground level and at time t; 'ρ' is the density; 'G' is the shear modulus and 'η' is the viscosity and = $\left(\frac{2G}{\omega}\right)\xi$; 'A' and 'B' are amplitudes of waves traveling in the upward (–z) and downward (+z) directions, respectively; 'k' (wave number)' = ω/Vs, where, 'ω' is wave frequency, Vs = shear wave velocity. k* is the complex wave number and is given by k* = k (1-iξ), where ξ = damping ratio. The amplification function is also derived as:

$$|F_2(\omega)| = \frac{1}{\sqrt{\cos^2\left(\frac{\omega H}{v_s}\right) + \left[\xi\left(\frac{\omega H}{v_s}\right)^2\right]}} \tag{6.5}$$

Where; H = thickness of the soil layer.

These expressions are also extended for layered and damped soils underlain by rigid as well as elastic rock (Figure 6.1). As mentioned under section 2.4.1.2, the frequency domain analysis (EQL) is based on assumption that the modulus and damping properties are constant and independent of strain level.

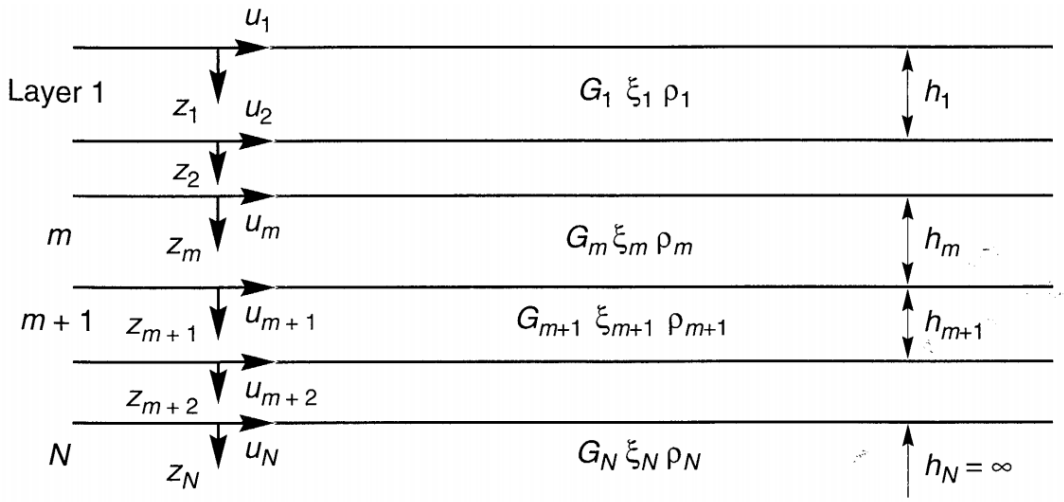

Figure 6.1 Nomenclature for layered soil deposit on elastic bedrock (After Kramer 1996)

6.2 Specification of Underlying Half-Space and Input Motions

One of the most important aspects of ground response analysis is the specification of the half-space (customarily called engineering bedrock) properties. In Japan, the term engineering seismic base layer is used instead because the base layer may sometimes be stiff/firm soil for sites such as deep basin (Yoshida 2015; Stewart et al. 2014).

Though there is no consensus regarding the definition, seismic base layer is preferably defined as bedrock or base layer with boundary conditions by which the response in the analyzed region is not affected (Yoshida 2015). It is also defined from the mechanics point of view as a layer that has sufficiently large impedance ratio to the surface layer or hard deposit that expands widely in the region. In Japan, the definition of engineering seismic base layer in design specifications is described by the S-wave velocity ranging from 300 m/s - 700 m/s (Yoshida 2015).

The half-space, in GRA, is required to match with the reference site condition for which the target spectra and the ground motion time series have been evaluated (Stewart et al. 2014). This reference site condition represents the condition below the geotechnical layers that are being analyzed in GRA. Therefore, the site condition used to develop the response spectrum for use in selecting ground motions was applied as an elastic half-space. This is the reference site condition of ground type A of ES EN 1998:2015 with corresponding shear wave velocity of 800 m/s. Its location, for some of the selected profiles, has been fixed to the depth of 30 m as the investigation data terminate at this

depth. However, for those profiles whose depth of investigations pass the 30 m, the entire soil profile to the terminal of the investigation has been considered.

From the perspective of the location as to where they are recorded, input ground motions are specified as outcropping or within motions (Figure 6.2). “Outcropping motions” refer to motions recorded at the ground surface whereas “within motions” are motions recorded in boring at rock level. A number of studies recommend the use of these ground motions along with appropriate bedrock condition (elastic or rigid half-space) based on the impedance ratio (ratio of the product of the density and shear wave velocity of two layers) between layers (Stewart et al. 2014; Stewart et al. 2008; Kwok et al. 2007). Accordingly, for time domain analysis (nonlinear analysis) bedrock should be modeled as an elastic half-space if the input motion is recorded at the free surface while within motions should be used with a rigid half-space. For within motions, depth of base of the soil profile that is to be analyzed in GRA is required to match with the depth at which the motions were recorded.

For use in frequency domain analysis, however, input motions are best defined as outcropping motions with elastic base (Kwok 2007). Stewart et al. (2014) also describe that input motions in GRA should be specified as outcropping motions with underlying half-space having S-wave velocity compatible with the reference site condition. Yoshida (2015) mentions that earthquake ground motions in North America are defined as outcrop motions at the rock/hard deposit surface. Having this in mind and assuming that the ground motions selected from PEER ground motion database were recorded on the ground surface (outcropping rock), the analysis was performed regarding these motions as outcropping. Because of the suggestions mentioned, the deconvolved historical ground motions were also applied as an outcropping motions (Haile 1996).

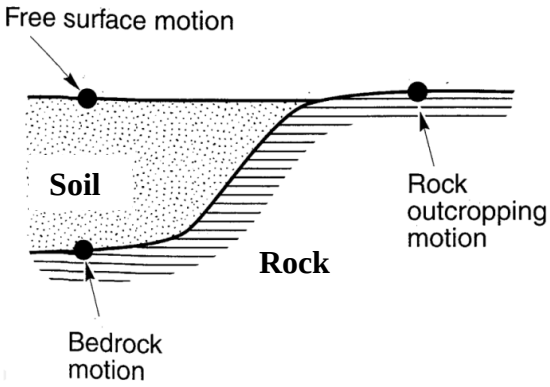

Figure 6.2 Ground response nomenclature (After Kramer 1996)

6.3 Summary Profiles

Ground response analyses using EQL method of analysis for 5% damping have been carried out at the selected sites. The input motions were scaled to peak acceleration value of 0.11g as per the seismicity of Addis Ababa city. Changes in ground motion parameters took place as the input motions passed through the modeled soil profiles. The potential in change (amplification/deamplification) depends on the soil type, thickness of the soft soil deposit, stiffness and impedance contrast with the underlying bedrock. The results of the analyses expressed in terms of peak ground acceleration (PGA) and maximum strain along the model profiles; and in terms of response spectra and Fourier amplitude spectra at the ground surface are presented in the following subsections.

The fundamental natural periods of the profiles computed using DEEPSOIL program (which are nearly the same results obtained using the expression $T = 4H / V_s$) are shown in Table 6.1. The periods from the seismic refraction data are observed to be shorter as the field survey results characterize the sites by higher shear wave velocity profiles.

Table 6.1 Fundamental natural periods (in seconds) of modeled profiles

Data Type	Ayat Site	CMC Site	Bole		Mexico		Jemmo	
			Site 1	Site 2	Site 1	Site 2	Profile 1	Profile 2
Geotechnical data	0.48	0.50	0.48	0.50	0.48	0.56	0.66	0.47
Seismic Refraction data	0.36	0.26	0.32		--------		0.32	

6.3.1 Maximum Strain Profiles

In the previous subsections of this study it was mentioned that the method of Equivalent Linear Analysis has been preferred because of two main reasons: the requirement of straightforward input soil parameters and the reality of obtaining satisfactory outputs for up to a certain threshold strain level. This threshold strain level is estimated to range up to about 5%. Moderately-seismic regions are predicted to sustain a strain not commonly exceeding this threshold level.

The maximum strain profiles resulted from the entire set of analyses using geotechnical data, excepting Bole site 2, induce maximum strain level well below 0.25%. Maximum strain from the Bole site 2 profile is about 0.6 % when it is shaken with the Northridge and the Loma Prieta earthquake ground motions. This peak value appears to happen due to two main reasons. The first likely cause is that the ground motions usually portray peculiar characteristics at about the predominant period of the site. Secondly, the site profile consists of relatively soft material of about 5 m thickness.

Generally, the maximum strain profiles from almost all analyses (62 of 64 analyses) vary roughly from 0.07% to 0.22% (Figure 6.3). This range is in close agreement with the strain level range for which reliable output using EQL method is expected.

The strain profiles from the seismic refraction survey are also found to fall well below a strain value of 0.04% (Figure 6.4). This shows that the analyses performed using seismic refraction survey data are in close agreement with the required threshold strain level, as well.

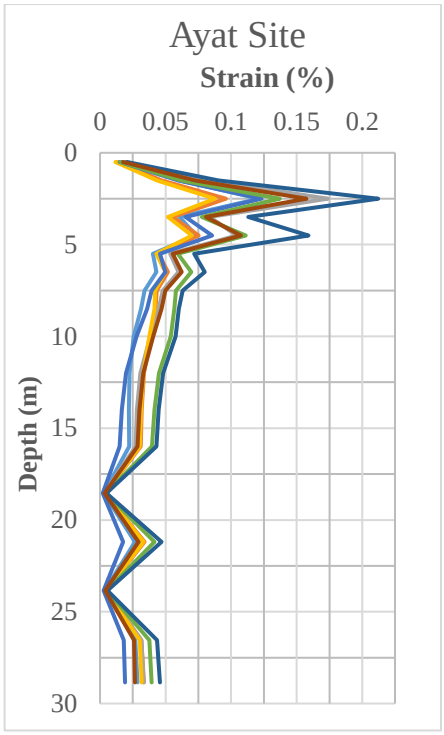
Ayat Site
Strain (%)
0 0.05 0.1 0.15 0.2
0 5 10 15 20 25 30
Depth (m)

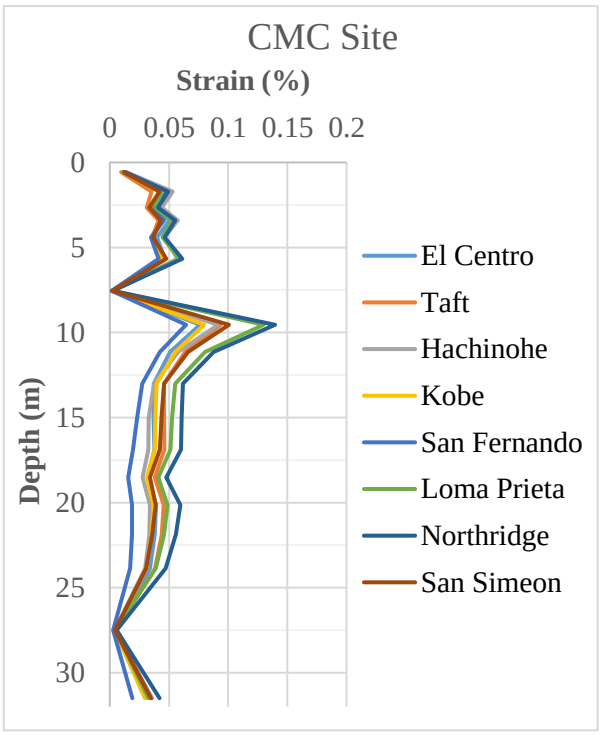
CMC Site
Strain (%)
0 0.05 0.1 0.15 0.2
0 5 10 15 20 25 30
Depth (m)
El Centro
Taft
Hachinohe
Kobe
San Fernando
Loma Prieta
Northridge
San Simeon

(a)

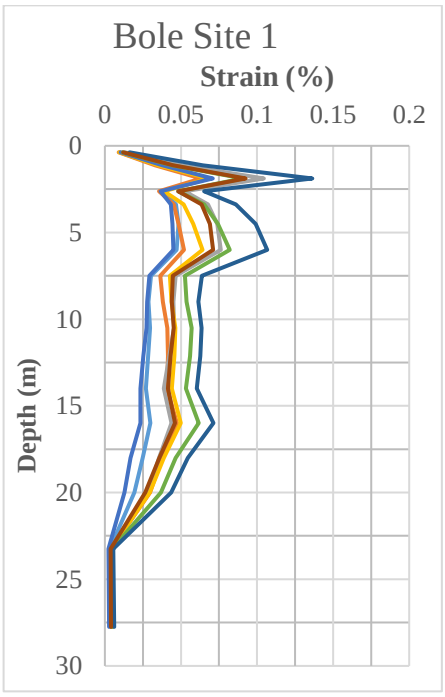
Bole Site 1
Strain (%)
0 0.05 0.1 0.15 0.2
0 5 10 15 20 25 30
Depth (m)

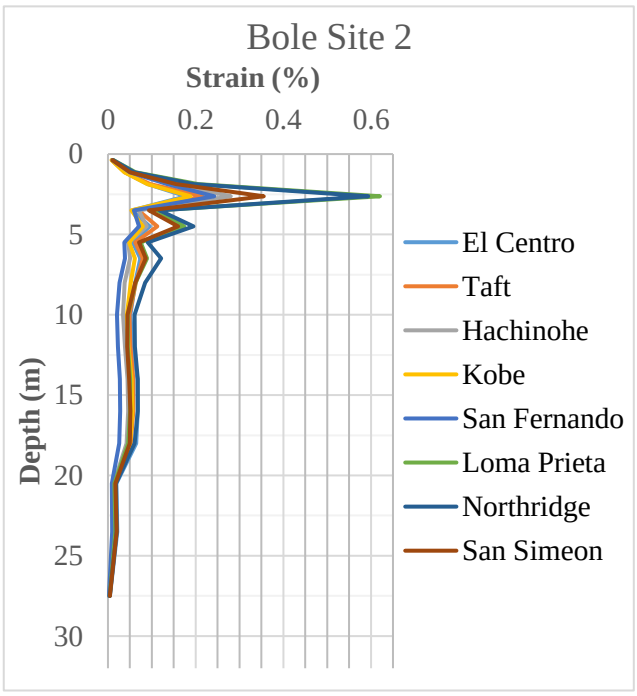
Bole Site 2
Strain (%)
0 0.2 0.4 0.6
0 5 10 15 20 25 30
Depth (m)
El Centro
Taft
Hachinohe
Kobe
San Fernando
Loma Prieta
Northridge
San Simeon

(b)

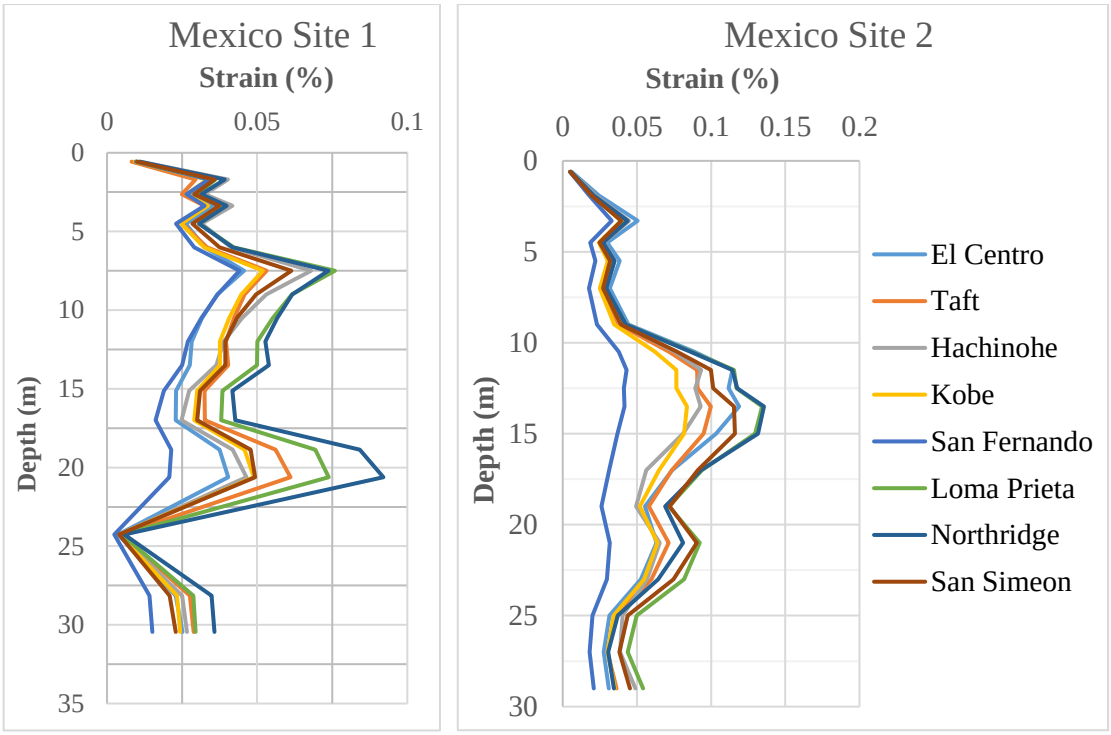

(c)

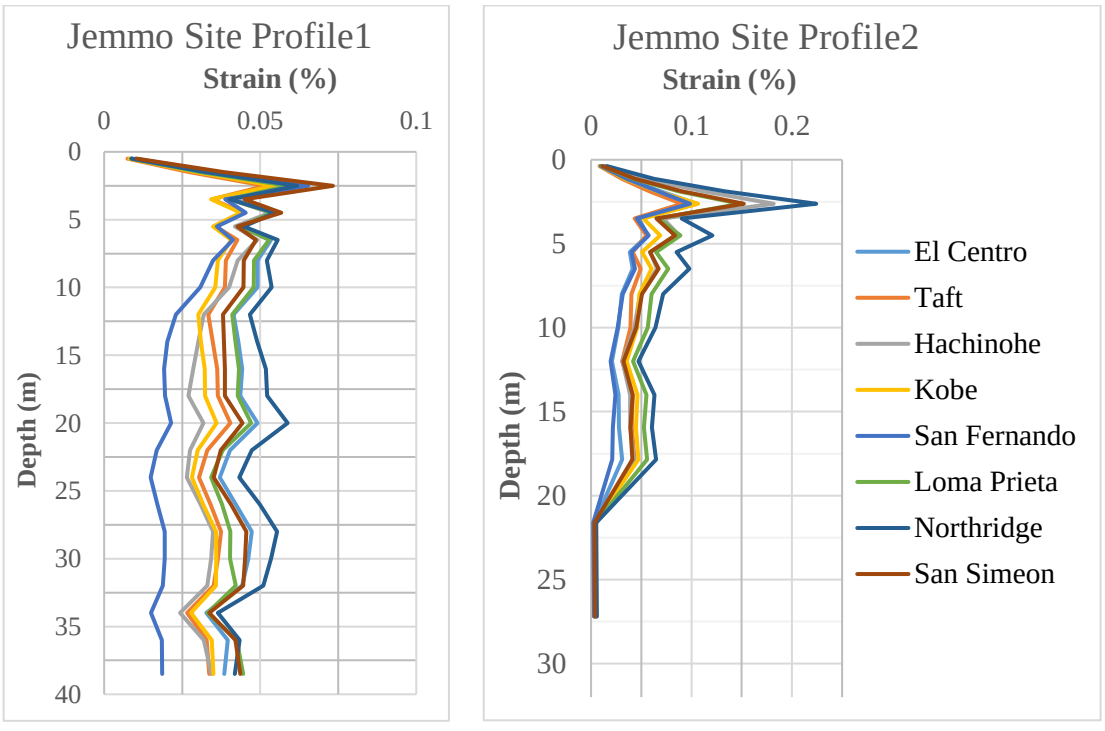

(d)

Figure 6.3 Maximum strain profiles from geotechnical data: Ayat and CMC sites (a); Bole sites (b); Mexico sites (c); and Jemmo site (d)

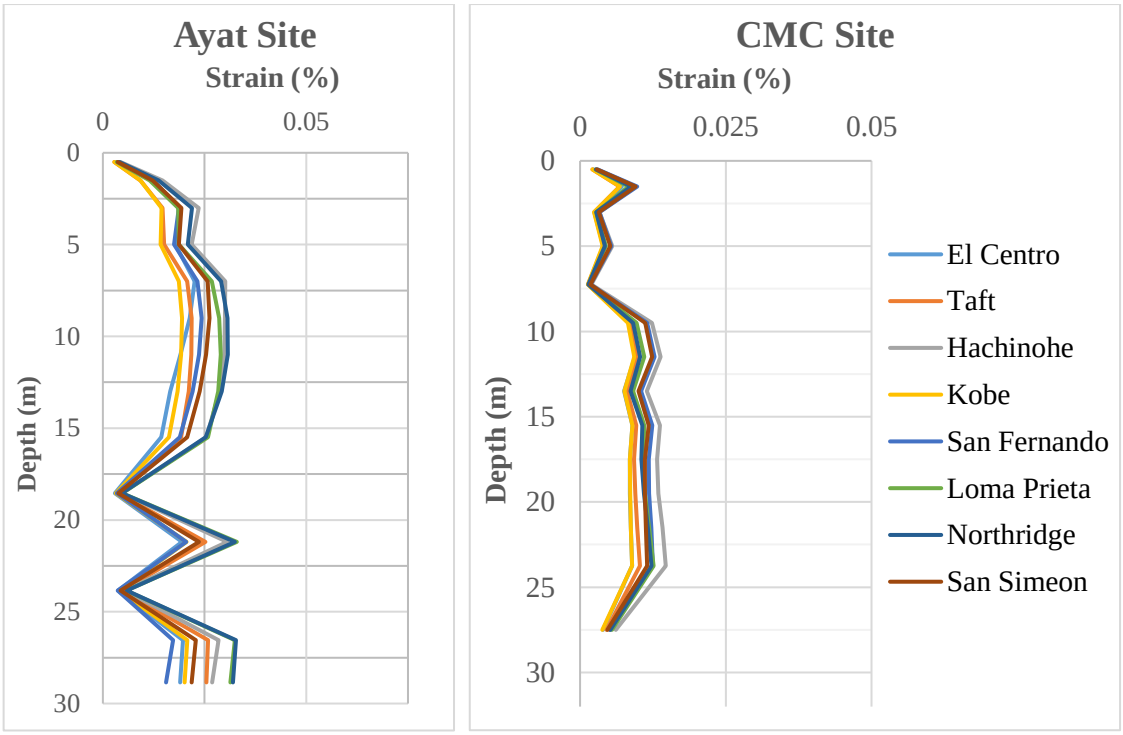

(a)

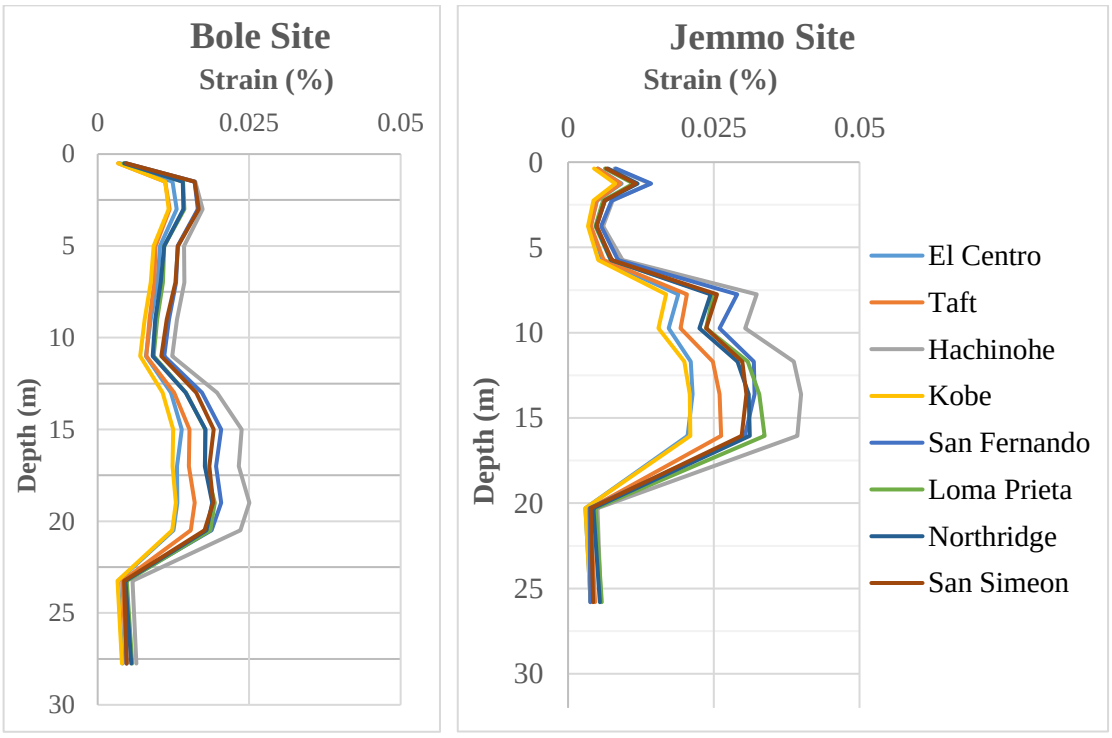

(b)

Figure 6.4 Maximum strain profiles from seismic refraction data: Ayat and CMC sites (a); Bole and Jemmo sites (b)

6.3.2 Peak Ground Acceleration (PGA) Profiles

The PGA profile results of the selected sites modeled using the data from geotechnical reports are summarized in Figure 6.5. In general, consistent amplification is observed at all profiles regardless of the input motions. The natural frequency of the profiles ranges from 1.80 Hz (Mexico site 2) to 2.14 Hz (Jemmo site). It is observed that the peak acceleration values of input ground motions (scaled to PGA of 0.11g) as they propagate along the soil profile show substantial changes. The PGA values found at the ground surface from these sites range from 0.18 (at Mexico site 2) to 0.41 (at Jemmo site profile 2) (Table 6.2).

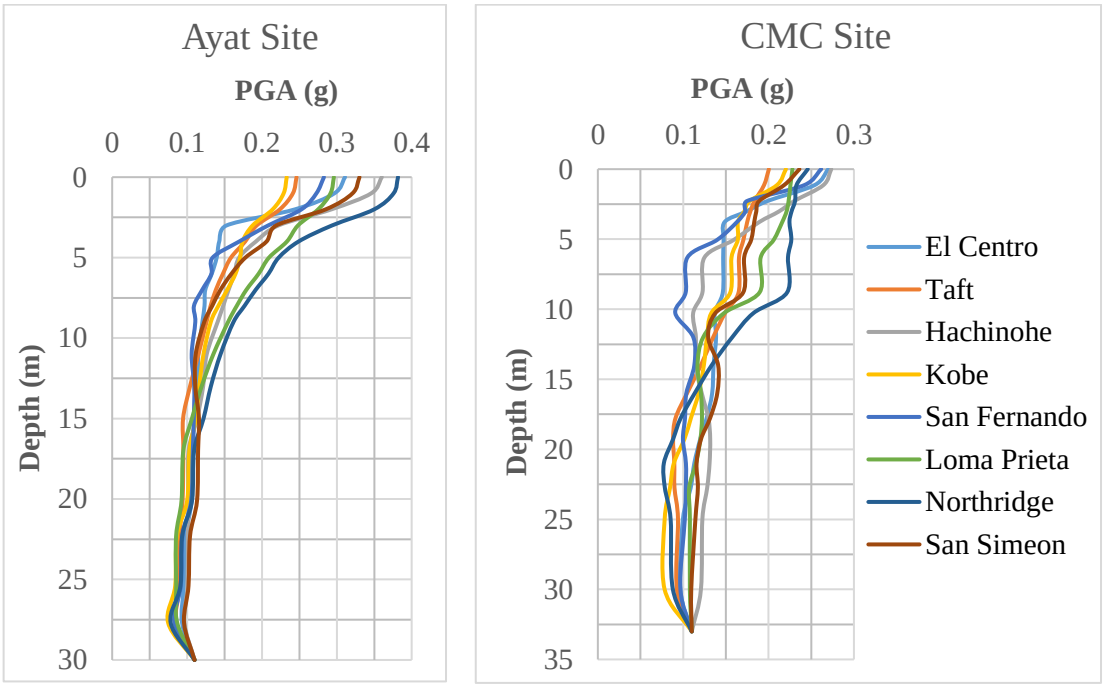

(a)

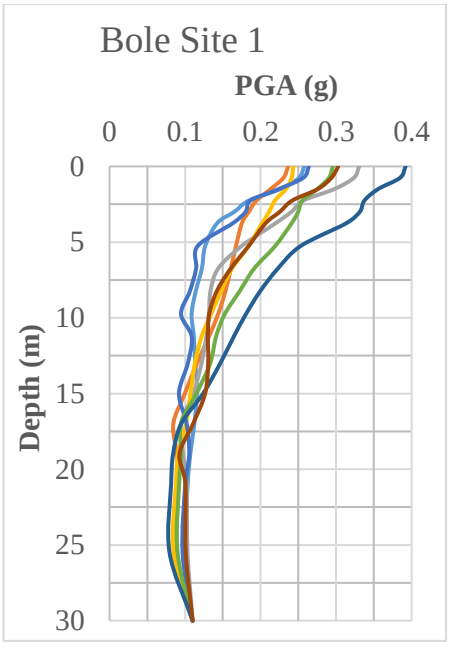
Bole Site 1
PGA (g)
0
0.1
0.2
0.3
0.4
Depth (m)
0
5
10
15
20
25
30

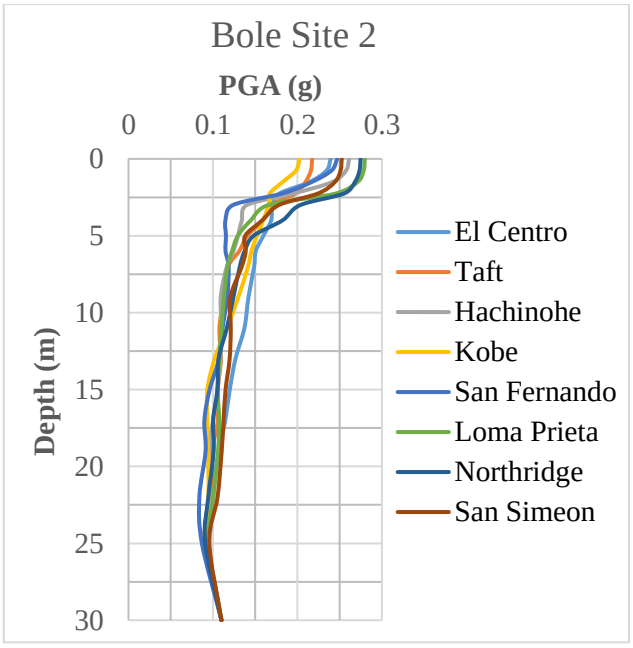
Bole Site 2
PGA (g)
0
0.1
0.2
0.3
Depth (m)
0
5
10
15
20
25
30
El Centro
Taft
Hachinohe
Kobe
San Fernando
Loma Prieta
Northridge
San Simeon

(b)

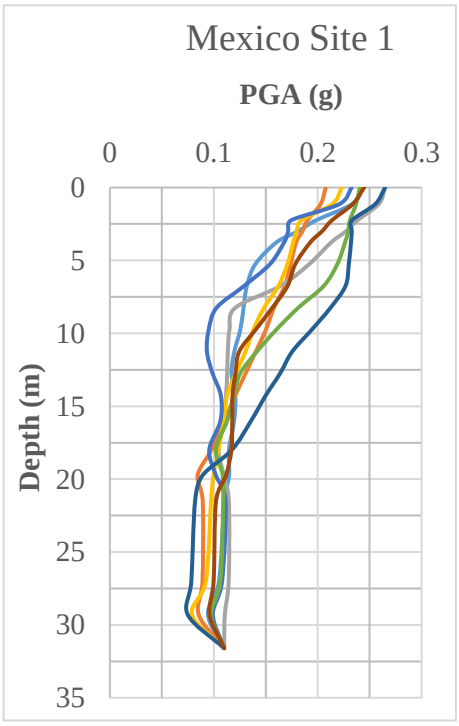
Mexico Site 1
PGA (g)
0
0.1
0.2
0.3
Depth (m)
0
5
10
15
20
25
30
35

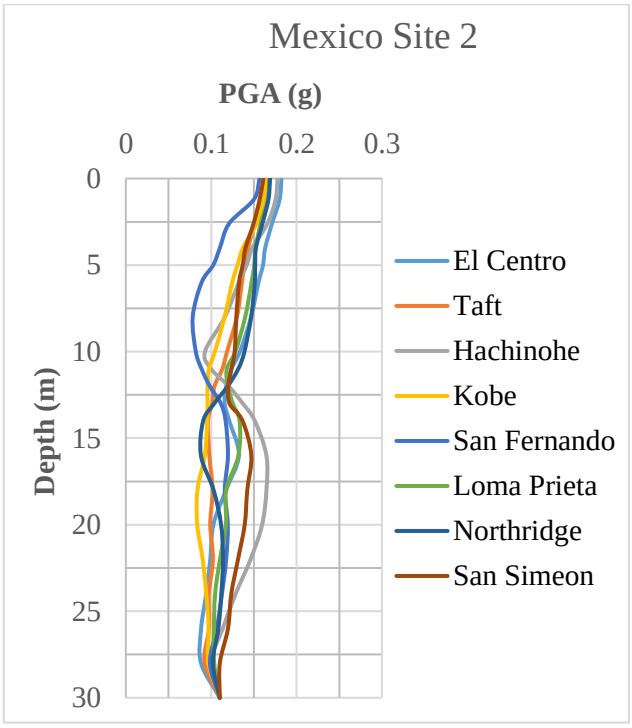
Mexico Site 2
PGA (g)
0
0.1
0.2
0.3
Depth (m)
0
5
10
15
20
25
30
El Centro
Taft
Hachinohe
Kobe
San Fernando
Loma Prieta
Northridge
San Simeon

(c)

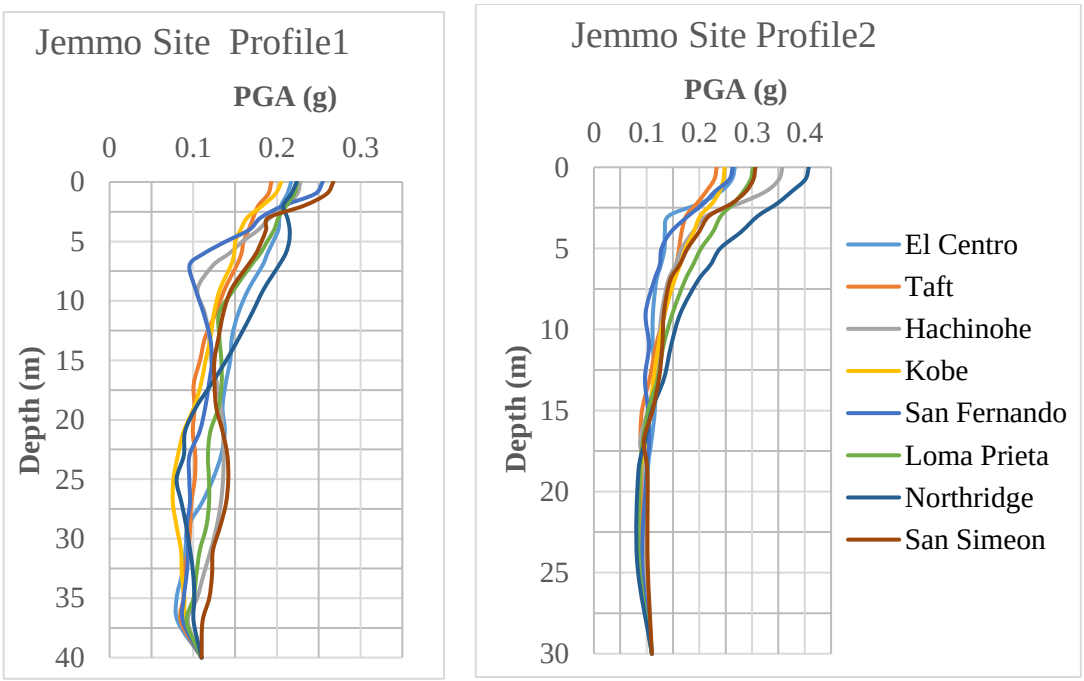

(d)

Figure 6.5 Peak ground acceleration (PGA) profiles using geotechnical data: Ayat and CMC sites (a); Bole sites (b); Mexico sites (c); and Jemmo site (d)

The maximum PGA value observed at most of the sites is mainly attributed to the presence of relatively soft soil at shallower depth. The absolute peak value is obtained from the analysis conducted by the use of Northridge earthquake ground motion which has predominant period around 0.4 sec (Figure 4.10) (while the characteristic period of the site is 0.5 sec; 2 Hz). The condition of resonance is more likely to occur with this ground motion. This is clearly seen in PGA profiles (Figure 6.5) that most of the profiles show substantial amplification under Northridge ground motion.

Profiles containing stiffer materials show less amplification potential at depths where the stiffer material is found and it finally converges to a PGA of 0.11g. However, profiles composed of thick soft soil formations indicate more significant amplification at greater depths. The PGA outputs at the ground surface resulted from the analyses using the set of input ground motions discussed in chapter four can be summarized as in Table 6.2.

Table 6.2 Summary of PGA values at the ground surface

Sites	Ayat Site	CMC Site	Bole		Mexico		Jemmo	
			Site 1	Site 2	Site 1	Site 2	Profile 1	Profile 2
Maximum PGA (g)	0.380	0.27	0.39	0.28	0.26	0.18	0.27	0.41

PGA profile results from the seismic refraction survey is depicted in Figure 6.6. Agreeable results with that of the results from the geotechnical data was not found because of a number of reasons. Absence of significant contrast in velocity between layers, positioning difference in borehole locations and refraction measurement, lateral geologic variability and presence of water table are among the main causes of the difference in results from the two methods of investigation. In addition, the precision of the seismic refraction survey depends on the energy source used, the soil condition, care involved in taking first arrival times and level and variation of noise impacting the measurement. In chapter five, it was described that shallow velocity profiles were obtained (mainly because of energy source used) and that they have been extrapolated to the required depth of 30 m.

The four sites modeled using the seismic refraction data show stiffer characteristics (shorter natural periods). Consequently, the amplification potential observed at these sites is lower when compared with geotechnical profiles. PGA values of 0.26, 0.19, 0.24 and 0.25 are experienced at the Ayat site, the CMC site, the Bole site and the Jemmo site respectively.

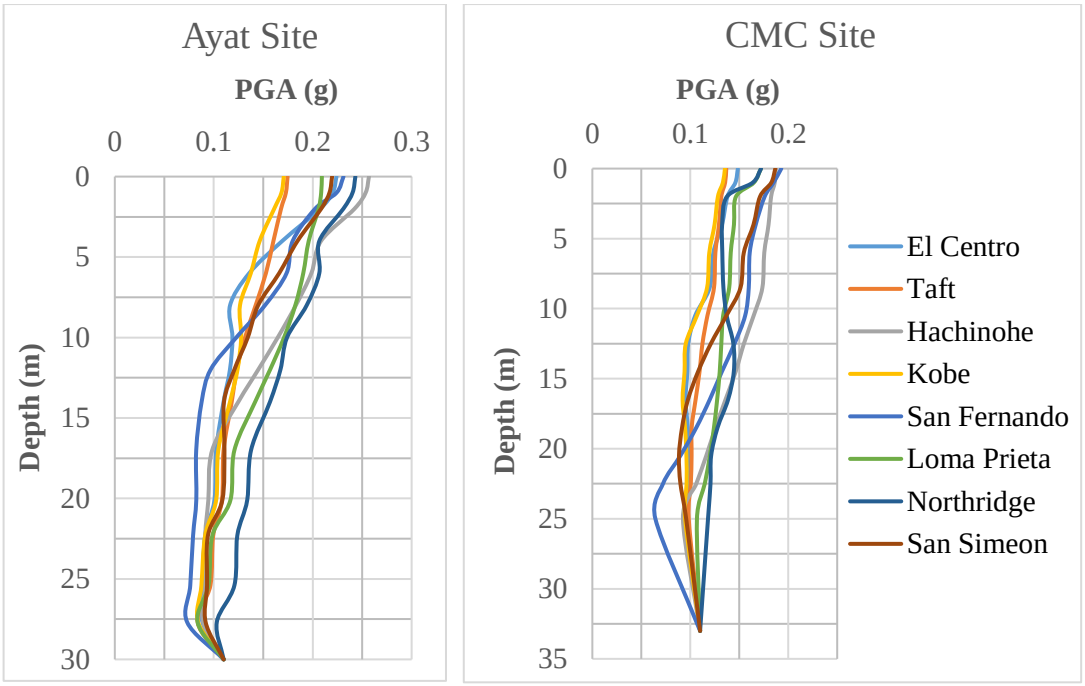

(a)

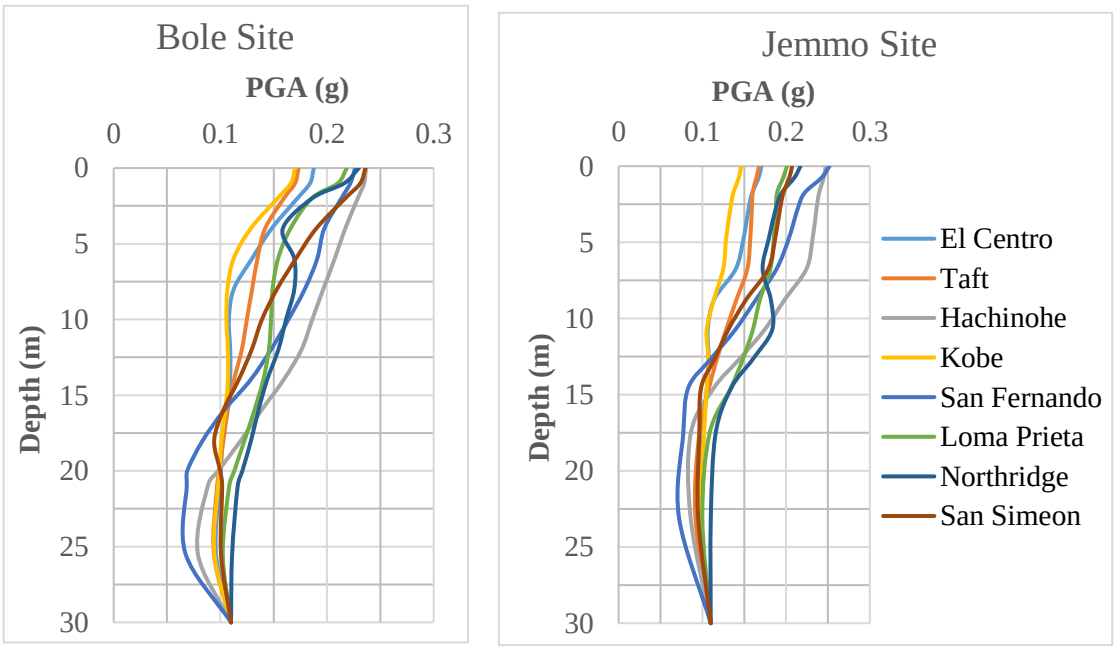

(b)

Figure 6.6 Peak ground acceleration (PGA) profiles using seismic refraction data: Ayat and CMC sites (a); Bole and Jemmo sites (b)

6.3.3 Fourier Amplitude Spectra

The tendency of the modeled soil profiles to amplify the input ground motions can plainly be detected from graphical representation of Fourier amplitude spectra. This method of characterizing motions at the ground surface provides clear understanding into the frequency content of motions and the way they are affected as they propagate to the ground surface. The plots of distribution of Fourier amplitude (as a ratio of Fourier amplitude of a motion at the ground surface to the Fourier amplitude of the motion at the base of the profile) with frequency content are depicted in Figures 6.7 and 6.8.

As discussed in the previous subsections, the fundamental natural periods of profiles from the seismic refraction survey demonstrate short periods (and hence high frequencies). The Fourier amplitude spectra obtained from these profiles show more or less lower peaks at higher frequencies (as compared to the spectra found from the geotechnical data). These plots (Appendix C) do have inconsistent feature with the corresponding plots from geotechnical data as a result of the disagreeable data acquired from the two methods.

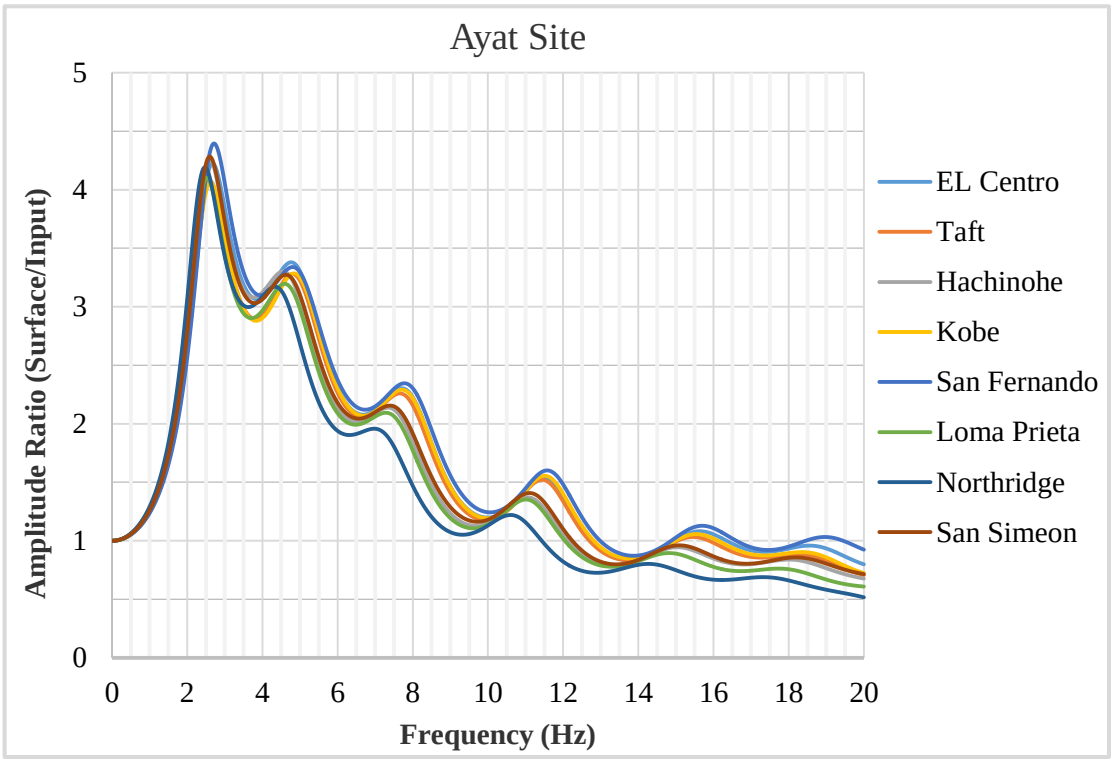

(a)

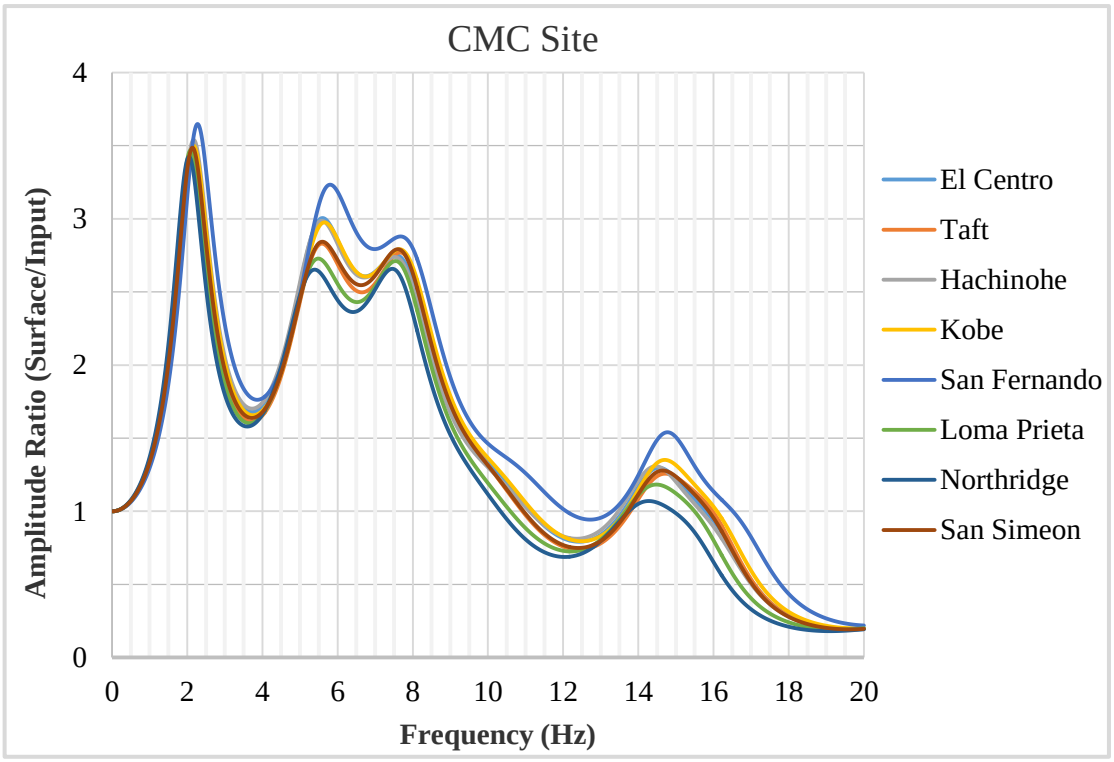
CMC Site
Amplitude Ratio (Surface/Input)
Frequency (Hz)
0
1
2
3
4
0
2
4
6
8
10
12
14
16
18
20
El Centro
Taft
Hachinohe
Kobe
San Fernando
Loma Prieta
Northridge
San Simeon

(b)

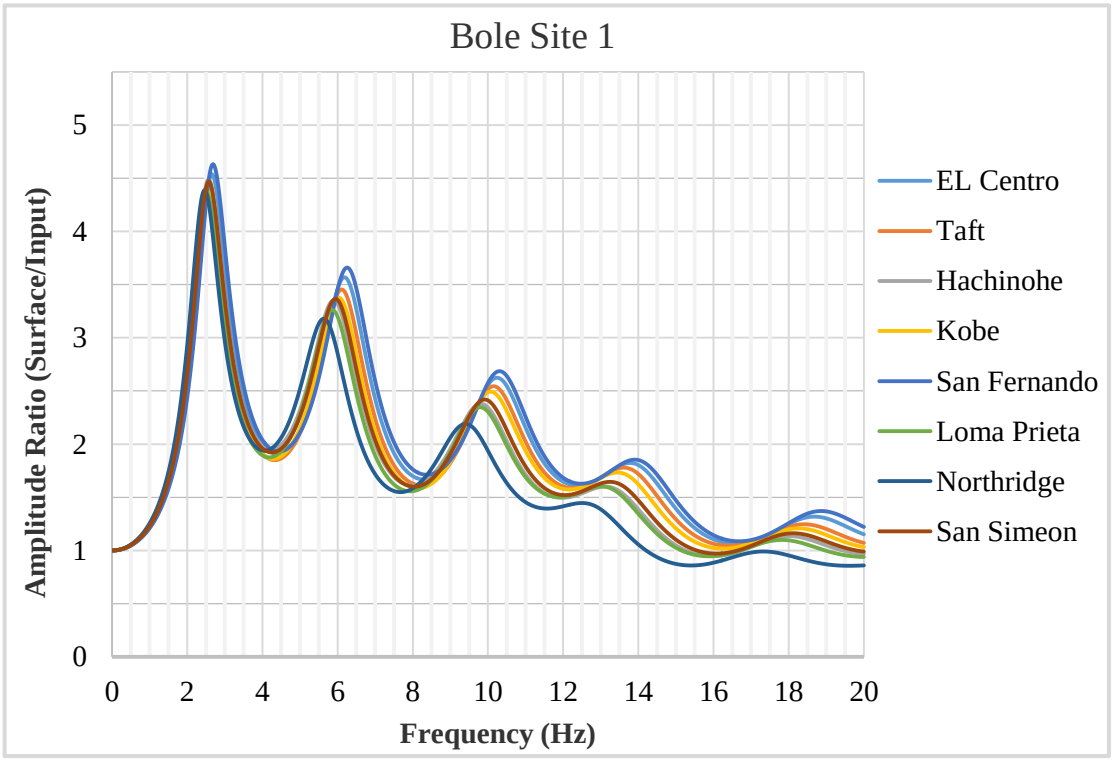
Bole Site 1
Amplitude Ratio (Surface/Input)
Frequency (Hz)
0
1
2
3
4
5
0
2
4
6
8
10
12
14
16
18
20
EL Centro
Taft
Hachinohe
Kobe
San Fernando
Loma Prieta
Northridge
San Simeon

(c)

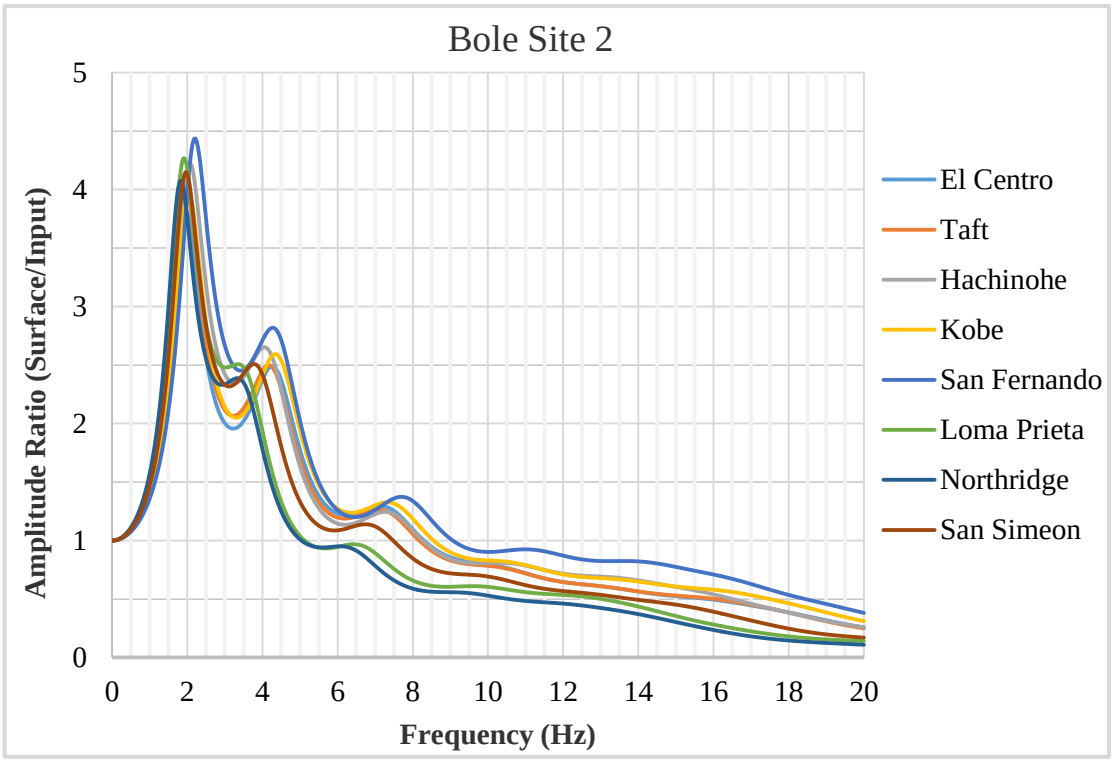
Bole Site 2
Amplitude Ratio (Surface/Input)
Frequency (Hz)
0
1
2
3
4
5
0
2
4
6
8
10
12
14
16
18
20
El Centro
Taft
Hachinohe
Kobe
San Fernando
Loma Prieta
Northridge
San Simeon

(d)

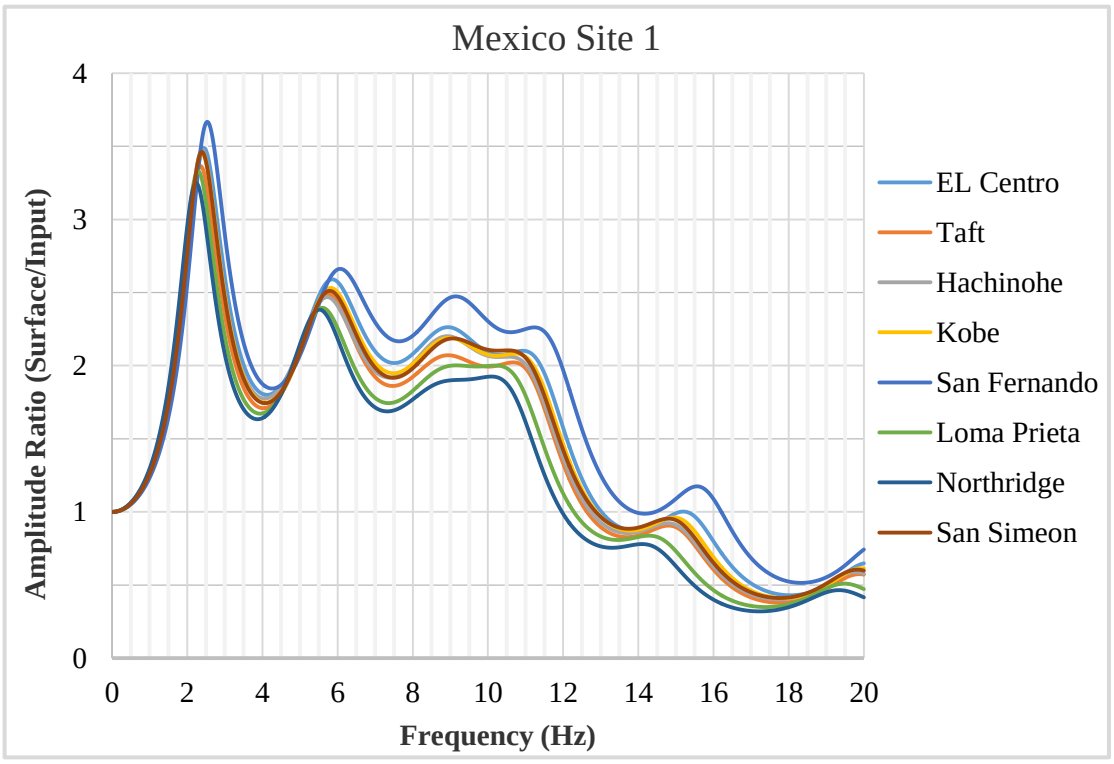
Mexico Site 1
Amplitude Ratio (Surface/Input)
Frequency (Hz)
0
1
2
3
4
0
2
4
6
8
10
12
14
16
18
20
EL Centro
Taft
Hachinohe
Kobe
San Fernando
Loma Prieta
Northridge
San Simeon

(e)

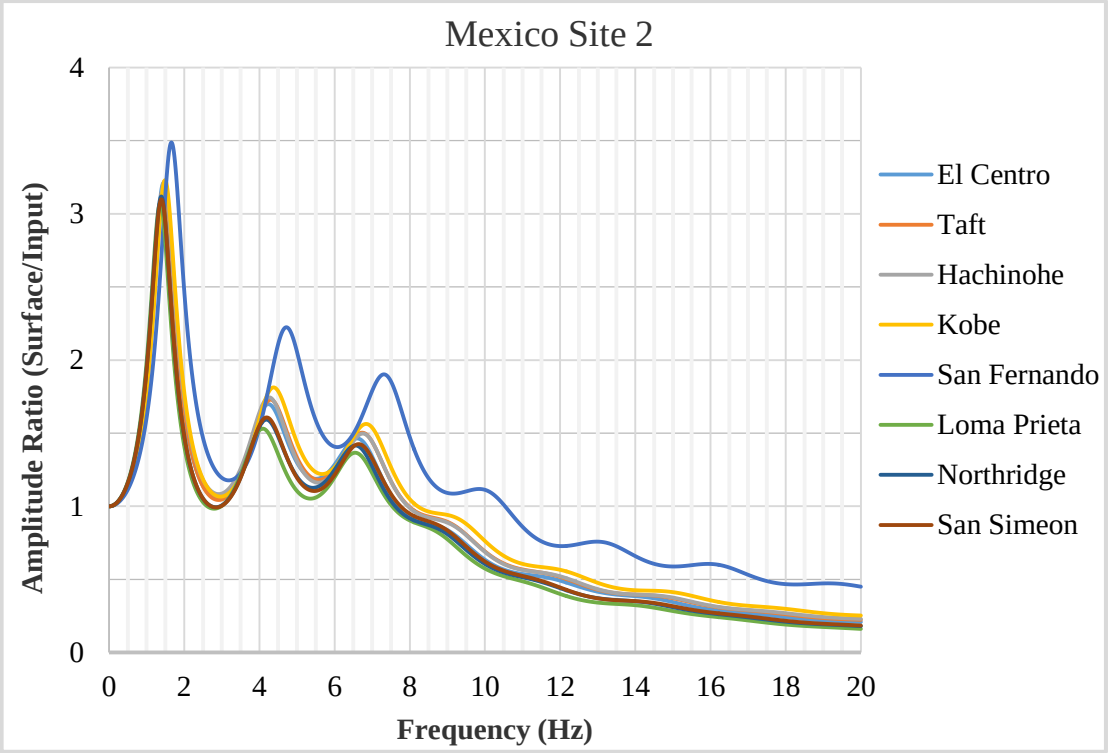

(f)

Figure 6.7 Fourier amplitude spectra (surface to input ratios) at the ground surface using geotechnical data: for Ayat site (a); for CMC site (b); for Bole site 1 (c); for Bole site 2 (d); for Mexico site 1 (e) and for Mexico site 2 (f)

Significant amplification ranging from about 3.5 to 4.5 times the Fourier amplitude of the input ground motions is observed at the ground surface of the above sites. Of all these sites, much greater amplification is observed at sites which comprise comparatively medium thickness of soft soil formation underlain by hard (usually rock) formation. The peak values are obtained at a frequency closer to the predominant frequency (or predominant period) of the profile irrespective of the ground motions.

A closer look at the consecutive curves gives two unique features that turn away from the coherent characteristics presented. The first feature is that the San Fernando earthquake ground motion shows highest peaks of all the motions at all site profiles. This appears to happen because of the fact that the ground motion has uniquely lower Fourier amplitude around the predominant period of the sites (Figure 4.10). The second notable inconsistent feature is that the local peaks at the CMC site and the Mexico site 1 are observed at their second and third natural frequencies. This also seems to occur as a result of the presence of the ignimbrite layers at different depths of the profiles.

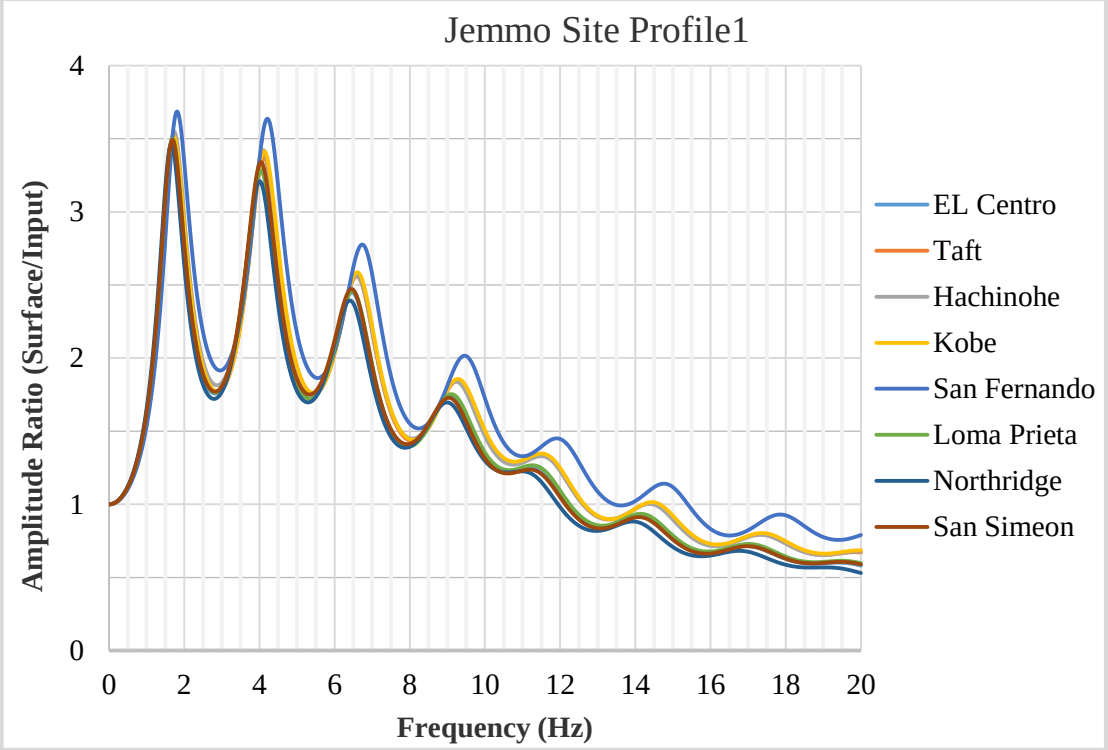

(a)

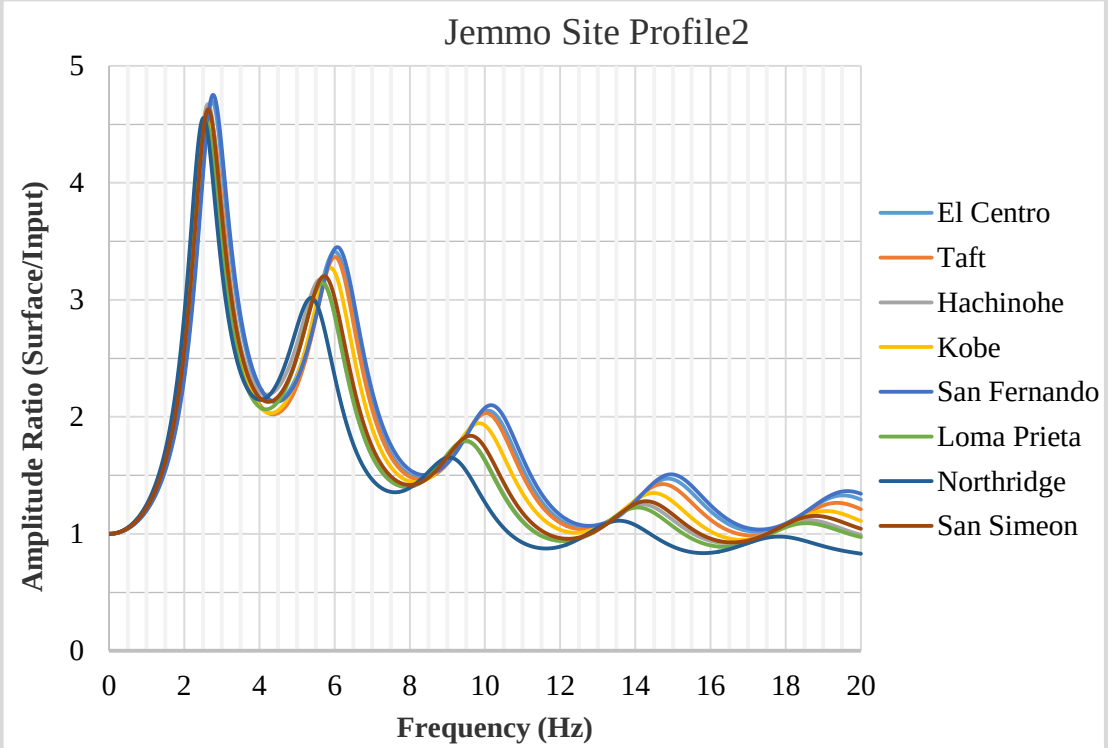

(b)

Figure 6.8 Fourier amplitude spectra (surface to input ratios): for Jemmo site profile 1 (a) and for Jemmo site profile 2 (b)

Figure 6.8 also shows that the soil profiles at Jemmo site demonstrate consistent amplification of the input motions by more than threefold at profile 1 and by more than fourfold at profile 2 at the ground surface. As usual, maximum amplification occurs at the predominant natural periods of the profiles. The effect of the presence of hard stratum (ignimbrite) at about 19 meters depth in profile 2 is found to show substantial amplification in comparison with another profile that consists of 40 meters thick soft soil.

Variations of the Fourier amplitude spectra characteristics with depth becomes essential when it comes to interaction of engineering structures with soil. Structures are rarely constructed on the ground surface. Figures 6.9 show the variation of Fourier amplitude spectra with depth for the CMC site, the Bole site and the two profiles of Jemmo site. Because of the consistent patterns observed in the results from all ground motions and the need to show succinct graphical presentation, statistical average values were used to draw the variations.

The four representative profiles present an amplification potential of greater than two-fold at a depth of about 10 meters below the natural ground level. The amplification is much important with profiles consisting of thick soft soil formations such as Jemmo site profile 1 (twice at 17 meters depth).

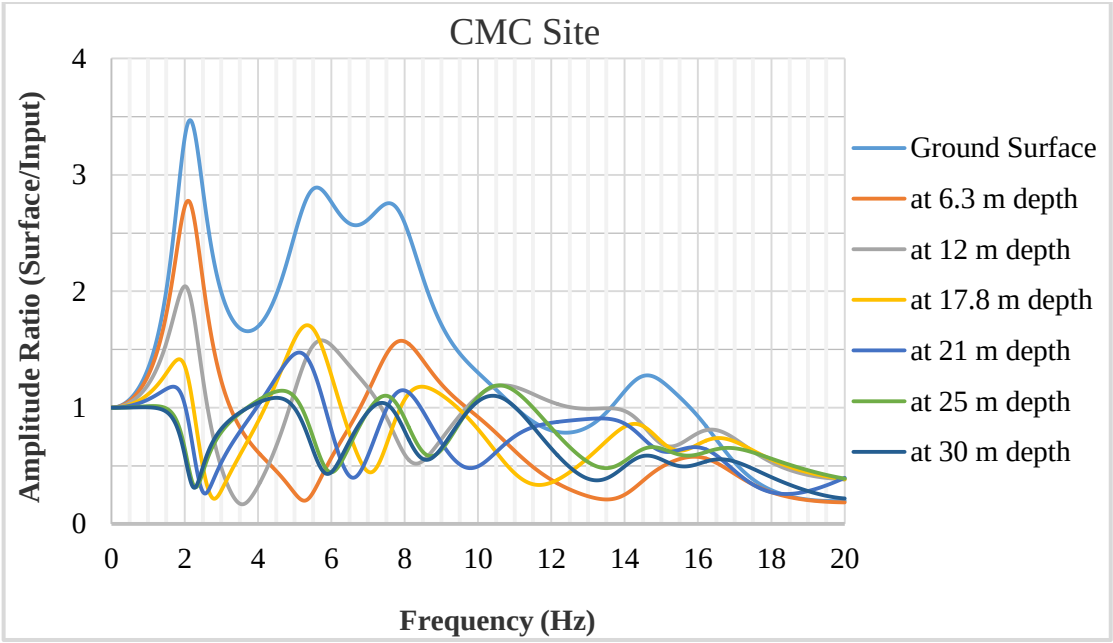

(a)

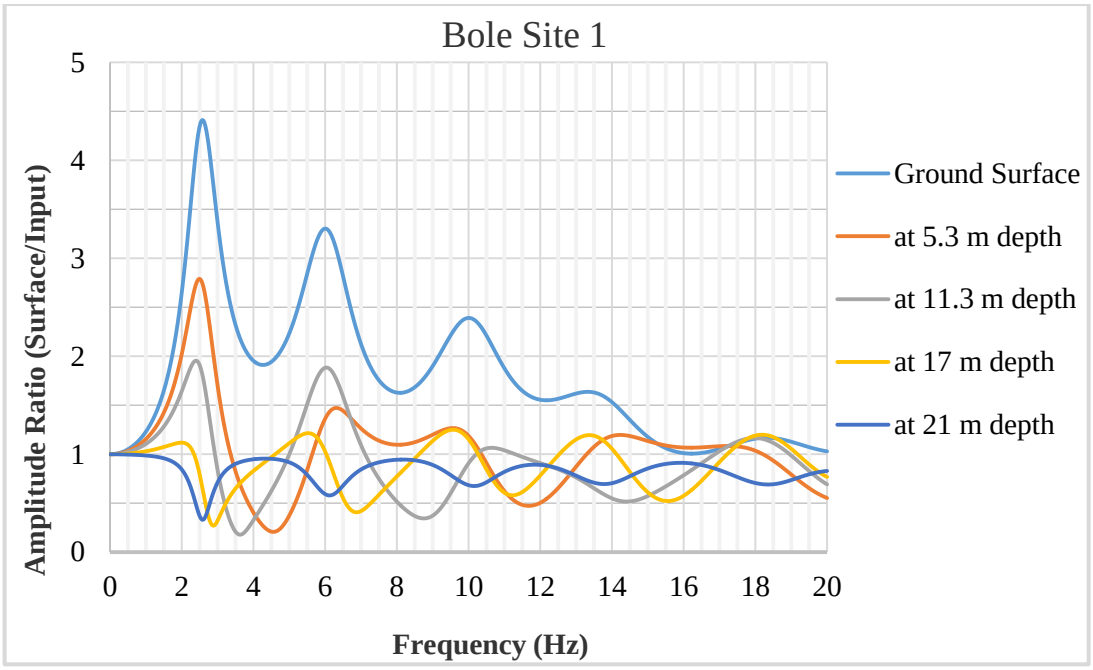
Bole Site 1
Amplitude Ratio (Surface/Input)
Frequency (Hz)
Ground Surface
at 5.3 m depth
at 11.3 m depth
at 17 m depth
at 21 m depth

(b)

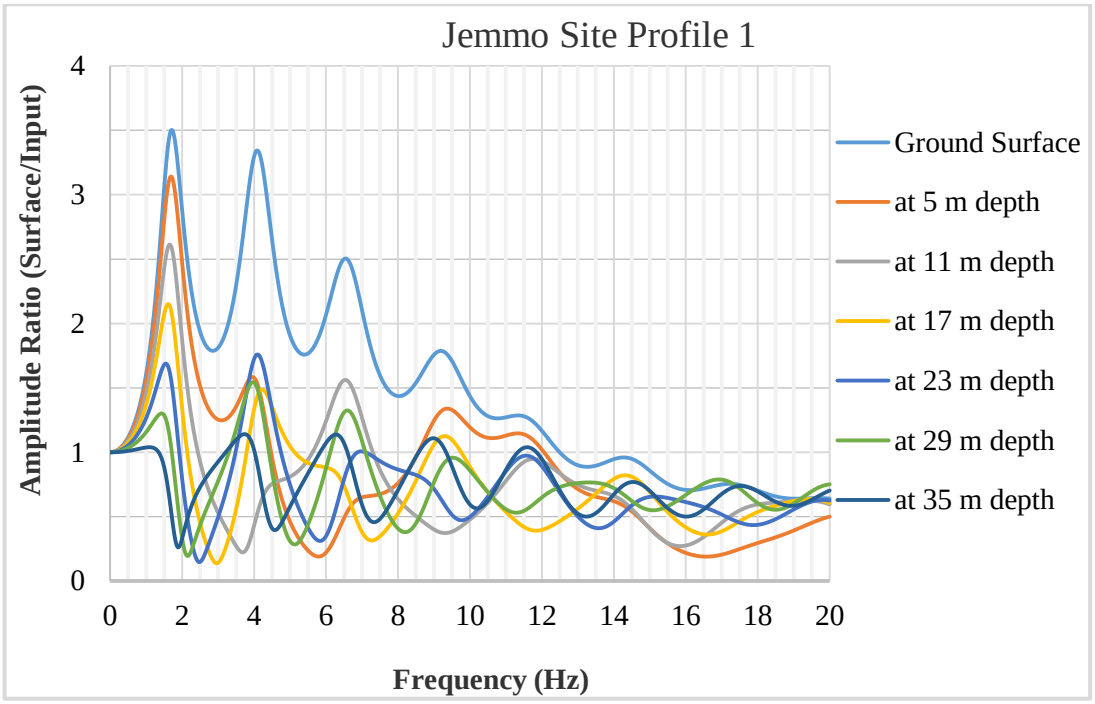
Jemmo Site Profile 1
Amplitude Ratio (Surface/Input)
Frequency (Hz)
Ground Surface
at 5 m depth
at 11 m depth
at 17 m depth
at 23 m depth
at 29 m depth
at 35 m depth

(c)

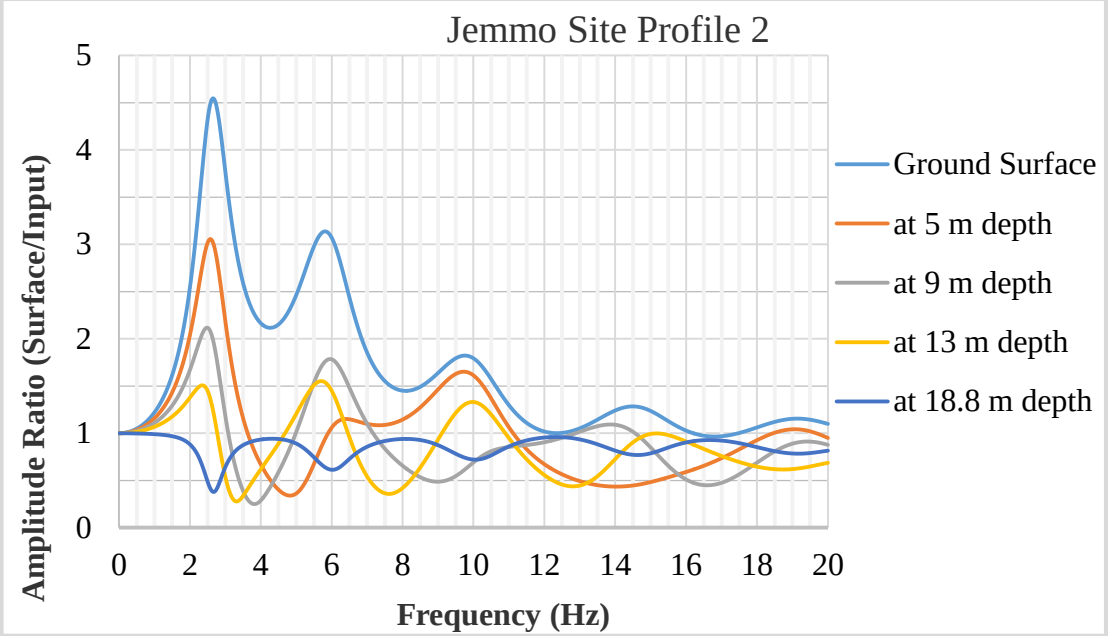

(d)

Figure 6.9 Fourier amplitude spectra variations with depth: for CMC site (a); for Bole site1 (b); for Jemmo site profile1 (c) and for Jemmo site profile 2 (d)

6.3.4 Response Spectra

The response of a single-degree-of-freedom (SDOF) system to a particular input motion (in this case, motions at the ground surface) as a function of natural frequency (or natural period) is another way of presenting output motion from ground response analyses. Response spectra curves shown in Figures 6.10 and 6.11 represent the response of SDOF systems to ground surface motions from ground response analyses (using geotechnical data) at the selected sites.

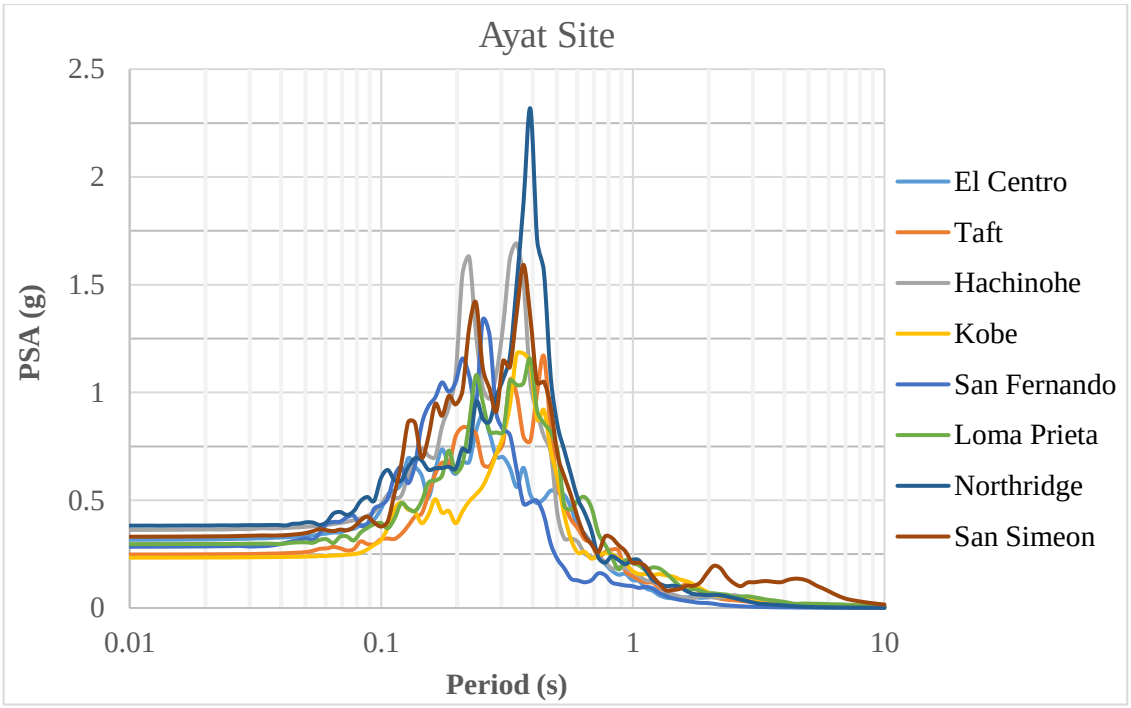
Ayat Site
2.5
2
1.5
1
0.5
0
PSA (g)
0.01
0.1
1
10
Period (s)
El Centro
Taft
Hachinohe
Kobe
San Fernando
Loma Prieta
Northridge
San Simeon

(a)

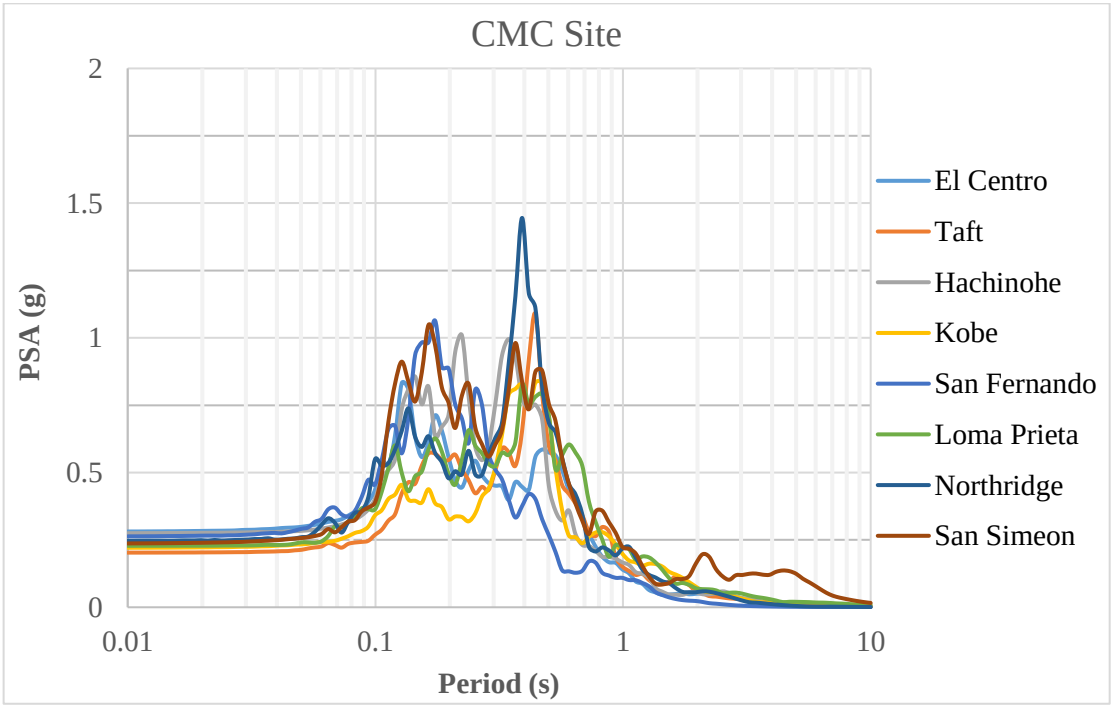
CMC Site
2
1.5
1
0.5
0
PSA (g)
0.01
0.1
1
10
Period (s)
El Centro
Taft
Hachinohe
Kobe
San Fernando
Loma Prieta
Northridge
San Simeon

(b)

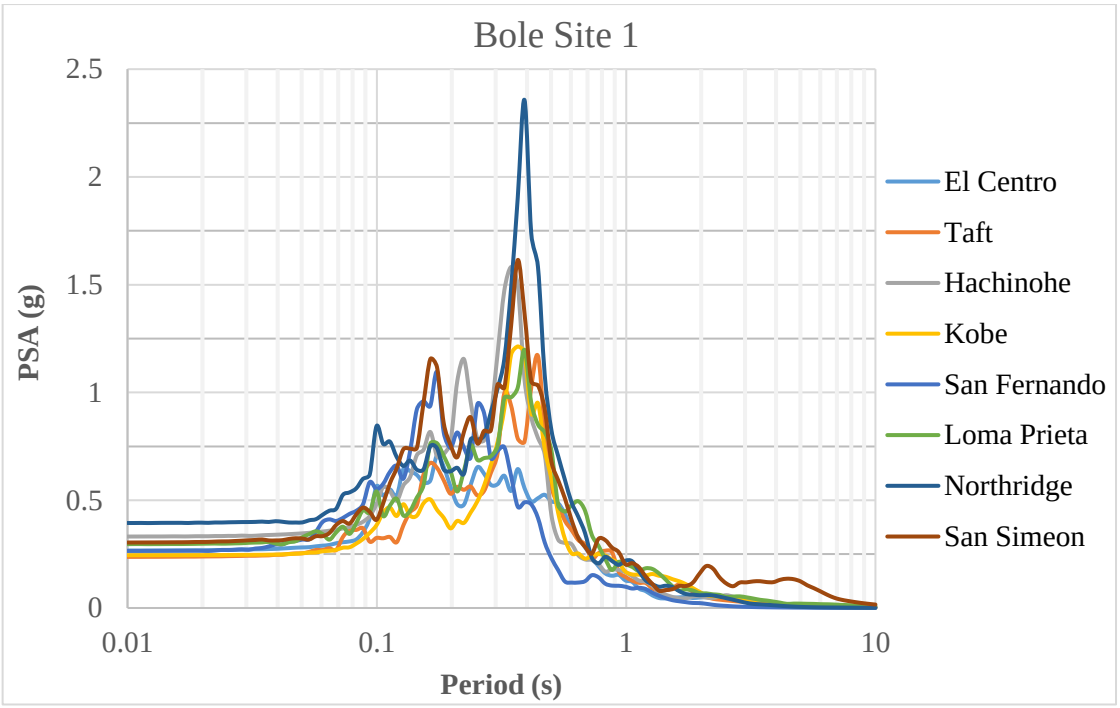
Bole Site 1
2.5
2
1.5
1
0.5
0
PSA (g)
0.01
0.1
1
10
Period (s)
El Centro
Taft
Hachinohe
Kobe
San Fernando
Loma Prieta
Northridge
San Simeon

(c)

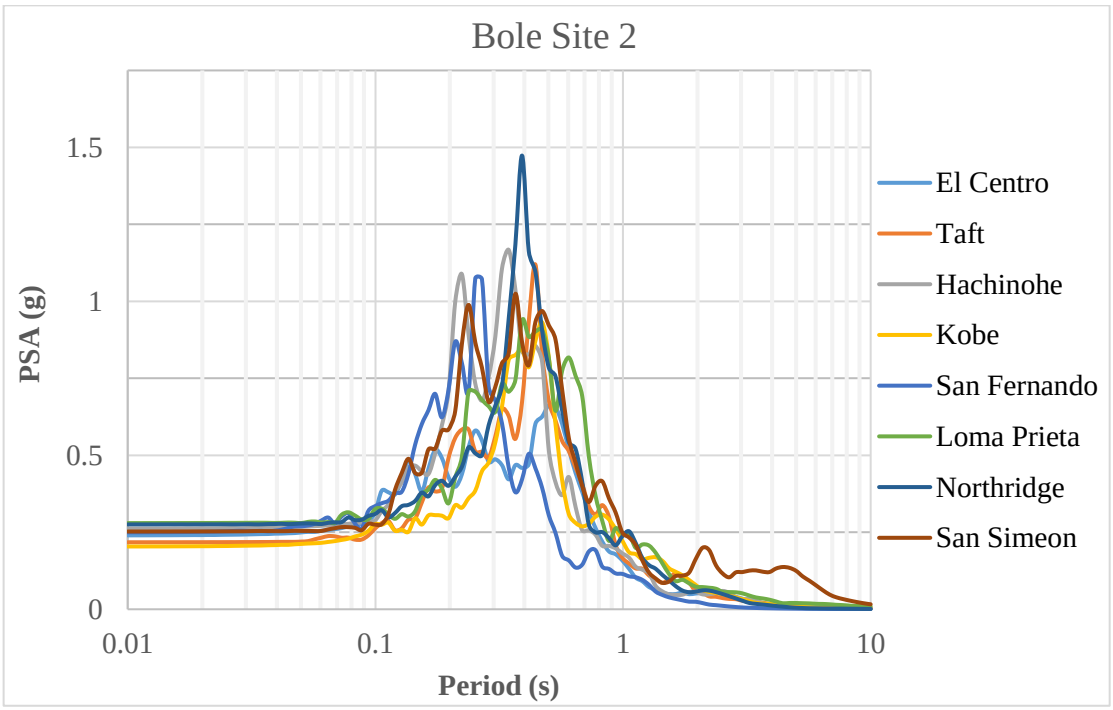
Bole Site 2
1.5
1
0.5
0
PSA (g)
0.01
0.1
1
10
Period (s)
El Centro
Taft
Hachinohe
Kobe
San Fernando
Loma Prieta
Northridge
San Simeon

(d)

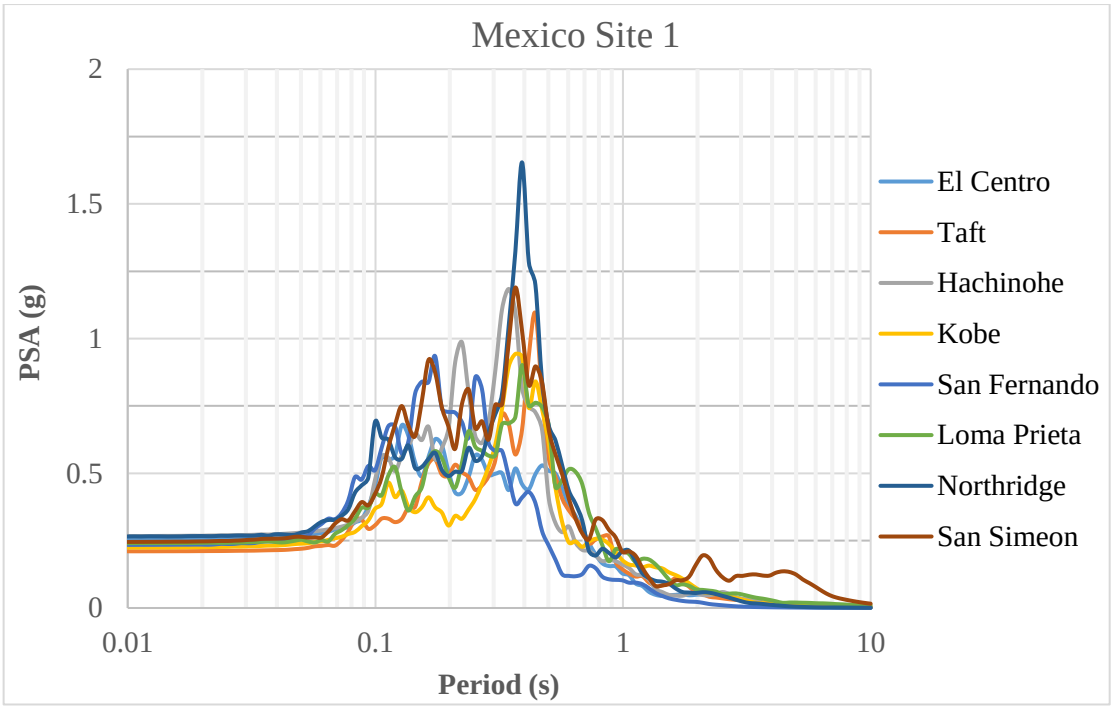

(e)

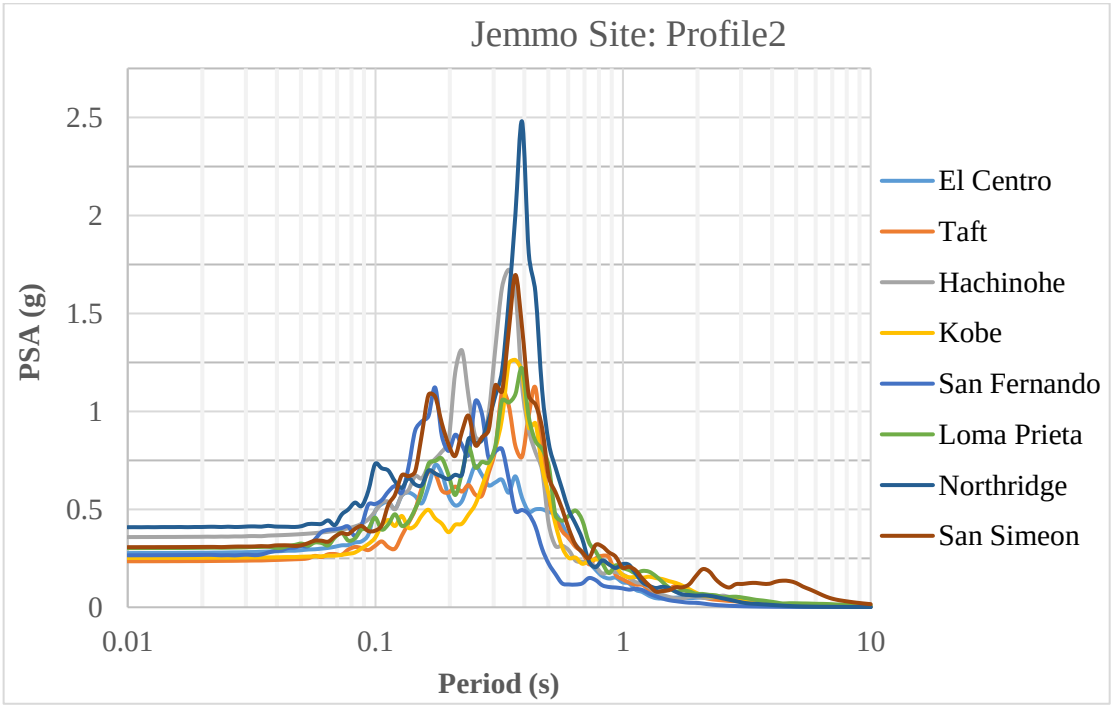

(f)

Figure 6.10 Response spectra from geotechnical data: for Ayat site (a); for CMC site (b); for Bole site 1 (c); for Bole site 2 (d); for Mexico site 1 (e) and for Jemmo site profile 2 (f)

As one glances at these curves, he/she right away finds out the substantial amplification obtained at all sites (omitting Mexico site 2 and Jemmo site profile 1) from the Northridge earthquake ground motion. This significant amplification ranges from PSA of 1.45 g at Bole site 2 to PSA of 2.5g at Jemmo site profile 2. The amplification occurs at a period of about 0.4 sec which is associated due to the fact that Northridge ground motion has ample Fourier amplitude than others near this period (Figure 4.10). The Hachinohe and the San Simeon ground motions possess moderate potential of amplification at these sites for this very reason.

On the other hand, Mexico site 2 and Jemmo site profile 1 which have longer predominant natural periods compared to the remaining sites (0.56 sec and 0.66 sec respectively) do not experience such a significant amplification when analyzed by using Northridge ground motion. Hachinohe, San Simeon, Loma Prieta and San Fernando motions provide higher peaks, instead (Figure 6.11). Variation of response spectra with depth for Jemmo site profile 1 is shown in Figure 6.11c.

Generally, the selected sites show consistent and fairly large amplifications that well exceed a PSA value of 1g. The least amplification is observed at Mexico site 2, which still experienced PSA of up to 0.75g.

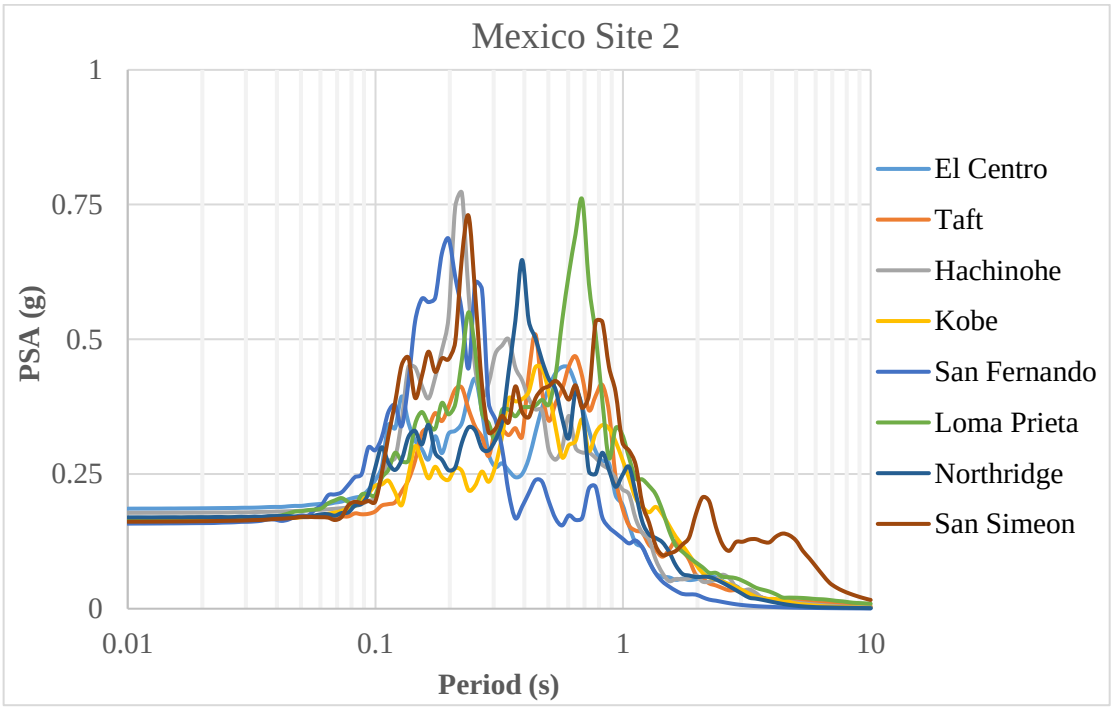

(a)

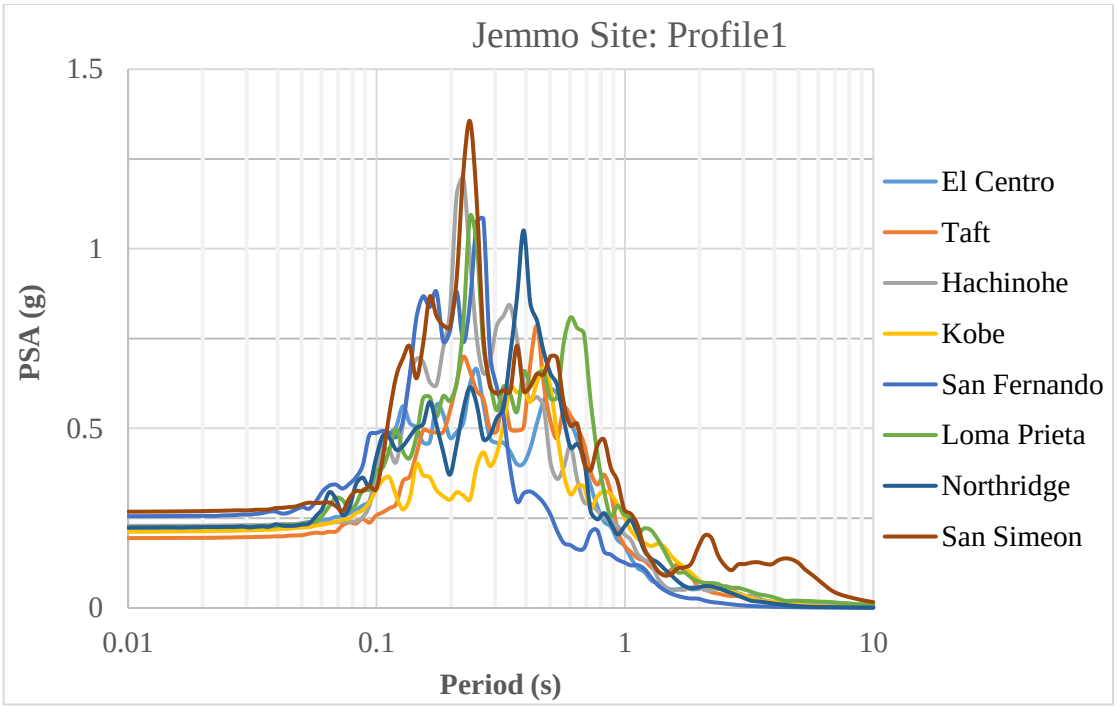

(b)

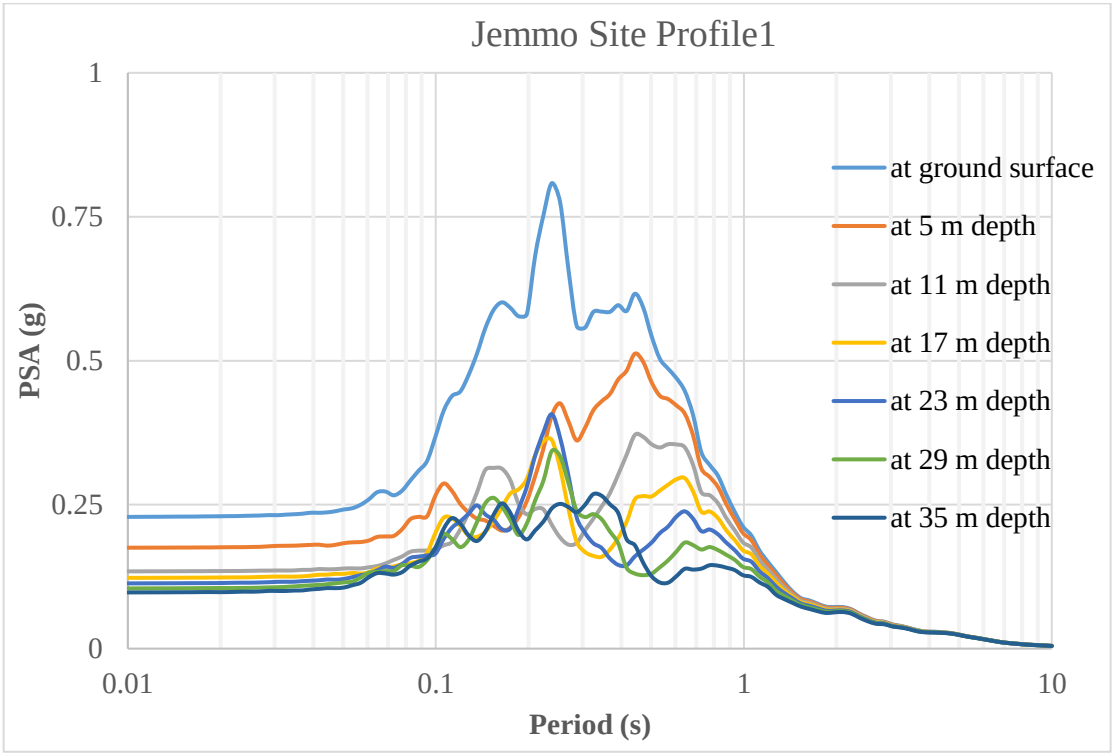

(c)

Figure 6.11 Response spectra from geotechnical data: for Mexico site 2 (a); Jemmo site profile 1 (b) and variation of response spectra with depth for Jemmo site profile 1 (c)

In a similar fashion as the case with PGA profile and Fourier amplitude spectra trends, the resulting response spectra from the seismic refraction survey data indicate lesser amplification potential in comparison with the geotechnical data. The four site profiles possess maximum spectral amplifications of lower than 1.25g (except at the Ayat site, when it is analyzed with the Northridge earthquake ground motion). The spectral plots are depicted in Figure 6.12.

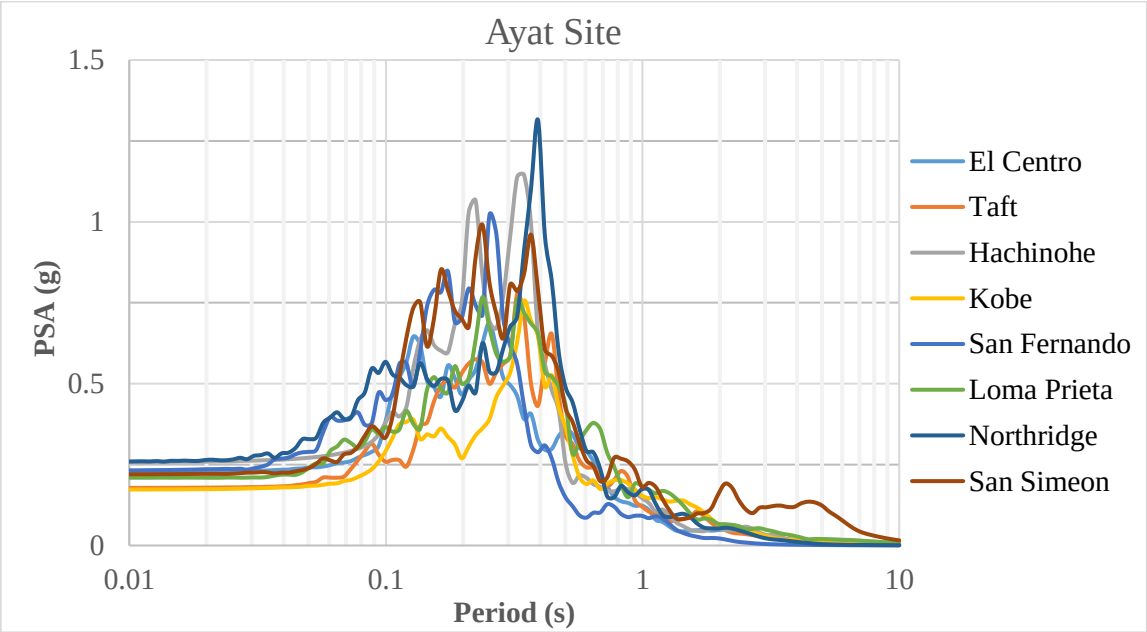

(a)

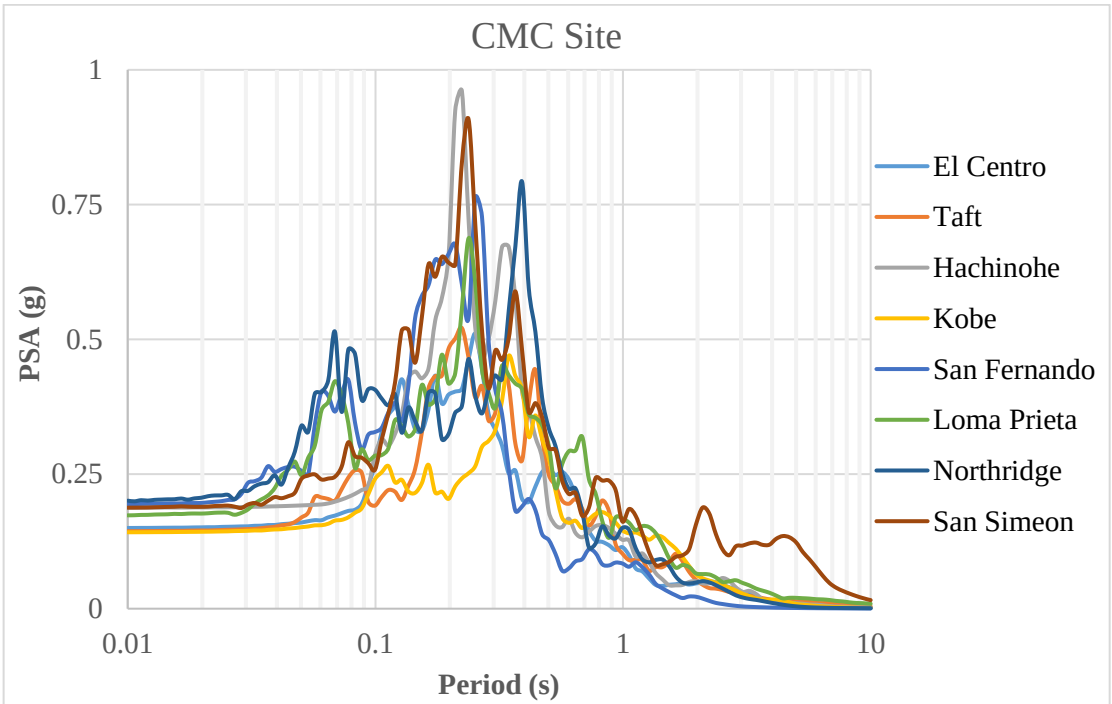

(b)

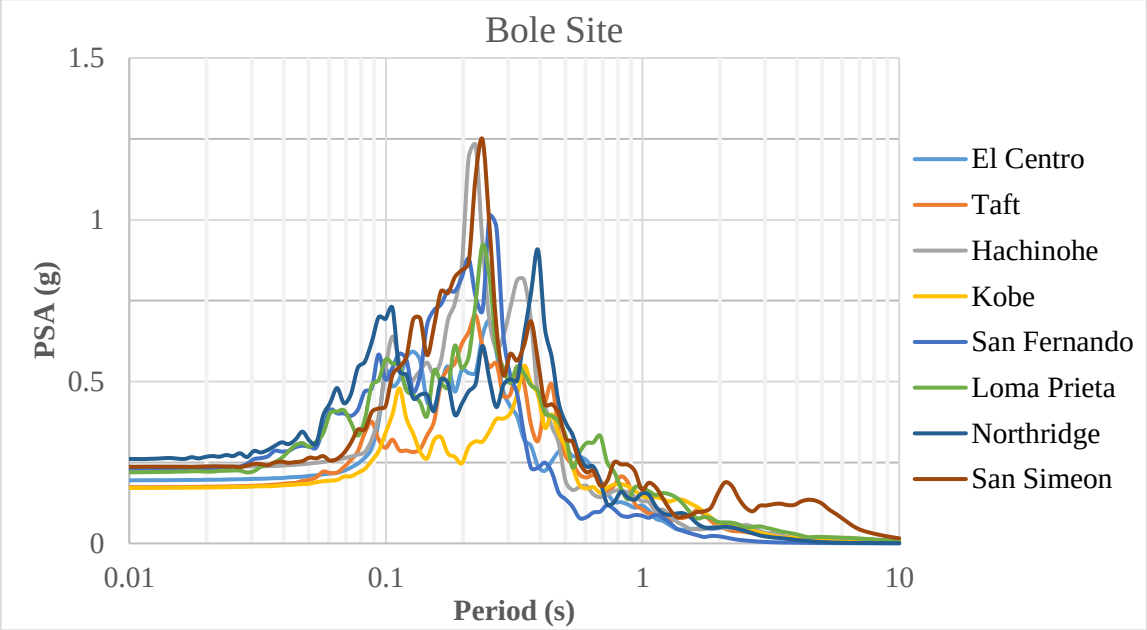

(c)

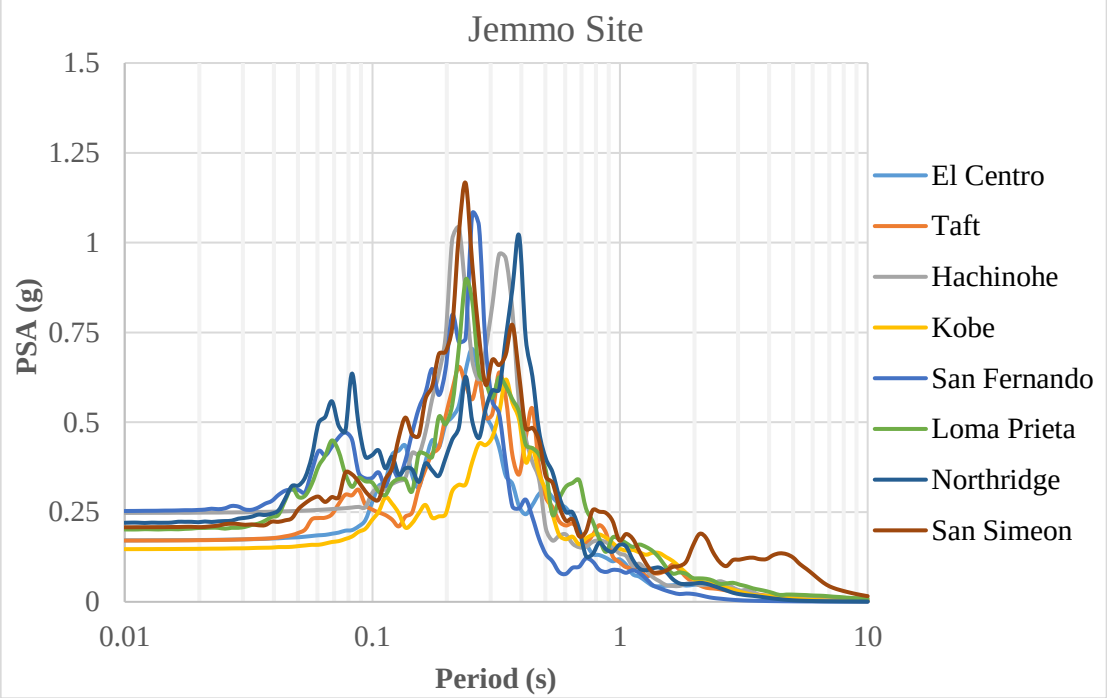

(d)

Figure 6.12 Response spectra from seismic refraction survey data: for Ayat site (a); for CMC site (b); for Bole site (c) and for Jemmo site (d)

6.4 Comparison of Mean Response Spectrum with Code-Specified Spectra

For the reason that the selected sites possess distinct soil formation (as explained in details in the previous subsections), a separate comparison of the response spectrum of each site with the code-specified spectra is found to be important. Figure 6.13 shows this comparison considering both the geotechnical and the seismic refraction data. The Ayat, Bole and Jemmo sites significantly affect ground motions and higher amplification is observed at periods up to about 0.7 sec. The amplification trends from the geotechnical and the seismic refraction data appear to be similar with the exception that much larger amplification is obtained from the geotechnical data at short periods (below about 1 sec). From figure 6.13, it is clear that this substantial amplification potential (observed almost at all sites) is severely underestimated by the currently applicable code provisions.

CMC site, associated with the existence of the ignimbrite and the basalt layers at different depths, can be described by a comparatively lesser amplification. On the other hand, sites consisting of soft soil formations (such as Mexico site 2 and Jemmo site profile 1; presented in Appendix C) show relatively higher amplification at longer periods but with less potential at short periods.

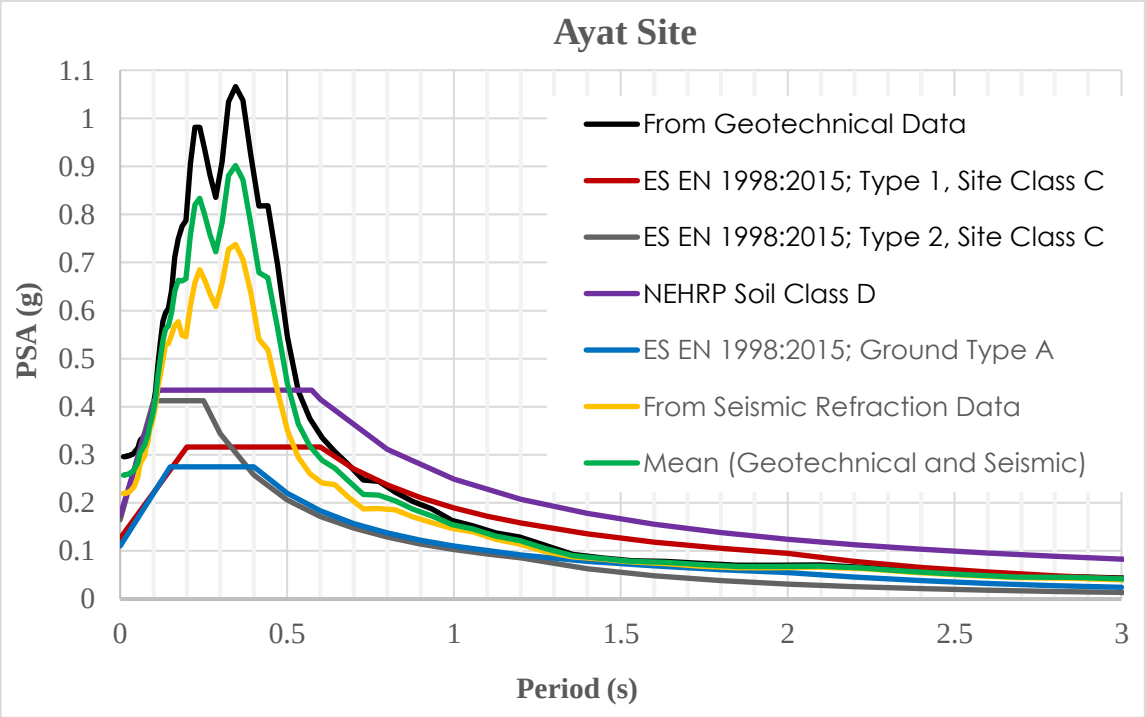

(a)

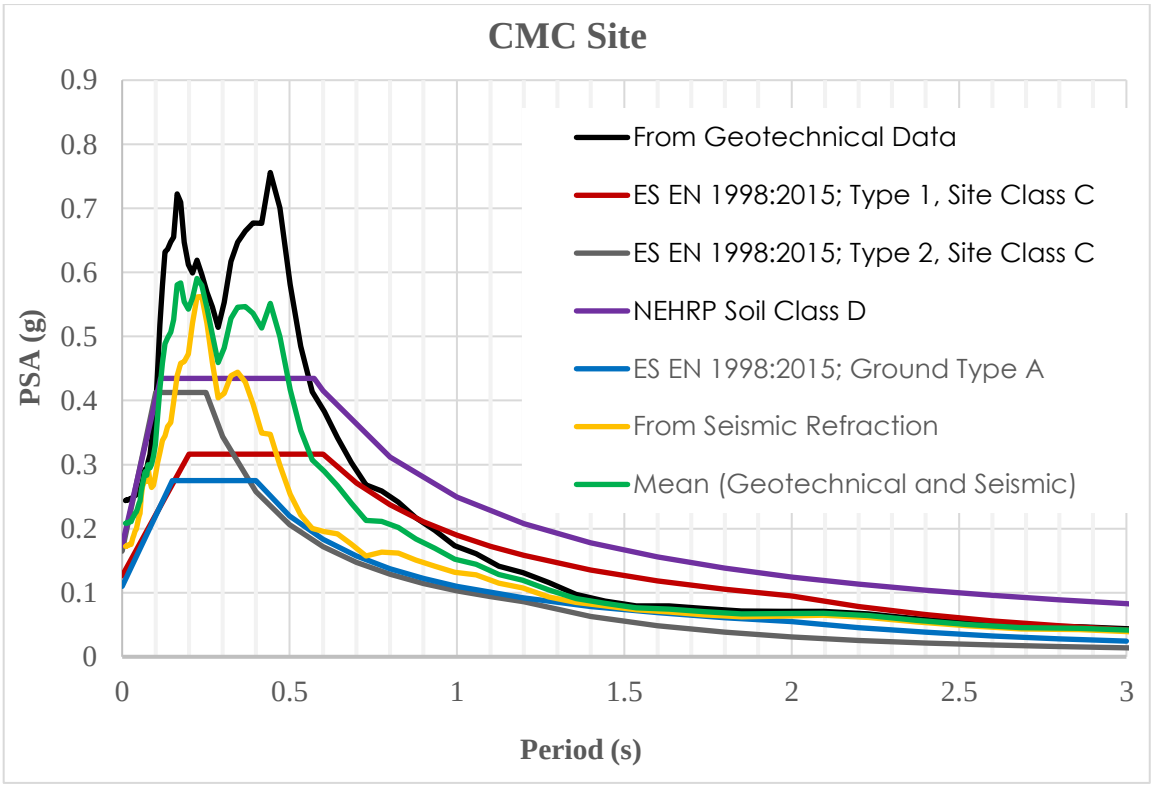
CMC Site
PSA (g)
Period (s)
From Geotechnical Data
ES EN 1998:2015; Type 1, Site Class C
ES EN 1998:2015; Type 2, Site Class C
NEHRP Soil Class D
ES EN 1998:2015; Ground Type A
From Seismic Refraction
Mean (Geotechnical and Seismic)

(b)

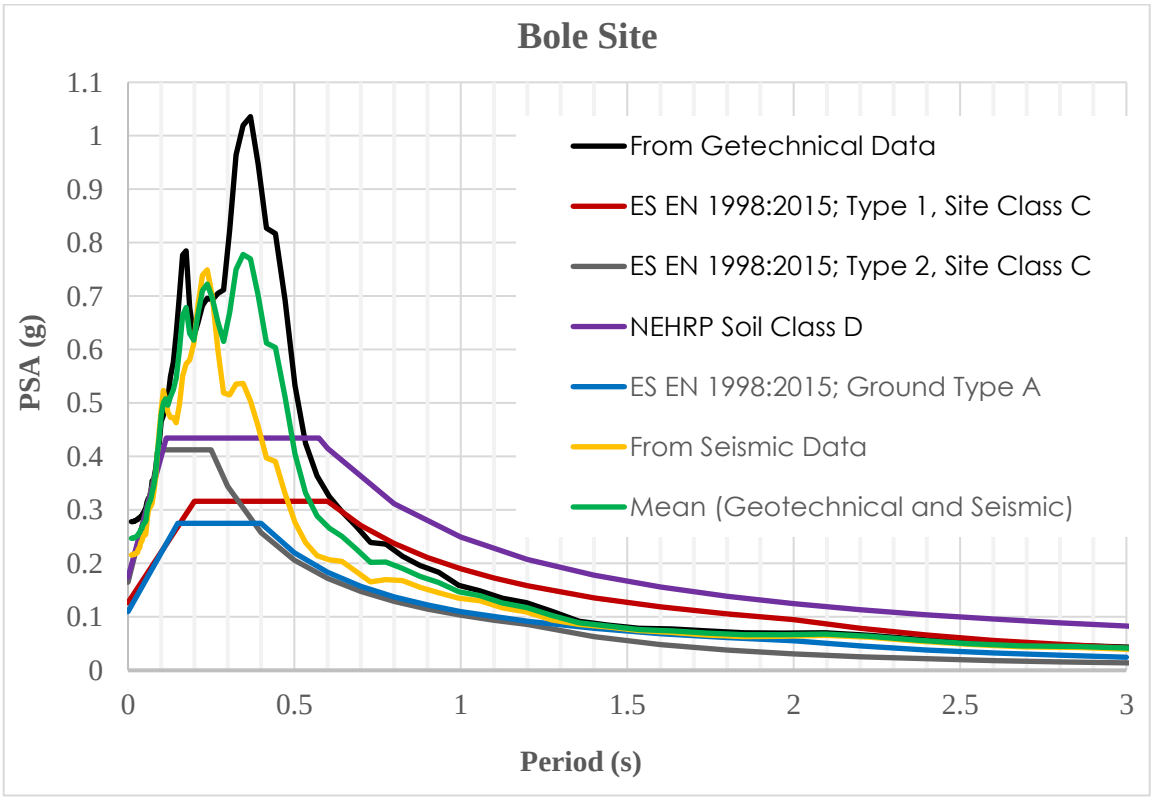
Bole Site
PSA (g)
Period (s)
From Getechnical Data
ES EN 1998:2015; Type 1, Site Class C
ES EN 1998:2015; Type 2, Site Class C
NEHRP Soil Class D
ES EN 1998:2015; Ground Type A
From Seismic Data
Mean (Geotechnical and Seismic)

(c)

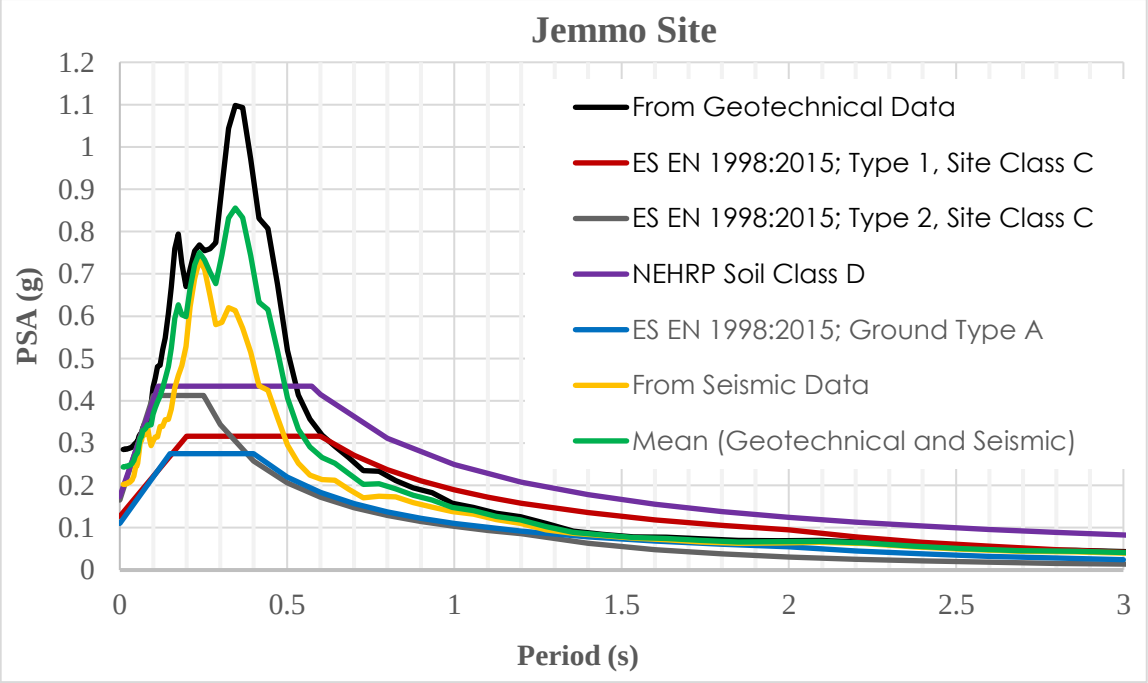

(d)

Figure 6.13 Response spectra of: (a) Ayat site, (b) CMC site, (c) Bole site1 and (d) Jemmo site profile 1 compared with code-specified spectra

For the general purpose of comparing and contrasting, the statistical mean of the response spectra at the ground surface has been computed for each profile and depicted in Figure 6.14. The computation (for profiles modeled using geotechnical data) was done by excepting the distinct and peak responses from Northridge ground motion. The mean peak amplification varies from PSA of about 0.5g (at Mexico site 2) to 1.1g (at Jemmo site profile 2) over a period range of 0.1 to 1.0 sec.

In the same way as the Fourier amplitude spectra, substantial amplification is perceived at Ayat, Bole site 1, and Jemmo site profile 1, for the same reason mentioned. Profiles composed of thick soft soil formations (hence longer natural period) like the Jemmo site profile 1, show higher amplification at longer periods: 0.6 -1.0 sec. The absolute mean response spectra also show that the PGA is amplified to 0.25g (more than twofold of the PGA) and the extreme effect is limited to a period range of 0.1 sec to 0.6 sec.

Because of the observed inconsistency in the acquired data from the two methods of investigation (and consequently inconsistent outputs), averaged response spectra from seismic refraction data were performed independently for the sake of comparing and contrasting results. Figure 6.15 shows the statistical mean of response spectra of the three sites (omitting the CMC site which falls under site class B of ES EN 1998:2015).

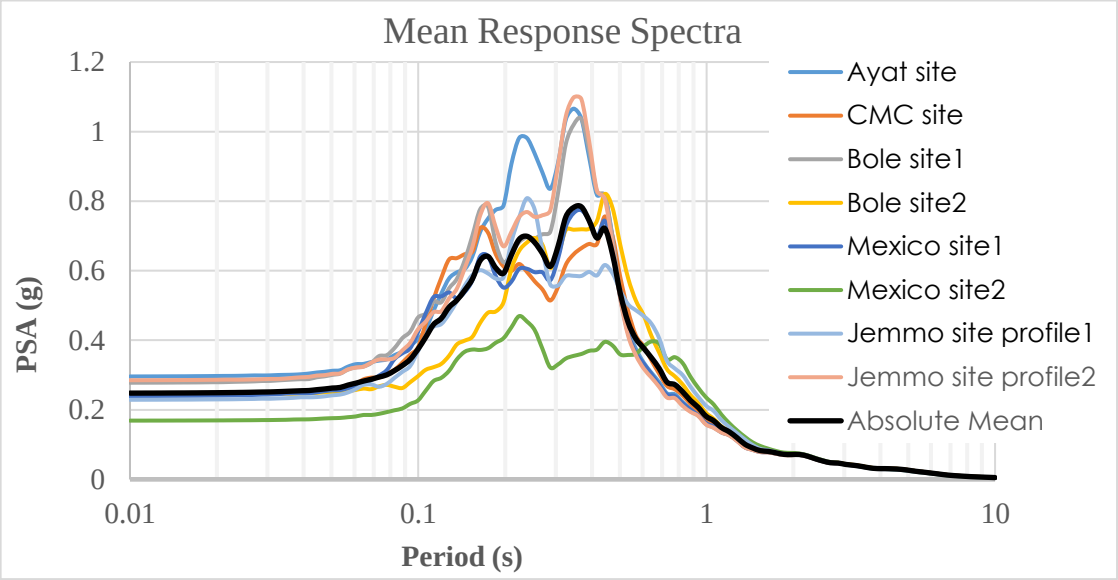

Figure 6.14 Statistical mean response spectra of the eight profiles (using geotechnical data) and the absolute mean response spectrum

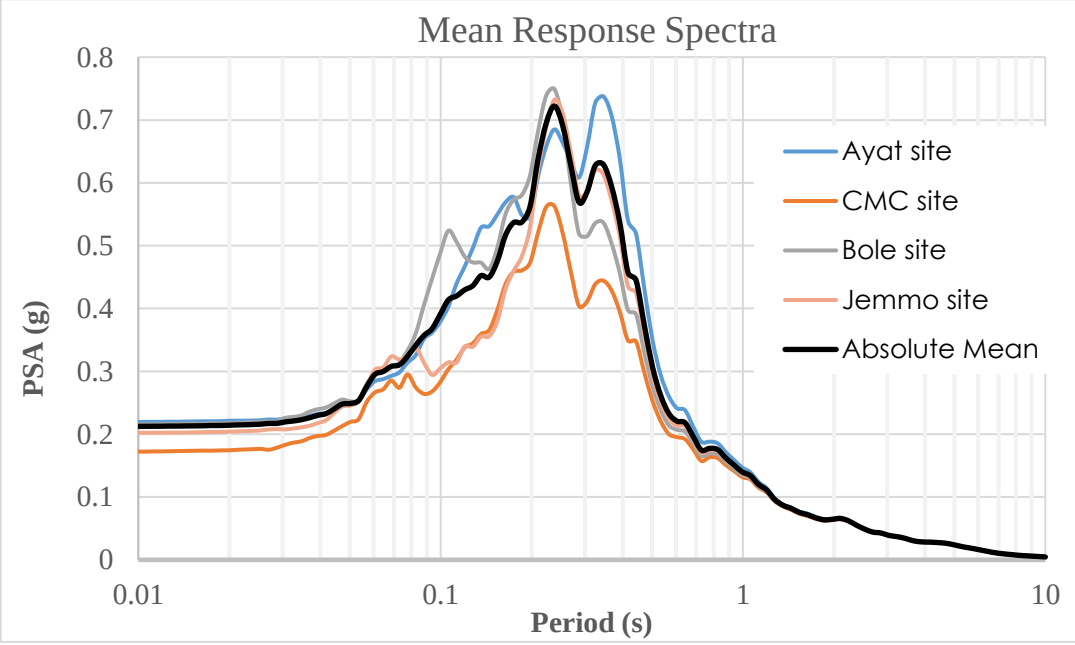

Figure 6.15 Statistical mean response spectra of the profiles (using seismic refraction data) and the absolute mean response spectrum of the three sites

It was previously mentioned that the selected sites were found to fall under “site class C” (using geotechnical data) as per the site classifications of ES EN 1998:2015 (or site class D in accordance with NEHRP code provision). Time-averaged shear wave velocity of the profiles considered in this response analysis varies from 215 - 275 m/s. Comparing the absolute mean of the response spectrum computed with that of site class C of ES EN 1998:2015 (both type 1 and type 2) and site class D of NEHRP, one can draw a number of interesting observations (Figure 6.16).

Both codes appear to critically underestimate the site effect at low periods. The PGA value of 0.11g that was found to represent the seismicity of Addis Ababa city (on ground type A) is amplified to 0.25g (at zero period) at the ground surface. At this period, however, the ES EN 1998:2015 (type 2 spectrum) and the NEHRP site class D provide lesser value of 0.17g and that of ES EN 1998:2015 (type 1 spectrum) gives even much lesser value of 0.13g.

In addition, NEHRP and ES EN 1998:2015 undervalue the absolute mean spectrum up to a period range of 0.55 sec and 1.0 sec, respectively. The deviation is found to be vital at low periods. The codes appear to render healthy predictions over periods greater than 1.0 sec.

The absolute mean response spectrum computed using seismic refraction data indicates lesser amplification and the amplification is restrained within the period range of 0.5 sec (when compared with ES EN 1998:2015; Type 1, Site Class C).

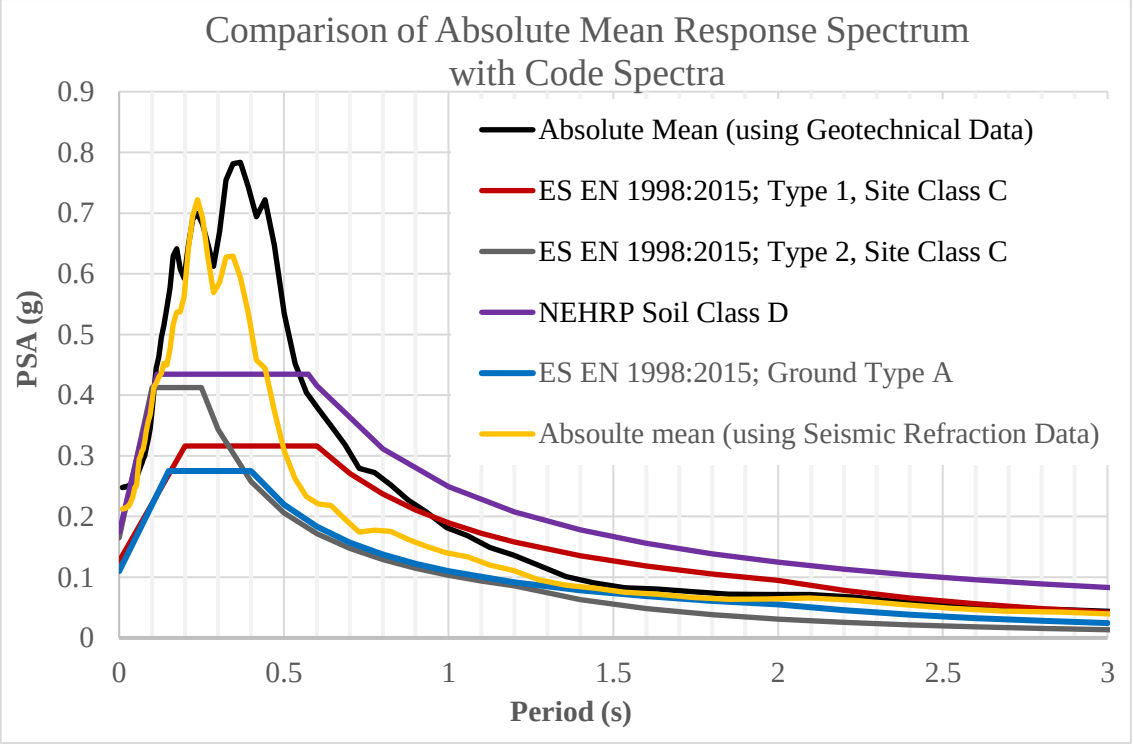

Figure 6.16 Comparison of absolute mean response spectrum with code-specified spectra

CHAPTER SEVEN

CONCLUSIONS AND RECOMMENDATION

7.1 Conclusions

To perform one-dimensional ground response analysis, soil data from geotechnical investigations and seismic refraction survey were collected at different locations basing certain filtering criteria. These data associated with the geological studies referred in this study show that the subsurface conditions within the city vary non-uniformly from site to site. Various types of slightly-to-moderately weathered rocks (such as ignimbrite, basalt and rhyolite) were encountered at different depths of several sites. Regardless of the presence of thin rock layer materials, the selected sites testify that thick soil formations exist in wide area of the city. Earthquake ground motions were principally selected from PEER ground motion database by considering the local geologic and tectonic conditions. Additional ground motions which have unique characteristics of motion parameters and which are customarily being used in engineering practices were included, as well.

Sites characterized using both the geotechnical and the seismic refraction data were employed to DEEPSOIL program of version v6.1 and were subjected to the selected input motions with EQL method of analysis. The following conclusions can be made related to the results.

- In spite of the inconsistency in data from the geotechnical and the seismic refraction sources, the eleven soil profile models (three from seismic refraction and eight from geotechnical data) have been found to fall under site class ‘C’ of ES EN 198:2015. The CMC site profile from seismic refraction data goes to site class ‘B’.
- Regarding to the justification of the threshold strain level (0.5%, Udaka (1983) as cited by Haile 1996) in the case of EQL method of analysis, more than 97% (94 analyses out of 96) of all analyses performed induce a strain value of well below 0.25% which most agrees with the suggestion.
- Ground motion characteristics are observed to be significantly affected by the soil formations of the selected sites. PGA values increase progressively

from the base of modeled profiles to the ground surface. Substantial potential of amplification at the ground surface is observed from geotechnical data (up to 0.41g). Still, profiles from seismic refraction data show amplification potential of greater than twofold (except at the CMC site).

- The Fourier amplitude spectra results of most profiles indicate that the proposed sites possess the potential to amplify input ground motions to three- to fourfold (yet some others show even more than this) at the ground surface. Sites comprising thick soft soil formations potentially amplify input motions even at greater depths below the ground level.
- A separate comparison of the response spectrum of the selected sites with the code-specified design spectra shows that the non-uniformity of the sites is also reflected in their potential of amplification. In spite of the variation in amplification extent, the current code-specified spectra are found to critically underestimate the existing condition.
- Comparing the mean response spectrum with that of the ES EN 1998:2015 site class 'C' (both Type 1 and Type 2) spectra, the code spectra were observed to critically underestimate the amplification potential of sites in the study area. The underestimation is even greater at short periods (periods of up to 1 sec).

7.2 Recommendation

In spite of the fact that the soil data and input ground motions used in the analysis have some limitations pertaining to quality and quantity, the investigation conducted on the amplification potential of selected sites in Addis Ababa city brings out that the soil formation of the city has significant potential of amplifying ground motions than the one specified in currently used code provisions. Accordingly, the result advocates intensive and city-wide investigation in order to come up with comprehensive appraisal.

REFERENCES

ASTM (American Society for Testing Materials). *Standard Guide for Using the Seismic Refraction Method for Subsurface Investigation (ASTM D 5777).* USA

Ayele, A. (2017). Probabilistic seismic hazard analysis (PSHA) for Ethiopia and the neighboring region. Journal of African Earth Sciences, 134, 257-264.

Bommer, J. J., Stafford, P. J., and Alarcon, J. E. (2009). "Empirical equations for the prediction of significant, bracketed and uniform duration of earthquake ground motion." *Bulletin of the Seismological Society of America,* 99(6), 3217-3233.

Boore, D.M. (2004). "Estimating $V_{s(30)}$ (or NEHRP Site Classes) from shallow velocity models (depths <30m)." *Bull. Seismo. Am.,* 94(2), 591-597.

Borcherdt, R.D. (1970). "Effects of local geology on ground motion near San Francisco Bay." *Bulletin of the Seismological Society of America,* 60, 29-61.

Briaud, J. L. (2013). *Geotechnical engineering: unsaturated and saturated soils*. Hoboken, New Jersey.

Budhu, M. (2011). *Soil mechanics and foundations.* USA

Chopra, A. K. (202). *Dynamics of structures*. Prentice Hall. Upper Saddle River

Darendeli, M. B. (2001). "Development of a new family of normalized modulus reduction and material damping curves." Ph.D. dissertation, University of Texas at Austin, Austin, TX.

Finn, W.D.L, Ventura, C.E., and Schuster, N.D., (1995). "Ground motions during the 1994 Northridge Earthquake." Candian Journal of Civil Engineering, vol. 22, 300-315

Getahun, A. (2007). *Geology of Addis Ababa city*. Ministry of Mines and Energy, Geological Survey of Ethiopia. Addis Ababa, Ethiopia

Giardini, D. and Basham, P. (1993). "The Global Seismic Hazard Assessment Program (GSHAP)." *Annali di Geofisica,* 36(3), 3-13.

Giardini, D., Grünthal, G., Shedlock, K. M. and Zhang, P. (1999). "The GSHAP Global Seismic Hazard Map." *Annali di Geofisica*, 42(6), 1225-1228.

Gouin, P. (1979). *Earthquake history of Ethiopia and the horn of Africa*. IDRC. Ottawa, Ontario.

Haile, M. (1996). "Critical assessment of site effect parameters for strong ground motion prediction." Ph.D. dissertation, Tokyo Institute of Technology, Tokyo.

Haile, M. (2004). *Seismic microzonation for the city of Addis Ababa by using Microtremors.* 13th World Conference on Earthquake Engineering. Vancouver, B.C., Canada. Paper No. 2092

Hashash, Y.M.A., Musgrove, M.I., Harmon, J.A., Groholski, D.R., Phillips, C.A., and Park, D. (2016) "DEEPSOIL 6.1, User Manual." Urbana, IL, Board of Trustees of University of Illinois at Urbana Champaign.

Hutabarat, D. (2016). "Evaluation of One-Dimensional Seismic Site Response Analyses at Small to Large Strain Levels." MSc. Thesis, University of Washington, Seattle, WA.

Kebede, F. and Asfaw, L.M. (1996). *Seismic hazard assessment for Ethiopia and the neighbouring countries*. SINET: Ehiop.J.Sci. 19, 15-50.

Kebede, F. and van Eck, T. (1997). "Probabilistic seismic hazard assessment for the Horn of Africa based on seismotectonic regionalization." *Tectonophysics,* 270, 221-237.

Kinde, S. (2002). *Earthquake Risks in Addis Ababa and other Major Ethiopian Cities - Will the Country be Caught Off-guarded?*

Kinde, S., K. (nd). *Proposed Considerations for Revision of EBCS-8:1995 for Conservative Seismic Zoning and Stringent Requirements for Torsionally Irregular Buildings.* Irvine, CA, USA.

Kottke, A.R. and Rathje, E.M. (2009). "Technical Manual for Strata." *Pacific Earthquake Research Center,* University of California at Berkeley.

Kramer, S. L. (1996). *Geotechnical Earthquake Engineering*. Prentice-Hall. Upper Saddle River.

Kramer, S. L., Arduino, P and Dideras, S. S. (2012). *Earthquake ground motion selection*. Research Project T4118, Task 69. University of Washington.

Kwok, A. O. L., Stewart, J. P., Hashash, Y. M. A., Matasovic, N., Pyke, R., Wang, Z. and Yang, Z. (2007). *Use of Exact Solutions of Wave Propagation Problems to Guide Implementation of Nonlinear Seismic Ground Response Analysis Procedures*. Journal of Geotechnical and Geoenvironmental Engineering, 133, 1385-1398.

Lubkowski, Z. Villani, M. Koates, K. Jirouskova, N. and Willis, M. (2014). *Seismic design considerations for East Africa.* Conference Paper, second European conference on earthquake engineering and seismology.

Mammo, T. (2005). *Site-specific ground motion simulation and seismic response analysis at the proposed bridge sites within the city of Addis Ababa, Ethiopia*. ELSEVIER, Engineering Geology, 79, 127-150Kramer, S. L. (1996). *Geotechnical Earthquake Engineering*. Prentice-Hall. Upper Saddle River.

Ministry of Construction. (2015) *Design of Structures for Earthquake Resistance, Ethiopian Standards based on Euro Norms* (EBCS EN 1998:2015), Addis Ababa.

Ministry of Works and Urban Development. (1995) *Design of Structures for Earthquake Resistance*, Ethiopian Building Code Standard (EBCS 8), Addis Ababa.

PEER (Pacific earthquake engineering center) (2010). *Ground motion database user manual*, Beta Version.

Poggi, V., Durrheim, R., Tuluka, G. M., Weatherill, G., Gee, R., Pagani. M., Nyblade, A., Delvaux, D. (2017). *Assessing seismic hazard of the East African Rift: a pilot study from GEM and AfricaArray.* Springer, Bull Earthquake Engineering.

Schnabel, P.B., Lysmer, J. and Seed, H.B. (1972). "SHAKE: A computer program for earthquake response analysis of horizontally layered sites." Report No. EERC 72-12, Earthquake Research Center, University of California, Berkeley, California.

Seed, H.B. and Idriss, I.M. (1970). "Soil Moduli and Damping Factors for Dynamic Response Analyses." *Report No. EERC-70-10*, Earthquake Engineering Research Center, University of California, Berkeley, CA.

Seed, H.B., Wong, R.T., Idriss, I.M. and Tokimatsu, K. (1986). "Moduli and Damping Factors for Dynamic Analyses of Cohesionless Soils." *Journal of the Soil Mechanics and Foundations Division*, ASCE, 112(11), 1016-1032.

Stewart, J.P. and Kwok, A.O.L. (2008). "Nonlinear Seismic Ground Response Analysis: Code Usage Protocols and Verification against Vertical Array Data." *Geotechnical Earthquake Engineering and Soil Dynamics IV*, ASCE, GSP 181.

Stewart, J.P., Afshari, K. and Hashash, Y.M.A. (2014). "Guidelines for Performing Hazard-Consistent One-Dimensional Ground Response Analysis for Ground Motion Prediction." *Pacific Earthquake Engineering Research Center*, University of California at Berkeley.

Srbulov, M. (2008). *Geotechnical Earthquake Engineering: Simplified Analysis with Case Studies and Examples.* Springer. U.K.

Srbulov, M. (2011). *Geotechnical, Geological and Earthquake Engineering, Practical Soil Dynamics: Case studies in earthquake and geotechnical engineering.* Springer. U.K.

Tsehayu, K. and H.Mariam, T. (1990). *Engineering geological map of Addis Ababa*. Addis Ababa

U.S Nuclear Regulatory Commission (2004). "Evaluation of the December 22, 2003 M_w = 6.5 San Simeon Earthquake." Final Report, Washington

U.S. Geological Survey professional paper 1551-A (1994). "The Lorna Prieta, California, Earthquake of October 17, 1989-Strong Ground Motion." Washington.

Villaverde, R. (2009). *Fundamental concepts of earthquake engineering*. CRC Press. Boca Raton

Vucetic, M. and Dobry, R. (1991). "Effect of Soil Plasticity on Cyclic Response." ASCE, *Journal of Geotechnical Engineering*, 117(1), 89-107.

Wair. B.R., DeJong, J.T. and Shantz, T. (2012). "Guidelines for Estimation of Shear Wave Velocity Profiles." *Pacific Earthquake Research Center,* University of California at Berkeley.

Worku, A. (2011). "Recent developments in the definition of design earthquake ground motions calling for a revision of the current Ethiopian seismic code – EBCS 8:1995." *Zede - Journal of EEA*, 28, 1-15.

Worku, A. (2014). "The status of basic design ground motion provisions in seismic design codes of sub-Saharan African countries, a critical review." *Journal of the S. African Institution of Civil Eng.,* 56(1), 40-53.

Yoshida, N. (2015). *Seismic Ground Response Analysis.* Springer. Dordrecht.

APPENDIX

Appendix A

Typical soil data as obtained from geotechnical reports

1. Ayat Site

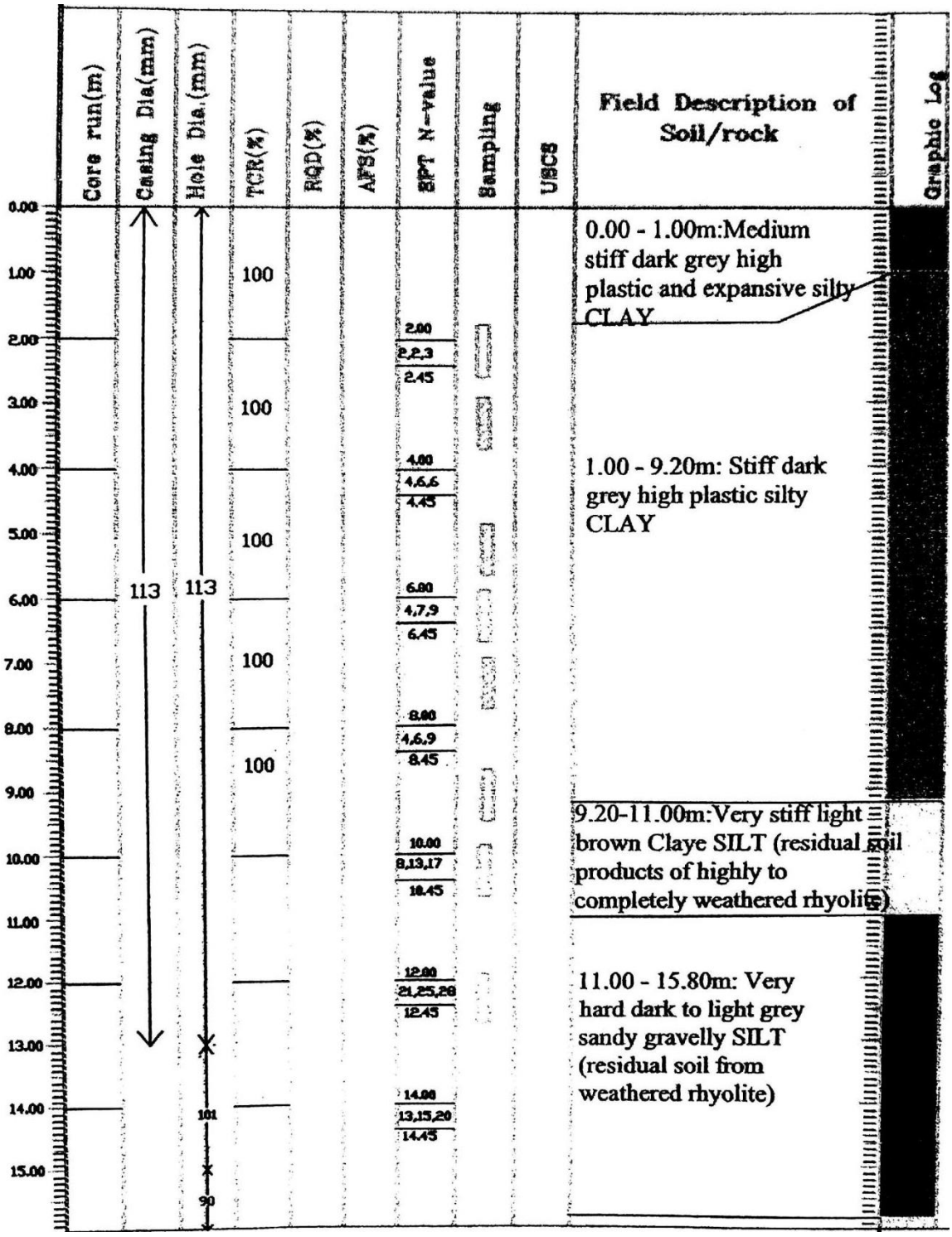

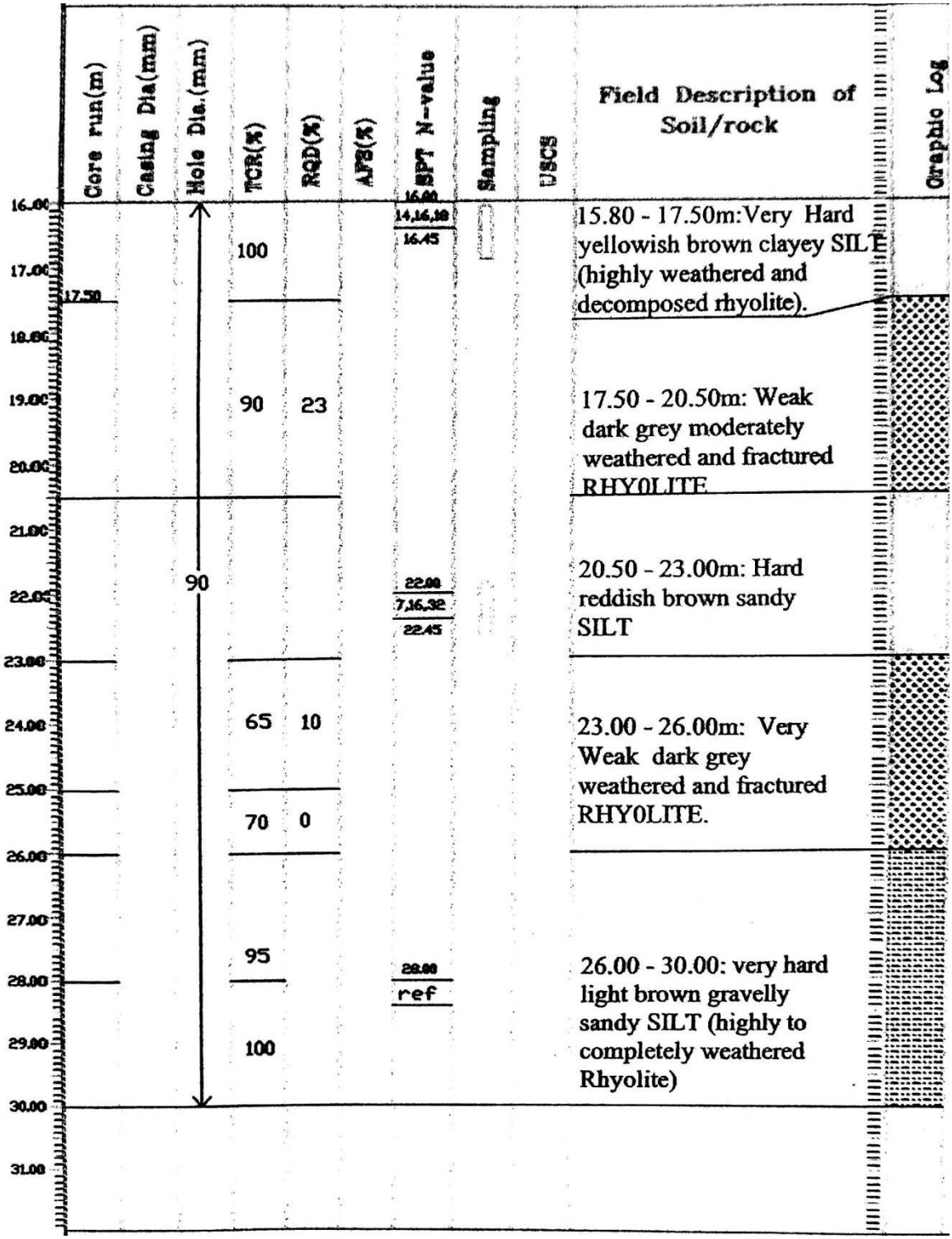

Figure A1: Typical borehole profile for Ayat site

2. CMC Site

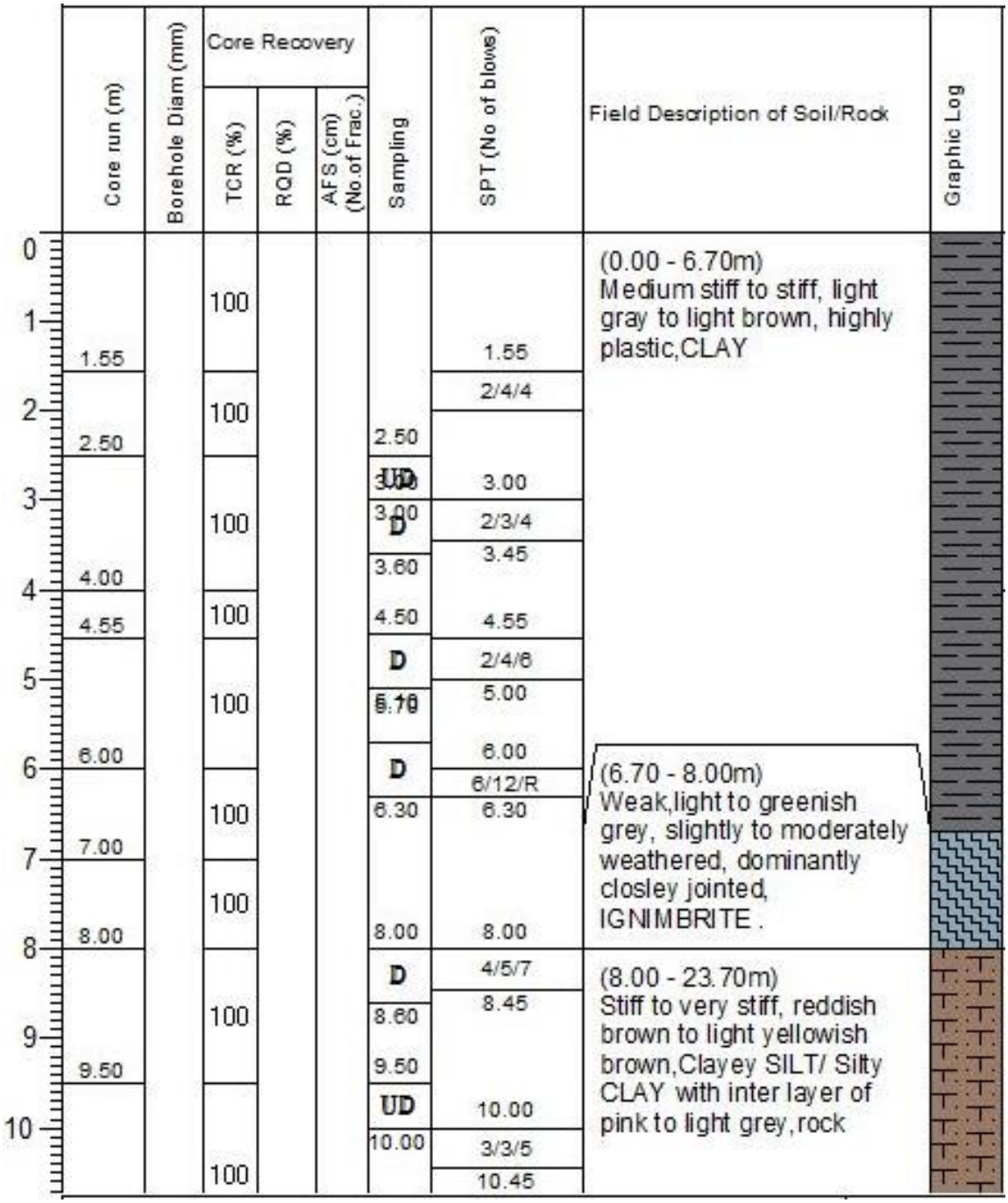
Core run (m)
Borehole Diam (mm)
Core Recovery
TCR (%)
RQD (%)
AFS (cm) (No.of Frac.)
Sampling
SPT (No of blows)
Field Description of Soil/Rock
Graphic Log
(0.00 - 6.70m)
Medium stiff to stiff, light gray to light brown, highly plastic,CLAY
(6.70 - 8.00m)
Weak,light to greenish grey, slightly to moderately weathered, dominantly closley jointed, IGNIMBRITE .
(8.00 - 23.70m)
Stiff to very stiff, reddish brown to light yellowish brown,Clayey SILT/ Silty CLAY with inter layer of pink to light grey,rock
1.55
2.50
4.00
4.55
6.00
7.00
8.00
9.50
100
1.55
2/4/4
2.50
UD
3.00
D
2/3/4
3.45
3.60
4.50
4.55
D
2/4/6
5.00
6.00
D
6/12/R
6.30
6.30
8.00
8.00
D
4/5/7
8.45
8.60
9.50
UD
10.00
10.00
3/3/5
10.45

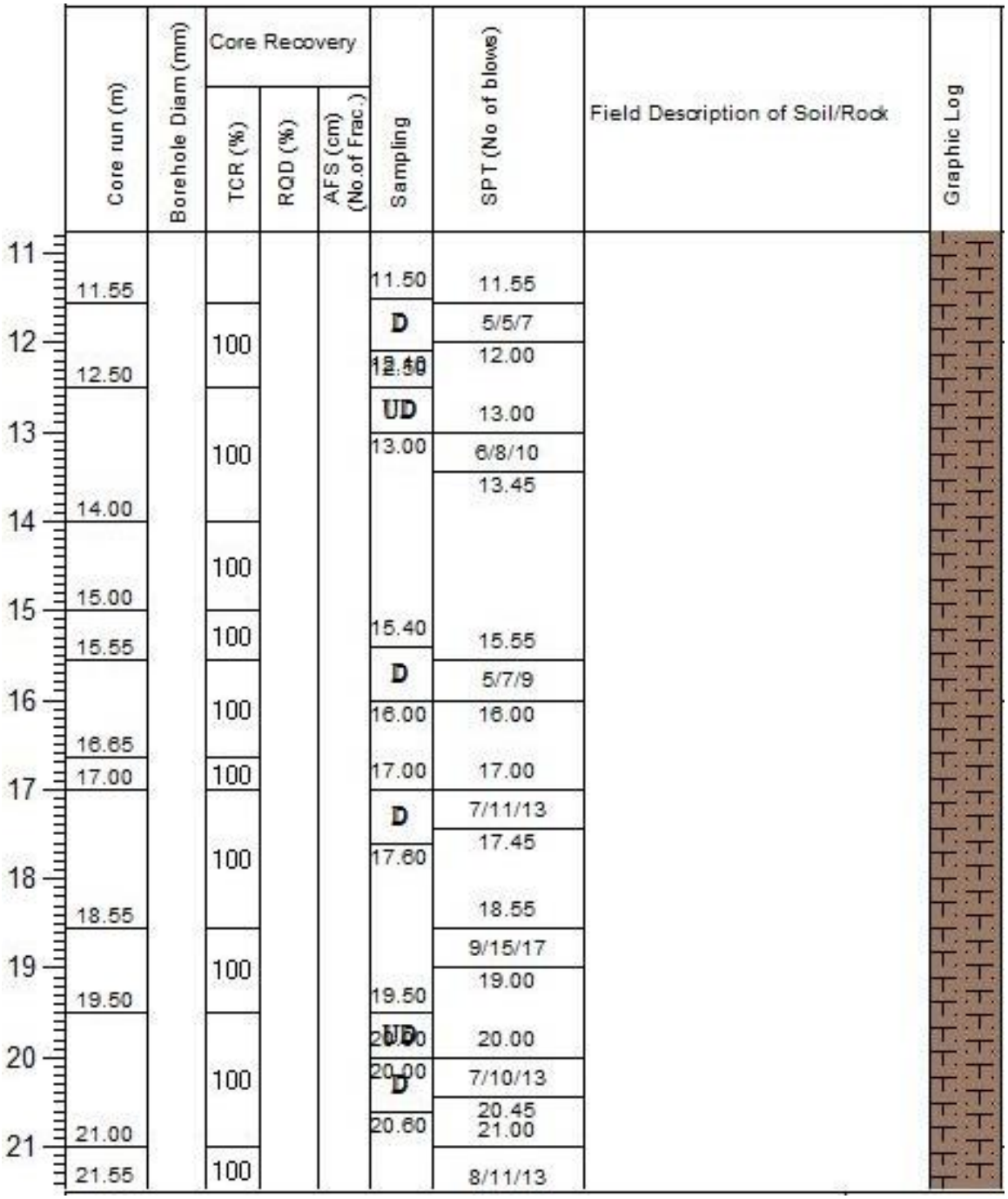
Core run (m)
Borehole Diam (mm)
Core Recovery
TCR (%)
RQD (%)
AFS (cm) (No.of Frac.)
Sampling
SPT (No of blows)
Field Description of Soil/Rock
Graphic Log
11
12
13
14
15
16
17
18
19
20
21
11.55
12.50
14.00
15.00
15.55
16.65
17.00
18.55
19.50
21.00
21.55
100
11.50
D
12.00
13.00
UD
13.00
6/8/10
13.45
15.40
15.55
D
5/7/9
16.00
16.00
17.00
17.00
D
7/11/13
17.60
17.45
18.55
9/15/17
19.00
19.50
20.00
UD
20.00
D
7/10/13
20.45
20.60
21.00
8/11/13

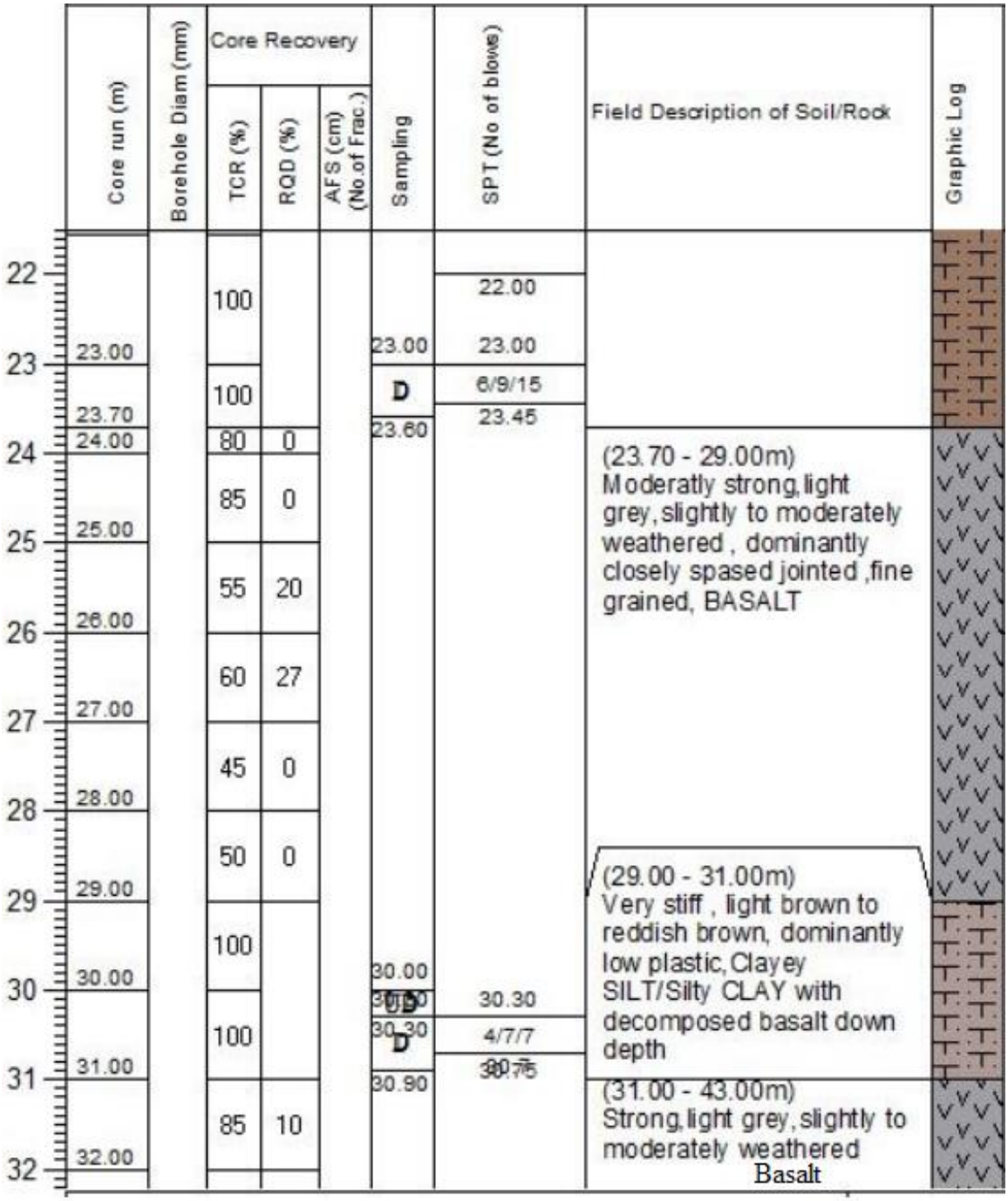

Figure A2: Typical borehole profile for CMC site

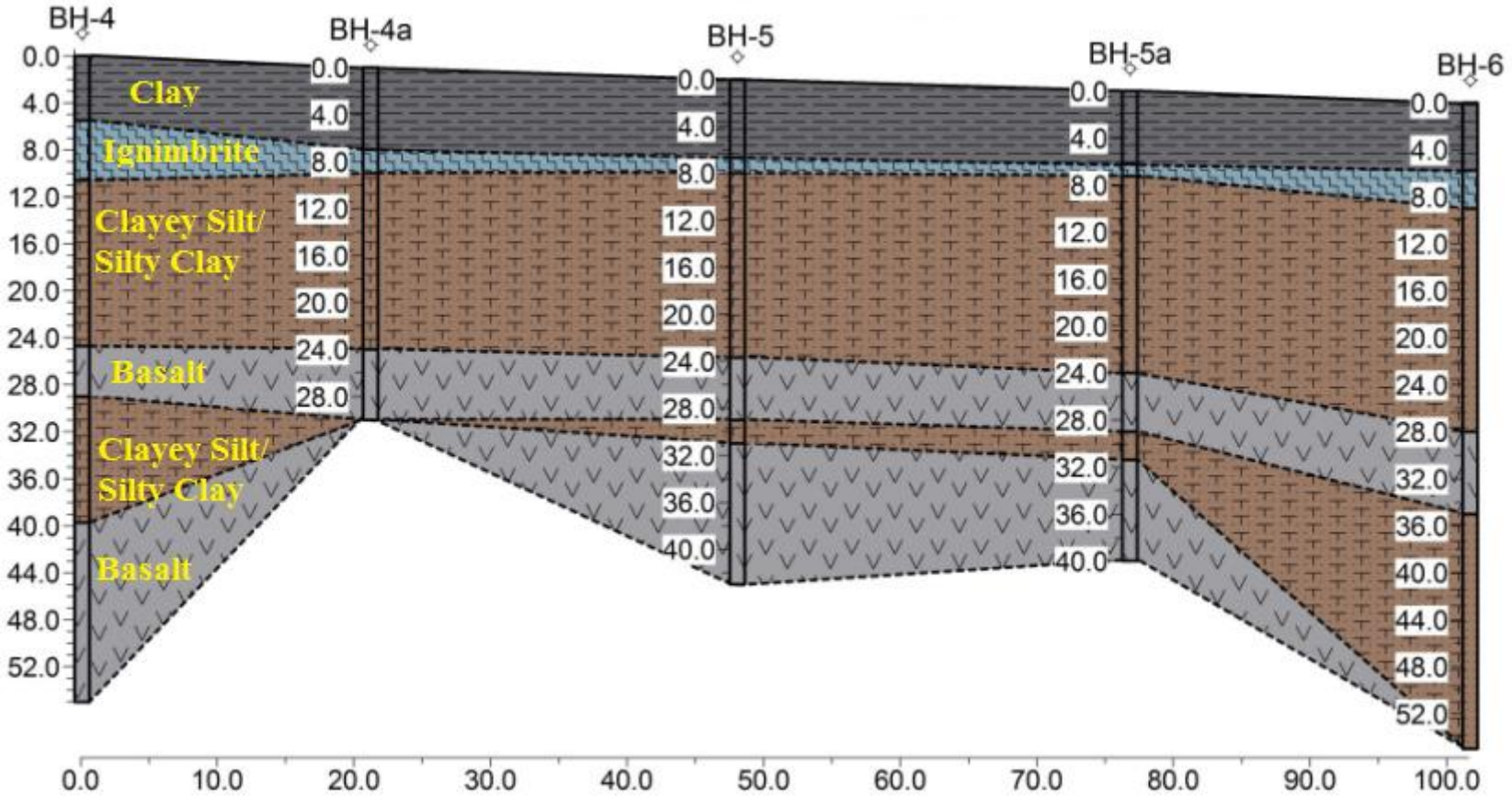

Figure A3: Possible cross section along boreholes for CMC site

3. Bole Site 1

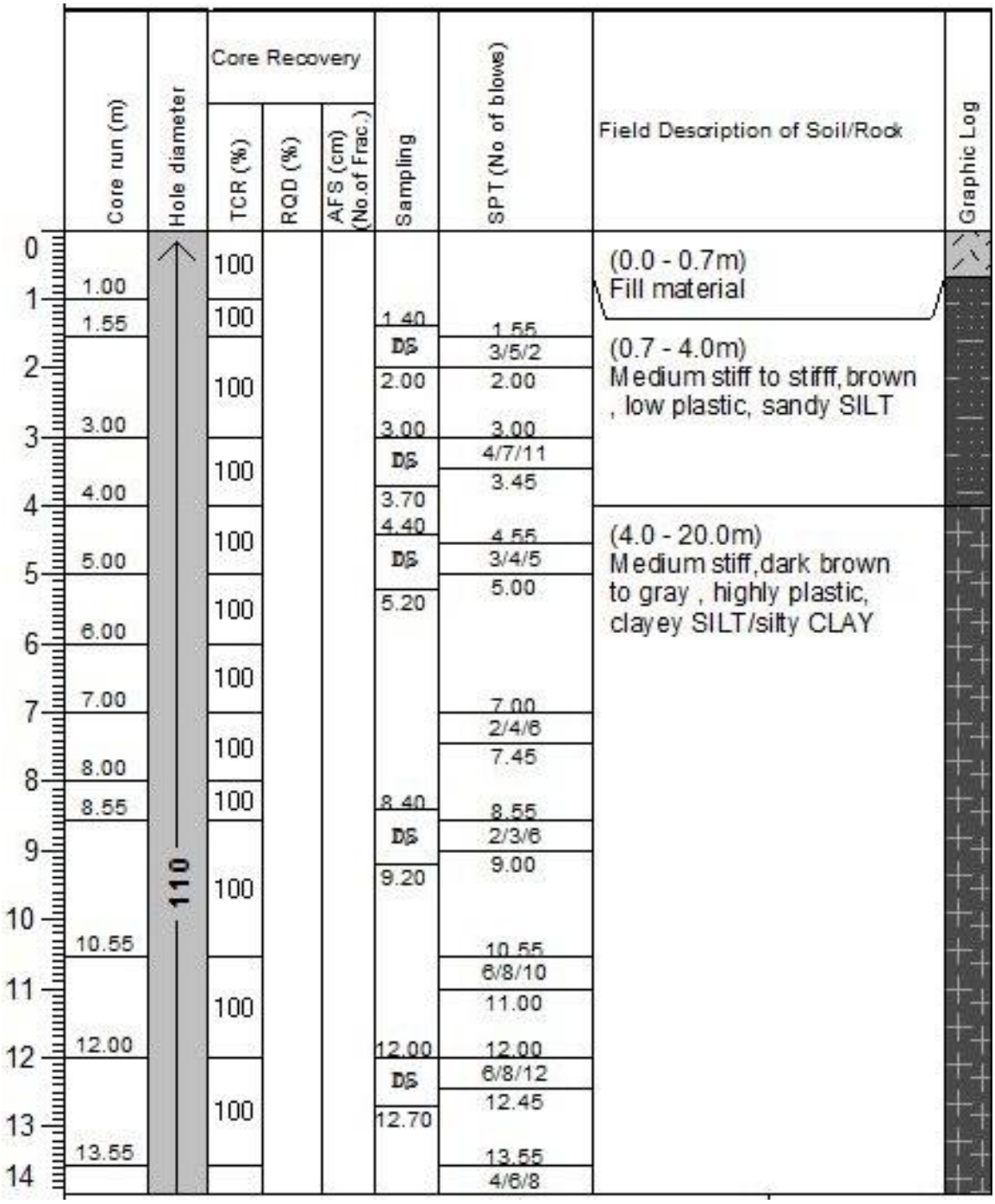
Core run (m)
Hole diameter
Core Recovery
TCR (%)
RQD (%)
AFS (cm) (No.of Frac.)
Sampling
SPT (No of blows)
Field Description of Soil/Rock
Graphic Log
(0.0 - 0.7m)
Fill material
(0.7 - 4.0m)
Medium stiff to stifff, brown , low plastic, sandy SILT
(4.0 - 20.0m)
Medium stiff, dark brown to gray , highly plastic, clayey SILT/silty CLAY
110
DS
1.00
1.55
3.00
4.00
5.00
6.00
7.00
8.00
8.55
10.55
12.00
13.55
1.40
2.00
3.00
3.70
4.40
5.20
8.40
9.20
12.00
12.70
3/5/2
4/7/11
3/4/5
2/4/6
2/3/6
6/8/10
6/8/12
4/6/8

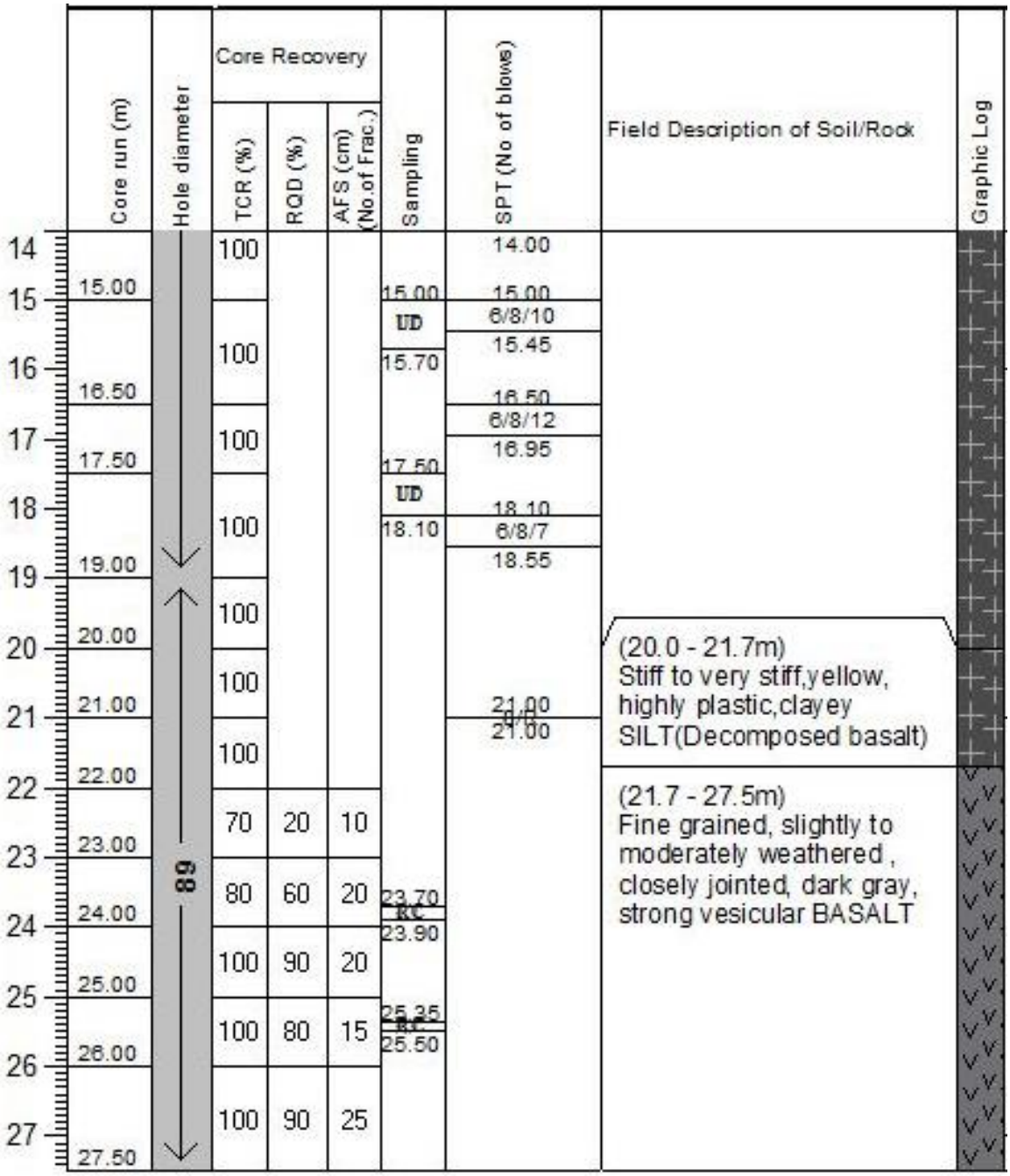

Figure A4: Typical borehole profile for Bole site 1

4. Bole Site 2

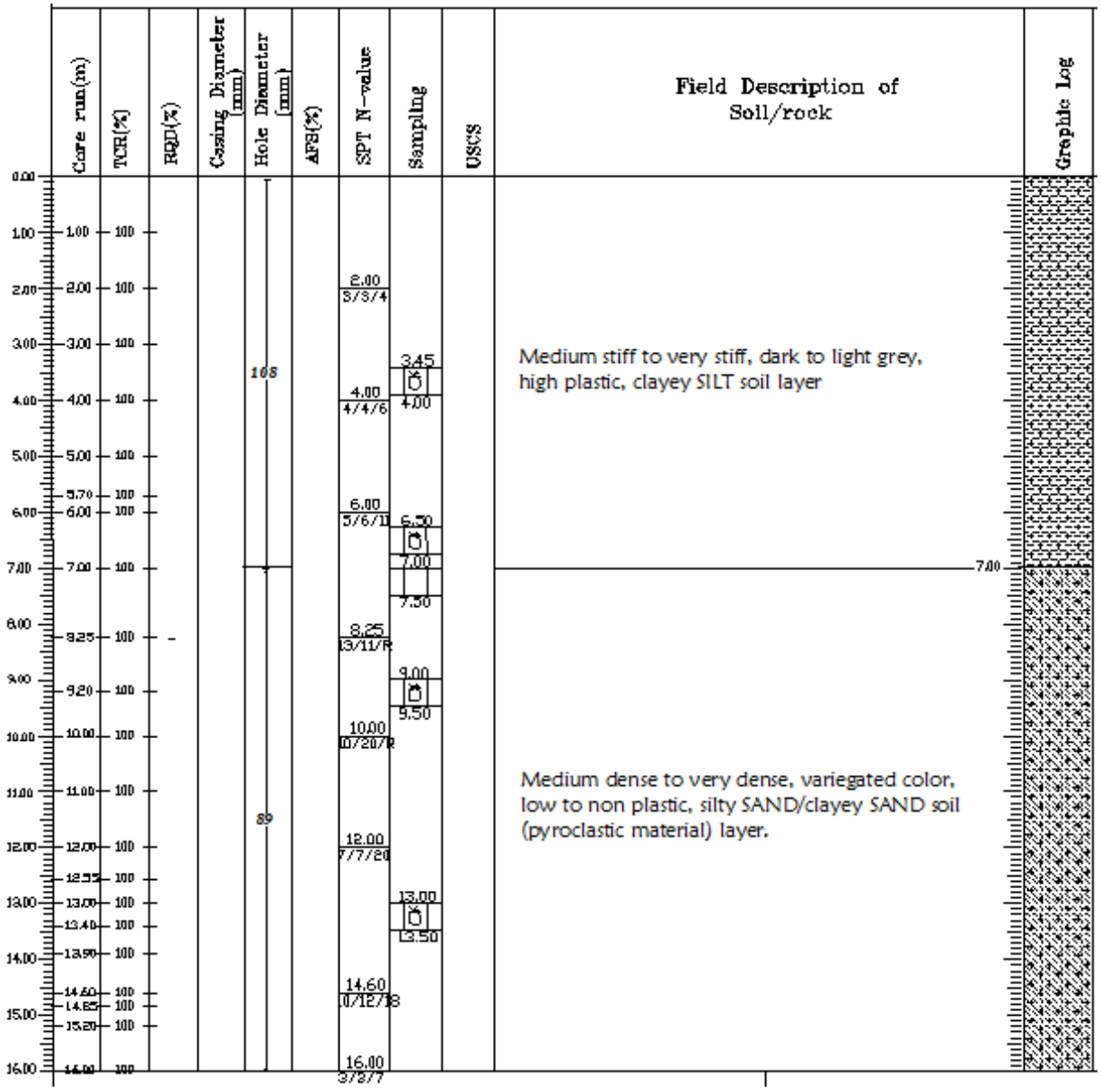
Core run(m)
TCR(%)
RQD(%)
Casing Diameter (mm)
Hole Diameter (mm)
AFS(%)
SPT N-value
Sampling
USCS
Field Description of Soil/rock
Graphic Log
Medium stiff to very stiff, dark to light grey, high plastic, clayey SILT soil layer
Medium dense to very dense, variegated color, low to non plastic, silty SAND/clayey SAND soil (pyroclastic material) layer.
7.00
168
89
2.00
3/3/4
3.45
4.00
4/4/6
4.00
6.00
5/6/11
6.50
7.00
7.50
8.25
13/11/R
9.00
9.50
10.00
10/20/R
12.00
7/7/20
13.00
13.50
14.60
10/12/18
16.00
9/8/7

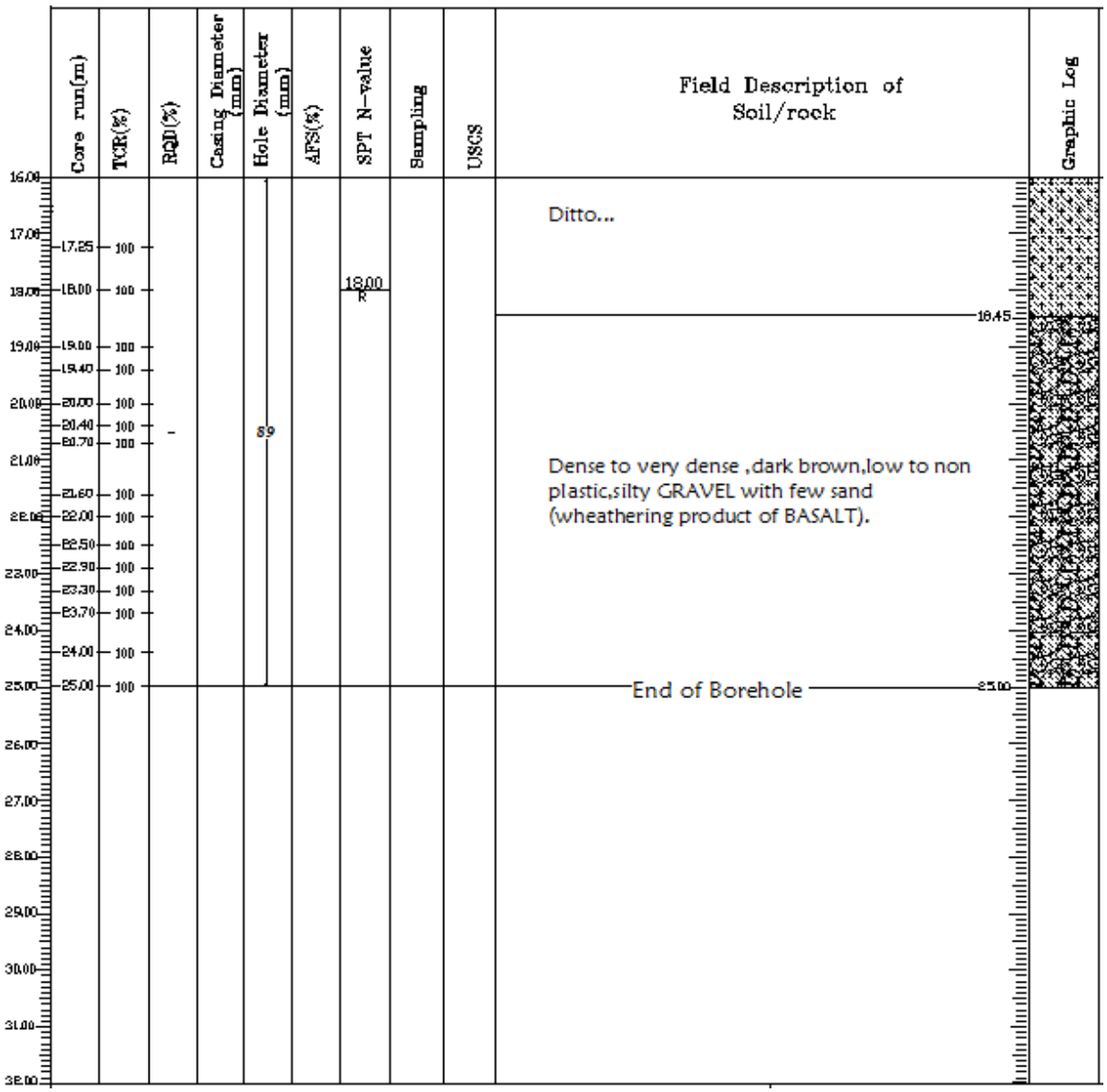

Figure A5: Typical borehole profile for Bole site 2

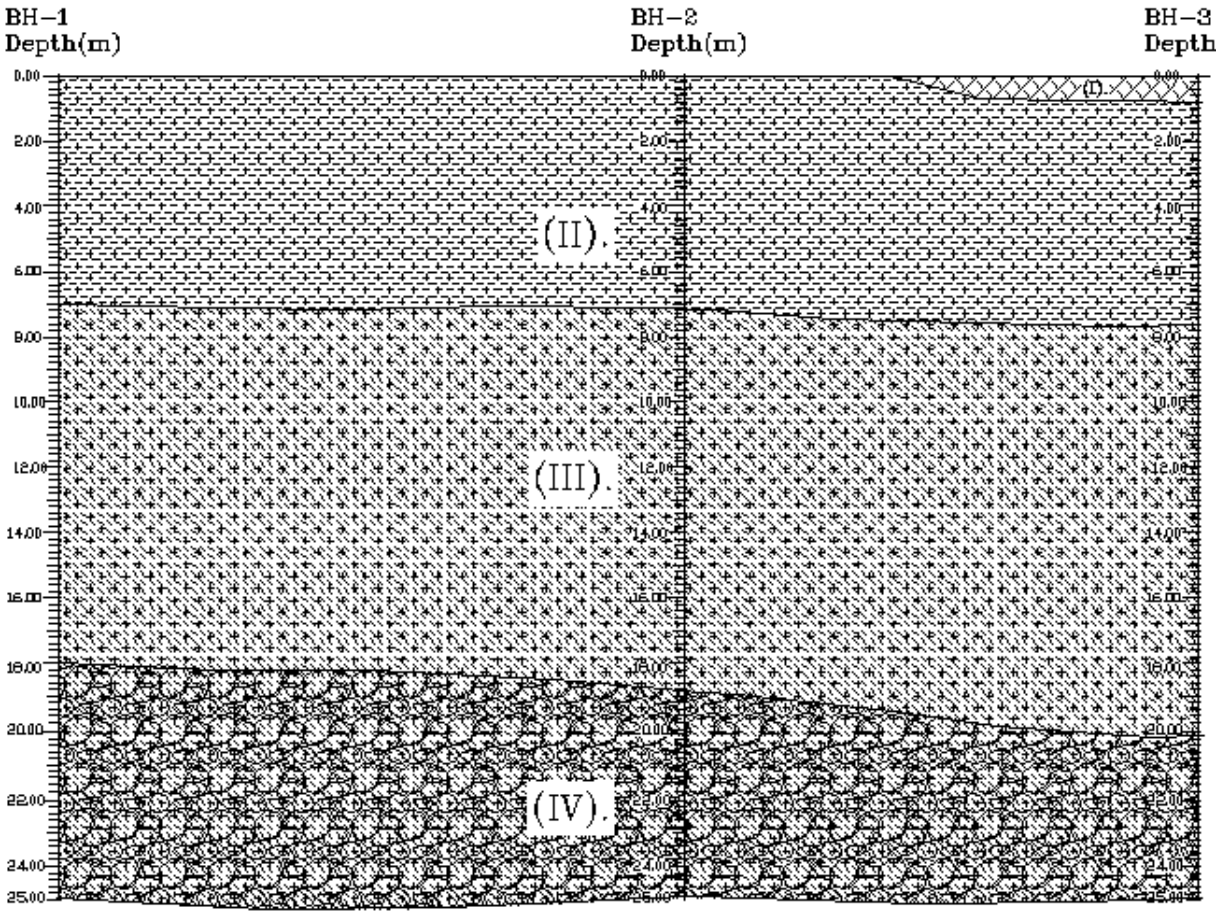

(I). Back fill:- construction stone

(II). Medium stiff to very stiff, dark to light grey, high plastic clayey SILT soil layer

(III). Medium dense to very dense, variegated color, low to non plastic silty SAND/clayey SAND soil (pyroclastic material) layer.

(IV). Dense to very dense, dark brown,low to non plastic silty GRAVEL with few sand (wheathering product of BASALT).

Figure A6: Cross section through boreholes for Bole site 2

5. Mexico Site 1

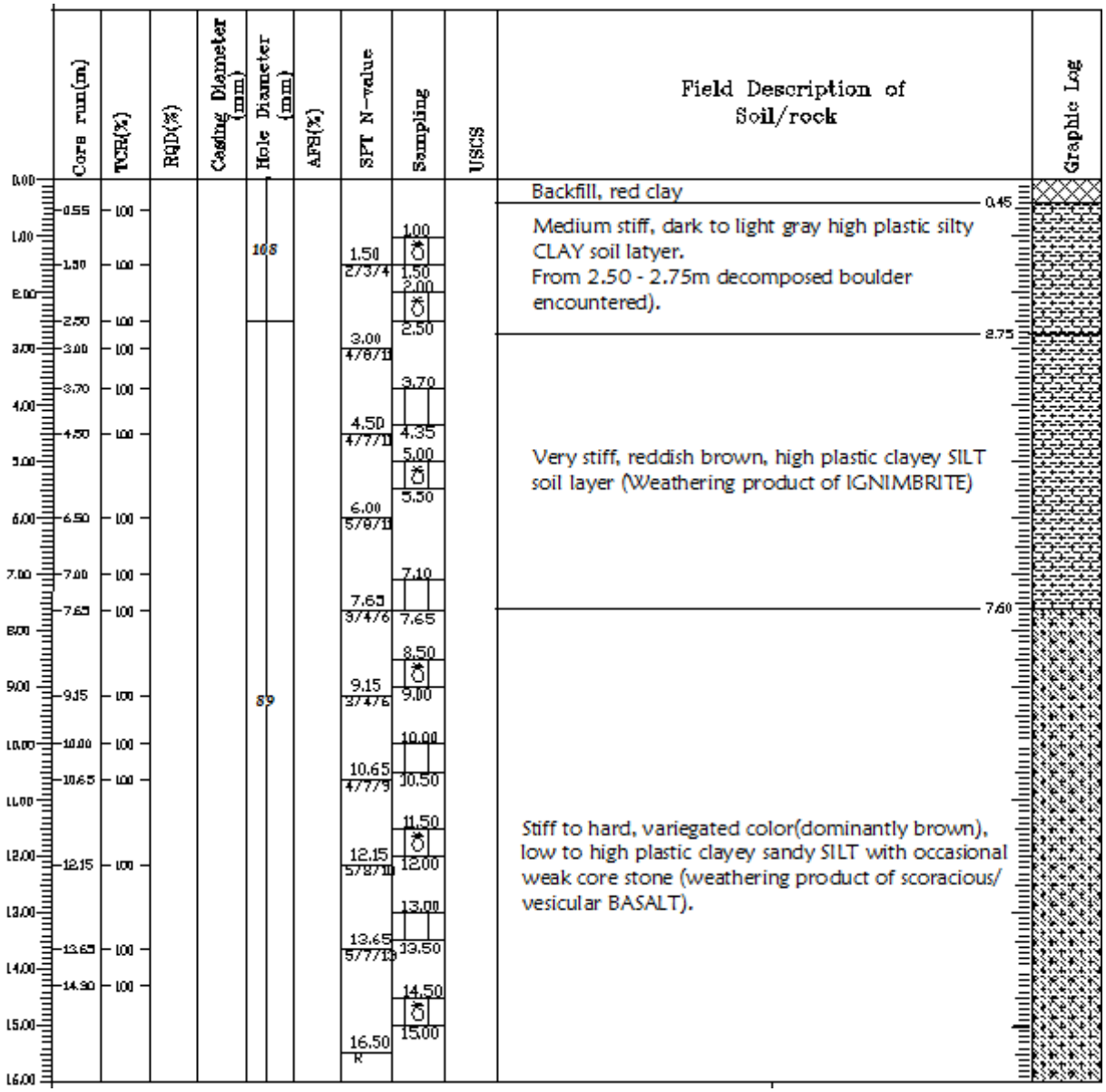

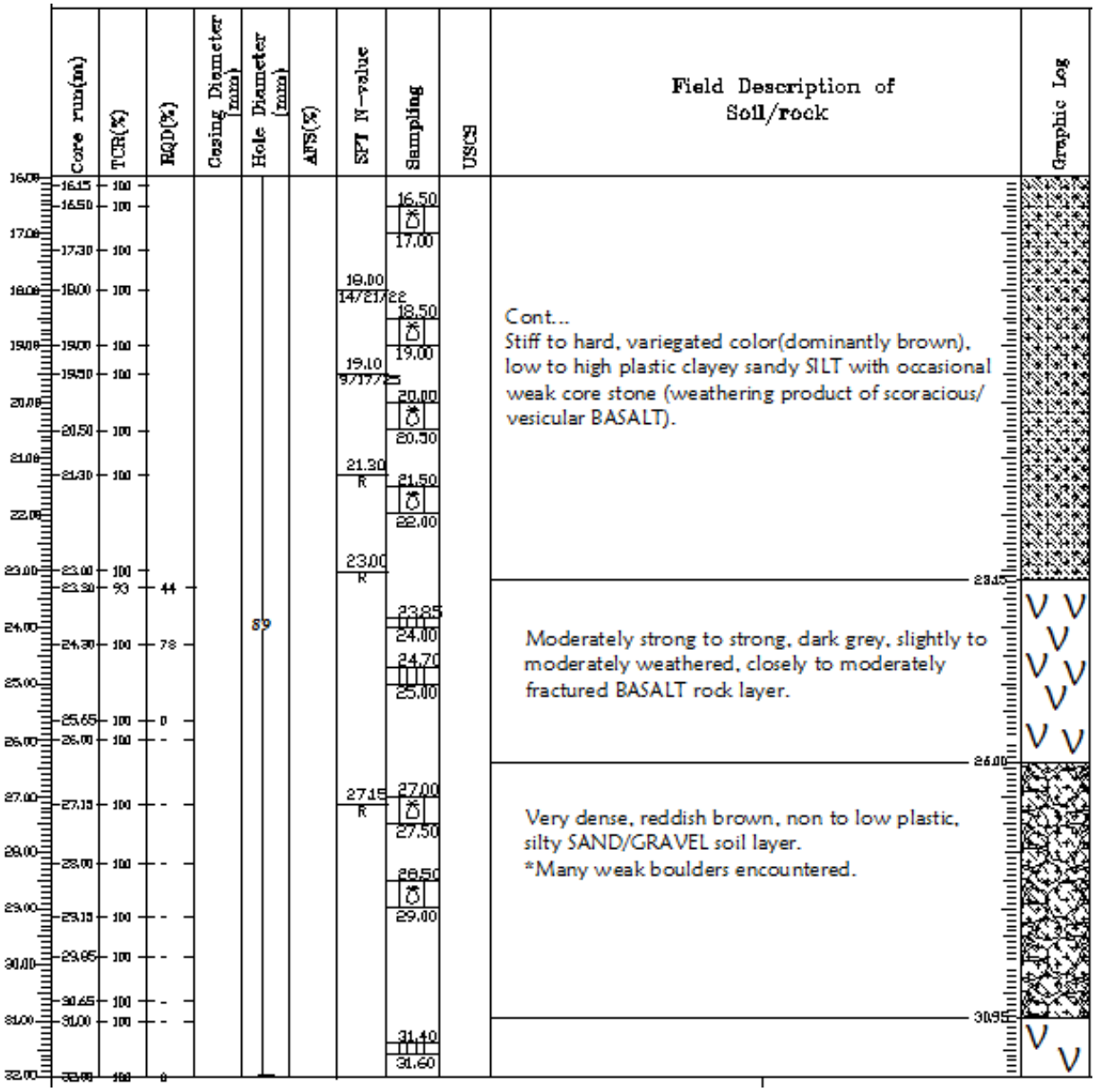

Figure A7: Typical borehole profile for Mexico site 1

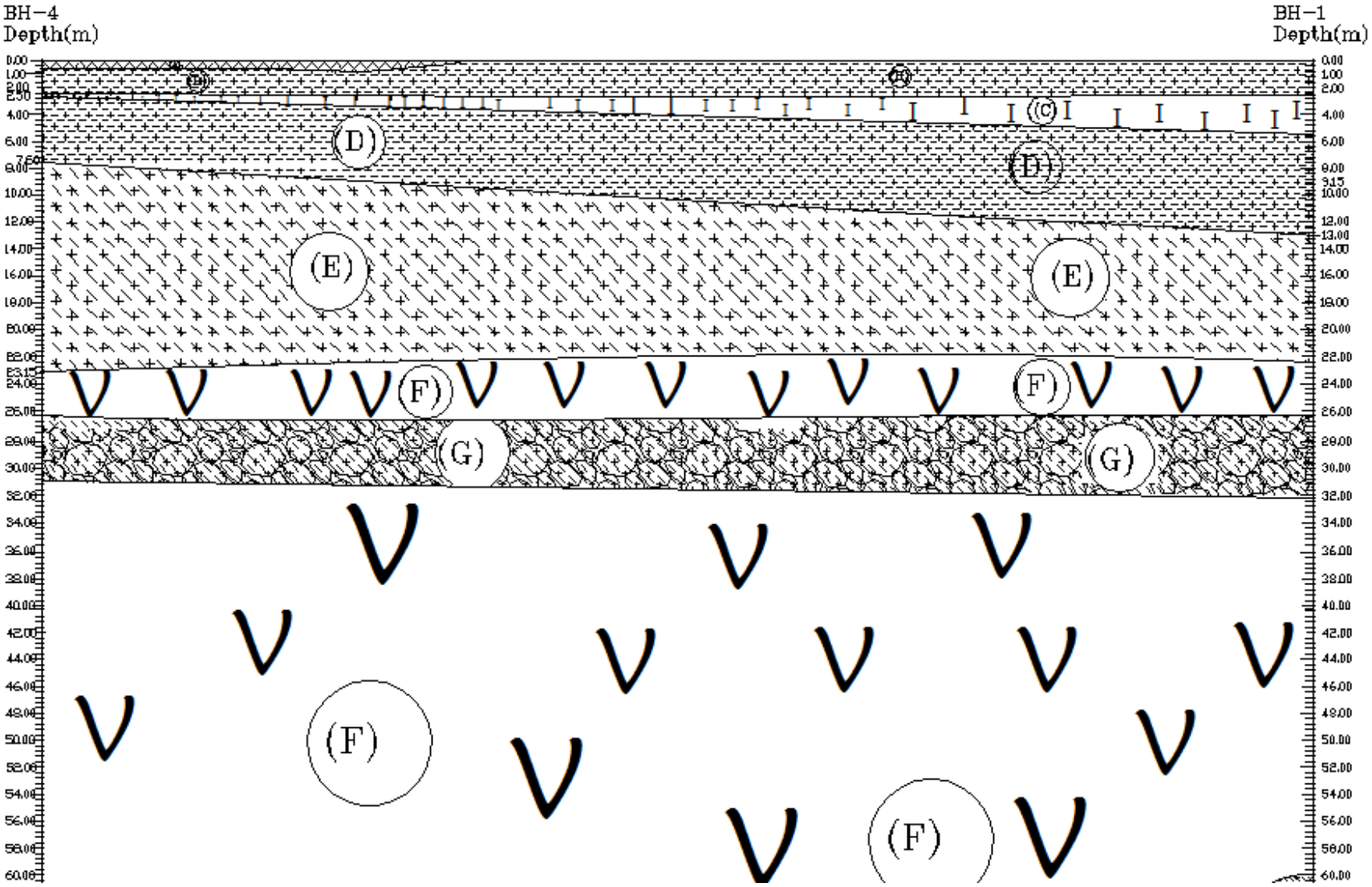
BH−4
Depth(m)
BH−1
Depth(m)
(D)
(E)
(F)
(G)

(A). Backfill-red clay.

(B). Medium stiff, dark to light gray high plastic silty CLAY soil layer .

(C). Weak to extremely weak, greenish grey, moderately weathered to decomposed and moderately jointed IGNIMBRITE. .(It can be found as variable size boulders).

(D). Stiff to hard, reddish brown, high plastic clayey SILT with trace sand soil layer.

(E). Stiff to hard, variegated color , low to high plastic sandy SILT with clay and weak core stone.

(F). Strong to weak, dark gray, slightly to moderately weathered and moderately fractured to crushed BASALT rock layer.

(G). Very dense, variegated color (dominantly brown), low to high plastic silty SAND/GRAVEL soil layer

(H). Hard, variegated color, non to high plastic sandy SILT/silty SAND with gravel.

Figure A8: Cross section through boreholes for Mexico site 1

6. Mexico Site 2

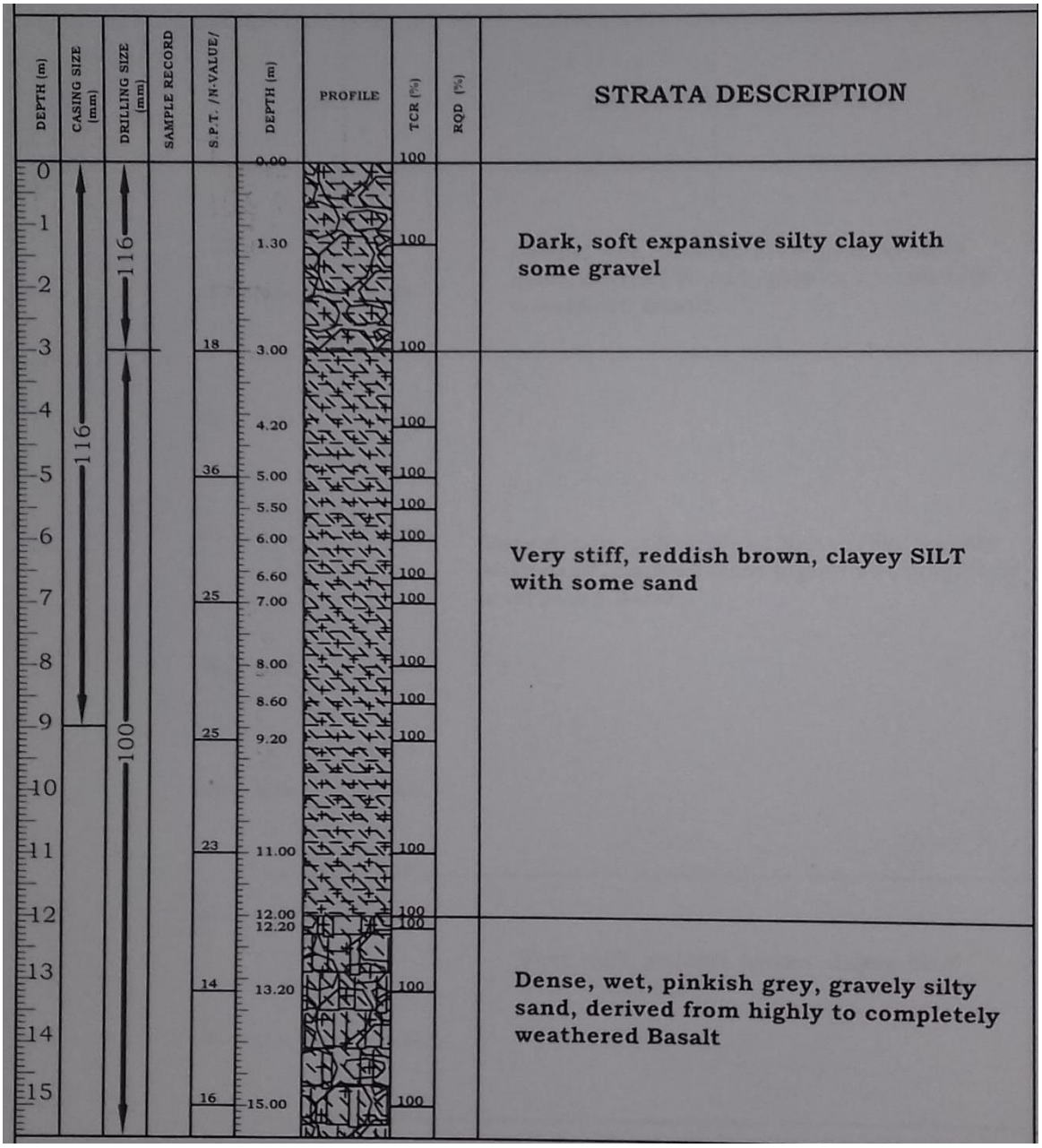

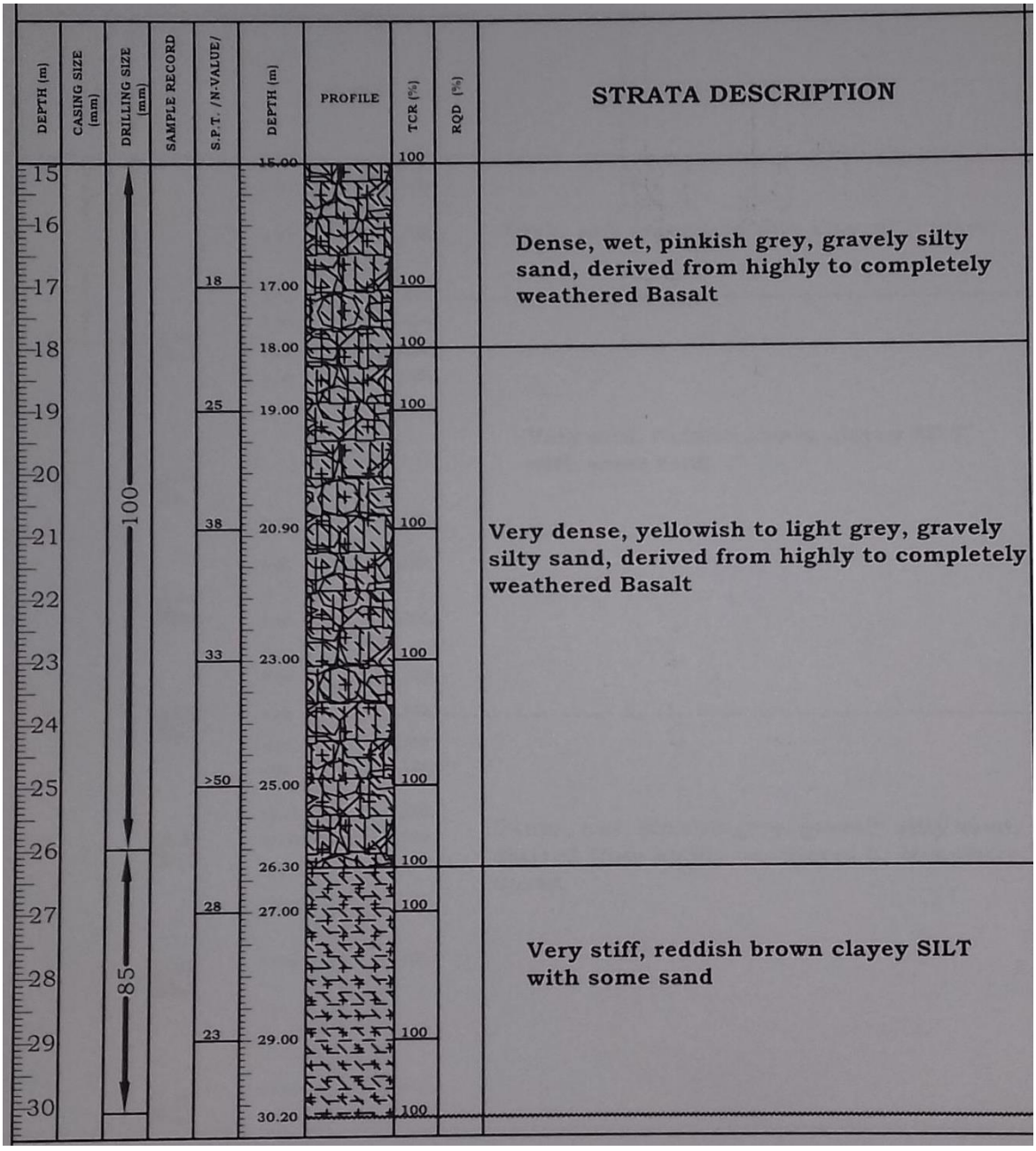

Figure A9: Typical borehole profile for Mexico site 2

7. Jemmo Site Profile 1

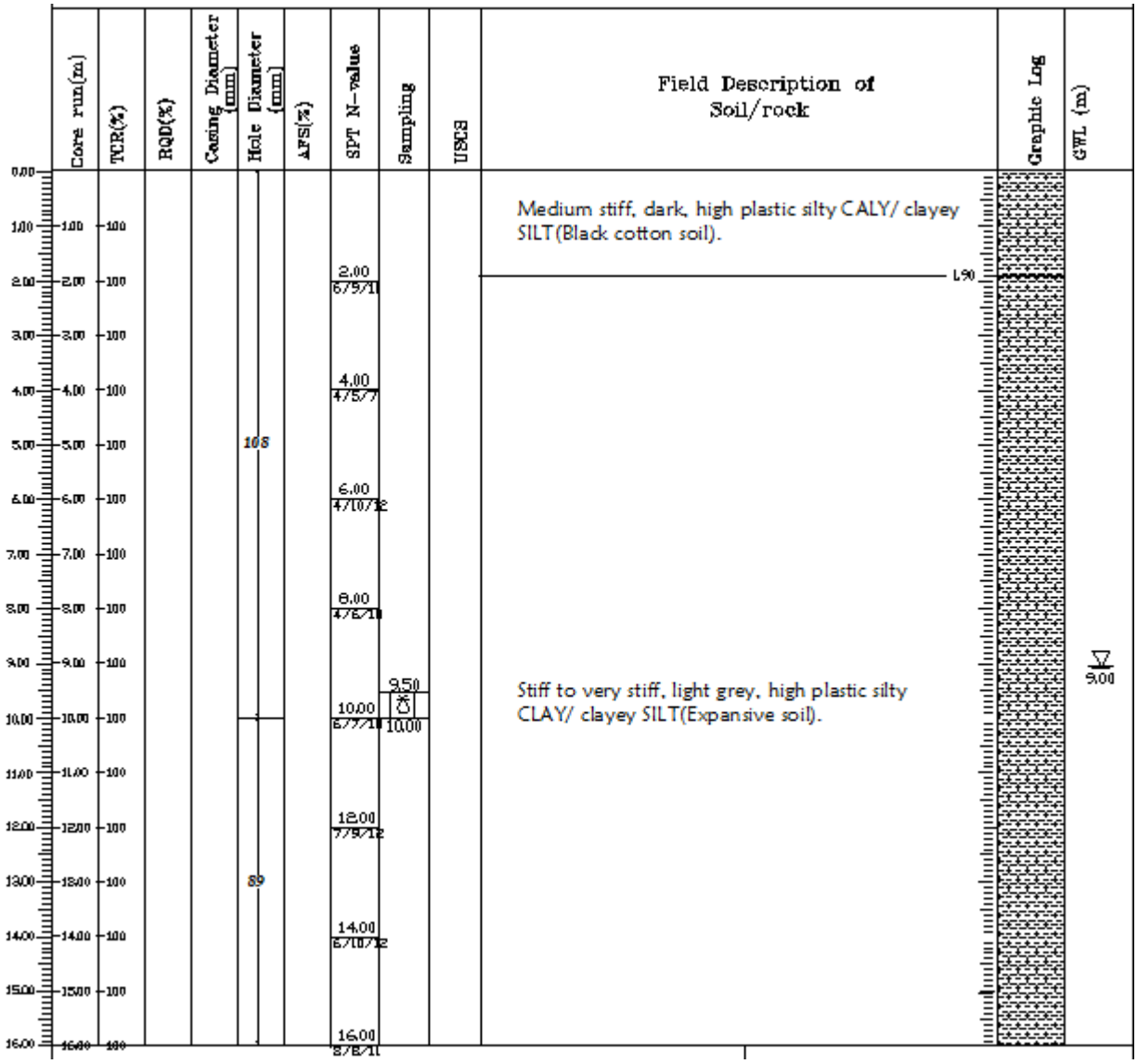

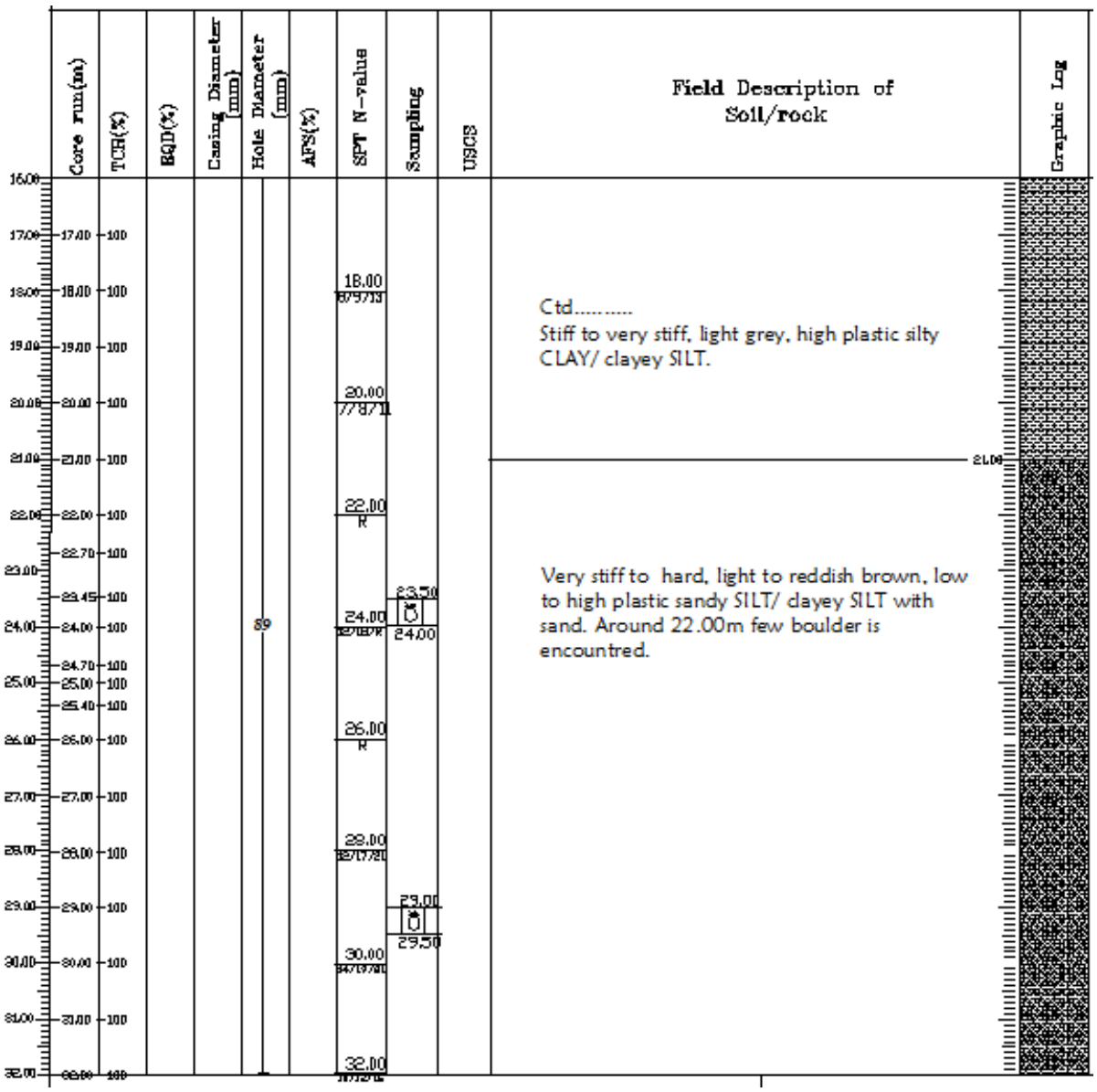
Core run(m)
TCR(%)
RQD(%)
Casing Diameter (mm)
Hole Diameter (mm)
APS(%)
SPT N-value
Sampling
USCS
Field Description of Soil/rock
Graphic Log
Ctd.....
Stiff to very stiff, light grey, high plastic silty CLAY/ clayey SILT.
21.00
Very stiff to hard, light to reddish brown, low to high plastic sandy SILT/ clayey SILT with sand. Around 22.00m few boulder is encountred.
18.00
20.00
22.00
R
23.50
U
24.00
24.00
26.00
R
28.00
29.00
U
29.50
30.00
32.00
89

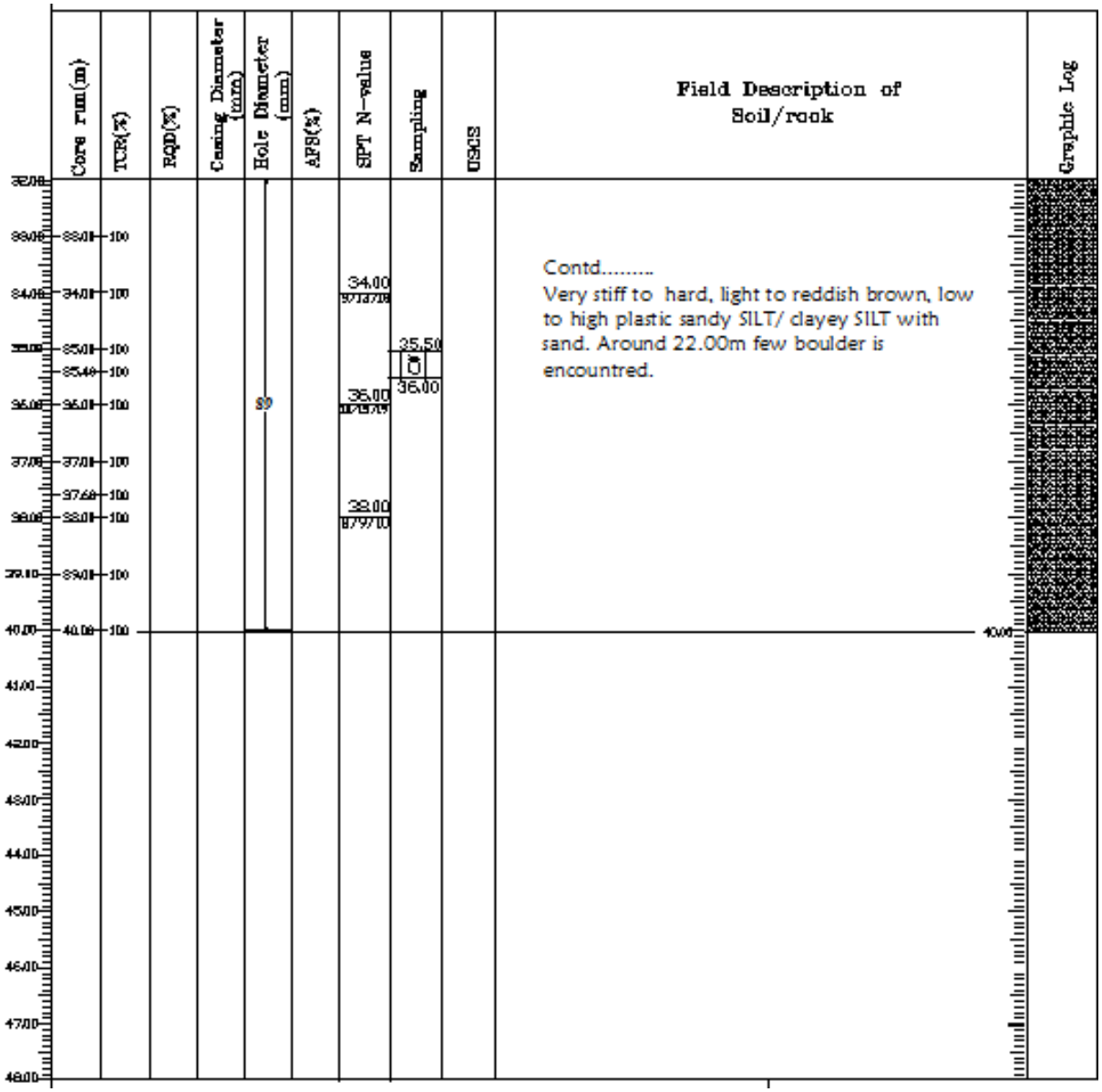
Core run(m)
TCR(%)
RQD(%)
Casing Diameter (mm)
Hole Diameter (mm)
AFR(%)
SPT N-value
Sampling
USCS
Field Description of Soil/rock
Graphic Log
Contd.....
Very stiff to hard, light to reddish brown, low to high plastic sandy SILT/ clayey SILT with sand. Around 22.00m few boulder is encountred.
34.00
35.50
36.00
38.00
40.00

8. Jemmo Site Profile 2

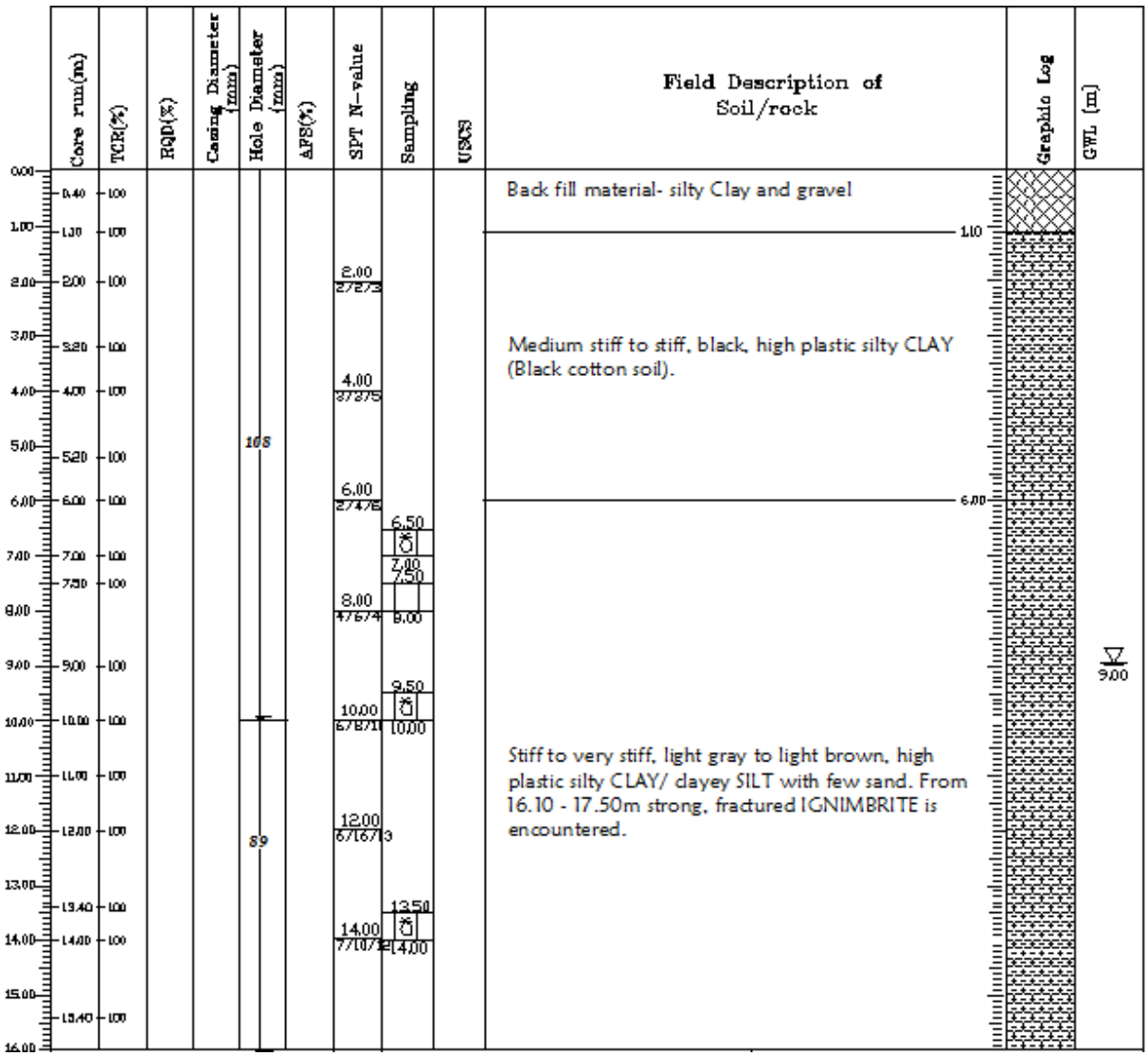

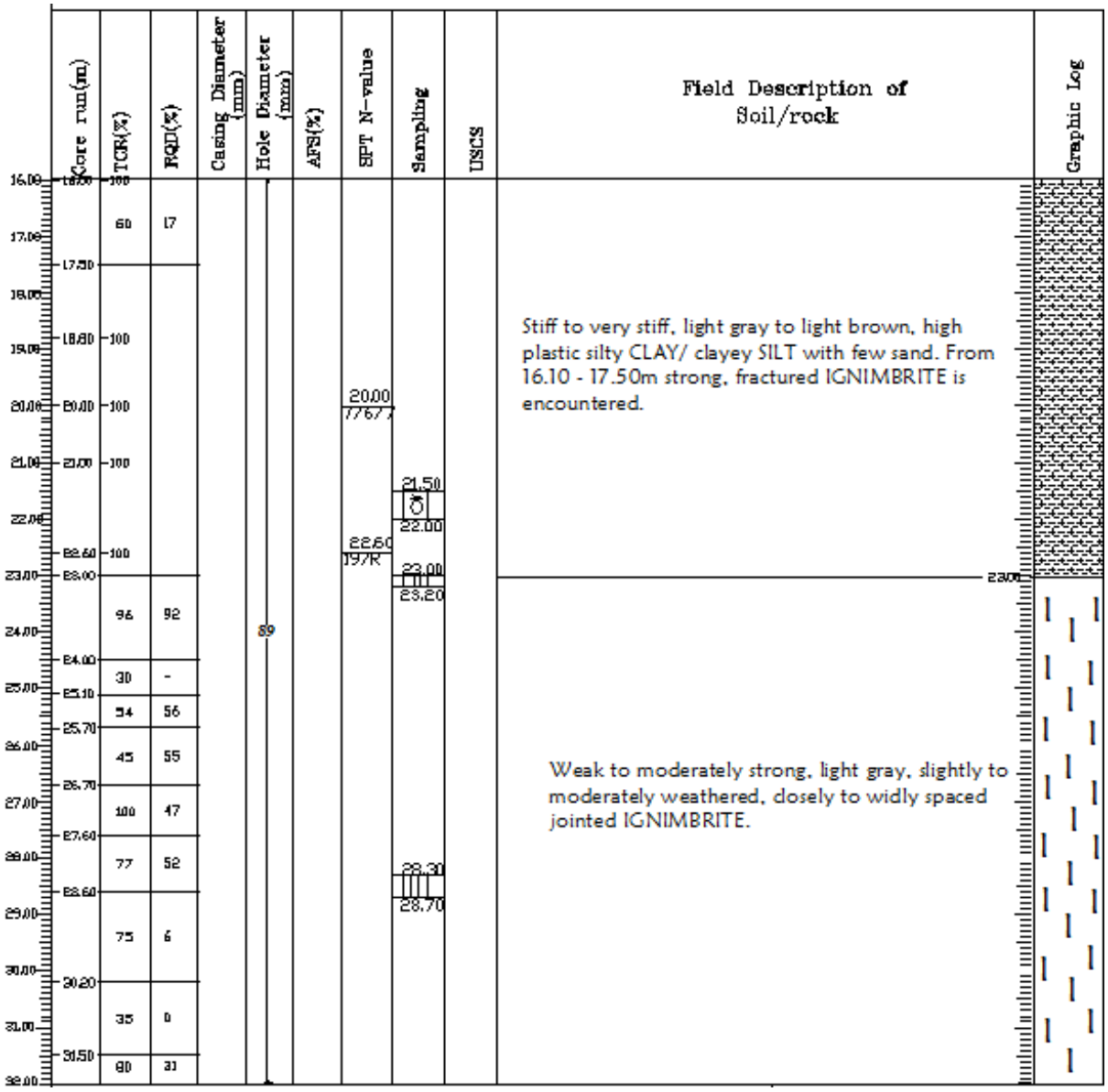

Figure A11: Typical borehole profile for Jemmo site profile 2

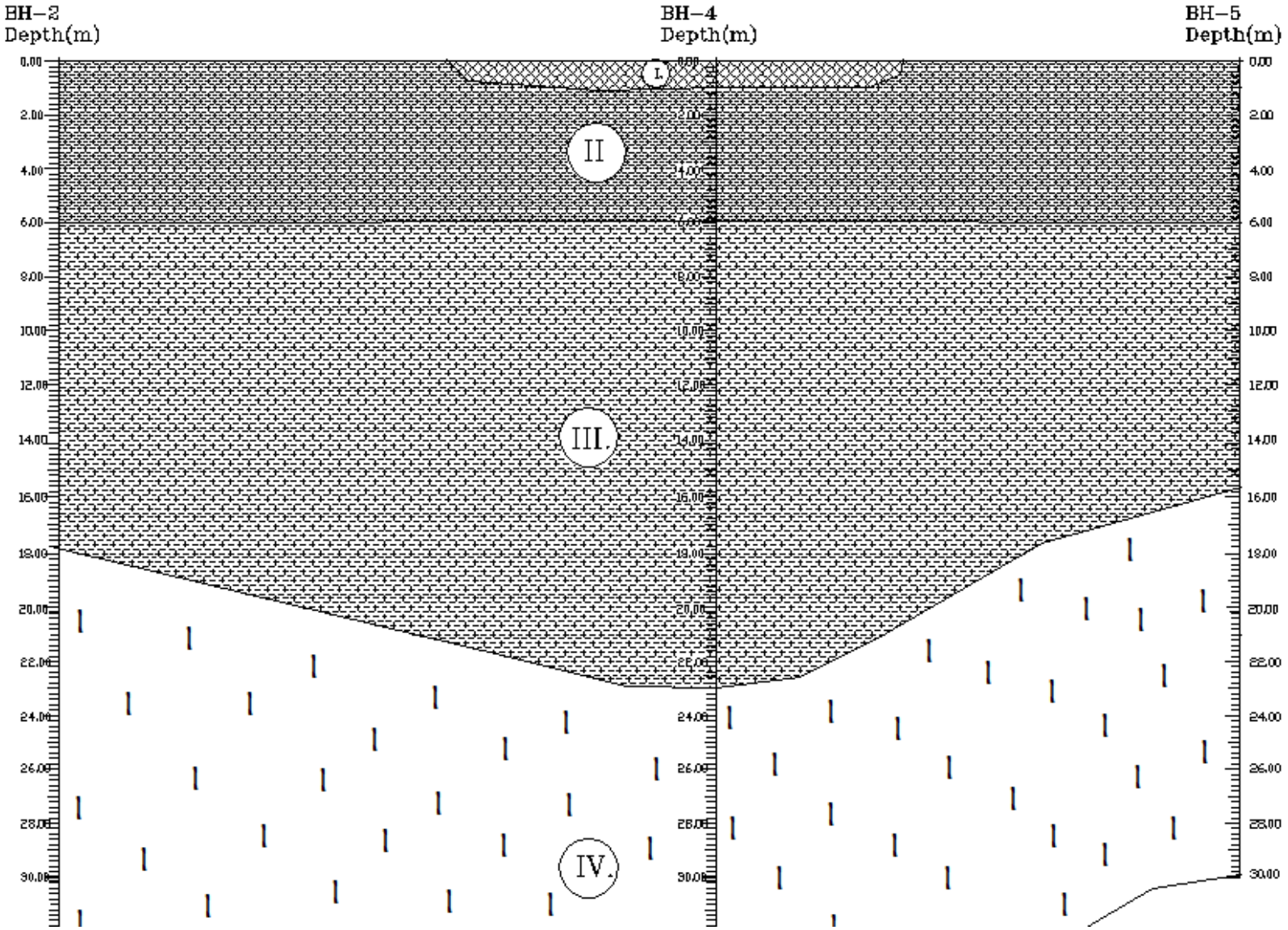
BH–2
Depth(m)
BH–4
Depth(m)
BH–5
Depth(m)
I.
II
III.
IV.

(I). Back fill material- silty sand with gravel

(II). Meduim stiff to stiff, black to dark grey, high plastic silty CLAY (Black cotton soil).

(III). Stiff to very stiff, light grey, high plastic silty CLAY/ clayey SILT.

(IV). Moderately strong, to moderately weak, light grey, slightly weatered, closely to widely sapce jointed IGNIMBRITE.

Figure A12: Cross section through boreholes for Jemmo site profile 2

Appendix B

Table B: Depth dependent Boore (2004) regression coefficients

Depth (m)		10	11	12	13	14
Regression Coefficients	**a**	0.042062	0.022140	0.012571	0.014186	0.012300
	b	1.0292	1.0341	1.0352	1.0318	1.0290

Depth (m)		15	16	17	18	19
Regression Coefficients	**a**	0.013795	0.013893	0.019565	0.024879	0.025614
	b	1.0263	1.0237	1.0190	1.0144	1.0117

Depth (m)		20	21	22	23	24
Regression Coefficients	**a**	0.025439	0.025311	0.026900	0.022207	0.016891
	b	1.0095	1.0072	1.0044	1.0042	1.0043

Depth (m)		25	26	27	28	29
Regression Coefficients	**a**	0.011483	0.006565	0.002519	0.000773	0.000431
	b	1.0045	1.0045	1.0043	1.0031	1.0015

Appendix C

Fourier Amplitude Spectra

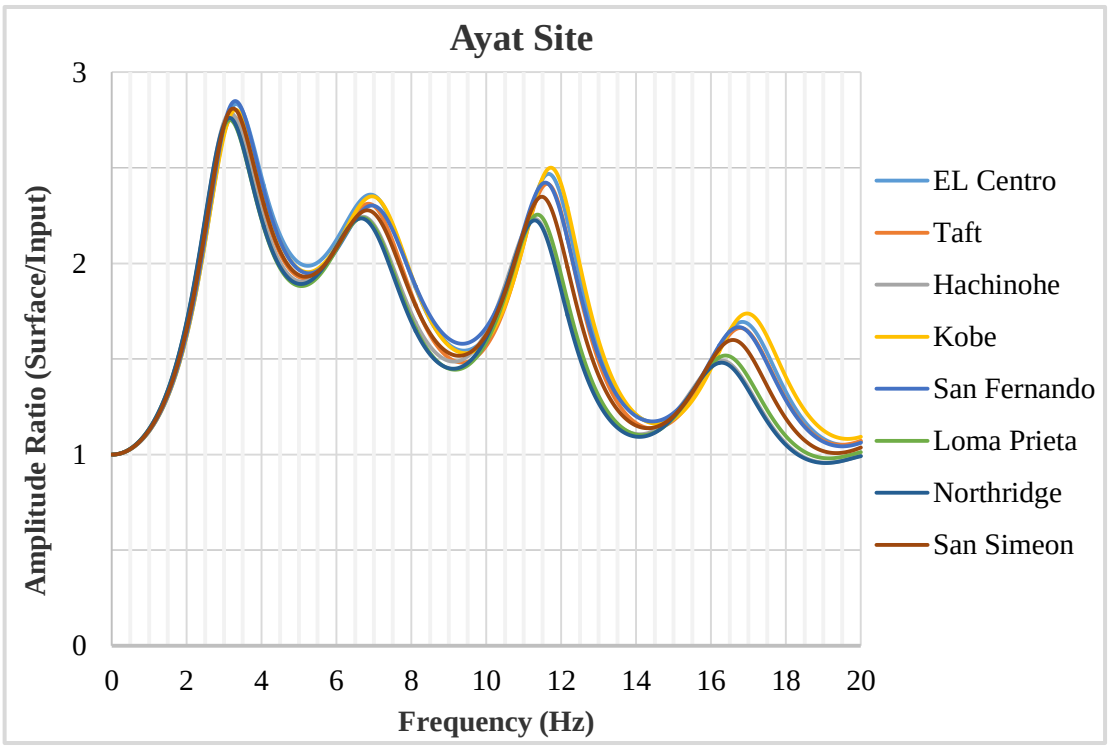

(a)

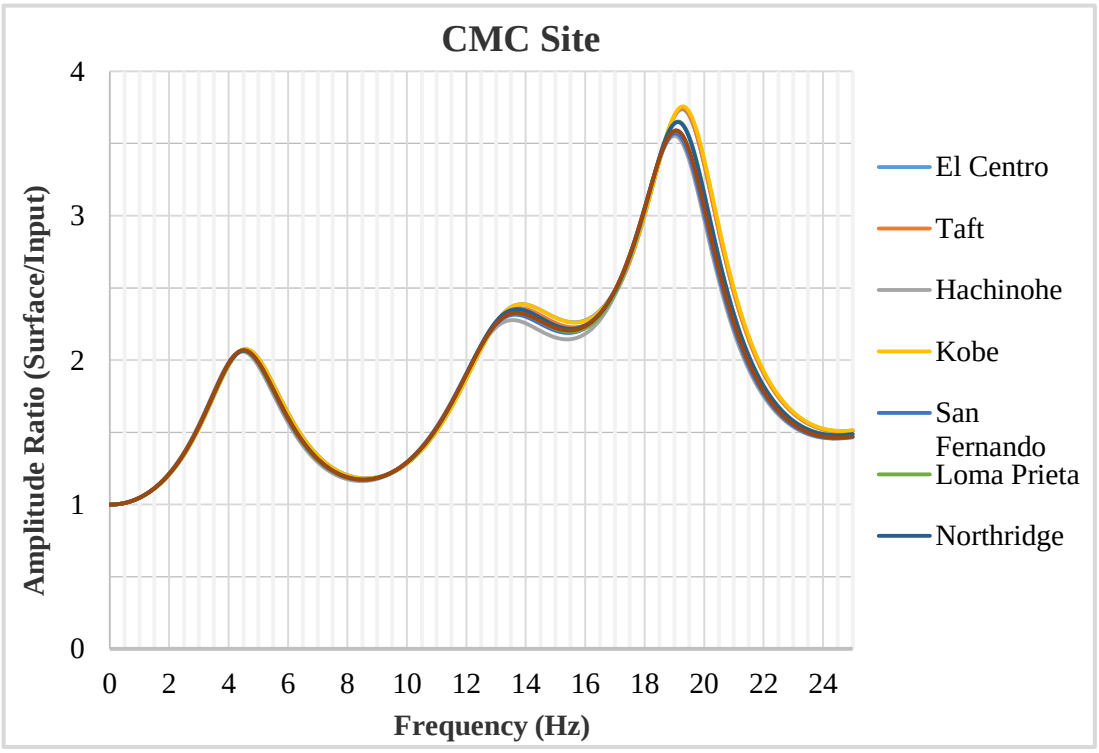

(b)

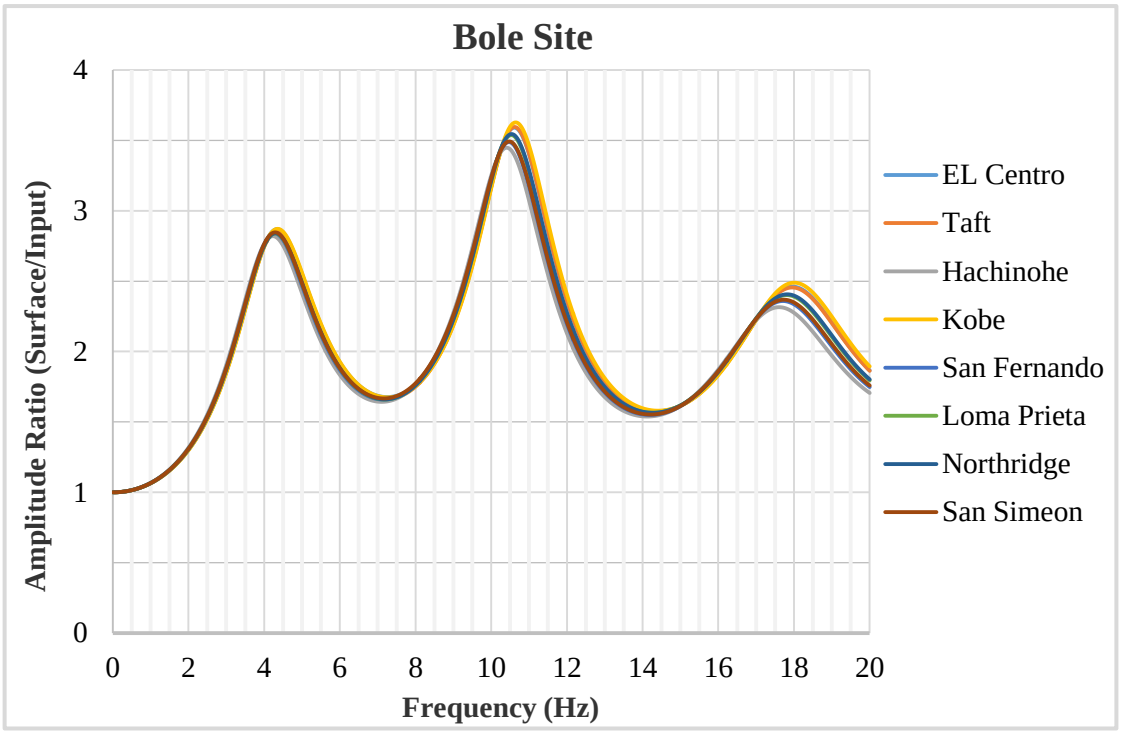

(c)

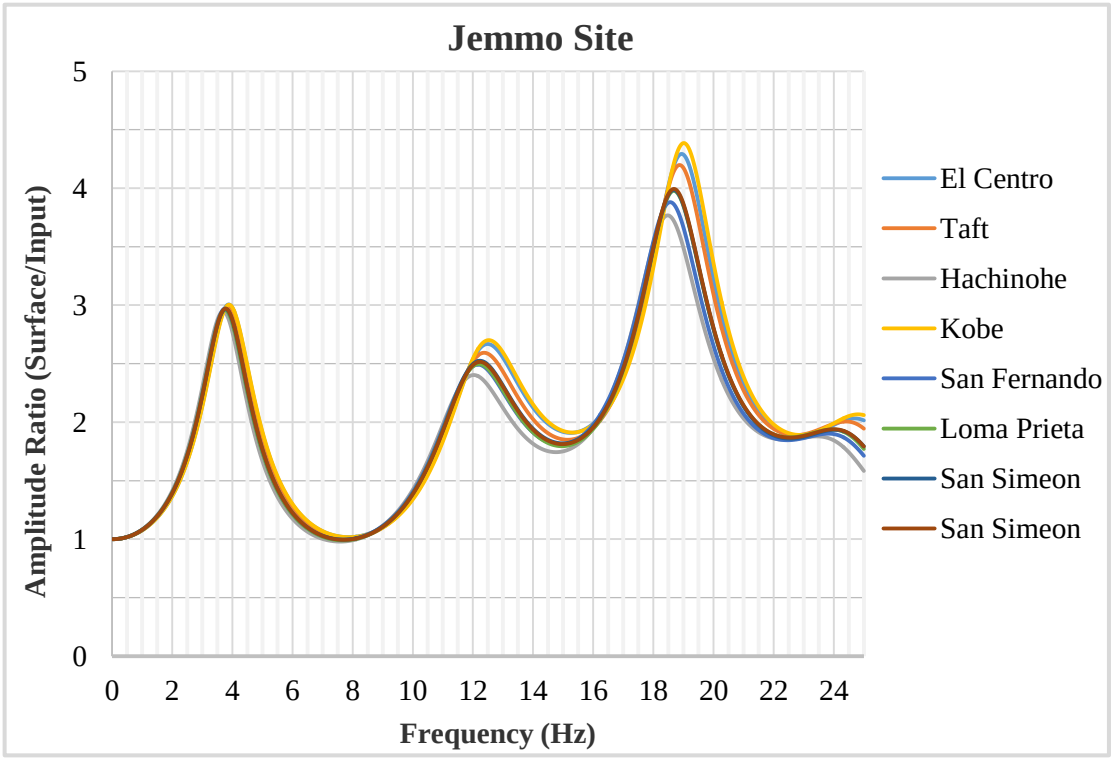

(d)

Figure C1: Fourier Amplitude Spectra of selected sites using Seismic refraction survey data: for Ayat site (a); for CMC site (b); for Bole site (c) and for Jemmo site (d)

Response spectra of sites compared with code-specified spectra

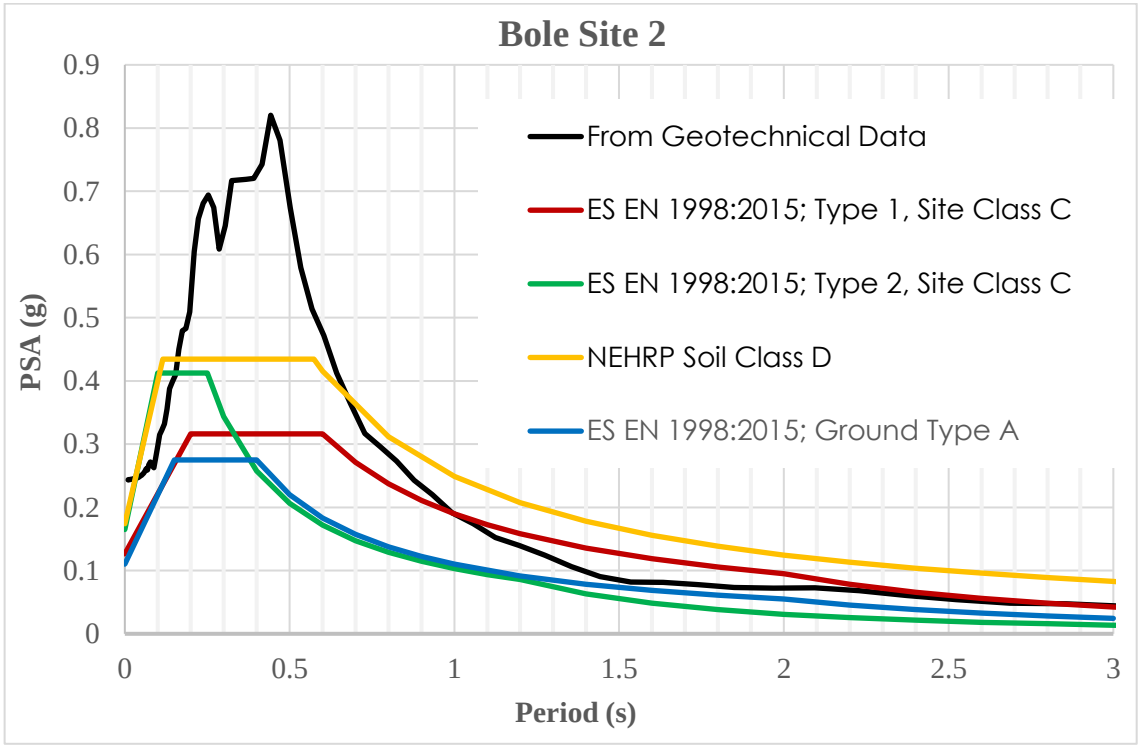

(a)

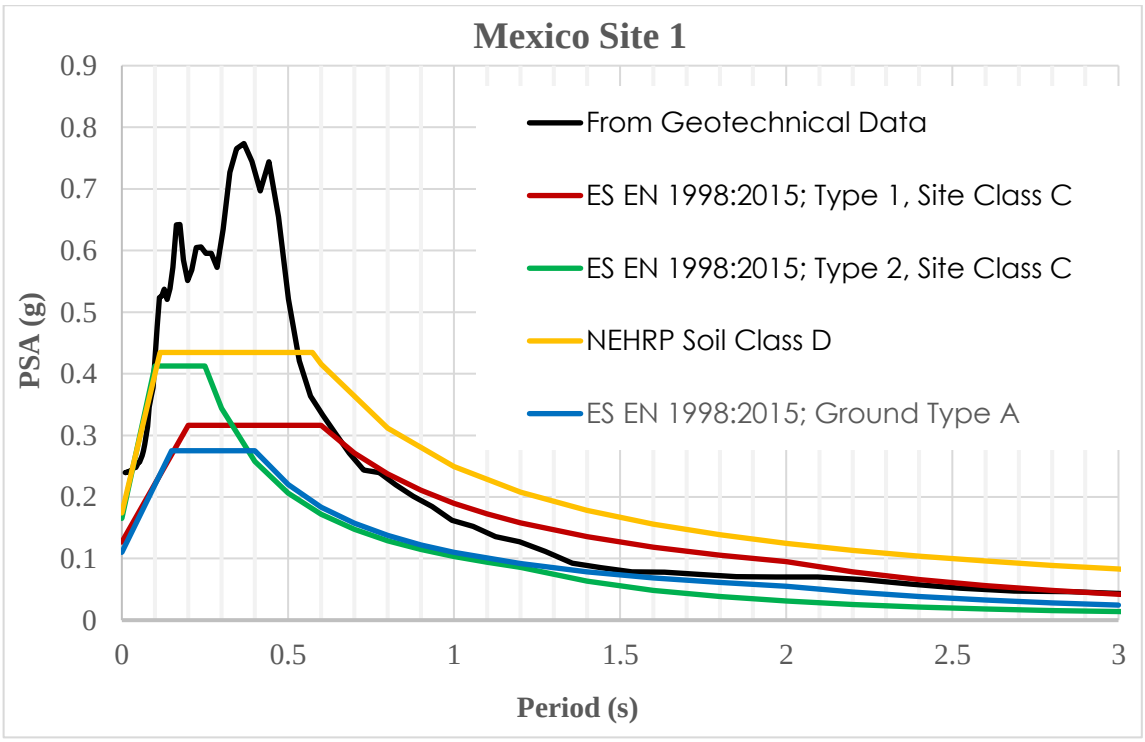

(b)

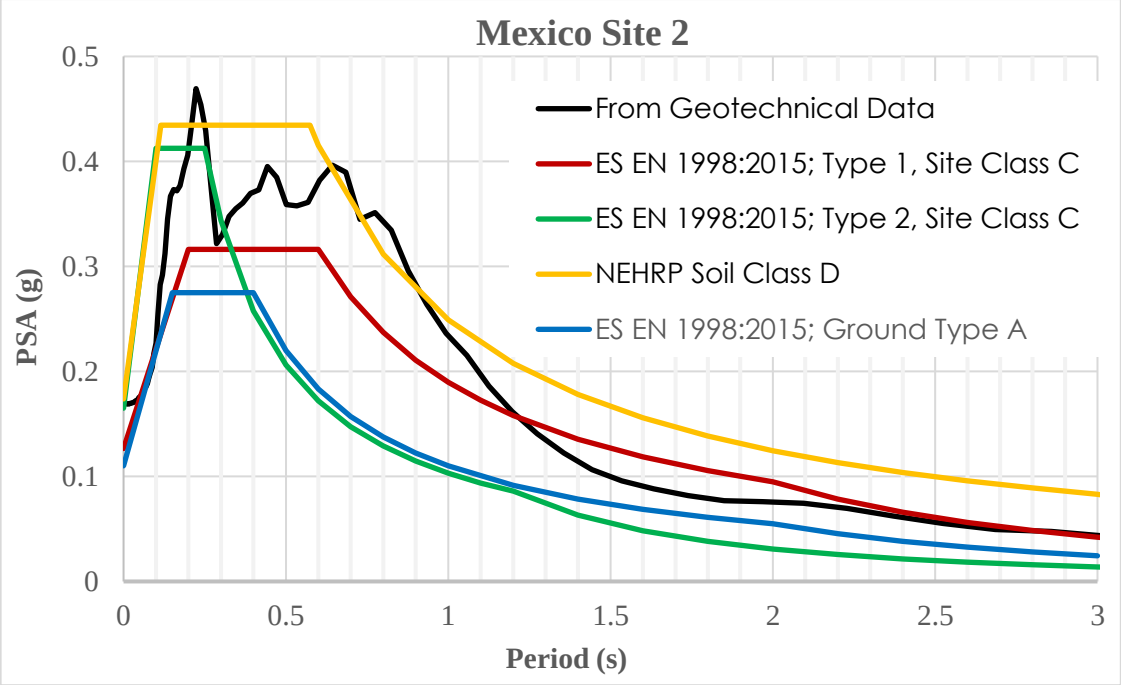

(c)

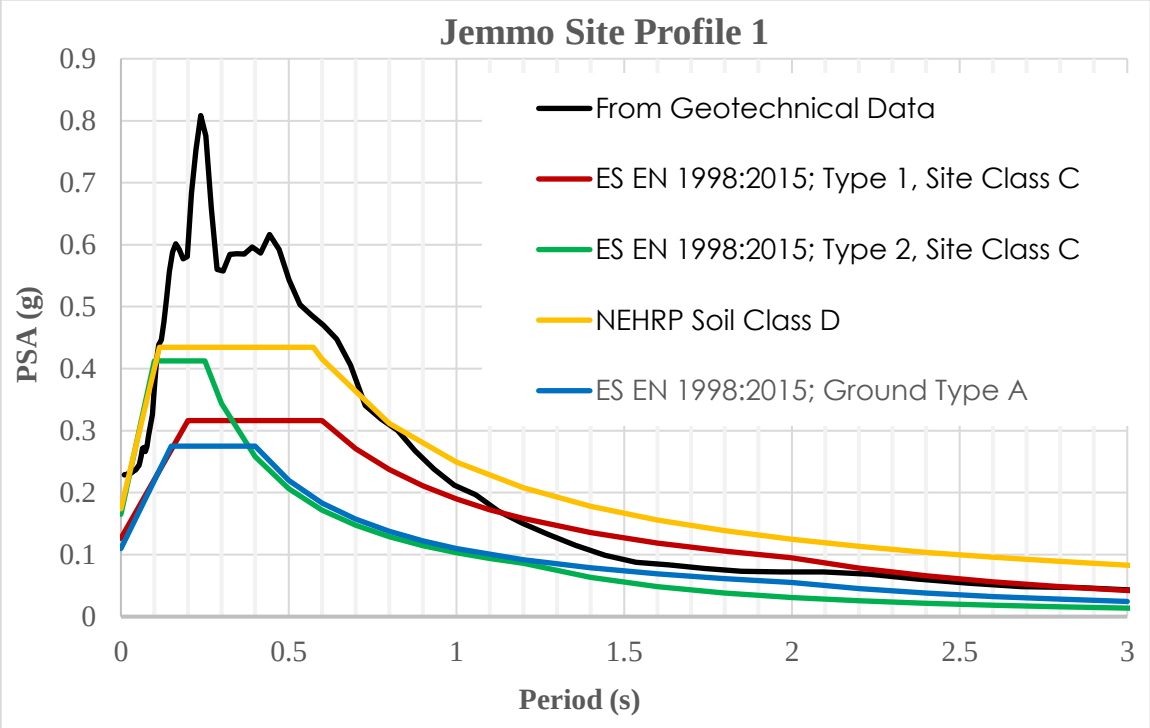

(d)

Figure C2: Mean response spectrum of: (a) Bole site1, (b) Mexico site 1, (c) Mexico site 2 and (d) Jemmo site profile 1, compared with code-specified spectra